

Deutsche Entomologische

Zeitschrift

69 (1) 2022

Deutsche Entomologische Zeitschrift

An International Journal of Systematic Entomology

Editor-in-Chief

Dominique Zimmermann

Natural History Museum Vienna
dominique.zimmermann@nhm-wien.ac.at

Managing Editor

Lyubomir Penev

Pensoft Publishers, Sofia, Bulgaria
phone: +359-2-8704281
fax: +359-2-8704282
e-mail: penev@pensoft.net

Editorial Secretary

Boryana Ovcharova

Pensoft Publishers, Sofia, Bulgaria
e-mail: journals@pensoft.net

Editorial Board

Ulrike Aspöck, Vienna, Austria
Silas Bossert, Pullman, United States of America
Jose Fernandez-Triana, Ottawa, Canada
Claudia Hemp, Bayreuth, Germany
Zoltán László, Cluj-Napoca, Romania
Harald Letsch, Vienna, Austria
James Liebherr, Ithaca, United States of America
Wolfram Mey, Berlin, Germany
Alessandro Minelli, Padova, Italy
Susanne Randolph, Vienna, Austria
Dávid Rédei, Tianjin, China
Matthias Seidel, Vienna, Austria
Nikolaus Szucsich, Vienna, Austria
Sonja Wedmann, Messel, Germany
Frank Wieland, Bad Dürkheim, Germany
Michael Wilson, Cardiff, United Kingdom
Dominique Zimmermann, Vienna, Austria

Deutsche Entomologische Zeitschrift

2022. Volume 69. Issue 1

ISSN: 1435-1951 (print), 1860-1324 (online)
Abbreviated keys title: Dtsch. Entomol. Z.

In Focus

The cover picture shows *Platyderus (Eremoderus) vanensis*, sp. nov., holotype

See paper of **Guéorguiev B, Wrase DW, Assmann T, Muilwijk J, Machard P** Taxonomic revision of the African and Southwest Asian species of *Platyderus* Stephens, subg. *Eremoderus* Jeanne (Coleoptera, Carabidae, Sphodrini)

Cover design

Pensoft



Deutsche Entomologische Zeitschrift
An International Journal of Systematic Entomology

Content of volume **69 (1)** 2022

Li X-R Phylogeny and age of cockroaches: a reanalysis of mitogenomes with selective fossil calibrations	1
Schmidt J, Scholz S, Will K Character analysis and descriptions of Eocene sphodrine fossils (Coleoptera, Carabidae) using light microscopy, micro-CT scanning, and 3D imaging	19
Morishita S, Watanabe K Revision of the genus <i>Woldstedtius</i> Carlson, 1979 (Hymenoptera, Ichneumonidae, Diplazontinae) from Japan	45
Kočárek P, Horká I Identity of <i>Zorotypus juninensis</i> Engel, 2000, syn. nov. revealed: it is conspecific with <i>Centrozoros hamiltoni</i> (New, 1978) (Zoraptera, Spiralizoridae)	65
Guéorguiev B, Wrase DW, Assmann T, Muilwijk J, Machard P Taxonomic revision of the African and Southwest Asian species of <i>Platyderus</i> Stephens, subg. <i>Eremoderus</i> Jeanne (Coleoptera, Carabidae, Sphodrini)	122

Abstract & Indexing Information

Biological Abstracts® (Thompson ISI)
BIOSIS Previews® (Thompson ISI)
Cambridge Scientific Abstracts (CSA/CIG)
Web of Science® (Thompson ISI)
Zoological Record™ (Thompson ISI)

Phylogeny and age of cockroaches: a reanalysis of mitogenomes with selective fossil calibrations

Xin-Ran Li^{1,2}

¹ State Key Laboratory of Palaeobiology and Stratigraphy, Nanjing Institute of Geology and Palaeontology, Chinese Academy of Sciences, Nanjing 210008, Jiangsu, China

² University of Science and Technology of China, Hefei 230026, Anhui, China

<http://zoobank.org/EAF5BD14-E52A-46D0-A7A0-B238B3DC727D>

Corresponding author: Xin-Ran Li (ConlinMcCat@gmail.com)

Academic editor: Harald Letsch ♦ Received 7 May 2021 ♦ Accepted 29 November 2021 ♦ Published 7 January 2022

Abstract

In spite of big data and new techniques, the phylogeny and timing of cockroaches remain in dispute. Apart from sequencing more species, an alternative way to improve the phylogenetic inference and time estimation is to improve the quality of data, calibrations and analytical procedure. This study emphasizes the completeness of data, the reliability of genes (judged via alignment ambiguity and substitution saturation), and the justification for fossil calibrations. Based on published mitochondrial genomes, the Bayesian phylogeny of cockroaches and termites is recovered as: Corydiinae + (((Cryptocercidae + Isoptera) + ((Anaplectidae + Lamproblattidae) + (Tryonicidae + Blattidae))) + (Pseudophyllodromiinae + (Ectobiinae + (Blattellinae + Blaberidae)))). With two fossil calibrations, namely, *Valditermes brenanae* and *Piniblattella yixianensis*, this study dates the crown Dictyoptera to early Jurassic, and crown Blattodea to middle Jurassic. Using the ambiguous ‘roachoid’ fossils to calibrate Dictyoptera+sister pushes these times back to Permian and Triassic. This study also shows that appropriate fossil calibrations are rarer than considered in previous studies.

Key Words

Blattaria, Blattodea, Dictyoptera, divergence time; mitochondrial DNA

Introduction

The family-level relationships of cockroaches have been in dispute for decades (Fig. 1; see also McKittrick 1964, Klass 2001, Roth 2003). The debate recently intensified with many incongruent phylogenies emerging. Most recent studies are based on molecular data (e.g., Djernæs et al. 2015, Legendre et al. 2015, Wang et al. 2017, Bourguignon et al. 2018, Evangelista et al. 2019), or rarely on morphological and ethological data (Klass and Meier 2006, Djernæs et al. 2015 in part). Despite big data studies, the evolutionary pattern of cockroaches remains ambiguous: mitochondrial genomes (Bourguignon et al. 2018) suggest the basal splits as (Blaberoidea + Corydioidea) + the blattoid complex (i.e. Blattoidea nesting Isoptera), while the much bigger transcriptome data (Evangelista et al. 2019) suggest Blaberoidea + (Corydioidea + blattoid

complex), not to mention more incongruent relationships of families and subfamilies.

Calibration has a major impact on divergence time estimation (Inoue et al. 2010, Dos Reis and Yang 2012, Sauquet et al. 2012, Sauquet 2013, Magallón et al. 2013). Fossils are common calibrations for phylogenetic dating, while choosing a suitable fossil is difficult (Parham et al. 2011, Wolfe et al. 2016). The lack of justified fossil calibrations for dating cockroaches is particularly acute (Evangelista et al. 2017, 2019, Li and Huang 2019). Of the calibrations used, the ‘roachoid’ fossils are a particular point of contention (Tong et al. 2015 vs. Kjer et al. 2015, Bourguignon et al. 2018 *per se*).

Phylogenetic inference and time estimation can be improved by enlarging the dataset with new loci and new samples, but also by improving the quality of

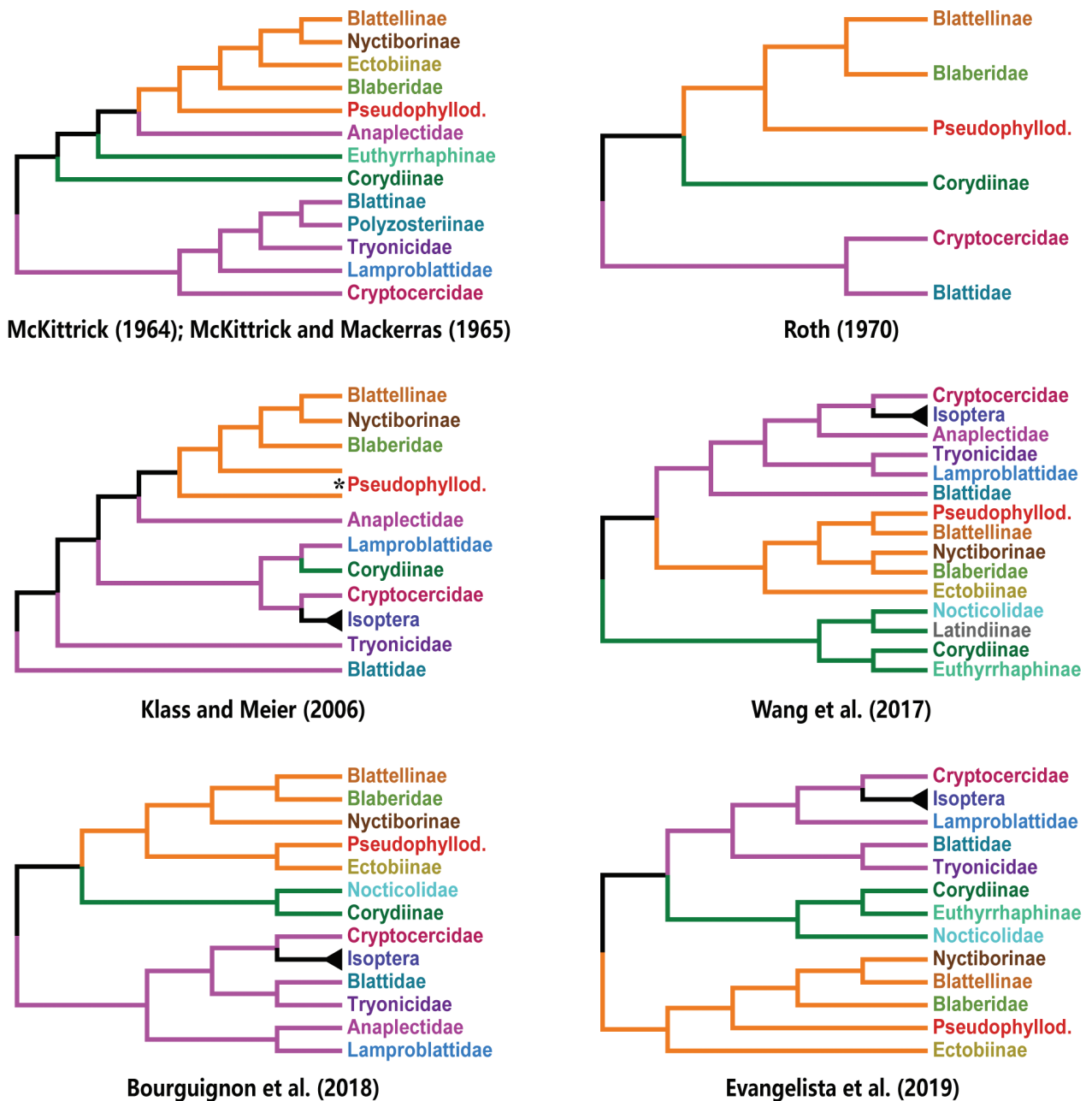


Figure 1. Representative phylogenetic inferences of cockroaches based on various data and methods. McKittrick (1964) and McKittrick and Mackerras (1965): female and male genitalia, proventriculus and oviposition behaviour; discussion. Roth (1970): oothecal rotation; discussion. Klass and Meier (2006): male genitalia, accompanied by ethology etc.; parsimony. Wang et al. (2017): gene fragments (three mitochondrial and two nuclear), incorporating the data from Djernæs et al. (2015) and others; maximum likelihood. Bourguignon et al. (2018): mitogenome; maximum likelihood and Bayesian. Evangelista et al. (2019): transcriptome; maximum likelihood. Taxa are shown in currently recognized rank instead of original designation. Branches in orange, Blaberoidea; in green, Corydioidea; in purple, Blattoidea. Asterisk, paraphyly.

published data, calibrations and analytical procedure. The latter approach is emphasized and presented herein. In the present study, the mitochondrial genome is preferred as the only type of data for the following reasons. First, taxon coverage is comparatively high; second, missing data can be essentially avoided; third, the computation load (i.e. time investment) is acceptable, allowing multiple analyses for comparisons among datasets.

Material and methods

Dataset

The present study focuses on true cockroaches (Blattaria), the major component of Dictyoptera. Taxa included in my analyses also cover other Dictyoptera, namely, termites (Isoptera) and mantises (Mantodea), and the living sister of Dictyoptera, namely Eukinolabia + Xenonomia, as

suggested by transcriptome data (Misof et al. 2014, Evangelista et al. 2019, Wipfler et al. 2019). In order to reduce the difficulty and inaccuracy in alignment, more distant insect groups were not included in this study. All DNA sequences were collected from whole mitogenome sequencing data deposited in GenBank. Isolated fragments do not conform to the main idea of the present study because they leave missing cells in the alignments. A certain number of missing cells may be harmless to phylogenetic inferences (Wiens 2006, Wiens and Moen 2008), but there is no universal standard for different datasets and methods to avoid pitfalls. Using fully sequenced mitogenome (thus avoiding isolated fragments) can also prevent concatenation of sequences from different specimens, of which the genetic distance is unknown. This practice also automatically rules out specimens that are misidentified as conspecific. Fundamentally, concatenation of sequences from different specimens is an artefact and does not represent a natural organism. This artefact may cause unpredictable errors (pers. observ.); however, the influence of this issue seemingly has not yet been addressed in the literature.

The initial data pool comprises 169 mitogenomes, including all available cockroaches and selected other insects (Suppl. material 1). GenBank files were imported to PHYLOSUITE v1.2.1 (Zhang D et al. 2020), in which duplicates were removed. To save time and computation resources, only one species was kept in each genus, with the exception of genetically diverse and speciose genera (e.g., *Cryptocercus*, *Allacta* and *Ischnoptera*). The final taxon set comprises 95 species (Suppl. material 2: Table S1). The DNA data in the GenBank files were extracted using PHYLOSUITE. Most of the mitogenomes (68.4%) are from Bourguignon et al. (2018), and the remaining from Yamauchi et al. (2004), Cameron et al. (2005, 2012), Zhang YY et al. (2009), Kômoto et al. (2010, 2012), Chen (2012), Wang et al. (2014), Jeon and Park (2015), Tian et al. (2015), Cheng et al. (2016), Ye et al. (2016), Chen et al. (2017), Dumans et al. (2017), Ma et al. (2017), Gong et al. (2018), and Zhang LP et al. (2018).

The character set includes 13 protein coding genes while all RNA genes were excluded. Aligning RNA gene sequences is dependent on the prediction of secondary structure (Buckley et al. 2000, Stocsits et al. 2009), the accuracy of which clearly influences alignment and tree reconstruction (Letsch et al. 2010). This approach is unfeasible in the present study, because even predicting the structure of a small fragment of closely related species is hard and exhausting (e.g., Li et al. 2017). To avoid errors introduced by inaccurate alignment, I do not use them. Besides, RNA gene sequences only account for a minor proportion in the mitochondrial genome, therefore excluding them does not virtually reduce the size of dataset.

Alignment and quality check

Sequences of protein coding genes were aligned using MUSCLE in MEGA7 with default settings of codon mode (Edgar 2004, Kumar et al. 2016). Uneven ends

were manually trimmed. 43 sequences were spotted containing missing or poorly-sequenced portions, which were deleted or question-marked (Suppl. material 3: Table S2). Then, all sequences were aligned again. The aligned sequences were translated into amino acids to check accuracy. Alignments of 13 genes were concatenated using PHYLOSUITE. The final alignment is 10932 bases long.

ALIGROOVE 1.05 (Kück et al. 2014) was used to assess alignment ambiguity for each gene, and DAMBE 7.2.7 (Xia 2018) to calculate the substitution saturation per codon position per gene (i.e. 3 bases \times 13 genes). Amino acid alignments (translated from the nucleotide alignments) instead of nucleotide alignments were imported to ALIGROOVE, because the alignments were based on codon model. Saturation was calculated under GTR model by default, or under F84 model when an overflow error occurs (the error itself is a sign of saturation).

ALIGROOVE suggests high ambiguity in ATP8 alignment, followed by ND6 (Suppl. material 4). Other genes exhibit low general ambiguity, but a few taxa with too many missing cells in alignments show high ambiguity. Even if several incomplete sequences can be excluded in the following analyses, ATP8, in general, is still too ambiguous. On the other hand, the dataset as a whole is not significantly affected by scattered ambiguous alignments (Suppl. material 4).

According to the 39 saturation plots (Suppl. material 5), ATP8, ND4L, ND6 and, as expected, the third codon positions are saturated. These three genes are among the less informative ones considered in Talavera and Vila (2011). Excluding ATP8, ND4L and ND6, data incompleteness was calculated by counting Ns and question-marks, both of which are regarded as missing cells. Eight taxa with missing cells greater than 1% were grouped into ‘BadSeq’: *Anallacta methanoides* (9.17% missing), *Aposthonia borneensis* (1.80%), *Beybienkoa kurandanensis* (1.18%), *Eublabeus distanti* (2.87%), *Galiblatia cribrosa* (3.64%), *Megaloblatta* sp. (2.92%), *Metallyticus* sp. (8.84%), and *Platyzosteria* sp. (2.19%).

Bayesian phylogenetic inference

Phylogenetic inferences were performed in MRBAYES 3.2.7 (Ronquist et al. 2012). Data were divided into two partitions: the first and the second bases of the codon. The third position of codon was excluded from all analyses. I did not use programs to select a ‘best-fit’ model, not only because this is unnecessary (Nascimento et al. 2017, Abadi et al. 2019), but also because the ‘best-fit’ is not necessarily the best or accurate (Gatesy 2007, Kelchner and Thomas 2007, Luo et al. 2010). Instead, I used the empirically universal model, GTR, with Gamma rates (+G). The manual and tutorials of MRBAYES (among others) recom-

mend GTR+I+G as the universal model, but the invariable-sites model (+I) generates a strong correlation between the proportion of invariable sites and the gamma shape parameter, and becomes undesirable (Sullivan et al. 1999, Yang 2014). Using PHYLOBAYES with the CAT-GTR model implemented therein accounting for more exhaustive heterogeneities may improve the resolution and accuracy of phylogenetic inference (Lartillot and Philippe 2004, Lartillot et al. 2009, Moran et al. 2015), but this approach is currently impossible given the computation resources available to this study. Instead, the alignment ambiguity of the final dataset (see below) was reported, because the alignment ambiguity assessed by ALIGROOVE is also a measure of heterogeneous sequence divergence (Kück et al. 2014). I did not perform maximum likelihood analysis because the interpretation of bootstrapping (the assessment of the uncertainty of maximum likelihood estimates) is vague (Yang 2014), in contrast to posterior probabilities of Bayesian estimates (Huelsenbeck and Rannala 2004). Instead, the maximum-likelihood tree sampled from MCMC is reported. Each MRBAYES analysis involved two runs, each of which comprises four chains, running 1.5–2.5 million iterations depending on the difficulty of converging. Samples were taken once every 500 iterations and the initial 1%–5% (depending on the difficulty of converging) of samples were discarded (burn-in). I used TRACER 1.7.1 (Rambaut et al. 2018) to ensure sufficient effective samples (200 at least, 300–1000 in general).

The first analysis utilized all 13 genes. The results are only used for comparison with the second step analyses, to observe the influence of ATP8, ND4L and ND6.

The second step is to compare the trees inferred from three taxon sets. All analyses excluded ATP8, ND4L and ND6. (1) All-species analysis using complete taxon set. (2) Good-species analysis, excluding ‘BadSeq’. (3) Short-species analysis, excluding long-branched taxa detected from the all-species analysis. This step aims to detect the impact of incomplete data and long branch.

The third step analysis used only the ‘safe’ taxa. In this step, all taxa within ‘BadSeq’ were excluded even if they do not virtually affect the topology of other species. It is learnt from experience that more missing or poorly-sequenced bases imply more potential errors in the superficially intact data. Potential pitfalls of incompleteness (e.g. erroneous positions of these taxa *per se*) violate the main idea of this study. Long-branched taxa with low support are also to be excluded. In the present study, they are *Aposthonia borneensis*, *Aposthonia japonica* and *Nocticola* sp.. ‘Safe’ taxa comprise 85 species (Suppl. material 2: Table S1).

The fourth, also the final, step yields the phylogeny that is regarded as the formal result. Prior to MRBAYES, sequences of ‘safe’ taxa were re-aligned and concatenated. This new, 9912-base-long alignment, as final dataset, was also imported to ALIGROOVE to assess alignment

ambiguity. This 85-species dataset is less ambiguous than the original one (Suppl. material 4). The resulted tree was used as the fixed topology in dating analyses.

Fossil calibration and dating

As calibrations, only two fossils fulfill the criteria of Parham et al. (2011) and are suitable for the present study. The earliest known termite *Valditermes brenanae* calibrates the split between Cryptocercidae and Isoptera (minimum age 130.3 Ma, see Wolfe et al. 2016), as in Misof et al. (2014) and Evangelista et al. (2019). The earliest known blattelline cockroach *Piniblattella yixianensis* Gao et al., 2018 (Gao et al. 2018) calibrates the split between Blattellinae and Blaberidae. *Piniblattella yixianensis* is used for calibration for the first time, setting a minimum age as 120.9 Ma (see Discussion). To observe the effect of this new calibration, I also ran an analysis without this fossil (i.e. only calibrated by *V. brenanae*) to compare with the two-fossil analysis. The minimum bounds of calibrated nodes were set to the minimum age of fossils. The minimum root age was set to 130.3 Ma, the age of the older calibration fossil. All maximum bounds were set to 412 Ma, the oldest age of Rhynie Chert, as justified in Evangelista et al. (2019).

Some studies used the so-called ‘roachoids’ (Eoblattoidea, see Li 2019) to calibrate Dictyoptera+sister (which is the root herein), based on the hypothesis that those ambiguous fossils are stem members of Dictyoptera (Legendre et al. 2015, Tong et al. 2015, Bourguignon et al. 2018, Evangelista et al. 2019). To detect the impact of such fossils, I performed another dating analysis with the earliest ‘roachoid’, namely *Qilianiblattea namurensis* Zhang et al., 2012 (Zhang ZJ et al. 2012, Guo et al. 2013), thus three fossil calibrations were used in this analysis. The radioisotopic age of the *Q. namurensis*-bearing stratum is unavailable, instead, a preliminary stratigraphic correlation gives latest Bashkirian to middle Moscovian (Trümper et al. 2020). Therefore, I used the top age of Moscovian (306.9 Ma).

I used the MCMCTREE program in PAML 4.9j (Yang 2007) to estimate divergence times. Dating analyses used autocorrelated relaxed clock model and GTR+G model. Rate prior was set to 1 substitution per site per 100 Ma by reference to the empirical estimations (Papadopoulou et al. 2010, Andújar et al. 2012). Estimation of divergence times used the approximate method implemented in MCMCTREE. The first 20000 iterations were discarded as burn-in. 5000 samples were gathered, once every 200 iterations. A replicating MCMC was performed to check for convergence in TRACER.

Figure preparation

Trees are visualized using FigTree 1.4.3 (Andrew Rambaut, <http://tree.bio.ed.ac.uk/software/figtree>) and modified using Adobe Illustrator CC 2017.

Taxonomy

For the reader's convenience and to enable a comparison of studies, familial taxonomy of cockroaches in this paper follows recent studies that are compared (e.g., Djernæs et al. 2015, Legendre et al. 2015, Wang et al. 2017, Bourguignon et al. 2018, Evangelista et al. 2019). It is noteworthy that recent molecular studies focusing on Blaberoidea raised subfamilies of Ectobiidae to families (Djernaes et al. 2020, Evangelista et al. 2020). Consequently, their Ectobiidae is identical to the Ectobiinae herein.

Results

The 13-gene tree recovers a sistergroup relationship between *Aposthonia* (Embioptera) and *Nocticola* (Blattaria), which is obviously erroneous regardless of posterior probability (Suppl. material 6). The 10-gene analyses removed this error (Suppl. material 7–9), and demonstrate that ATP8, ND4L and ND6 are detrimental to the analyses. The results from the all-species analysis (Suppl. material 7) and the good-species analysis (Suppl. material 8) are very close, with some divergences in small clades, and the posterior probabilities are similar in general. In the all-species analysis, three species have extremely long branches (*Aposthonia borneensis*, *Aposthonia japonica* and *Nocticola* sp.), and the posterior probabilities of corresponding nodes are low. Excluding these species increases the general supports (Suppl. material 9).

The 'safe'-taxa analysis yields higher posterior probabilities (Suppl. material 10) than all analyses above. The final dataset, which is from the realignment of the ten genes of 'safe' taxa, yields the formal result (Fig. 2). The maximum-likelihood tree (log-likelihood = -155715.20) sampled from MCMC has only one topological difference with Fig. 2: *Neostylopyga rhombifolia* and *Periplaneta brunnea* are exchanged (not shown). The phylogeny recovers major splits in Dictyoptera as Mantodea + (Corydiinae + (Blaberoidea + Blattoidea-Isoptera complex)). These major splits have at least 95% posterior probability. Owing to the absence of Nocticolidae and Latindiinae, the relationships in Corydioidea are unknown.

The dating result of two-fossil-calibration analysis (without *Q. namurensis*) is regarded as the formal result of this paper (Fig. 3: middle), suggesting that the age of crown Dictyoptera is 191.08 Ma (95% credibility interval 168.96–218.82 Ma), of crown Blattodea 171.2 Ma (95% CI 153.26–194.23 Ma). *Qilianiblattea namurensis* considerably pushes the ages back (Fig. 3: top): the age of crown Dictyoptera is 270.01 Ma (95% CI 236.69–309.31 Ma), of crown Blattodea 237.82 Ma (95% CI 204.46–276.04 Ma). In comparison, there is little difference in the estimated ages between the two-calibration analysis and the one-calibration one (Fig. 3: middle vs. bottom). Even though it is insufficient to conclude that *P. yixianensis* is a

calibration as competent as *V. brenanae*, *P. yixianensis* is at least harmless to dating analyses. The time trees showing species are given in Suppl. material 11–13.

Discussion

Phylogeny of cockroaches

The relationship of major clades (suborder, superfamily, family, and subfamily) recovered herein is not identical to any previous studies. At the superfamily level, the sistergroup relationship of Corydioidea (only represented by Corydiinae) to the rest of Blattodea is consistent with that in Wang et al. (2017) and Djernæs et al. (2015, in part), both of which used three mitochondrial and at least two nuclear gene fragments, whereas conflicting with other recent phylogenies (Djernæs et al. 2015 in part, Legendre et al. 2015, Bourguignon et al. 2018, Evangelista et al. 2019). The superfamilial relationship of cockroaches is in dispute. On the other hand, the monophyletic Blaberoidea and the monophyletic blattoid complex (Blattoidea and Isoptera) are always supported.

Corydioidea are always undersampled. Species of Nocticolidae, Latindiinae, and Corydiidae *incertae sedis* (e.g. *Ctenoneura*) are lacking. Although one mitogenome of *Nocticola* is available, it is hardly serviceable unless the long branch is broken up by increased sampling (Poe 2003). Nonetheless, the transcriptome data support a monophyletic Corydioidea that include Corydiidae and Nocticolidae (Evangelista et al. 2019).

In the blattoid complex, only the sistergroup relationship between Cryptocercidae and Isoptera is universally recognized. These taxa constitute Xylophagodea (Engel 2011). The new phylogeny recovers Xylophagodea as sister to the remaining blattoid complex, of which the internal relationship is (Blattidae + Tryonicidae) + (Anaplectidae + Lamproblattidae). This is significantly different from other studies. Three major groups of Blattoidea are still undersampled, namely, Anaplectidae, Lamproblattidae and Tryonicidae. In addition, some mysterious taxa of Blattoidea *incertae sedis* (e.g. *Oulopteryx*) have not yet been sampled.

The paraphyly of Ectobiidae with respect to Blaberidae is a consensus among studies; the present study is not an exception. However, the relationships among Blaberidae and ectobiid subfamilies are conflicting among studies, especially in the positions of Ectobiinae and Pseudophyllodromiinae. The Ectobiinae contributes a weak point in the new phylogeny (pp = 79%), i.e. the node of Ectobiinae + (Blattellinae + Blaberidae). Regardless of the Nyctiborinae, which is not included in the final phylogeny herein, the sistergroup relationship between Blattellinae and Blaberidae is also supported in Bourguignon et al. (2018) and Evangelista et al. (2019, 2020). Although the considerably diversified Blaberidae are typically densely sampled, the phylogeny of them recovered by various studies is inconsistent.

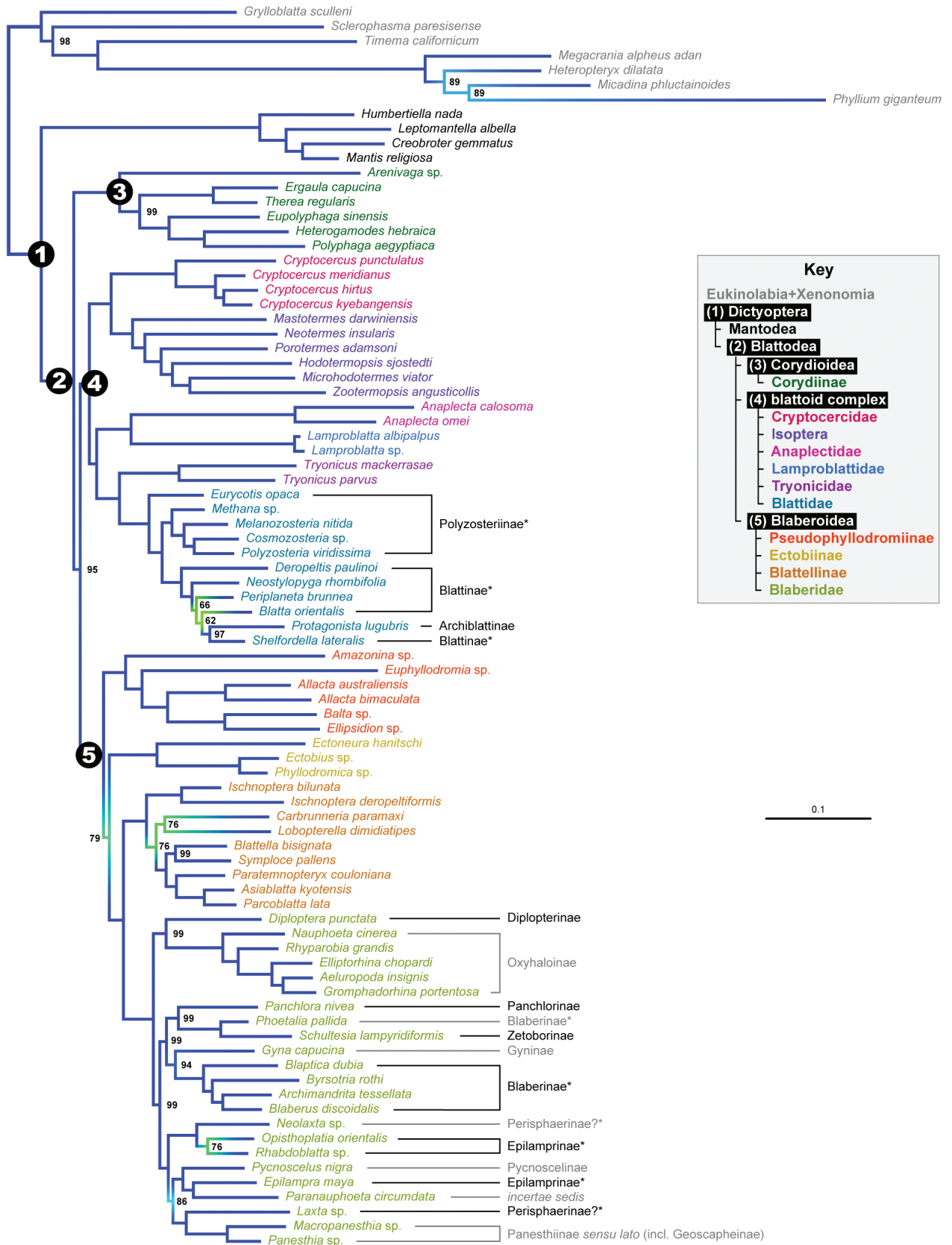


Figure 2. Bayesian phylogeny of Dictyoptera inferred from ten protein-coding genes of 85 mitogenomes, excluding the third base of codon. Posterior probabilities are shown in percentage otherwise are 100%. Clades of superfamilies or higher rank are numbered, as indicated by black background in the key. Species of major taxonomic identities (all are clades) are coloured, as indicated in the key. Subfamilies of Blattidae and Blaberidae are labeled; asterisked ones are not monophyletic. For comparison with trial analyses, see Suppl. material 6–10.

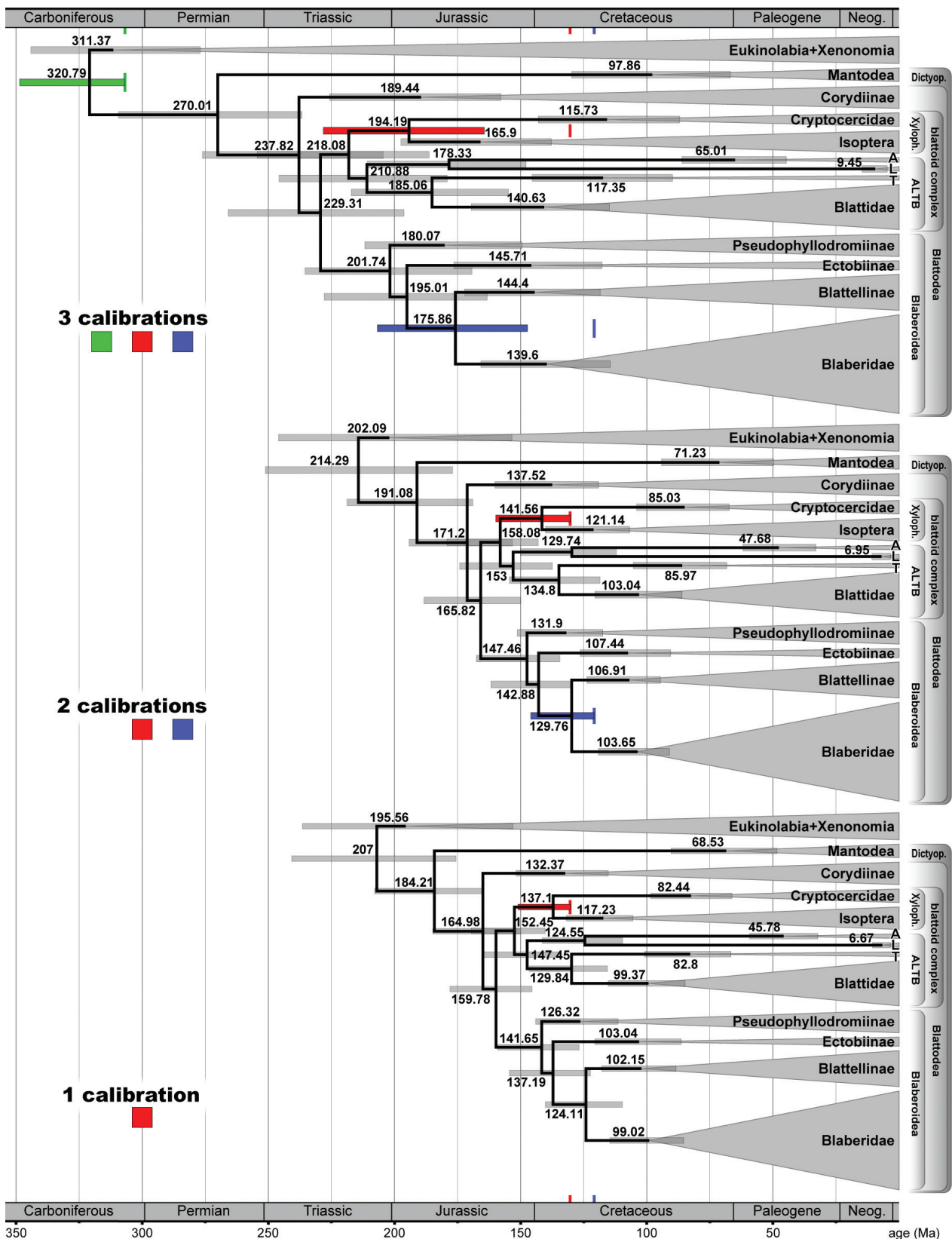


Figure 3. Time trees of Dictyoptera estimated by MCMCTREE. Two-calibration result (middle) is regarded as the formal result of this study. Calibrated nodes are coloured, with vertical bars denoting bounds. Calibrations: *Qilianiblatta namurensis* (green), *Valditermes brenanae* (red), *Piniblattella yixianensis* (blue). Abbreviations: A[naplectidae], Dictyop[tera], L[amproblattidae], T[ryonicidae], Xyloph[agodea]. For detailed phylogenies showing species, see Suppl. material 11–13.

A challenge to all molecular phylogenies is the reconciliation with morphological, behavioral, and other evidence. For example, oothecal property and rotation behavior are various and the taxonomic distribution of them in Blaberoidea is comparatively well known (McKittrick 1964, Roth 1967, 1968a, Bell et al. 2007). Note that the rotation behavior assigned to Ectobiinae in Evangelista et al. (2019) is contrary to the literature. The parsimonious scenario is that Pseudophyllodromiinae are sister to, or paraphyletic with respect to, the remaining Blaberoidea, which constitute a clade (e.g. McKittrick 1964, Klass and Meier 2006). The present study supports this scenario but the posterior probabilities of the “remaining Blaberoidea” node is relatively low (pp = 79%). Other studies, in which the phylogenies do not recover Pseudophyllodromiinae as sister to the remaining Blaberoidea, imply either parallel evolution of oothecal rotation in Ectobiinae and in Blattellinae + Nyctoborinae + Blaberidae, or an ancestral state of oothecal rotation in Blaberoidea and a loss in Pseudophyllodromiinae. At least, the relationship of Ectobiinae and Pseudophyllodromiinae to other Blaberoidea is debatable.

Fossil calibrations and divergence times

The only appropriate fossil calibration in Blattaria in the present study is *Piniblattella yixianensis* Gao et al., 2018 (Gao et al. 2018), which is used as a calibration for the first time. In the following, this fossil calibration is justified according to the five criteria in Parham et al. (2011).

Criteria 1 and 4. Information about the fossil-bearing stratum and museum collection is provided in Gao et al. (2018).

Criterion 2. Regardless of the determination of genus (which is in dispute, see Hinkelman 2019), *P. yixianensis* belongs in Blattellinae as evidenced by the oothecal rotation, reproduction type oviparity B, and the wing venation pattern, as explained below. Rotation feature and physical property of ootheca are crucial to the family-level phylogeny of cockroaches: the “advanced rotation” (i.e. rotating the ootheca and containing the anterior eggs inside vestibulum) is considered as a significant apomorphy in cockroaches, and distributed in Blaberoidea other than Pseudophyllodromiinae (McKittrick 1964, Roth 1967, 1968a, Bell et al. 2007). The rotation of the oothecae of *P. yixianensis* is unlikely due to taphonomic process: all preserved oothecae are horizontally positioned, none is perpendicularly or randomly positioned (Gao et al. 2018, Hinkelman 2019). The “primitive rotation” of Corydiidae is also ruled out: in the primitive rotation, the anterior eggs are outside the abdomen and the ootheca is obliquely positioned (Roth 1967) – this is not the case with *P. yixianensis*. Another difference between primitive and advanced rotation is the presence and absence of the flange, but which cannot be clearly observed in those fossils. In the phylogenies of the present study and some previous studies (e.g., McKittrick 1964, Klass and Meier

2006), Pseudophyllodromiinae are sister to or paraphyletic with the remaining Blaberoidea, supporting that the advanced rotation is autapomorphic for Blaberoidea excluding Pseudophyllodromiinae, and therefore *P. yixianensis* can at least calibrate the node of crown Blaberoidea (regardless of other evidence discussed below). However, other studies support several origins of the advanced rotation in Blaberoidea or loss of the advanced rotation in Pseudophyllodromiinae (e.g., Wang et al. 2017, Bourguignon et al. 2018, Evangelista et al. 2019). Under this hypothesis and regardless of other evidence (discussed below), *P. yixianensis* may only calibrate the split between Blaberoidea and the sister group with caution.

The reproduction type of *P. yixianensis* is oviparity B: (1) during reproduction, female cockroaches have a period of carrying the ootheca (if present) outside, but only the oviparity B carries the ootheca externally until hatching; other types only carry shortly before oviposition (oviparity A) or before retraction (ovoviviparity and viviparity) (Roth 1967, 2003, Bell et al. 2007), and have much less chance to leave fossils. Oviparity B likely contributes a lot to the preservation of ootheca-bearing fossils like *P. yixianensis*. (2) Based on the author’s observation during collecting, the oviparity A ootheca is easily dropped when the cockroach is caught, and almost certainly detached in the end. In comparison, some of the oviparity B oothecae remain attached in the abdomen even when the cockroach is preserved. This implies that it is unlikely that oviparity A cockroaches preserve fossils carrying oothecae, but oviparity B cockroaches may. (3) The oothecal keel of *P. yixianensis* is relatively underdeveloped and unornamented (Gao et al. 2018, Hinkelman 2019), and so accords with the characteristics of oviparity type B (Roth 1968a, 1971, Bell et al. 2007). Among living cockroaches, only some species of *Blattella*, *Chorisia* and *Onycholobus* are known of both the oviparity type B and the advanced rotation (McKittrick 1964, Roth 1967, 1968a, 1971, 1983, 2003, Bell et al. 2007). *Chorisia* and *Onycholobus* are not included in analyses here, but the former is considered as closest to *Blattella* (Roth 1983), while the latter has the ootheca resembling that of *Blattella* (Roth 1971).

However, oviparity B is homoplastic among Blaberoidea. Roth (1968b) found *Lophoblatta*, a pseudophyllodromiine genus, carrying the ootheca until the eggs hatch, but not rotating the ootheca. This discovery demonstrated that the oviparity B originated independently more than once within Blaberoidea. According to the reasonable hypothesis of Roth (1968a), oviparity B is the intermediate form between the ovoviviparity and the plesiomorphic oviparity A, i.e., ovoviviparity derived from oviparity B, which derived from oviparity A. Ovoviviparity occurs in most Blaberidae (with advanced rotation) but also, homoplastically, in two genera of Blattellinae, which rotate the ootheca (Roth 1982, 1984: *Stayella*, Roth 1995: *Pseudoanaplectinia*), and two genera of Pseudophyllodromiinae, which do not rotate the ootheca (Roth 1989: *Sliferia*, Roth 1997: *Pseudobalta*) (see also

a review by Djernæs et al. 2020). Provided that Roth's hypothesis is true, the homoplasy of ovoviviparity further demonstrates that the oviparity B is highly homoplastic.

Accordingly, it appears that Blaberoidea are preadapted to the advanced rotation and oviparity B (consequently ovoviviparity), but as far as known, these two features only co-occur in Blaberidae and Blattellinae. Blaberidae and Blattellinae were recovered as sister groups (Bourguignon et al. 2018 and the present study), or form a clade together with Nyctiborinae (Klass and Meier 2006, Evangelista et al. 2019), which is not included in analyses herein. This implies that species of the clade Blaberidae + Blattellinae (or Blaberidae + Blattellinae + Nyctiborinae) are more preadapted to allow (if not achieved) the co-occurrence of advanced rotation and oviparity B (consequently ovoviviparity). Therefore, the combination of advanced rotation and oviparity B may tentatively place *P. yixianensis* into that clade but outside of Blaberidae.

Other characters preserved in the fossils of *P. yixianensis* are barely discernible except the wing venation. The forewing of *P. yixianensis* conforms to the general form of Blattellinae (see Rehn 1951, Li et al. 2018): ScP with few branches, R pectinate proximally and dichotomous or irregular distally, M and CuA both developed and not essentially pectinate, claval furrow with sharp apical turn, and claval veins diagonal. These traits are distinct from other subfamilies of Ectobiidae. The hindwing has a simple ScP, a pectinate RA with four branches or so, a non-pectinate RP, a simple and feeble M, and a nearly pectinate CuA (Gao et al. 2018). This combination of hindwing traits is not characteristic of any taxon, although these traits are more common in Blaberoidea, particularly Blaberidae (see Rehn 1951, Li et al. 2018). Unfortunately, the polarity of wing venation characters above is barely clear, so that it is premature to conclude a phylogenetic position through these similarities in venation. It is noteworthy that both the tegmen and hindwing of *P. yixianensis* exhibit a developing characteristic posterior branch of R, i.e., the apicoposterior part of R is a branch with terminal branching only. Most cockroaches do not have a characteristic posterior branch (cpb), and this specialization is homoplastically derived among cockroaches, principally Ectobiidae (see Rehn 1951, Li et al. 2018). Nonetheless, the cpb and developing cpb vary in morphology, whereas the branching pattern of *P. yixianensis* is found in *Blattella* and related genera such as *Episymphloe*, but not seen in others (Li et al. 2018, and unpublished observation). This evidence reinforces the hypothesis that *P. yixianensis* belongs in Blattellinae, although it is premature to conclude that *P. yixianensis* is a close relative of *Blattella* or even sister to *Blattella*.

So far, the evolution of reproduction type, ootheca handling behaviour and wing venation of cockroaches is not well understood, and might be more complicated than currently known. In view of this, the phylogenetic position of *P. yixianensis* is not securely settled. Nevertheless, *P. yixianensis* can be tentatively considered as a member of Blattellinae, and thus calibrates the node of

Blattellinae + sister (Blaberidae herein). In summary, *P. yixianensis* as a calibration should be used with caution, and comparative analyses with/without this fossil should be performed to accommodate its uncertainty.

Criterion 3. Reconciliation between molecular and morphological phylogenies is partially achieved. As mentioned above, regardless of the Nyctiborinae that is not included in the final data, the sistergroup relationship between Blattellinae and Blaberidae is supported herein and in recent big data analyses (Bourguignon et al. 2018, Evangelista et al. 2019, 2020), and Ectobiinae and Pseudophyllodromiinae are not nested in the clade of Blattellinae + Blaberidae + Nyctiborinae. In the most comprehensive ever morphological (and ethological) phylogeny of Dictyoptera (Klass and Meier 2006), the above relationships within Blaberoidea are also recovered, except the absence of Ectobiinae. According to the phylogenetic discussion in McKittrick (1964), the Ectobiinae is nested in the clade of Blattellinae + Blaberidae + Nyctiborinae (Fig. 1), but that study is somewhat outdated and not strictly phylogenetic. There is a lack of recent morphological phylogeny covering all major groups; therefore, it is impossible to thoroughly compare the morphological phylogeny with the molecular phylogeny.

Criterion 5. *Piniblattella yixianensis* is from Huangbanjigou, Beipiao, Liaoning, northeastern China (Gao et al. 2018). Isotopic age of the fossiliferous layers in Huangbanjigou ranges from 121.2 Ma to 129.8 Ma (Swisher et al. 1999, Yang et al. 2007). However, the horizontal correlation between this fossil and the radiometric samples is unknown, and the radiometric sampling is insufficient, therefore the age range above does not necessarily represent the age of fossils. I conservatively use the age of the overlying stratum (of top Yixian Formation), 120.9 Ma (Smith et al. 1995), as the minimum age of *P. yixianensis*.

The other fossil for calibration, *V. brenanae*, has been frequently used for Xylophagodea (e.g., Misof et al. 2014, Bourguignon et al. 2018, Evangelista et al. 2019). Its identity as a termite is secured by the presence of basal suture (Jarzembowski 1981), one of the defining characters (autapomorphies) of Isoptera (Ax 1999, Krishna et al. 2013). Its validity as a calibration was justified by Wolfe et al. (2016), and I have no comments on this fossil.

Fossil calibrations contribute considerably to the discrepancy in the age estimation among studies. The 'roachoid' fossils, remarkably, were frequently assigned as "stem Dictyoptera" (e.g., Legendre et al. 2015, Tong et al. 2015, Bourguignon et al. 2018, Evangelista et al. 2019). Although the ambiguity of them and alternative interpretations were considered (e.g., Kjer et al. 2015, Bourguignon et al. 2018, Li and Huang 2019), a formal report on the impact of them is lacking. Because of the same assignment of 'roachoid' fossils, the age estimates with three calibrations herein (which is only for comparison) are close to that in Bourguignon et al. (2018) and Evangelista et al. (2019) (Permian origin of crown Dictyoptera and Triassic origin of crown Blattodea), and only somewhat younger than that in Legendre et al. (2015).

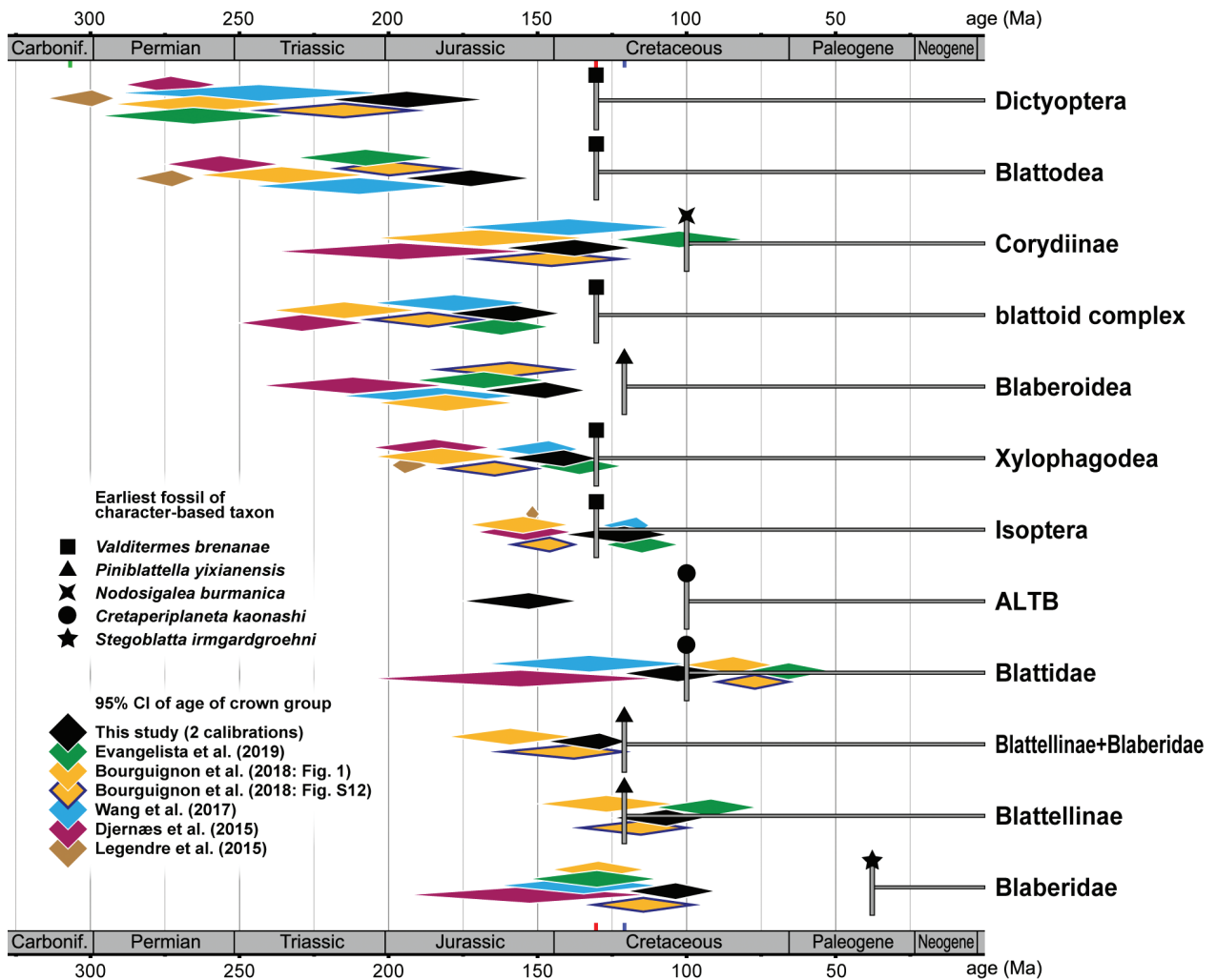


Figure 4. Comparison among the ages estimated in various studies. The fossils are: *Valditermes brenanae* Jarzembowski, 1981; *Piniblattella yixianensis* Gao et al., 2018; *Nodosigalea burmanica* Li & Huang, 2018; *Cretaperiplaneta kaonashi* Qiu et al., 2020; *Stegoblatta irmgardgroehni* Anisutkin & Gröhn, 2012. Abbreviation: ALTB, Anaplectidae + Lamproblattidae + Tryonicidae + Blattidae.

‘Roachoid’ fossils often play a decisive role in the dating of cockroaches, pushing the age estimates older. In comparison, the formal age estimates herein (two fossil calibrations) are close to that in Misof et al. (2014), both studies do not use ‘roachoid’ fossils as calibrations, suggesting Jurassic origins of crown Dictyoptera and crown Blattodea. Without the ‘roachoids’, other fossils will take over them as decisive calibrations and result in various, and usually younger, estimations (e.g., Wang et al. 2017, Bourguignon et al. 2018: fig. S12). A comparison of age estimates among studies is shown in Fig. 4.

Unfortunately, many of the fossil calibrations other than ‘roachoids’ are also unjustified. Subsequently, comparisons among the age estimates from various studies could be pointless. For example, the “stem Mantodea” *Homocladus grandis* (Djernæs et al. 2015, Bourguignon et al. 2018) is highly questionable (Evangelista et al. 2019 and references therein); the “oldest Mantoidea fossil” *Prochaeradodis enigmaticus* (Djernæs et al. 2015, Wang et al. 2017) may be a cockroach (Cui et al. 2018); the “blattid” *Balatronis libanensis* is unlikely a true cockroach (Blattaria), not to mention Blattidae (Evangelista

et al. 2017, Qiu L et al. 2020a); the “*Diploptera* fossils” (Bourguignon et al. 2018) cannot be identified to *Diploptera* and the higher-rank placement of those fossils also remains undetermined (Evangelista et al. 2017, Li et al. 2017); the “first modern cockroach” *Zhujiblatta anofissilis* (Bourguignon et al. 2018) is phylogenetically unsettled and has to be redescribed, which I am preparing elsewhere. Even more surprisingly, an unnamed “*Epilampra* fossil” found in an extant cockroach database was used (Bourguignon et al. 2018).

A critical review of cockroach fossil calibrations was not achieved until Evangelista et al. (2017), who recommended four cockroach fossils for node calibration. Evangelista et al. (2019) discarded one of them and retained corydiid *Cretaholocompsa montsecana* Martinez-Delclos, 1993, blaberid “*Gyna*” *obesa* (Piton, 1940) and ectobiid *Ectobius kohlsi* Vršanský et al., 2014. However, these fossils are still debatable.

Cretaholocompsa montsecana was determined as a close relative of extant *Holocompsa* (Martinez-Delclos 1993), and used as a calibration for corydiid nodes (Legendre et al. 2015, Wang et al. 2017, Evangelista et al.

2019). However, *Cretaholocompsa* significantly differs from *Holocompsa* in the presence of large spines along the ventral margin of midfemora (other legs unknown) (Qiu L et al. 2020b). Besides, according to recent accounts of Corydiidae, such spines are absent from all femora in this family (e.g., Estrada-Alvarez and Guadarrama 2012, Hopkins 2014, Crespo et al. 2015, Qiu L 2017, Qiu L et al. 2017, 2019a, 2019b, 2020b).

“*Gyna*” *obesa* was used as a calibration for blaberid nodes (Bourguignon et al. 2017, Evangelista et al. 2019). Evangelista et al. (2017) identified this fossil to Blaberidae based on (1) the stout cerci, (2) approximately parallel edges of tegmina, (3) elongated CuP, (4) shape of the pronotum, (5) asymmetrical male subgenital plate and (6) large body size. Although this fossil appears to be blaberid in overall appearance, the evidence above is weak or invalid to place “*Gyna*” *obesa* in Blaberidae. First, as acknowledged by Evangelista et al. (2017), traits 1, 2 and 3 are homoplastic with Blattidae. Second, the shape of the pronotum is not entirely clear (Evangelista et al. 2017). Third, the subgenital plate is not clearly discernible: according to the figures in Evangelista et al. (2017), the “concave margin” is implausible in favour of poor preservation. Besides, the subgenital plate appears to be large and cover three segments as in extant female cockroaches, in comparison to the male subgenital plate that is as small as one normal segment; therefore, the specimen may be a female. Fourth, large-sized species are common in Blattidae and Corydiidae in addition to Blaberidae.

Ectobius kohlsi was identified based on a comparison with extant species (Vršanský et al. 2014). However, the preserved characters are not unique enough to indicate the genus; i.e., diagnostic characters of *Ectobius* or of Ectobiinae are not clearly observed, e.g., elongate male genital elements (Roth 2003) and a pinnate R+M+CuA system of tegmina (unpublished observation). Instead, spot-and-line macula patterns on the pronotum and forewings are common in Ectobiinae and Pseudophyllodromiinae. Vršanský et al. (2014) reported a female with valvate subgenital plate. If this is true, then this species likely belongs to Pseudophyllodromiinae because suchlike females do exist in Pseudophyllodromiinae (e.g. *Euphyllodromia*, Anisyutkin 2011). If this fossil is a male, then it is more likely to be a member of Pseudophyllodromiinae, some genera of which have a valvate subgenital plate in males (e.g. *Balta*, Qiu ZW et al. 2017).

Interestingly, the fossil discarded by Evangelista et al. (2019), *Cariblattoides labandeirai* Vršanský et al., 2011, is likely to be a genuine pseudophyllodromiine species, even though the genus is uncertain. According to Vršanský et al. (2011b), the forewing of *C. labandeirai* bears venational characters in common with most Pseudophyllodromiinae: ScP simple and short, R essentially pectinate, M pectinate and more developed than CuA, claval veins oblique or diagonal (see Rehn 1951, Li et al. 2018). The venation alone is a weak indicator of the taxonomic identity, whereas the combination of venation and macula pattern is stronger reasoning. Unfortunately, *C. labandeirai* is not suitable for calibrating Pseudophyl-

lodromiinae + sister (= Blaberoidea herein) even if its inclusion in Pseudophyllodromiinae is proven, because it would be suppressed by the older fossil, *P. yixianensis*, which already calibrates an internal node.

Only one true-cockroach fossil is used as a calibration in the present study, but this does not imply that other fossils are substandard. Every informative fossil (with high phylogenetic resolution and ascertained geological context) has the potential to be a competent calibration, but the incorporation of them is hampered by the fact that relevant living species are under-sampled or have not yet been sequenced. Noteworthy examples of fossils include those of extant genus, e.g. *Supella* (*Nemosupella*) *miocenica* Vršanský et al., 2011 (see Vršanský et al. 2011a), and those of Corydioidea, e.g., *Proholocompsa fossilis* (Shelford, 1910) (see Gorokhov 2007), *Paraethyrrhapha groehni* Anisyutkin, 2008 (see Anisyutkin 2008), *Crenoticticola* Li & Huang, 2019 (see Li and Huang 2019). These fossils could become powerful calibrations for smaller clades (younger nodes) if the data of related extant species are available, otherwise they can only calibrate larger clades (older nodes), and become ineffective when older fossils (e.g. those used herein) calibrate the same or internal nodes.

Conclusions

Based on published mitochondrial genomes, the present study infers a phylogeny of cockroaches and termites as Corydiinae + (((Cryptocercidae + Isoptera) + ((Anaplectidae + Lamproblattidea) + (Tryonicidae + Blattidae))) + (Pseudophyllodromiinae + (Ectobiinae + (Blattellinae + Blaberidae))). The sistergroup relationship between (Cryptocercidae + Isoptera) and (Anaplectidae + Lamproblattidae + Tryonicidae + Blattidae) is recovered for the first time. This study suggests that the phylogenetic reconstruction of cockroaches is in urgent need of the data of Corydioidea (particularly the Nocticolidae), of which the phylogenetic relationships are poorly known. This study dates the crown Dictyoptera to early Jurassic, and crown Blattodea to middle Jurassic. Using the ambiguous ‘roachoid’ fossils to calibrate Dictyoptera+sister pushes these times back to Permian and Triassic. Given currently available data and fossils, few nodes within true cockroaches can be calibrated. This can be overcome by discovering more fossils, or by sampling fossil-related species to allow the incorporation of well-justified fossils. In view of the scarcity of suitable fossils for calibration, the latter approach may be more promising.

Acknowledgements

I deeply thank Dr Klaus Klass and Dr Dominic Evangelista for constructive comments and critiques, and thank the authors of mitogenome data which are fundamental to the present study. This study was motivated by my interest and not funded.

References

- Abadi S, Azouri D, Pupko T, Mayrose I (2019) Model selection may not be a mandatory step for phylogeny reconstruction. *Nature Communications* 10: e934. <https://doi.org/10.1038/s41467-019-08822-w>
- Andújar C, Serrano J, Gómez-Zurita J (2012) Winding up the molecular clock in the genus *Carabus* (Coleoptera: Carabidae): assessment of methodological decisions on rate and node age estimation. *BMC Evolutionary Biology* 12: e40. <https://doi.org/10.1186/1471-2148-12-40>
- Anisuyutkin LN (2008) *Paraeuthyrhapha groehni* gen. et sp. nov., a new genus of the family Polyphagidae (Dictyoptera) from Baltic amber and its phylogenetical position. *Alavesia* 2: 77–85.
- Anisuyutkin LN (2011) A review of the genus *Euphyllodromia* Shelford, 1908 (Dictyoptera: Ectobiidae), with description of three new species. *Proceedings of the Zoological Institute RAS* 315 (4): 369–398. <https://www.zin.ru/journals/trudyzin/publication.html?id=110>
- Ax P (1999) *Das System der Metazoa II. Ein Lehrbuch der phylogenetischen Systematik*. Gustav Fischer, Stuttgart/Jena/Lübeck-Ulm, 384 pp.
- Bell WJ, Nalepa CA, Roth LM (2007) *Cockroaches: Ecology, Behavior, and Natural History*. Johns Hopkins University Press, Baltimore, 230 pp.
- Bourguignon T, Lo N, Cameron SL, Šobotník J, Hayashi Y, Shigenobu S, Watanabe D, Roisin Y, Miura T, Evans TA (2014) The evolutionary history of termites as inferred from 66 mitochondrial genomes. *Molecular Biology and Evolution* 32(2): 406–421. <https://doi.org/10.1093/molbev/msu308>
- Bourguignon T, Tang Q, Ho SYW, Juna F, Wang ZQ, Arab DA, Cameron SL, Walker J, Rentz D, Evans TA, Lo N (2018) Transoceanic dispersal and plate tectonics shaped global cockroach distributions: evidence from mitochondrial phylogenomics. *Molecular Biology and Evolution* 35: 970–983. <https://doi.org/10.1093/molbev/msy013>
- Buckley TR, Simon C, Flook PK, Misof B (2000) Secondary structure and conserved motifs of the frequently sequenced domains IV and V of the insect mitochondrial large subunit rRNA gene. *Insect Molecular Biology* 9(6): 565–580. <https://doi.org/10.1046/j.1365-2583.2000.00220.x>
- Cameron SL, Barker SC, Whiting MF (2005) Mitochondrial genomics and the new insect order Mantophasmatodea. *Molecular Phylogenetics and Evolution* 38(1): 274–279. [print version 2006] <https://doi.org/10.1016/j.ympev.2005.09.020>
- Cameron SL, Lo N, Bourguignon T, Svenson GJ, Evans TA (2012) A mitochondrial genome phylogeny of termites (Blattodea: Termitoidea): Robust support for interfamilial relationships and molecular synapomorphies define major clades. *Molecular Phylogenetics and Evolution* 65(1): 163–173. <https://doi.org/10.1016/j.ympev.2012.05.034>
- Chen AH (2012) Complete mitochondrial genome of the double-striped cockroach *Blattella bisignata* (Insecta: Blattaria: Blaberoidea). *Mitochondrial DNA* 24(1): 14–16. [print version 2013] <https://doi.org/10.3109/19401736.2012.710228>
- Chen Z-T, Lü L, Lu M-X, Du Y-Z (2017) Comparative mitogenomic analysis of *Aposthonia borneensis* and *Aposthonia japonica* (Embioptera: Oligotomidae) reveals divergent evolution of web-spinners. *Scientific Reports* 7: 8279. <https://doi.org/10.1038/s41598-017-09003-9>
- Cheng XF, Zhang LP, Yu DN, Storey KB, Zhang JY (2016) The complete mitochondrial genomes of four cockroaches (Insecta: Blattodea) and phylogenetic analyses within cockroaches. *Gene* 586(1): 115–122. <https://doi.org/10.1016/j.gene.2016.03.057>
- Crespo FA, Di Iorio O, Valverde ADC (2015) Contributions to the knowledge of *Hypercompsa*, new register from Argentina (Blattaria: Corydiidae). *Revista de la Sociedad Entomológica Argentina* 74(3–4): 203–207.
- Cui Y, Evangelista DA, Béthoux O (2018) Prayers for fossil mantis unfulfilled: *Prochaeradodis enigmaticus* Piton, 1940 is a cockroach (Blattodea). *Geodiversitas* 40(15): 355–362. <https://doi.org/10.5252/geodiversitas2018v40a15>
- Djernæs M, Klass KD, Eggleton P (2015) Identifying possible sister groups of Cryptocercidae + Isoptera: A combined molecular and morphological phylogeny of Dictyoptera. *Molecular Phylogenetics and Evolution* 84: 284–303. <https://doi.org/10.1016/j.ympev.2014.08.019>
- Djernæs M, Varadínová ZK, Kotyk M, Eulitz U, Klass K-D (2020) Phylogeny and life history evolution of Blaberoidea (Blattodea). *Arthropod Systematics & Phylogeny* 78(1): 29–67. <https://doi.org/10.26049/ASP78-1-2020-03>
- Dos Reis M, Yang Z (2012) The unbearable uncertainty of Bayesian divergence time estimation. *Journal of Systematics and Evolution* 51(1): 30–43. [bound in 2013] <https://doi.org/10.1111/j.1759-6831.2012.00236.x>
- Dumans ATN, Grimaldi DB, Furtado C, Machado EA, Prosdociimi F (2017) The complete mitochondrial genome of the subsocial cockroach *Nauphoeta cinerea* and phylogenomic analyses of Blattodea mitogenomes suggest reclassification of superfamilies. *Mitochondrial DNA Part B* 2(1): 76–78. <https://doi.org/10.1080/23802359.2017.1285207>
- Edgar RC (2004) MUSCLE: multiple sequence alignment with high accuracy and high throughput. *Nucleic Acids Research* 32(5): 1792–1797. <https://doi.org/10.1093/nar/gkh340>
- Engel MS (2011) Family-group names for termites (Isoptera), redux. *ZooKeys* 148: 171–184. <https://doi.org/10.3897/zookeys.148.1682>
- Estrada-Alvarez JC, Guadarrama CA (2012) Primeros registros de *Homoeogamia mexicana* Burmeister, 1838 (Blattaria: Polyphagidae) para el Estado de México. *Dugesiana* 19(1): 11–12.
- Evangelista DA, Djernæs M, Kohli MK (2017) Fossil calibrations for the cockroach phylogeny (Insecta, Dictyoptera, Blattodea), comments on the use of wings for their identification, and a redescription of the oldest Blaberidae. *Palaeontologia Electronica* 20: 1FC. [23 pp.] <https://doi.org/10.26879/711>
- Evangelista DA, Wipfler B, Béthoux O, Donath A, Fujita M, Kohli MK, Legendre F, Liu S, Machida R, Misof B, Peters RS, Podsiadlowski L, Rust J, Schuette K, Tollenaar W, Ware JL, Wappler T, Zhou X, Meusemann K, Simon S (2019) An integrative phylogenomic approach illuminates the evolutionary history of cockroaches and termites (Blattodea). *Proceedings of the Royal Society B: Biological Sciences* 286: 20182076. <https://doi.org/10.1098/rspb.2018.2076>
- Evangelista D, Simon S, Wilson MM, Kawahara AY, Kohli MK, Ware JL, Wipfler B, Béthoux O, Grandcolas P, Legendre F (2020) Assessing support for Blaberoidea phylogeny suggests optimal locus quality. *Systematic Entomology* 46(1)[bound in 2021]: 157–171. <https://doi.org/10.1111/syen.12454>
- Gao T, Shih C, Labandeira CC, Liu X, Wang Z, Che Y, Yin X, Ren D (2018) Maternal care by Early Cretaceous cockroaches. *Journal of Systematic Palaeontology* 17(5): 379–391. [bound in 2019] <https://doi.org/10.1080/14772019.2018.1426059>
- Gatesy J (2007) A tenth crucial question regarding model use in phylogenetics. *Trends in Ecology and Evolution* 22: 509–510. <https://doi.org/10.1016/j.tree.2007.08.002>
- Gong R, Guo X, Ma J, Song X, Shen Y, Geng F, Price M, Zhang X, Yue B (2018) Complete mitochondrial genome of *Periplaneta brunnea*

- (Blattodea: Blattidae) and phylogenetic analyses within Blattodea. *Journal of Asia-Pacific Entomology* 21(3): 885–895. <https://doi.org/10.1016/j.aspen.2018.05.006>
- Gorokhov AV (2007) New and little known orthopteroid insects (Polyneoptera) from fossil resins: communication 2. *Paleontological Journal* 41: 156–166. <https://doi.org/10.1134/S0031030107020062>
- Guo Y, Béthoux O, Gu JJ, Ren D (2013) Wing venation homologies in Pennsylvanian ‘cockroachoids’ (Insecta) clarified thanks to a remarkable specimen from the Pennsylvanian of Ningxia (China). *Journal of Systematic Palaeontology* 11: 41–46. <https://doi.org/10.1080/14772019.2011.637519>
- Hennig W (1969) *Die Stammesgeschichte der Insekten*. Waldemar Kramer, Frankfurt am Main, 436 pp.
- Hinkelman J (2019) *Spinaeblattina myanmarensis* gen. et sp. nov. and *Blattothecichnus argenteus* ichnogen. et ichnosp. nov. (both Mesoblattinidae) from mid-Cretaceous Myanmar amber. *Cretaceous Research* 99: 229–239. <https://doi.org/10.1016/j.cretres.2019.02.026>
- Hopkins H (2014) A revision of the genus *Arenivaga* (Rehn) (Blattodea, Corydiidae), with descriptions of new species and key to the males of the genus. *ZooKeys* 384: 1–256. <https://doi.org/10.3897/zookeys.384.6197>
- Huelsenbeck JP, Rannala B (2004) Frequentist properties of Bayesian posterior probabilities of phylogenetic trees under simple and complex substitution models. *Systematic Biology* 53(6): 904–913. <https://doi.org/10.1080/10635150490522629>
- Inoue J, Donoghue PCJ, Yang Z (2010) The impact of the representation of fossil calibrations on Bayesian estimation of species divergence times. *Systematic Biology* 59(1): 74–89. <https://doi.org/10.1093/sysbio/syp078>
- Jarzemkowski EA (1981) An early Cretaceous termite from southern England (Isoptera: Hodotermitidae). *Systematic Entomology* 6(1): 91–96. <https://doi.org/10.1111/j.1365-3113.1981.tb00018.x>
- Jeon MG, Park YC (2015) The complete mitogenome of the wood-feeding cockroach *Cryptocercus kyebangensis* (Blattodea: Cryptocercidae) and phylogenetic relations among cockroach families. *Animal Cells and Systems* 19(6): 432–438. <https://doi.org/10.1080/19768354.2015.1105866>
- Kelchner SA, Thomas MA (2007) Model use in phylogenetics: nine key questions. *Trends in Ecology and Evolution* 22: 87–94. <https://doi.org/10.1016/j.tree.2006.10.004>
- Kjer KM, Ware JL, Rust J, Wappler T, Lanfear R, Jermini LS, Zhou X, Aspöck H, Aspöck U, Beutel RG, Blanke A, Donath A, Flouri T, Frandsen PB, Kapli P, Kawahara AY, Letsch H, Mayer C, McKenna DD, Meusemann K, Niehuis O, Peters RS, Wiegmann BM, Yeates DK, von Reumont BM, Stamatakis A, Misof B (2015) Response to Comment on “Phylogenomics resolves the timing and pattern of insect evolution”. *Science* 349: 487. <https://doi.org/10.1126/science.aaa7136>
- Klass KD (2001) Morphological evidence on blattarian phylogeny: “phylogenetic histories and stories” (Insecta, Dictyoptera). *Deutsche Entomologische Zeitschrift* 48: 223–265. <https://doi.org/10.1002/mmnd.4800480203>
- Klass KD, Meier R (2006) A phylogenetic analysis of Dictyoptera (Insecta) based on morphological characters. *Entomologische Abhandlungen* 63: 3–50.
- Kômoto N, Yukuhiro K, Ueda K, Tomita S (2010) Exploring the molecular phylogeny of phasmids with whole mitochondrial genome sequences. *Molecular Phylogenetics and Evolution* 58(1): 43–52. [bound in 2011] <https://doi.org/10.1016/j.ympev.2010.10.013>
- Kômoto N, Yukuhiro K, Tomita S (2012) Novel gene rearrangements in the mitochondrial genome of a webspinner, *Aposthonia japonica* (Insecta: Embioptera). *Genome* 55(3): 222–233. <https://doi.org/10.1139/g2012-007>
- Krishna K, Grimaldi DA, Krishna V, Engel MS (2013) *Treatise on the Isoptera of the World*. *Bulletin of the American Museum of Natural History* 377, 2704 pp. <https://doi.org/10.1206/377.7>
- Kück P, Meid SA, Groß C, Wägele JW, Misof B (2014) AliGROOVE – visualization of heterogeneous sequence divergence within multiple sequence alignments and detection of inflated branch support. *BMC Bioinformatics* 15: 294. <https://doi.org/10.1186/1471-2105-15-294>
- Kumar S, Stecher G, Tamura K (2016) MEGA7: Molecular Evolutionary Genetics Analysis version 7.0 for bigger datasets. *Molecular Biology and Evolution* 33(7): 1870–1874. <https://doi.org/10.1093/molbev/msw054>
- Lartillot N, Philippe H (2004) A Bayesian mixture model for across-site heterogeneities in the amino-acid replacement process. *Molecular Biology and Evolution* 21(6): 1095–1109. <https://doi.org/10.1093/molbev/msh112>
- Lartillot N, Lepage T, Blanquart S (2009) PhyloBayes 3: a Bayesian software package for phylogenetic reconstruction and molecular dating. *Bioinformatics* 25(17): 2286–2288. <https://doi.org/10.1093/bioinformatics/btp368>
- Legendre F, Nel A, Svenson GJ, Robillard T, Pellens R, Grandcolas P (2015) Phylogeny of Dictyoptera: Dating the origin of cockroaches, praying mantises and termites with molecular data and controlled fossil evidence. *PLoS ONE* 10: e0130127. <https://doi.org/10.1371/journal.pone.0130127>
- Letsch HO, Kück P, Stocsits RR, Misof B (2010) The Impact of rRNA Secondary Structure Consideration in Alignment and Tree Reconstruction: Simulated Data and a Case Study on the Phylogeny of Hexapods. *Molecular Biology and Evolution* 27(11): 2507–2521. <https://doi.org/10.1093/molbev/msq140>
- Li XR (2019) Disambiguating the scientific names of cockroaches. *Palaeoentomology* 2: 390–402. <https://doi.org/10.11646/palaeoentomology.2.4.13>
- Li XR, Huang D (2019) A new mid-Cretaceous cockroach of stem Nocticolidae and reestimating the age of Corydioidea (Dictyoptera: Blattodea). *Cretaceous Research* 106: 104202. [bound in 2020] <https://doi.org/10.1016/j.cretres.2019.104202>
- Li XR, Li M, Wang ZQ (2017) Preliminary molecular phylogeny of beetle cockroaches (*Diploptera*) and notes on male and female genitalia (Blattodea: Blaberidae: Diplopterinae). *Zootaxa* 4320(3): 523–534. <https://doi.org/10.11646/zootaxa.4320.3.7>
- Li XR, Zheng YH, Wang CC, Wang ZQ (2018) Old method not old-fashioned: parallelism between wing venation and wing-pad tracheation of cockroaches and a revision of terminology. *Zoomorphology* 137: 519–533. <https://doi.org/10.1007/s00435-018-0419-6>
- Luo A, Qiao H, Zhang Y, Shi W, Ho SYW, Xu W, Zhang A, Zhu C (2010) Performance of criteria for selecting evolutionary models in phylogenetics: a comprehensive study based on simulated datasets. *BMC Evolutionary Biology* 10: 242. <https://doi.org/10.1186/1471-2148-10-242>
- Ma J, Du C, Zhou C, Sheng Y, Fan Z, Yue B, Zhang X (2017) Complete mitochondrial genomes of two blattid cockroaches, *Periplaneta australasiae* and *Neostylopyga rhombifolia*, and phylogenetic relationships within the Blattaria. *PLoS ONE* 12(5): e0177162. <https://doi.org/10.1371/journal.pone.0177162>

- Magallón S, Hilu KW, Quandt D (2013) Land plant evolutionary timeline: Gene effects are secondary to fossil constraints in relaxed clock estimation of age and substitution rates. *American Journal of Botany* 100(3): 556–573. <https://doi.org/10.3732/ajb.1200416>
- Martínez-Delclòs X (1993) Blátidos (Insecta, Blattodea) del Cretácico Inferior de España. Familias Mesoblattinidae, Blattulidae y Poliphagidae. *Boletín Geológico y Minero* 104(5): 516–538.
- McKittrick FA (1964) Evolutionary studies of cockroaches. Cornell University Agricultural Experiment Station Memoir 389: 1–197. http://reader.library.cornell.edu/docviewer/digital?id=chla7251474_8564_009
- McKittrick FA, Mackerras MJ (1965) Phyletic relationships within the Blattidae. *Annals of the Entomological Society of America* 58(2): 224–230. <https://doi.org/10.1093/aesa/58.2.224>
- Misof B, Liu SL, Meusemann K, Peters RS, Donath A, Mayer C, Frandsen PB, Ware J, Flouri T, Beutel RG, Niehuis O, Petersen M, Izquierdo-Carrasco F, Wappler T, Rust J, Aberer AJ, Aspöck U, Aspöck H, Bartel D, Blanke A, Berger S, Böhm A, Buckley TR, Calcott B, Chen JQ, Friedrich F, Fukui M, Fujita M, Greve C, Grobe P, Gu SC, Huang Y, Jermini LS, Kawahara AY, Krogmann L, Kubiak M, Lanfear R, Letsch H, Li YY, Li ZY, Li JG, Lu HR, Machida R, Mashimo Y, Kapli P, McKenna DD, Meng GL, Nakagaki Y, Navarrete-Heredia JL, Ott M, Ou YX, Pass G, Podsiadlowski L, Pohl H, von Reumont BM, Schütte K, Sekiya K, Shimizu S, Slipinski A, Stamatakis A, Song WH, Su X, Szucsich NU, Tan MH, Tan XM, Tang M, Tang JB, Timelthaler G, Tomizuka S, Trautwein M, Tong XL, Uchifune T, Walz MG, Wiegmann BM, Wilbrandt J, Wipfler B, Wong TKF, Wu Q, Wu GX, Xie YL, Yang SZ, Yang Q, Yeates DK, Yoshizawa K, Zhang Q, Zhang R, Zhang WW, Zhang YH, Zhao J, Zhou CR, Zhou LL, Ziesmann T, Zou SJ, Li YR, Xu X, Zhang Y, Yang HM, Wang J, Wang J, Kjer KM, Zhou X (2014) Phylogenomics resolves the timing and pattern of insect evolution. *Science* 346: 763–767. <https://doi.org/10.1126/science.1257570>
- Moran RJ, Morgan CC, O’Connell MJ (2015) A guide to phylogenetic reconstruction using heterogeneous models—a case study from the root of the placental mammal tree. *Computation* 3: 177–196. <https://doi.org/10.3390/computation3020177>
- Nascimento FF, dos Reis M, Yang Z (2017) A biologist’s guide to Bayesian phylogenetic analysis. *Nature Ecology & Evolution* 1: 1446–1454. <https://doi.org/10.1038/s41559-017-0280-x>
- Papadopoulou A, Anastasiou I, Vogler AP (2010) Revisiting the insect mitochondrial molecular clock: the mid-Aegean trench calibration. *Molecular Biology and Evolution* 27(7): 1659–1672. <https://doi.org/10.1093/molbev/msq051>
- Parham JF, Donoghue PCJ, Bell CJ, Calway TJ, Head JJ, Holroyd PA, Inoue JG, Irmis RB, Joyce WG, Ksepka DT, Patané JSL, Smith ND, Tarver JE, van Tuinen M, Yang Z, Angielczyk KD, Greenwood JM, Hipsley CA, Jacobs L, Makovicky PJ, Müller J, Smith KT, Theodor JM, Warnock RCM, Benton MJ (2011) Best practices for justifying fossil calibrations. *Systematic Biology* 61: 346–359. <https://doi.org/10.1093/sysbio/syr107>
- Poe S (2003) Evaluation of the strategy of long-branch subdivision to improve the accuracy of phylogenetic methods. *Systematic Biology* 52(3): 423–428. <https://doi.org/10.1080/10635150390197046>
- Qiu L (2017) Taxonomic revision of the family Corydiidae from China (Blattodea: Corydioidea). M.S. thesis, Southwest University, Chongqing, China.
- Qiu L, Che YL, Wang ZQ (2017) Contribution to the cockroach genus *Ctenoneura* Hanitsch, 1925 (Blattodea: Corydioidea: Corydiidae) with descriptions of seven new species from China. *Zootaxa* 4237: 265–299. <https://doi.org/10.11646/zootaxa.4237.2.3>
- Qiu L, Wang ZQ, Che YL (2019a) New and little known Latindiinae (Blattodea, Corydiidae) from China, with discussion of the Asian genera and species. *ZooKeys* 867: 23–44. <https://doi.org/10.3897/zookeys.867.35991>
- Qiu L, Yang ZB, Wang ZQ, Che YL (2019b) Notes on some corydiid species from China, with the description of a new genus (Blattodea: Corydioidea: Corydiidae). *Annales de la Société entomologique de France (N.S.)* 55(3): 261–273. <https://doi.org/10.1080/00379271.2019.1603081>
- Qiu L, Liu YC, Wang ZQ, Che YL (2020a) The first blattid cockroach (Dictyoptera: Blattodea) in Cretaceous amber and the reconsideration of purported Blattidae. *Cretaceous Research* 109: 104359. <https://doi.org/10.1016/j.cretres.2019.104359>
- Qiu L, Wang ZQ, Che YL (2020b) Discovery of the second Asian *Holocompsa* species from China, and supplemental description of the male of *H. debilis* (Blattodea: Corydiidae: Euthyrrhaphinae). *Annales de la Société entomologique de France (N.S.)* 56(6): 481–487. <https://doi.org/10.1080/00379271.2020.1852889>
- Qiu ZW, Che YL, Zheng YH, Wang ZQ (2017) The cockroaches of *Balta* Tepper from China, with the description of four new species (Blattodea, Ectobiidae, Pseudophyllodromiinae). *ZooKeys* 714: 13–32. <https://doi.org/10.3897/zookeys.714.14041>
- Rambaut A, Drummond AJ, Xie D, Baele G, Suchard MA (2018) Posterior summarisation in Bayesian phylogenetics using Tracer 1.7. *Systematic Biology* 67(5): 901–904. <https://doi.org/10.1093/sysbio/syy032>
- Rehn JWH (1951) Classification of the Blattaria as indicated by their wings (Orthoptera). *Memoirs of the American Entomological Society* 14: 1–134.
- Ronquist F, Teslenko M, Der Mark PV, Ayres DL, Darling A, Höhna S, Larget B, Liu L, Suchard MA, Huelsenbeck JP (2012) MrBayes 3.2: Efficient Bayesian phylogenetic inference and model choice across a large model space. *Systematic Biology* 61(3): 539–542. <https://doi.org/10.1093/sysbio/sys029>
- Roth LM (1967) The evolutionary significance of rotation of the oötheca in the Blattaria. *Psyche* 74: 85–103. <https://doi.org/10.1155/1967/898454>
- Roth LM (1968a) Oöthecae of the Blattaria. *Annals of the Entomological Society of America* 61(1): 83–111. <https://doi.org/10.1093/aesa/61.1.83>
- Roth LM (1968b) Oviposition behavior and water changes in the oöthecae of *Lophoblatta brevis* (Blattaria: Blattellidae: Plectopterinae). *Psyche* 75: 99–106. <https://doi.org/10.1155/1968/46283>
- Roth LM (1970) Evolution and taxonomic significance of reproduction in Blattaria. *Annual Review of Entomology* 15(1): 75–96. <https://doi.org/10.1146/annurev.en.15.010170.000451>
- Roth LM (1971) Additions to the oöthecae, uricose glands, ovarioles, and tergal glands of Blattaria. *Annals of the Entomological Society of America* 64(1): 127–141. <https://doi.org/10.1093/aesa/64.1.127>
- Roth LM (1982) Ovoviviparity in the blattellid cockroach, *Symptloce bimaculata* (Gerstaecker) (Dictyoptera: Blattaria: Blattellidae). *Proceedings of the Entomological Society of Washington* 84(2): 277–280.
- Roth LM (1983) The genus *Chorisia* Princis (Dictyoptera, Blattaria: Blattellinae). *Entomologica Scandinavica* 14: 297–302. <https://doi.org/10.1163/187631283X00290>
- Roth LM (1984) *Stayella*, a new genus of ovoviviparous cockroaches from Africa (Dictyoptera: Blattariae, Blattellidae). *Entomologica Scandinavica* 15: 113–139. <https://doi.org/10.1163/187631284X00109>
- Roth LM (1989) *Sliferia*, a new ovoviviparous cockroach genus (Blattellidae) and the evolution of ovoviviparity in Blattaria (Dictyoptera). *Proceedings of the Entomological Society of Washington* 91(3): 441–451.

- Roth LM (1995) *Pseudoanaplectinia yumotoi*, a new ovoviviparous myrmecophilous cockroach genus and species from Sarawak (Blattaria: Blattellidae; Blattellinae). *Psyche* 102: 79–87. <https://doi.org/10.1155/1995/92482>
- Roth LM (1997) *Pseudobalta*, a new Australian ovoviviparous cockroach genus (Dictyoptera: Blattaria: Blattellidae: Pseudophyllo-dromiinae). *Australian Journal of Entomology* 36: 101–108. <https://doi.org/10.1111/j.1440-6055.1997.tb01440.x>
- Roth LM (2003) Systematics and phylogeny of cockroaches (Dictyoptera: Blattaria). *Oriental Insects* 37: 1–186. <https://doi.org/10.1080/00305316.2003.10417344>
- Sauquet H (2013) A practical guide to molecular dating. *Comptes Rendus Palevol* 12: 355–367. <https://doi.org/10.1016/j.crpv.2013.07.003>
- Sauquet H, Ho SYW, Gandolfo MA, Jordan GJ, Wilf P, Cantrill DJ, Bayly MJ, Bromham L, Brown GK, Carpenter RJ, Lee DM, Murphy DJ, Kale Sniderman JM, Udovicic F (2012) Testing the impact of calibration on molecular divergence times using a fossil-rich group: the case of *Nothofagus* (Fagales). *Systematic Biology* 61(2): 289–313. <https://doi.org/10.1093/sysbio/syr116>
- Smith PE, Evensen NM, York D, Chang M, Jin F, Li J, Cumbaa S, Russell D (1995) Dates and rates in ancient lakes: ^{40}Ar – ^{39}Ar evidence for an Early Cretaceous age for the Jehol Group, northeast China. *Canadian Journal of Earth Sciences* 32: 1426–1431. <https://doi.org/10.1139/e95-115>
- Stocsits RR, Letsch H, Hertel J, Misof B, Stadler PF (2009) Accurate and efficient reconstruction of deep phylogenies from structured RNAs. *Nucleic Acids Research* 37(18): 6184–6193. <https://doi.org/10.1093/nar/gkp600>
- Sullivan J, Swofford DL, Naylor GJP (1999) The effect of taxon sampling on estimating rate heterogeneity parameters of maximum-likelihood models. *Molecular Biology and Evolution* 16(10): 1347–1356. <https://doi.org/10.1093/oxfordjournals.molbev.a026045>
- Swisher CC III, Wang Y, Wang X, Xu X, Wang Y (1999) Cretaceous age for the feathered dinosaurs of Liaoning, China. *Nature* 400(6739): 58–61. <https://doi.org/10.1038/21872>
- Talavera G, Vila R (2011) What is the phylogenetic signal limit from mitogenomes? The reconciliation between mitochondrial and nuclear data in the Insecta class phylogeny. *BMC Evolutionary Biology* 11: 315. <https://doi.org/10.1186/1471-2148-11-315>
- Tian X, Ma G, Cui Y, Dong P, Zhu Y, Gao X (2015) The complete mitochondrial genomes of *Opisthoptalia orientalis* and *Blaptica dubia* (Blattodea: Blaberidae). *Mitochondrial DNA Part A* 28(1): 139–140. [bound in 2017] <https://doi.org/10.3109/19401736.2015.1111360>
- Tong KJ, Duchêne S, Ho SYW, Lo N (2015) Comment on “Phylogenomics resolves the timing and pattern of insect evolution”. *Science* 349(6247): 487-b. <https://doi.org/10.1126/science.aaa5460>
- Trümper S, Schneider JW, Nemyrovskaya T, Korn D, Linnemann U, Ren D, Béthoux O (2020) Age and depositional environment of the Xiaheyan insect fauna, embedded in marine black shales (Early Pennsylvanian, China). *Palaeogeography, Palaeoclimatology, Palaeoecology* 538: 109444. <https://doi.org/10.1016/j.palaeo.2019.109444>
- Vršanský P, Cifuentes-Ruiz P, Vidlička E, Čiampor F, Vega F (2011a) Afro-Asian cockroach from Chiapas amber and the lost Tertiary American entomofauna. *Geologica Carpathica* 62(5): 463–475. <https://doi.org/10.2478/v10096-011-0033-8>
- Vršanský P, Vidlička E, Čiampor Jr F, Marsh F (2011b) Derived, still living cockroach genus *Cariblattoides* (Blattida: Blattellidae) from the Eocene sediments of Green River in Colorado, USA. *Insect Science* 19(2): 143–152. [bound in 2012] <https://doi.org/10.1111/j.1744-7917.2010.01390.x>
- Vršanský P, Oružinský R, Barna P, Vidlička E, Labandeira CC (2014) Native *Ectobius* (Blattaria: Ectobiidae) from the Early Eocene Green River Formation of Colorado and its reintroduction to North America 49 million years later. *Annals of the Entomological Society of America* 107: 28–36. <https://doi.org/10.1603/AN13042>
- Wang T, Yu P, Ma Y, Cheng H, Zhang J (2014) The complete mitochondrial genome of *L. albella* (Mantodea: Iridopterygidae). *Mitochondrial DNA Part A* 27: 465–466. [bound in 2016] <https://doi.org/10.3109/19401736.2014.900669>
- Wang ZQ, Shi Y, Qiu ZW, Che YL, Lo N (2017) Reconstructing the phylogeny of Blattodea: robust support for interfamilial relationships and major clades. *Scientific Reports* 7: 3903. <https://doi.org/10.1038/s41598-017-04243-1>
- Wiens JJ (2006) Missing data and the design of phylogenetic analyses. *Journal of Biomedical Informatics* 39(1): 34–42. <https://doi.org/10.1016/j.jbi.2005.04.001>
- Wiens JJ, Moen DS (2008) Missing data and the accuracy of Bayesian phylogenetics. *Journal of Systematics and Evolution* 46(3): 307–314.
- Wipfler B, Letsch H, Frandsen PB, Kapli P, Mayer C, Bartel D, Buckley TR, Donath A, Ederly-Rooks JS, Fujita M, Liu SL, Machida R, Mashimo Y, Misof B, Niehuis O, Peters RS, Petersen M, Podsiadlowski L, Schütte K, Shimizu S, Uchifune T, Wilbrandt J, Yan E, Zhou X, Simon S (2019) Evolutionary history of Polyneoptera and its implications for our understanding of early winged insects. *Proceedings of the National Academy of Sciences* 116: 3024–3029. <https://doi.org/10.1073/pnas.1817794116>
- Wolfe JM, Daley AC, Legg DA, Edgecombe GD (2016) Fossil calibrations for the arthropod Tree of Life. *Earth-Science Reviews* 160: 43–110. <https://doi.org/10.1016/j.earscirev.2016.06.008>
- Xia X (2018) DAMBE7: New and improved tools for data analysis in molecular biology and evolution. *Molecular Biology and Evolution* 35: 1550–1552. <https://doi.org/10.1093/molbev/msy073>
- Yamauchi MM, Miya MU, Nishida M (2004) Use of a PCR-based approach for sequencing whole mitochondrial genomes of insects: two examples (cockroach and dragonfly) based on the method developed for decapod crustaceans. *Insect Molecular Biology* 13(4): 435–442. <https://doi.org/10.1111/j.0962-1075.2004.00505.x>
- Yang W, Li S, Jiang B (2007) New evidence for Cretaceous age of the feathered dinosaurs of Liaoning: zircon U-Pb SHRIMP dating of the Yixian Formation in Sihetun, northeast China. *Cretaceous Research* 28(2): 177–182. <https://doi.org/10.1016/j.cretres.2006.05.011>
- Yang Z (2007) PAML 4: Phylogenetic Analysis by Maximum Likelihood. *Molecular Biology and Evolution* 24(8): 1586–1591. <https://doi.org/10.1093/molbev/msm088>
- Yang Z (2014) *Molecular Evolution: A Statistical Approach*. Oxford University Press, Oxford, 492 pp.
- Ye F, Lan XE, Zhu WB, You P (2016) Mitochondrial genomes of praying mantises (Dictyoptera, Mantodea): rearrangement, duplication, and reassignment of tRNA genes. *Scientific Reports* 6: 25634. <https://doi.org/10.1038/srep25634>
- Zhang YY, Xuan WJ, Zhao JL, Zhu CD, Jiang GF (2009) The complete mitochondrial genome of the cockroach *Eupolyphaga sinensis* (Blattaria: Polyphagidae) and the phylogenetic relationships within the Dictyoptera. *Molecular Biology Reports* 37(7): 3509–3516. [bound in 2010] <https://doi.org/10.1007/s11033-009-9944-1>

Zhang ZJ, Schneider JW, Hong YC (2012) The most ancient roach (Blattodea): a new genus and species from the earliest Late Carboniferous (Namurian) of China, with a discussion of the phylomorphogeny of early blattids. *Journal of Systematic Palaeontology* 11: 27–40. [bound in 2013] <https://doi.org/10.1080/14772019.2011.634443>

Zhang L-P, Yu D-N, Storey KB, Cheng H-Y, Zhang J-Y (2018) Higher tRNA gene duplication in mitogenomes of praying mantises (Diptera, Mantodea) and the phylogeny within Mantodea. *International Journal of Biological Macromolecules* 111: 787–795. <https://doi.org/10.1016/j.ijbiomac.2018.01.016>

Zhang D, Gao F, Jakovlić I, Zou H, Zhang J, Li WX, Wang GT (2020) PhyloSuite: An integrated and scalable desktop platform for streamlined molecular sequence data management and evolutionary phylogenetics studies. *Molecular Ecology Resources* 20(1): 348–355. <https://doi.org/10.1111/1755-0998.13096>

Supplementary material 1

Initial pool of 169 mitochondrial genomes

Authors: Xin-Ran Li

Data type: document/list (pdf. file)

Explanation note: Initial pool of 169 mitochondrial genomes found in GenBank.

Copyright notice: This dataset is made available under the Open Database License (<http://opendatacommons.org/licenses/odbl/1.0>). The Open Database License (ODbL) is a license agreement intended to allow users to freely share, modify, and use this Dataset while maintaining this same freedom for others, provided that the original source and author(s) are credited.

Link: <https://doi.org/10.3897/dez.1.68373.suppl1>

Supplementary material 2

Table S1

Authors: Xin-Ran Li

Data type: Table (pdf. file)

Explanation note: Metadata of the 95 selected mitochondrial genomes.

Copyright notice: This dataset is made available under the Open Database License (<http://opendatacommons.org/licenses/odbl/1.0>). The Open Database License (ODbL) is a license agreement intended to allow users to freely share, modify, and use this Dataset while maintaining this same freedom for others, provided that the original source and author(s) are credited.

Link: <https://doi.org/10.3897/dez.2.68373.suppl2>

Supplementary material 3

Table S2

Authors: Xin-Ran Li

Data type: Table (pdf. file)

Explanation note: Sequence correction record.

Copyright notice: This dataset is made available under the Open Database License (<http://opendatacommons.org/licenses/odbl/1.0>). The Open Database License (ODbL) is a license agreement intended to allow users to freely share, modify, and use this Dataset while maintaining this same freedom for others, provided that the original source and author(s) are credited.

Link: <https://doi.org/10.3897/dez.3.68373.suppl3>

Supplementary material 4

Figure S1

Authors: Xin-Ran Li

Data type: statistic plot (jpeg. image)

Explanation note: Pairwise similarity scores calculated by ALIGROOVE.

Copyright notice: This dataset is made available under the Open Database License (<http://opendatacommons.org/licenses/odbl/1.0>). The Open Database License (ODbL) is a license agreement intended to allow users to freely share, modify, and use this Dataset while maintaining this same freedom for others, provided that the original source and author(s) are credited.

Link: <https://doi.org/10.3897/dez.4.68373.suppl4>

Supplementary material 5

Figure S2

Authors: Xin-Ran Li

Data type: statistic plot (tiff. image)

Explanation note: Substitution saturation plots per codon position per gene.

Copyright notice: This dataset is made available under the Open Database License (<http://opendatacommons.org/licenses/odbl/1.0>). The Open Database License (ODbL) is a license agreement intended to allow users to freely share, modify, and use this Dataset while maintaining this same freedom for others, provided that the original source and author(s) are credited.

Link: <https://doi.org/10.3897/dez.5.68373.suppl5>

Supplementary material 6

Figure S3

Authors: Xin-Ran Li

Data type: phylogram (tiff. image)

Explanation note: Bayesian phylogeny of 13 protein-coding genes of 95 species, excluding the third base of codon.

Copyright notice: This dataset is made available under the Open Database License (<http://opendatacommons.org/licenses/odbl/1.0>). The Open Database License (ODbL) is a license agreement intended to allow users to freely share, modify, and use this Dataset while maintaining this same freedom for others, provided that the original source and author(s) are credited.

Link: <https://doi.org/10.3897/dez.6.68373.suppl6>

Supplementary material 7

Figure S4

Authors: Xin-Ran Li

Data type: phylogram (tiff. image)

Explanation note: Bayesian phylogeny of 10 protein-coding genes of 95 species, excluding the third base of codon.

Copyright notice: This dataset is made available under the Open Database License (<http://opendatacommons.org/licenses/odbl/1.0>). The Open Database License (ODbL) is a license agreement intended to allow users to freely share, modify, and use this Dataset while maintaining this same freedom for others, provided that the original source and author(s) are credited.

Link: <https://doi.org/10.3897/dez.7.68373.suppl7>

Supplementary material 8

Figure S5

Authors: Xin-Ran Li

Data type: phylogram (tiff. image)

Explanation note: Bayesian phylogeny of 10 protein-coding genes of 87 species (Good-species analysis), excluding the third base of codon.

Copyright notice: This dataset is made available under the Open Database License (<http://opendatacommons.org/licenses/odbl/1.0>). The Open Database License (ODbL) is a license agreement intended to allow users to freely share, modify, and use this Dataset while maintaining this same freedom for others, provided that the original source and author(s) are credited.

Link: <https://doi.org/10.3897/dez.8.68373.suppl8>

Supplementary material 9

Figure S6

Authors: Xin-Ran Li

Data type: phylogram (tiff. image)

Explanation note: Bayesian phylogeny of 10 protein-coding genes of 92 species (Short-species analysis), excluding the third base of codon.

Copyright notice: This dataset is made available under the Open Database License (<http://opendatacommons.org/licenses/odbl/1.0>). The Open Database License (ODbL) is a license agreement intended to allow users to freely share, modify, and use this Dataset while maintaining this same freedom for others, provided that the original source and author(s) are credited.

Link: <https://doi.org/10.3897/dez.9.68373.suppl9>

Supplementary material 10

Figure S7

Authors: Xin-Ran Li

Data type: phylogram (tiff. image)

Explanation note: Bayesian phylogeny of 10 protein-coding genes of 85 species (Safe-species analysis), excluding the third base of codon.

Copyright notice: This dataset is made available under the Open Database License (<http://opendatacommons.org/licenses/odbl/1.0>). The Open Database License (ODbL) is a license agreement intended to allow users to freely share, modify, and use this Dataset while maintaining this same freedom for others, provided that the original source and author(s) are credited.

Link: <https://doi.org/10.3897/dez.10.68373.suppl10>

Supplementary material 11

Figure S8

Authors: Xin-Ran Li

Data type: time tree (tiff. image)

Explanation note: Time tree estimated by MCMCTREE with three fossil calibrations (incl. *Qilianiblatta namurensis*).

Copyright notice: This dataset is made available under the Open Database License (<http://opendatacommons.org/licenses/odbl/1.0>). The Open Database License (ODbL) is a license agreement intended to allow users to freely share, modify, and use this Dataset while maintaining this same freedom for others, provided that the original source and author(s) are credited.

Link: <https://doi.org/10.3897/dez.11.68373.suppl11>

Supplementary material 12

Figure S9

Authors: Xin-Ran Li

Data type: time tree (tiff. image)

Explanation note: Time tree estimated by MCMCTREE with two fossil calibrations (excl. *Qilianiblatta namurensis*).

Copyright notice: This dataset is made available under the Open Database License (<http://opendatacommons.org/licenses/odbl/1.0>). The Open Database License (ODbL) is a license agreement intended to allow users to freely share, modify, and use this Dataset while maintaining this same freedom for others, provided that the original source and author(s) are credited.

Link: <https://doi.org/10.3897/dez.12.68373.suppl12>

Supplementary material 13

Figure S10

Authors: Xin-Ran Li

Data type: time tree (tiff. image)

Explanation note: Time tree estimated by MCMCTREE with only one fossil calibration (*Valditermes breanae*).

Copyright notice: This dataset is made available under the Open Database License (<http://opendatacommons.org/licenses/odbl/1.0>). The Open Database License (ODbL) is a license agreement intended to allow users to freely share, modify, and use this Dataset while maintaining this same freedom for others, provided that the original source and author(s) are credited.

Link: <https://doi.org/10.3897/dez.13.68373.suppl13>

Character analysis and descriptions of Eocene sphodrine fossils (Coleoptera, Carabidae) using light microscopy, micro-CT scanning, and 3D imaging

Joachim Schmidt¹, Stephan Scholz¹, Kipling Will²

¹ University of Rostock, Institute of Biosciences, General and Systematic Zoology, Universitätsplatz 2, 18055 Rostock, German

² Essig Museum of Entomology, 1101 Valley Life Sciences Building, #4780 University of California, Berkeley, CA 94720-4780, USA

<http://zoobank.org/02E8488B-DDA7-464C-ABC2-39424200939E>

Corresponding author: Joachim Schmidt (schmidt@agonum.de)

Academic editor: Sonja Wedmann ♦ Received 29 December 2021 ♦ Accepted 2 February 2022 ♦ Published 9 February 2022

Abstract

Of the 12 specimens of *Calathus*-like sphodrine beetles presently known from Baltic and Rovno amber deposits, 11 specimens were investigated using light microscopy, micro-CT scanning, and 3D imaging techniques. For the first time, many significant diagnostic characters of the external morphology and male and female genitalia of Eocene Sphodrini were studied in detail. Based on these data, three fossil species are diagnosed and placed in a natural group characterized by a derived pattern in elytral chaetotaxy and microsculpture and therefore the genus *Quasicalathus* Schmidt & Will, gen. nov. is described to comprise these species. Due to the presence of a styloid right paramere, *Quasicalathus* gen. nov. is considered a member of the sphodrine “P clade” of Ruiz et al. (2009). However, given the absence of synapomorphies of any species group of the P clade, the systematic position of *Quasicalathus* gen. nov. within this clade remains unresolved. The Baltic amber species *Calathus elpis* Ortuño & Arillo, 2009 is redescribed based on additional, fossil, non-holotype material and transferred to *Quasicalathus* gen. nov. Identification of the additional *C. elpis* fossil material remains slightly uncertain due to the non-availability of the holotype for direct comparison coupled with doubts regarding the accuracy of certain character states presented in its original description. Two species are newly described: *Quasicalathus agonicollis* Schmidt & Will, sp. nov., from Baltic amber, and *Q. conservans* Schmidt & Will, sp. nov., from Rovno amber.

Key Words

Baltic amber, micro-computed tomography, paleoentomology, Rovno amber, systematics, taxonomy

Introduction

Beetles of the tribe Sphodrini Laporte, 1834 are known from Eocene fossil deposits only as species in the genus *Calathus* Bonelli, 1810 of the subtribe Calathina Laporte, 1834. Occurrence of *Calathus* fossils in Eocene Baltic amber (50–35 Ma; Standke 2008) was first noted by Handlirsch (1908), then Klebs (1910), and later listed in several amber catalogues (e.g., Bachofen-Echt 1949, Larsson 1978, Spahr 1981). Ortuño and Arillo (2009) described *Calathus elpis* from

Baltic amber, which stood as the only sphodrine species from the Paleogene.

The subtribe Calathina of the tribe Sphodrini is a moderately diverse carabid beetle group comprising 173 species distributed in the Holarctic region. The bulk of the species (152) occurs in the Palearctic, 21 species in the Nearctic, and additionally at least 31 endemic species are known to have an extralimital distribution in the Ethiopian Highlands (Bousquet 2012, Hovorka 2017a, Schmidt 2018). The majority of Calathina species are currently placed in the genus *Calathus* Bonelli, 1810. However, a molecular

analysis by Ruiz et al. (2010) showed that *Calathus* and Calathina are paraphyletic, but Calathina in the sense of Hovorka (2017a) is now monophyletic given that the North American *Calathus* (*Certocalathus*) *advena* (LeConte, 1846) was transferred from the subtribe Dolichina Brullé, 1834 to Calathina (Schmidt and Will 2020).

The definition of *Calathus* or Calathina by morphology alone was shown to be challenging because no morphological, autapomorphic character state is known to define these taxa (Schmidt and Will 2020). As a consequence, the monophyly of the subtribe Calathina is well supported by molecular data but can only be defined morphologically by a combination of plesiomorphic characters: i) antennae pubescent from fourth antennomere; ii) elytra with at least one or more discal seta on third interval; iii) dorsal surface of tarsi without pubescence or wrinkles; iv) tarsal claws pectinate; v) one of the aedeagal parameres styloid; vi) presence of a well-developed gonocoxal sensory pit (Lindroth 1956, Ball and Nègre 1972, Sciaky and Facchini 1997, Sciaky and Wrase 1998).

The lack of ostensible morphological synapomorphies creates a problem for the systematic treatment of Calathina fossils and is a significant, and often underappreciated issue for the use of fossils in time calibration of phylogenetic analyses (Ruiz et al. 2008, 2012, Ober and Heider 2010). Given this, previously published works covering representatives of the genus *Calathus* in Paleogene fossil deposits need careful reinvestigation.

Calathus elpis was placed in the tribe Sphodrini due to presence of pectinate claws in addition to a combination of morphological features characteristic for Platynini-like Harpalinae beetles (Ortuño and Arillo 2009). The authors did not further discuss their decision of placing the fossil into the subtribe Calathina or genus *Calathus*. The authors suggest that “*C. elpis* could be an ancestor of the ‘*C. mollis* group’ due to similarities in body size and overall shape (Ortuño and Arillo 2009: 60). However, as shown by Schmidt and Will (2020) these features are not sufficient for placement of the fossil into the genus *Calathus*, the subgenus *Neocalathus* Ball & Nègre, 1972 [including *C. mollis* (Marsham)], or even as evidence for a placement relative to the subtribes of Sphodrini. As a consequence, given the current state of knowledge, *C. elpis* is best treated as a member of Sphodrini with uncertain position within that tribe.

The limited availability of many morphological features for analysis is a serious problem for the study of fossils. In particular, this applies to features hidden in the internal parts of the body. Genitalia play a critical role for the systematic placement of species and lineages in many groups of ground beetles, e.g., character states v) and vi) mentioned above for Calathina. In addition, amber fossils are often obscured by a milky coating and refracting flow lines that prevent standard, visual investigation of characters. For example, preservation conditions unfavorable for light microscopic study are

present in the holotype specimen of *Calathus elpis* (see Ortuño and Arillo 2009: 57, fig. 1). Micro-CT scanning techniques offer a possible solution for these problems if amber and embedded fossils (or their imprints) show sufficient density contrast (Schmidt et al. 2016, 2019, Schmidt and Michalik 2017).

As discussed above, morphological evidence for relationships among clades of sphodrine is problematic but given that such characters are all that is available for fossil taxa it is necessary to critically assess all possible features even if the result can only be considered a working hypothesis. The present study is therefore intended as a first attempt to deal with these problems while comprehensively reviewing the fossil evidence discernible in Paleogene Sphodrini. This study includes a total of 11 inclusions of *Calathus*-like beetles, each preserved in different pieces of Baltic and Rovno ambers, using both light microscopy and micro-CT scanning techniques. All the fossilized specimens studied share character states in the original description of *C. elpis* by Ortuño and Arillo (2009) and, based on a much more comprehensive set of morphological features developed during this investigation, including those from male and female genitalia, the systematic position of *C. elpis* is reviewed. The morphological variability of all the Eocene sphodrine species is reviewed, and two additional species are described.

While in most regards the study is comprehensive and based on first-hand observations, our study is not definitive in some points because important issues related to species-specific taxonomy and morphology cannot be resolved at this juncture. The primary limiting factor was the lack of access to the holotype specimen of *C. elpis*, for reasons we were unable to ascertain (see section Material and Methods). Therefore, this study also stands to point out the consequences when nomenclaturally relevant material is not made available by scientific institutions or private collectors for reinvestigation by subsequent researchers in an appropriate manner.

Materials and methods

Investigated material

Type material: The holotype of *Calathus elpis* Ortuño & Arillo, 2009 could not be studied. Based on the original description, the type with collection number MCNA-13638 should be deposited in the Álava Museum of Natural Sciences (Vitoria, Spain) (Ortuño and Arillo 2009: 56). Between 2016 and 2020 email messages sent to the museum address found online at various sources (e.g., <https://www.gbif.org/publisher/4c91866b-3c2e-4568-aca0-3ab0a1c1a45e>) and emails sent to the authors of the fossil *Calathus* species remained unanswered. Multiple attempts to make contact by telephone using the number

Table 1. Micro-CT scan settings.

	<i>Quascalathus elpis</i>						<i>Q. agonicollis</i>			<i>Q. conservans</i>			
	Groehn 4879	Groehn 7814	Groehn 7889	Abdomen	Groehn 7962	CCHH 952	OSAC 265	MAIG 76	GZG 16185	Holotype SDEI 2528	GZG 16188	Abdomen	Holotype SDEI 2529
Voltage [V]	40	40	40	40	40	30	50	40	40	50	40	40	50
Power [W]	8	8	8	8	8	5	8	8	8	8	8	8	8
Object lens	4	4	4	4	0.4	0.4	4	0.4	4	4	4	20	4
Lens filter	none	none	none	none	none	LE 1	none	none	none	LE 4	none	none	LE 4
Cam binning	2	2	2	2	2	2	2	2	2	2	2	2	2
Distance to source [mm]	122	100	80	40	40	27	96	37	106	40	110	40	96
Distance to detector [mm]	36	40	50	80	300	177	37	260	21	30	70	9	45
Vertical stitch	2	2	3	none	none	none	2	none	2	3	2	none	2
Voxel size [µm]	5.2	4.77	4.14	2.24	7.84	8.73	4.87	8.3	5.63	3.84	4.15	1.09	4.58
Exposure time [sec]	variable 15–22.5	20	10	18	20	30	20	10	15	10	12	25	24
Number of images/ segment	2201 (360°)	2201 (360°)	2001 (360°)	2301 (360°)	2001 (360°)	2001 (360°)	2001 (360°)	1011 (198°)	2001 (360°)	1321 (188°)	1601 (360°)	2101 (360°)	2001 (360°)

listed at the same internet sources failed to connect with personnel at the museum.

Additional material: Ten *Calathus*-like sphodrine specimens preserved in pieces of Baltic amber and one specimen preserved in Rovno amber were studied. For details of the collection data and the respective preservation state of the fossils see species diagnoses and Acknowledgements below.

Investigation techniques

The fossil specimens were studied and imaged via light microscopy and micro-computed tomography (micro-CT) using the Xradia 410 Versa-X-ray microscope (Zeiss, Pleasanton USA). These methods were described in detail in our previous papers (Schmidt et al. 2019, 2021). Micro-CT scan settings used for 3D imaging of the specimens are shown in Table 1. Volume rendering of image stacks was performed by using Amira 6.1 software (FEI Visualization Science Group, Burlington, USA) using the “Volren”, “Volume Rendering” and “Segmentation” functions.

Measurements and proportions

The measurement software of Amira was used and applied to the X-ray scanning results of the fossils (Table 2). The length of the head was measured from anterior margin of clypeus to a point on the midline at the level of the posterior margin of the compound eye. The width of the head was measured in two ways: first, across the widest portion including the compound eyes [‘head width including eyes’ = HW(+)] and second, across the shortest distance between the eyes [‘head width between eyes’ = HW(-)]. The length of the eye and the length of the third antennomere were measured between their most distant points (for the eye in lateral aspect). Length of the pronotum was measured from apical to basal mar-

gin along the midline. The width of the pronotum and the width of each elytron were measured at their widest points (in dorsal aspect). The width of the pronotal apical margin was measured between the tips of the front angles. The width of the pronotal base was measured between the tips of the hind angles at the level of the laterobasal seta. The elytral humeral width was measured between the tips of the humeral angles. The length of each elytron was measured from the apex of scutellum to the apex of the respective elytron. The length of the metepisternum was measured along the lateral margin, its width along the anterior margin. The length of the femur, the apical gonocoxites and the aedeagal median lobe were measured along their greatest lengths. Measurements are not presented from body parts that were deformed due to gas formation (Fig. 61), and those, that yield insufficient contrast during micro-CT scan.

Body length is given as standardized body length (SBL), which equals the sum of the lengths of the head, pronotum, and the longer elytron.

Ratios were presented as follows:

- A3L/HL** length of third antennomere to length of head;
- EyL/ HW(-)** length of eye to head width between eyes;
- PW/HW(+)** pronotal width to head width including eyes;
- PW/PL** width to length of pronotum;
- PW/PWb** width of pronotum to width of pronotal base;
- PWb/PWa** width of pronotal base to width of pronotal apical margin;
- EW/PW** width of elytra to width of pronotum;
- EL/EW** length of the longer elytron to width of elytra;
- EpL/EpW** length to width of the metepisternum;
- EL/FL** length of the longer elytron to length of the longer femur;
- EL/AedL** length of the longer elytron to length of the aedeagal median lobe.

Table 2. Measurements [μm].

	<i>Quasicalathus elpis</i>					<i>Q. agonicolis</i>		<i>Q. conservans</i>			
	Groehn 4879	Groehn 7814	Groehn 7889	Groehn 7962	CCHH 952	OSAC 265	MAIG 76	GZG 16185	Holotype SDEI 2528	GZG 16188	Holotype SDEI 2529
Head length	933	898	950	n.a.	960	930	1038	1057	730	842	899
Head width including eyes	1440	1407	1427	1441	1380	1427	1524	1584	1258	1260	1392
Head width between eyes	885	822	801	827	848	813	875	888	750	779	779
Eye length (left)	577	587	582	652	560	608	622	676	465	503	560
Eye length (right)	n.a.	573	552	627	550	609	620	677	474	475	570
Antennomere 3 length (left)	406	359	382	404	411	396	429	n.a.	325	367	396
Antennomere 3 length (right)	416	366	n.a.	403	398	n.a.	429	446	n.a.	372	n.a.
Pronotal length	1732	1662	1584	1724	1637	1690	1590	1883	1450	1459	1537
Pronotal width	2238	2090	2053	2183	2110	2120	2111	2510	1824	1837	1952
Pronotal apical width	1328	1223	1283	1299	1275	1282	1377	1473	n.a.	1170	1213
Pronotal basal width	2046	1969	1864	2046	1872	1931	2051	2238	1559	1633	1770
Pronotal basal angle	115°	115°	110°	110°	115°	110°	110°	95°	115°	125°	115°
Elytral humeral width	2101	1988	1992	1926	1962	1998	n.a.	2254	1881	1852	1958
Elytral length (left)	5705	4953	5107	5264	5425	5151	4870	5868	4561	4575	4833
Elytral length (right)	5693	4977	5101	5284	5419	5149	4837	5889	4517	4568	4841
Elytral width (left)	1779	1633	1640	1777	1732	1721	n.a.	1995	1483	1465	1610
Elytral width (right)	1745	1569	1690	1706	1731	1682	1730	1857	1438	1531	1600
Metepisternum length (left)	1152	1060	1014	1110	n.a.	1111	n.a.	n.a.	937	971	1060
Metepisternum width (left)	724	689	637	699	n.a.	723	n.a.	n.a.	671	598	742
Metepisternum length (right)	1116	1035	1016	n.a.	n.a.	1162	1104	n.a.	917	1016	1025
Metepisternum width (right)	717	689	652	n.a.	n.a.	725	750	n.a.	631	639	718
Metafemoral length (left)	2163	1912	n.a.	2069	2004	2034	2042	2436	1886	1814	1874
Metafemoral length (right)	2158	1890	n.a.	2058	2093	2068	2069	n.a.	1865	1772	1880
Apical gonocoxite (left)	n.a.	n.a.	178	n.a.	n.a.	n.a.	n.a.	n.a.	n.a.	150	n.a.
Apical gonocoxite (right)	n.a.	n.a.	179	n.a.	n.a.	n.a.	n.a.	n.a.	n.a.	154	n.a.
Aedeagus length	n.a.	1230	n.a.	n.a.	n.a.	n.a.	n.a.	n.a.	1120	n.a.	1331

Description of male genitalia

Herein we use the orientation terms (left and right lateral, dorsal, ventral) for male genitalia that are homologous across Coleoptera and not with respect to the orientation found in Carabidae that is the result of torsion when genitalia are retracted within the apex of the abdomen.

Results

Taxonomic chapter

Genus *Quasicalathus* Schmidt & Will, gen. nov.

<http://zoobank.org/389A05CE-C2C1-4C31-9E8D-F0F9C1CBC1FD>

Type species. *Quasicalathus conservans* Schmidt & Will, sp. nov., fossil species from the Eocene Rovno amber, herein designated.

Species included. Three fossil species from Eocene amber deposits of Central Europe:

Quasicalathus agonicolis Schmidt & Will, sp. nov. (Baltic amber).

Quasicalathus conservans Schmidt & Will, sp. nov. (Rovno amber).

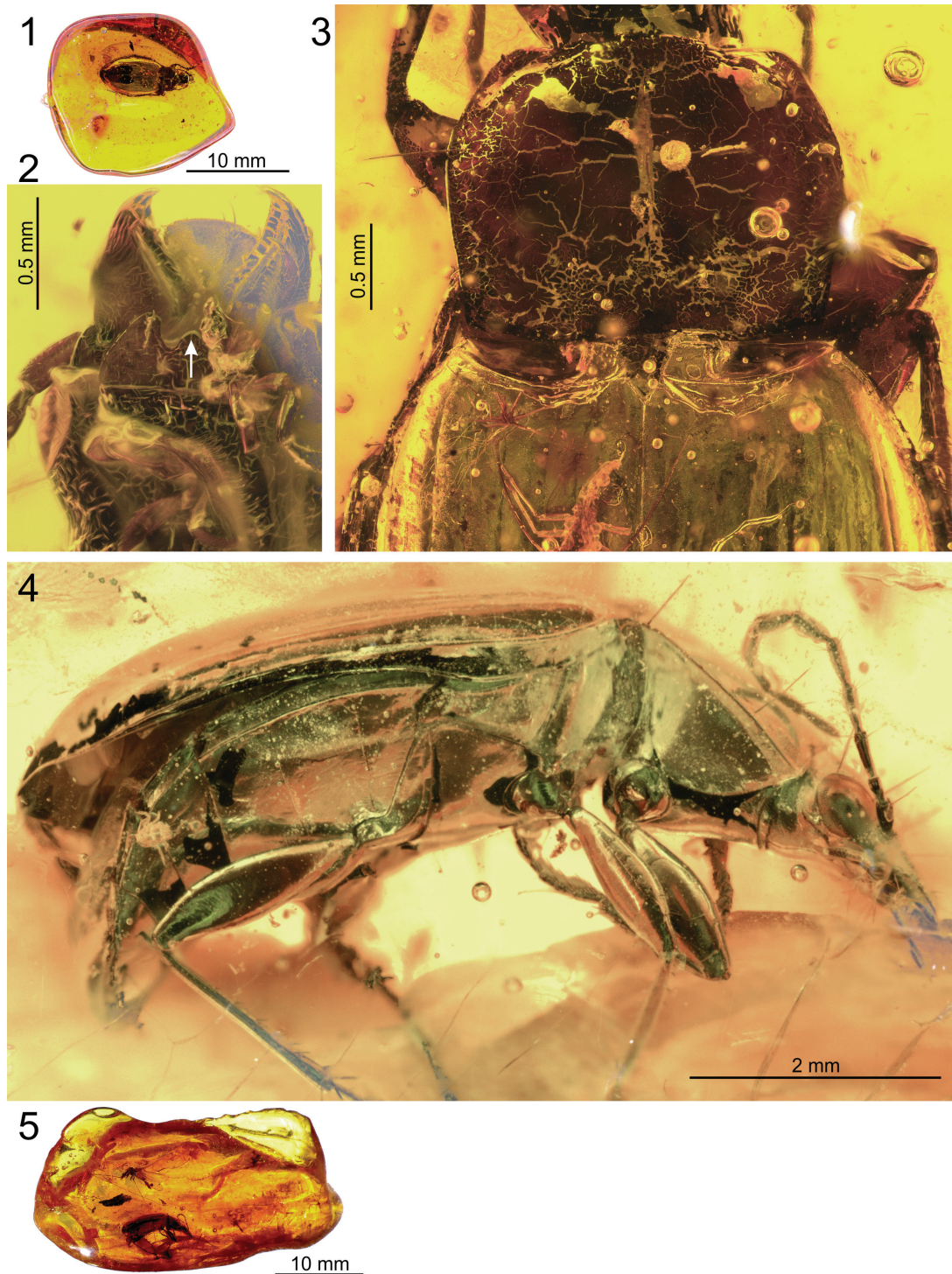
Quasicalathus elpis (Ortuño & Arillo, 2009), new combination (Baltic amber).

Diagnostic characters. Taxon with characteristics of *Calathina* and *Calathus*, respectively, as defined by Lindroth (1956) and Ball and Negre (1972). The combination of the following character states defines the group:

Head: normal for *Calathina*, not thickened (Figs 24, 41, 81); mandibles normal for *Calathina*, not broadened, not elongated (Figs 2, 52); eye size averaged for *Calathina*, normally protruded (Figs 24, 41); antennae pubescent from fourth antennomere (Fig. 20); mentum tooth simple or slightly truncated at tip, with two fine setae near its base (Figs 52, 82); submentum with two setae each side in normal position, with the internal setae robust and the external setae markedly short and thin (Figs 31, 52, 84).

Prothorax: pronotal shape subquadrate (“calathoid” form; Figs 3, 14, 34, 42, 50, 58–60, 63, 64, 73, 78), slightly or moderately constricted toward base, with lateral margin straight or slightly concave before base, and with basolateral angles slightly or moderately obtuse (Figs 9, 14, 25, 42, 50, 63, 64, 74, 78); basolateral angles not protruded posteriorly; basal margin beaded laterally (level of basolateral angles); basolateral seta situated at margin (Figs 9, 14, 20, 25, 42, 50, 66, 74); pronotal disc with sculpticells of microsculpture transverse, very narrow (magnification 80 \times). Prosternum impunctate, smooth, prosternal process with or without apical bead (Figs 37, 38, 51, 75, 85).

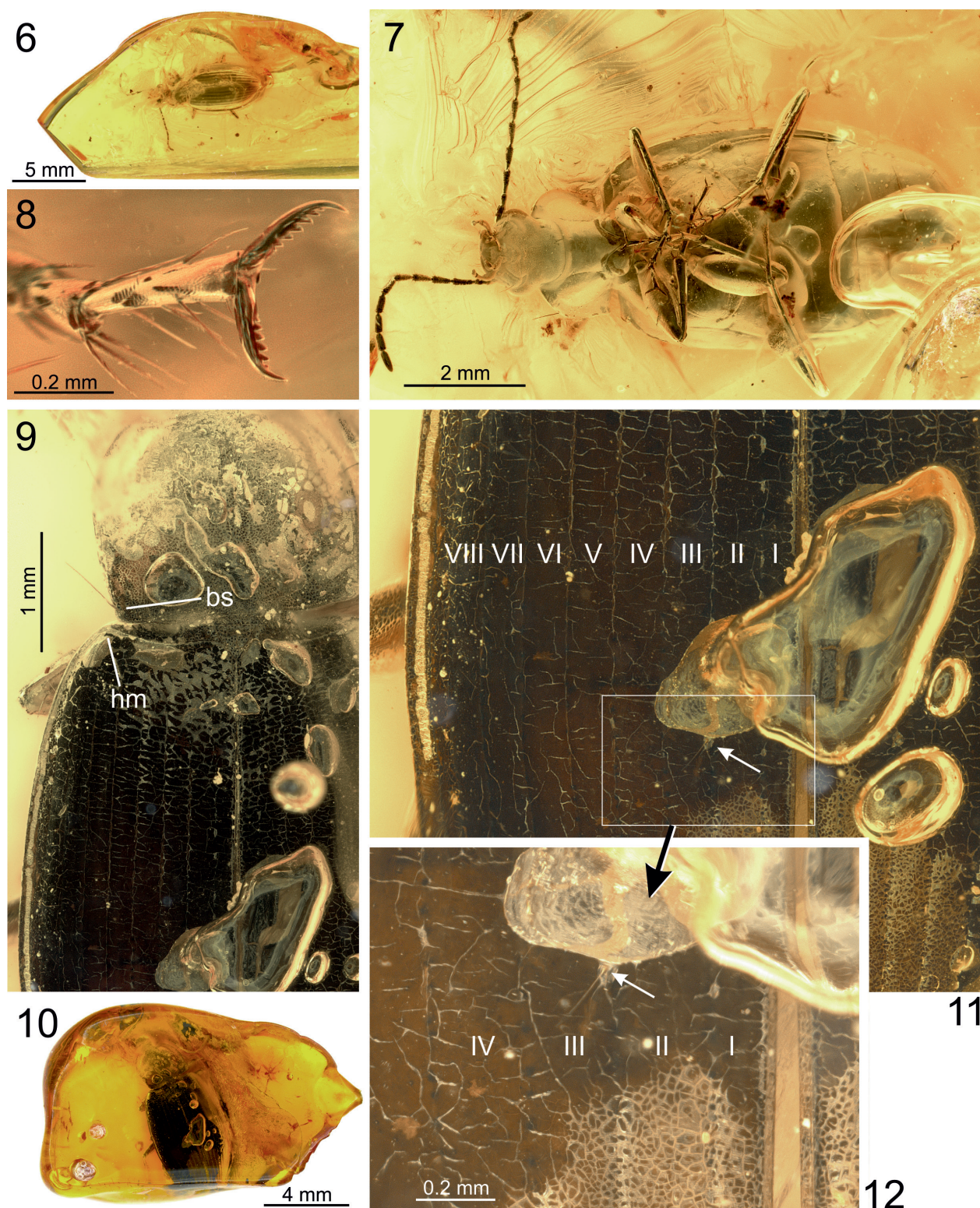
Pterothorax: elytra slender, ovate, glabrous, humeral tooth absent; basal bead moderately or markedly concave with humeral angle +/- markedly protruded anteriorly (Figs 9, 14, 25, 34, 47, 58–61, 66, 74, 78); epipleuron without plica (Fig. 53); striae slightly to moderately deeply engraved, with punctures evident (Figs 25, 27, 58); intervals flat to moderately convex; parascutellar seta present (Figs 14, 66, 74); third interval with a single rather short, thin discal seta situated near the end of the apical elytral 2/3, adjoining second stria (Figs 11, 12, 16, 27, 29);



Figures 1–5. *Quascalathus elpis* (Ortuño and Arillo 2009), light microscopic images of specimens “Groehn 4879” (1–3.) and “Groehn 7814” (4, 5.). 1, 5. General view of the amber pieces; 2. Ventral side of head (the white arrow points to the mentum tooth; note that the mentum is somewhat detached from the head capsule); 3. Pronotum and anterior part of elytra showing the markedly concave basal margin and projected humeri; 4. Right lateral view of body.

but see comments to the redescription of *Q. elpis*, below), with surroundings of setigerous puncture not depressed; external intervals without setae; intervals with sculpticells of microsculpture transverse, very narrow, narrower than on pronotum (Fig. 26; magnification 100×, elytra appearing polished at 40×). Metepisternum elongate (Figs 4, 62, 83). Hindwings fully developed.

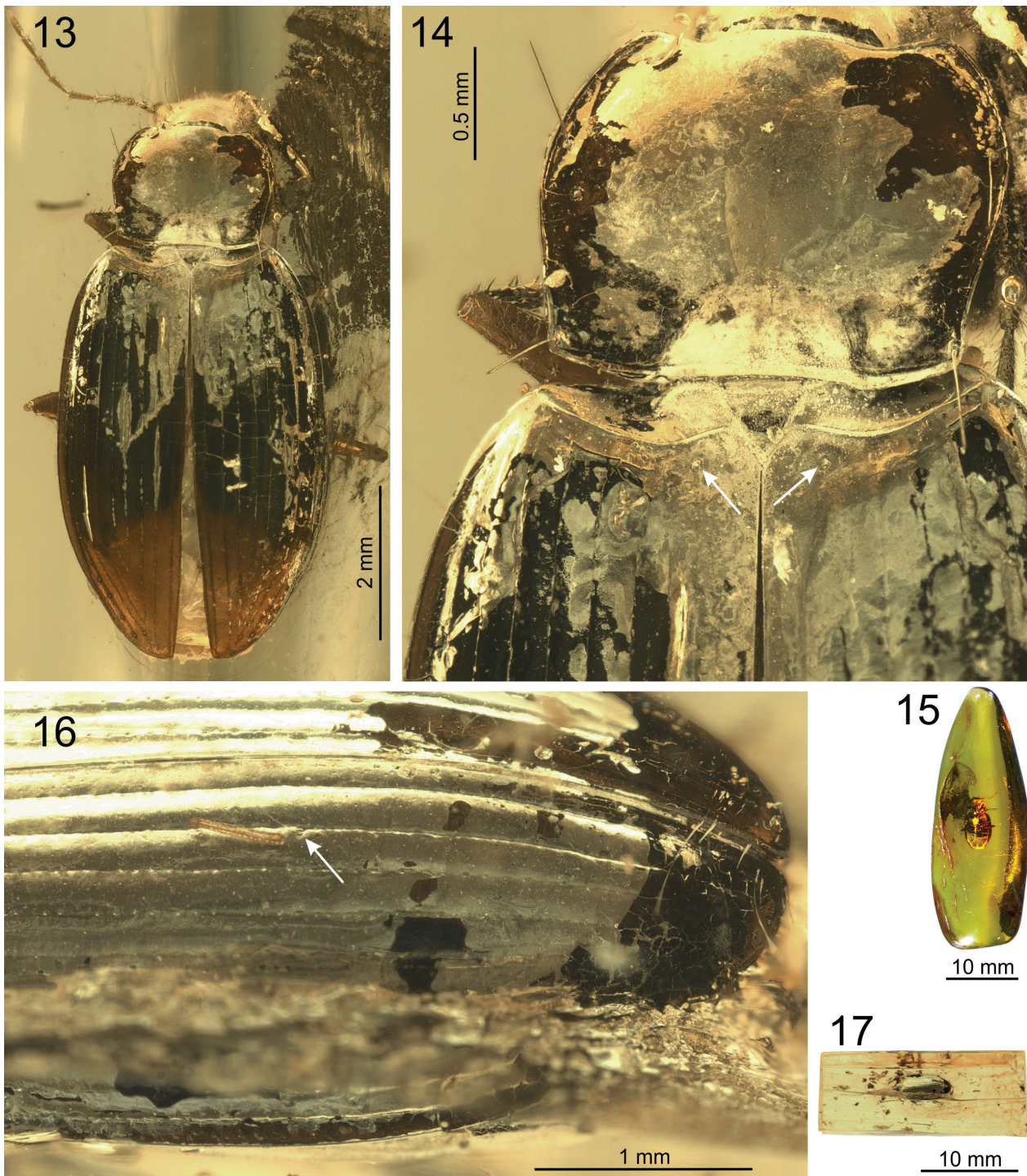
Legs: length average for Calathina, neither markedly slender nor particular robust (Figs 4, 7, 30, 36, 49, 62); male protarsomeres dilated; mesocoxa with a single ridge seta; metacoxa trisetose, with anterior seta large and with the two posterior setae small and thin, one located near external, one near internal margin (Figs 54, 67, 86; but see comments to the redescription of *Q. elpis*



Figures 6–12. *Quasicalathus elpis* (Ortuño and Arillo 2009), light microscopic images of specimens “Groehn 7889” (6–8.) and “Groehn 7962” (9–12.). **6, 10.** General view of the amber pieces (in Fig. 6, only the part of the large amber piece bearing the *Quasicalathus* fossil is shown); **7.** Ventral side of body; **8.** Left mesotarsi iv + v; **9.** Pronotum and anterior part of elytra, left side of body; **11, 12.** Medial part of left elytron (Fig. 12 shows the enlarged part of the elytron marked by the white frame in Fig. 11; the white arrow points to the insertion of the discal seta). Abbreviations: **bs** – insertion of the pronotal laterobasal seta; **hm** – humerus; **I–VIII** – elytral intervals 1–8.

below); metatrochanter with seta present (but see comments to the redescription of *Q. elpis*, below); metafemur with two setae on ventral surface, and with dorsoapical

setae present; metatibia in male not densely pubescent; tarsi without pubescence or wrinkles on dorsal surface; meso- and metatarsomeres I–IV without external and in-



Figures 13–17. *Quasicalathus elpis* (Ortuño and Arillo 2009), light microscopic images of specimens “CCHH 952” (13–15.) and “OSAC 269” (16, 17). **13.** Dorsal view of body; **14.** Pronotum and anterior part of elytra showing the markedly concave basal margin and projected humeri (the white arrows point the insertion pores of the parascutellary setae); **15, 17.** General view of the amber pieces; **16.** Posterior part of left elytron (the white arrow points to the insertion of the discal seta).

ternal lateral grooves; fifth tarsomeres with a single pair of dorsal setae, and with two pairs of ventral setae; claws pectinate (Fig. 8).

Abdomen: ventrites smooth aside from normal setation; apical ventrite in both sexes with one pair of seta near apical margin (Fig. 53).

Female genitalia (Figs 55–57, 76, 77): basal gonocoxite about two times longer than apical gonocoxite; apical

gonocoxite short, sickle-shaped, with one ensiform seta at dorsal and two ensiform setae at external margin, and with sensory pit large, well-developed, with two setae; basal gonocoxite without setae near apical margin; bursa copulatrix not markedly sclerotized.

Male genitalia (Figs 43–46, 68–72, 80, 87–89): aedeagus right side ventral in repose; right paramere styloid with distal portion very long and slender, not terminat-

ed in a distinct apical hook; left paramere ovoid; median lobe with long apical lamella, without apical disc.

Etymology. The name of the new subgenus is derived from the Latin conjunction “quasi” (like; as it were) and the name of the ground beetle genus *Calathus*, and thus refers to the morphological similarity to representatives of this genus.

Recognition and systematic placement within Sphodrini. Presence of a styloid right paramere (an apomorphic character state within Sphodrini) differentiates *Quasicalathus gen. nov.* from *Atranopsina* and *Synuchina*. Additionally, *Quasicalathus* lacks the stridulation organ that is an autapomorphy for *Atranopsina* (Casale 1988). Presence of well-developed sensory pit of the apical gonocoxite (plesiomorphic state) differentiates *Quasicalathus* from *Synuchina* (Casale 1988) and *Dolichina sensu* Sciaky and Facchini (1997), Sciaky and Wrase (1998) and Hovorka (2017b). Aedeagus with right side ventral in repose (right paramere styloid, left paramere ovoid; plesiomorphic state) differentiates *Quasicalathus* from *Pristosiina*. The combination of the following characters states places *Quasicalathus* outside of *Sphodrina sensu* Casale (1988): Mentum tooth not bifid (plesiomorphic state); antennae pubescent from fourth antennomere (plesiomorphic state); tarsomeres without pubescence and smooth on dorsal surfaces (plesiomorphic state); claws pectinate (symplesiomorph with Sphodrini except *Atranopsina*, reversed in some Sphodrini); aedeagal median lobe slender with long terminal lamella. The shape of the aedeagal median lobe and its terminal lamella is rather variable within *Calathina*, *Dolichina* and *Synuchina* (Lindroth 1956, Habu 1978, Casale 1988).

Based on the overall similarity in external and genital characters the new, fossil genus *Quasicalathus* strongly resembles extant species of subtribe *Calathina* and genus *Calathus* (see next section). However, as it was comprehensively discussed by Schmidt and Will (2020), monophyly of *Calathina* is supported by molecular data (Ruiz et al. 2009, 2010) while *Calathus* seems to be paraphyletic, and morphological data supporting *Calathina* monophyly are currently unknown. As a consequence, the definite, evidence-based, placement of fossil *Quasicalathus* species in this subtribe is currently impossible. What can be stated regarding the systematic placement of this taxon is the following:

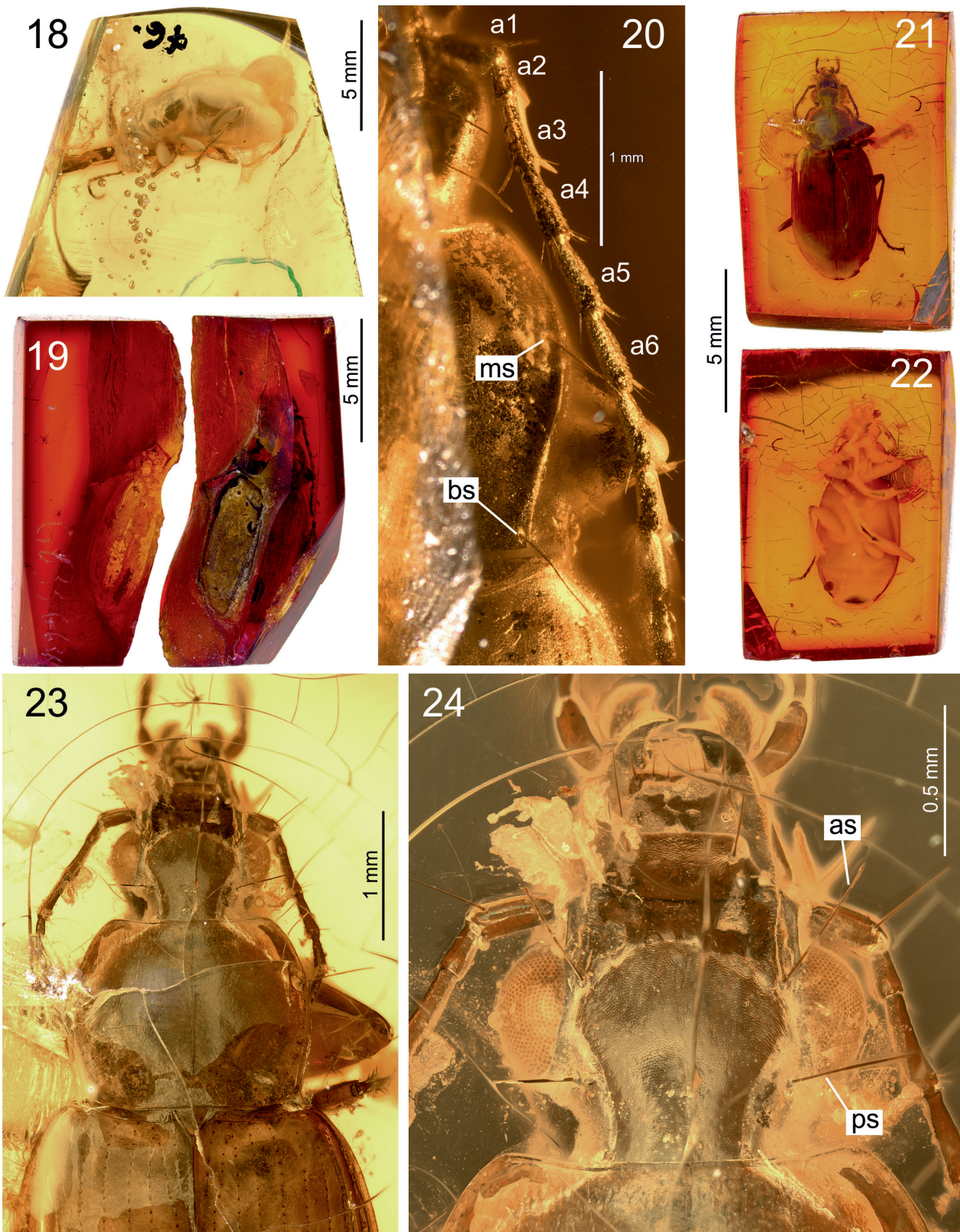
- i. *Quasicalathus* is included in the “P clade” of Ruiz et al. (2009) based on the shared presence of the markedly styloid right paramere, which is most likely an autapomorphy of this clade. *Atranopsina* and all but one outgroup, *Zabrini*, are characterized by much shorter parameres. The styloid right paramere shows a pattern of homoplasy across carabids and is considered a separate transformation in *Zabrini* as this group has not been shown to be the sister group to Sphodrini in relevant phylogenetic analyses (Ruiz et al. 2009, Gomez et al. 2016).
- ii. *Quasicalathus* is not a member of *Synuchina*, *Dolichina* or *Pristosiina*, as each of these sphodrine sub-

tribes is characterized by respective autapomorphic states that are not present in the fossil specimens.

- iii. *Quasicalathus* is not a member of *Sphodrina sensu* Casale (1988) because each of the genera affiliated to this subtribe is characterized by at least one autapomorphic state that is not present in *Quasicalathus* (see above).
- iv. Given the lack of apparent morphological synapomorphies for subtribe *Calathina* and the genus *Calathus* there is currently no evidence that places *Quasicalathus* within, or as sister of, any one of these clades.

Fossils are basic for understanding the evolutionary history of species groups and fossil specimens are critical for time calibration of phylogenetic hypotheses. Therefore, in order to prevent misleading interpretations—e.g., the incorrect assignment of fossils that lack evidence of their placement—we propose the systematic position of *Quasicalathus* using a conservative, synapomorphy-based approach. This requires establishing the genus without a certain position within the sphodrine “P clade” of Ruiz et al. (2009), i.e., Sphodrini, informal group P clade, *incertae sedis*.

Recognition with respect to *Calathina*. The overall similarity of *Quasicalathus gen. n.* with species of the genus *Calathus* makes it necessary to provide a detailed differential diagnosis of the new genus. Recently, Schmidt and Will (2020) presented an overview to the diagnostic characters of the currently accepted genera and subgenera placed within *Calathina*, and respectively *Calathus sensu* Hovorka (2017a). The Eocene *Quasicalathus* differs from all calathine species groups by presence of a single elytral discal seta (but see Remarks section to the redescription of *Calathus elpis*, below). All but one *Calathina* are characterized by presence of at least two elytral discal setae, while the elytra of *Tachalus* Ball & Nègre lacks discal setae. *Quasicalathus* additionally differs from all calathine taxa, with the exception of *Bedelinus* Ragusa, by having a simple mentum tooth (entire instead of bifid), and trisetose metacoxa. *Quasicalathus* differs from all but the Himalayan *Spinocalathus* Schmidt by narrow transverse sculpticells of elytral microsculpture (nearly isodiametric in other *Calathina*). A slightly transverse pattern of elytral microsculpture is developed in some species of *Dentalcalathus* Schmidt, however, species of this group differ by pubescent third antennomere in addition to other characters mentioned above and below. *Bedelinus* and *Spinocalathus* differ from *Quasicalathus* additionally by removal of the pronotal laterobasal pronotal seta from the lateral margin, plus presence of lateral grooves on metatarsomeres I–IV. *Quasicalathus* differs from *Spinocalathus* by the short metepisternum, and from *Bedelinus* and most *Spinocalathus* by presence of an apical hook on the right paramere. *Quasicalathus* shares meso- and metatarsomeres I–IV without external and internal lateral grooves with *Iberocalathus* Toribio, *Lindrothius* Kurnakov, some species of *Calathus s. str.*, *Dentalcalathus*, and *Neocalathus* Ball & Nègre. However, species of these groups differ by presence of an apical hook on the aedeagal



Figures 18–24. *Quasicalathus*, light microscopic images of *Q. elpis* Ortuño & Arillo, 2009 (18–20.) and *Q. agonicolis* sp. nov. (21–24.). 18. General view of the amber piece “MAIG 76” (only that part of the large amber piece bearing the *Quasicalathus* fossil is shown; the fossil is widely covered by milky coating); 19. General view of the two fragments of specimen “GZG 16185”; the left one bears only the negative imprint of the left elytra on the inclusion wall; 20. Right anterior part of body of specimen “GZG 16185” showing part of head, pronotum and humerus; 21, 22. General view of the amber piece “GZG 16188” (21. With fossil in dorsal view; 22. In ventral view); 23. Anterior part of specimen “GZG 16188”; 24. Head of specimen “GZG 16188”. Abbreviations: **a1–a6** – antennomeres 1–6; **as** – anterior supraorbital seta; **bs** – pronotal laterobasal seta; **ms** – pronotal lateral seta; **ps** – posterior supraorbital seta.

right paramere (*Lindrothius*, *Calathus* s. str., *Denticalathus*, *Neocalathus*) and by a markedly sclerotized spermatheca plus presence of a single ensiform seta along the external margin of the apical gonocoxite (*Iberocalathus*).

Here we hypothesize that i) presence of a single elytral discal seta and ii) presence of narrow transverse sculpticells of elytral microsculpture are synapomorphies of *Quasicalathus* gen. n.; the similarly developed pattern of elytral microsculpture in *Spinocalathus* and some *Denticalathus* are hypothesized as homoplasious as these groups share more derived patterns in some morphological features (e.g., bifid mentum tooth, bisetose metacoxa) together with other Calathina groups.

***Quasicalathus elpis* (Ortuño & Arillo, 2009) comb. nov.**

Figs 1–20, 34–64

Calathus elpis Ortuño & Arillo, 2009: 56–60.

Type material. Not studied; see Material and methods, above.

Remarks on original description and recognition.

The original description of the fossil species *C. elpis* is doubtful or confusing with respect to some important diagnostic characters, these are:

- i. Elytra near middle with two setiferous pores in the 5th interval. This pattern of chaetotaxy was not found in any of the fossil species we investigated. In contrast to what was presented by Ortuño and Arillo (2009), we believe that discal setae are absent in the 5th interval of the *C. elpis* holotype specimen. It seems likely that the observation of the authors is based on a misinterpretation of micro-structures on the elytral surface of the fossil that are preservation artifacts and thus produce a false impression of existing setiferous pores. This interpretation is supported by the following three facts:

First, in the reconstruction drawing of the holotype specimen, Ortuño and Arillo (2009: 57, fig. 1d) figured a seta corresponding to each of the reconstructed setiferous pores in the 3rd interval (these pores were found in all fossils we studied by us) but do not show those of the external intervals. Therefore, we believe that the authors may have observed structures in the external intervals that appear similar to (but not identical with) setiferous pores but do not bear setae.

Second, Ortuño and Arillo (2009: 57, fig. 1d) figured pore-like structures in the 6th elytral intervals close to the 5th striae but not in the 5th interval (as reported in their description). Such setation pattern is unknown in sphodrine beetles, fossil or extant. Presence of setiferous pores in the 6th elytral interval would also represent a markedly anomalous setation pattern, last but not least because the path of the cubital-1 nerve follows the 5th elytral interval (Jeannel 1926).

Third, the character combination ‘3rd interval uni-setose + one of the external intervals pluri-setose’ is absent in all other fossil and extant sphodrine species and therefore it is also very likely absent in *C. elpis*.

- ii. Ortuño and Arillo (2009: 58, fig. 2d) presented a reconstruction drawing of the *C. elpis* metacoxa that is bisetose in an irregular way: adjacent to the anterior seta an additional seta on the interior side of the posterior metacoxal surface was figured. Because this setation pattern is unknown in all Sphodrini and other Harpalinae, we believe that it is based on an erroneous interpretation of the actual coxal chaetotaxy of *C. elpis*. Although the majority of sphodrine species are characterized by bisetose metacoxae with one anterior and one posterior seta present, the posterior seta is always located near the external metacoxal margin. Very few Sphodrini possess a trisetose metacoxa with an additional seta interior of the external posterior seta, these include, some Atranopsina, *Bedelinus* of Calathina sensu Hovorka (2017a), *Anchomenidius* Heyden and *Casaleius* Sciaky & Wrase of Dolichina sensu Hovorka (2017b), and all the fossil species from Eocene amber that we investigated. In these extant and fossil taxa, the seta near the internal metacoxal margin is located at the same place as it was figured for *C. elpis* by Ortuño and Arillo (2009: 58, fig. 2d). Therefore, we believe that the external setiferous pore on posterior metacoxal area of *C. elpis* is present but was overlooked by the authors, probably because the seta was broken off or the view obscured, and that the metacoxa of *C. elpis* is actually trisetose as it is in all the other fossil specimens listed in the present study.
- iii. Ortuño and Arillo (2009: 58, fig. 2d) further presented a reconstruction drawing of the *C. elpis* metatrochanter that is asetose. However, the metatrochanters of the holotype specimen actually each are bearing a setiferous pore (Ortuño pers. comm., 2009) as in the diagnosis of *Quasicalathus* gen. n. (see above).

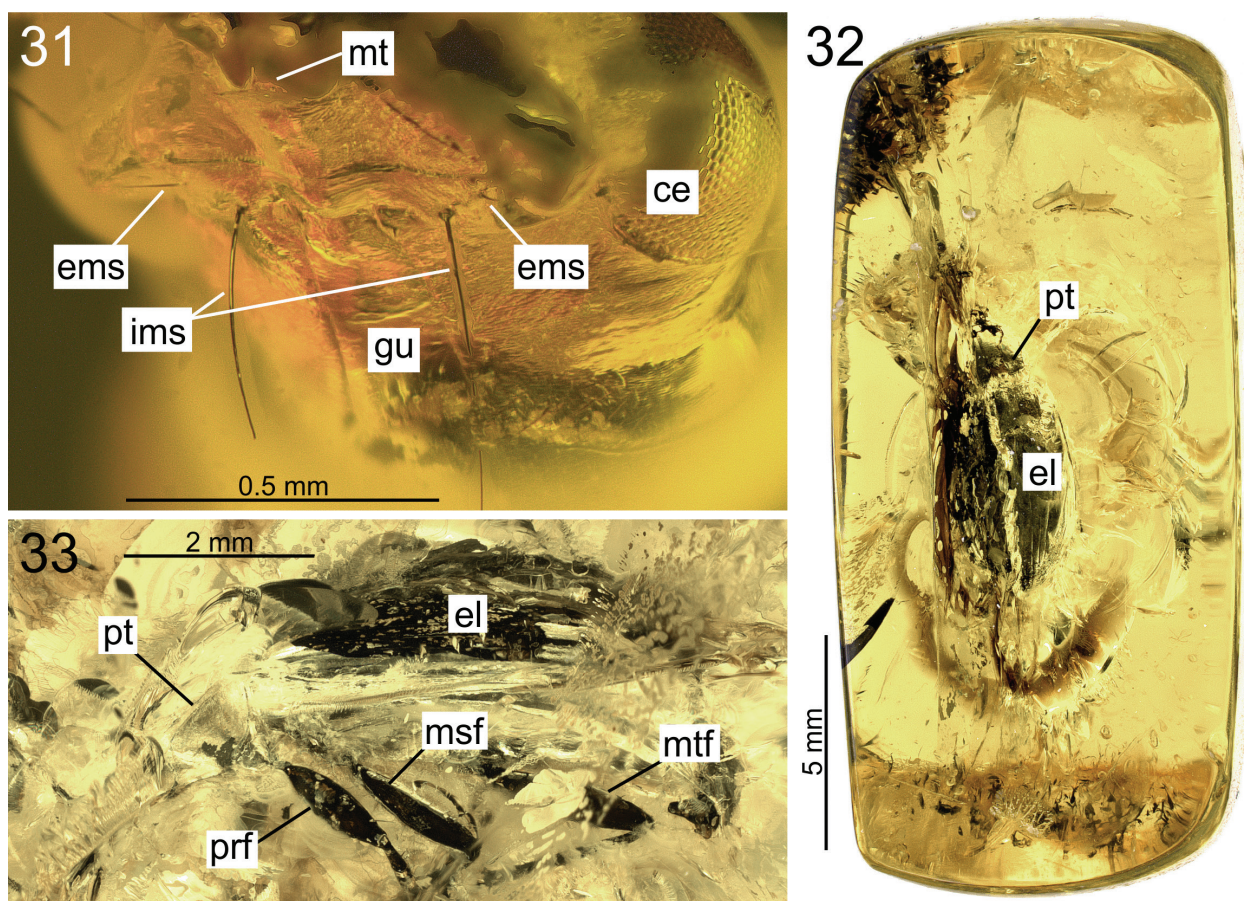
In addition to the doubtful character states discussed above, the original description of *C. elpis* provides few indications that lead to recognition of specimens of this species without direct comparison to the holotype. The ten sphodrine specimens from Baltic amber available for us to study, belong to at least two different species of *Quasicalathus*, and all but one of the diagnostic characters we found to be relevant for these species are absent in the description presented by Ortuño and Arillo (2009). Our interpretation of *C. elpis* as a member of *Quasicalathus* gen. n. is based on the assumption that elytral and coxal chaetotaxy was misinterpreted by the authors of the species as discussed above and, additionally, on the following morphological features evident in the photographs of the holotype specimen provided by Ortuño and Arillo (2009: figs 1b, c): pronotal lateral margin moderately narrowed toward base, straight before laterobasal angles, with



Figures 25–30. *Quasicalathus agonicollis* sp. nov., light microscopic images of specimen “GZG 16188” (25–26.) and the holotype (28–30.). 25. Posterior part of pronotum and anterior part of elytra, right side; 26. Anterior part of fifth interval of left elytra showing microsculpture; 27. Posterior part of elytra (the arrows point to the insertions of the discal setae); 28. General view of the amber piece; 29. Right dorsal view of beetle body (the arrow points to the insertion of the discal seta on left elytron); 30. Left ventral view. Abbreviations: **bs** – insertion of the pronotal laterobasal seta; **hm** – humerus; **m** – mite (syninclusion).

the latter moderately obtuse (instead of more rounded pronotal lateral margin with more obtuse laterobasal angles in the Baltic amber fossil species *Q. agonicollis* sp. nov.; see description below). Based on this character, we assume eight of the fossil specimens that are listed under Additional material (below) belong to *C. elpis*.

As a consequence, the redescription of *Quasicalathus elpis* comb. nov. and information about additional morphological characters that we use to distinguish this species from other Eocene sphodrine species (see descriptions of the new fossil species, below) are based on investigation of these eight additional specimens.



Figures 31–33. *Quascalathus*, light microscopic images of the holotypes of *Q. agonicollis* sp. nov. (31.) and *Q. conservans* sp. nov. (32, 33.). 31. Ventral side of head showing chaetotaxy of mentum; 32. General view of the amber piece with fossil in dorsal view; 33. Left lateral view. Abbreviations: **ce** – compound eye; **el** – elytron; **ems** – external seta of submentum; **gu** – gula; **ims** – internal seta of submentum; **msf** – mesofemur; **mt** – mentum; **mtf** – metafemur; **prf** – profemur; **pt** – pronotum.

Additional material. Eight specimens, with the following identification numbers, collection data, preservation state, and syninclusions:

Groehn 4879. Male in Baltic amber, with specimen label data “Groehn 4879”, deposited in Coll. Carsten Gröhn, Hamburg. Size of the piece approx. 15 × 15 × 4 mm (Fig. 1).

Preservation status: The amber is clear but pervaded by numerous air bubbles; most details of external morphology of the embedded fossil are well visible using light microscope (Figs 2, 3). Some parts of the exoskeleton (head, pronotum, elytral apex) are discoloured black. Using micro-CT, the fossilized beetle body yields moderate to low contrast so that parts of its external shape could only be coarsely imaged (Figs 34–37). The aedeagus is not preserved.

Syninclusions: Stellate hairs, additional plant remains, dust particles.

Groehn 7814. Male in Baltic amber, with specimen label data “Groehn 7814”, deposited in Coll. Carsten Gröhn, Hamburg. Size of the piece approx. 35 × 17 × 9 mm (Fig. 5).

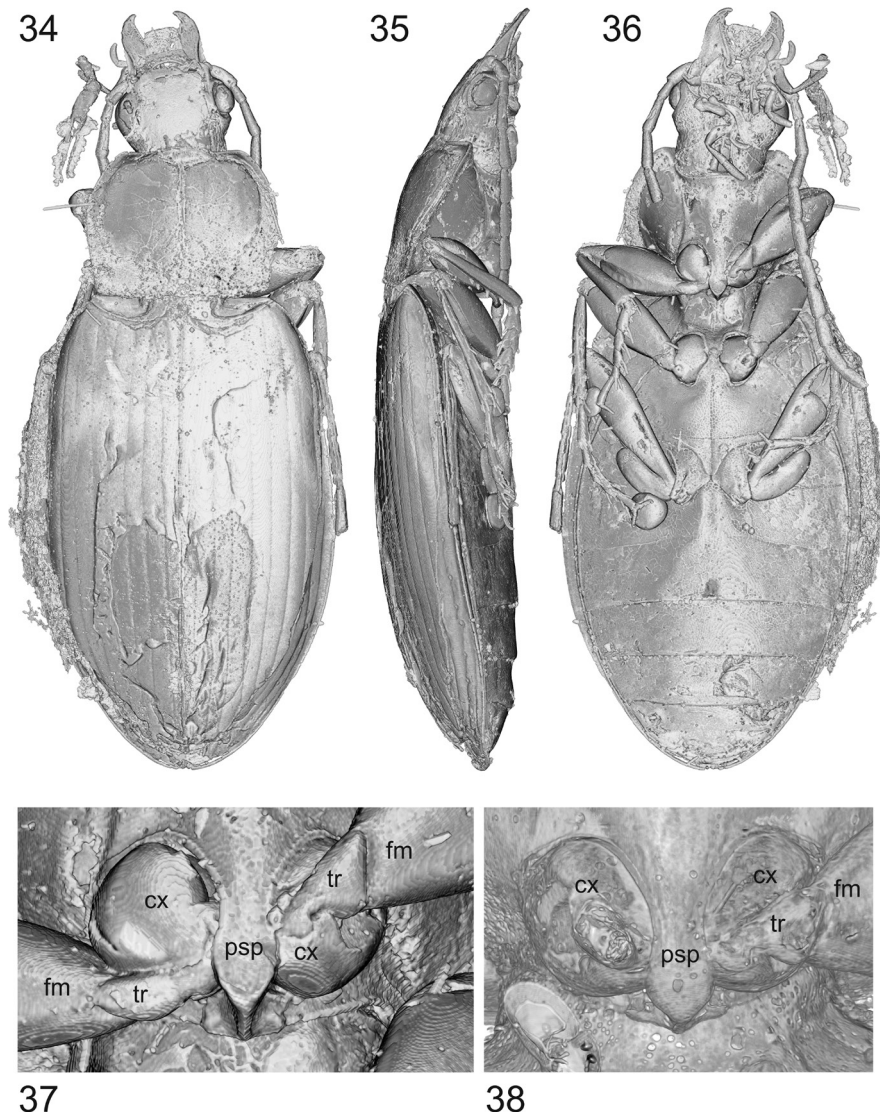
Preservation status: The amber is pervaded by numerous flowlines and air bubbles and therefore; the embedded fossil is only visible ventrad and right laterad using light microscopy (Fig. 4). The exoskeleton of the fossil is moderately well preserved and important diagnostic characters

could be imaged using micro-CT (Figs 38, 41, 42). The aedeagus is preserved in most parts (Figs 43–46), however, it was completely detached from the terminal abdominal segments during fossilization of the specimen. Most likely it moved through the abdomen and was finally wedged in the tight connection of meso- and metathorax (Figs 39, 40) after drying out of the internal parts of the beetle.

Syninclusions: Stellate hairs, two Nematocera flies, one mite.

Groehn 7889: Female in Baltic amber, with specimen label data “Groehn 7889”, deposited in Coll. Carsten Gröhn, Hamburg. The original size of the amber piece was approx. 35 × 23 × 10 mm and was separated into two pieces (Groehn 7889) in order to get better micro-CT scanning results. The size of the amber piece bearing the calathine fossil measures approx. 30 × 11 × 10 mm (Fig. 6).

Preservation status: The amber is pervaded by an extend flowline attached to the beetle laterally, and a large air bubble is attached to its abdomen ventrally, but most external characters of the beetle are visible using light microscope (Figs 6, 7). The exoskeleton of the fossil is well preserved and could be imaged to show most details using micro-CT (Figs 47–54) including the gonocoxites (Figs 55–57).



Figures 34–38. *Quascalathus elpis* (Ortuño and Arillo 2009), volume rendering of specimens “Groehn 4879” (34–37.) and “Groehn 7814” (38.). 34. Dorsal aspect; 35. Right lateral aspect; 36. Ventral aspect; 37, 38. Prothorax and basal portions of prolegs. Abbreviations: **cx** – procoxa; **fm** – profemur; **psp** – prosternal process; **tr** – prothorax.

Syninclusions: Plant remains, dust particles.

Groehn 7962: Male in Baltic amber, with specimen label data “Groehn 7962”, deposited in Coll. Carsten Gröhn, Hamburg. Size of the amber piece approx. $14 \times 10 \times 6$ mm, irregularly cut and polished (Fig. 10).

Preservation status: The amber is pervaded by numerous flowlines and air bubbles attached to the beetle body, mostly to its ventral surface; the fossil is therefore only partly visible using light microscope (Figs 9–12). Using micro-CT, the fossilized beetle body yields low contrast so that its external shape could only be coarsely imaged (Fig. 58). The aedeagus is not preserved.

Syninclusions: None.

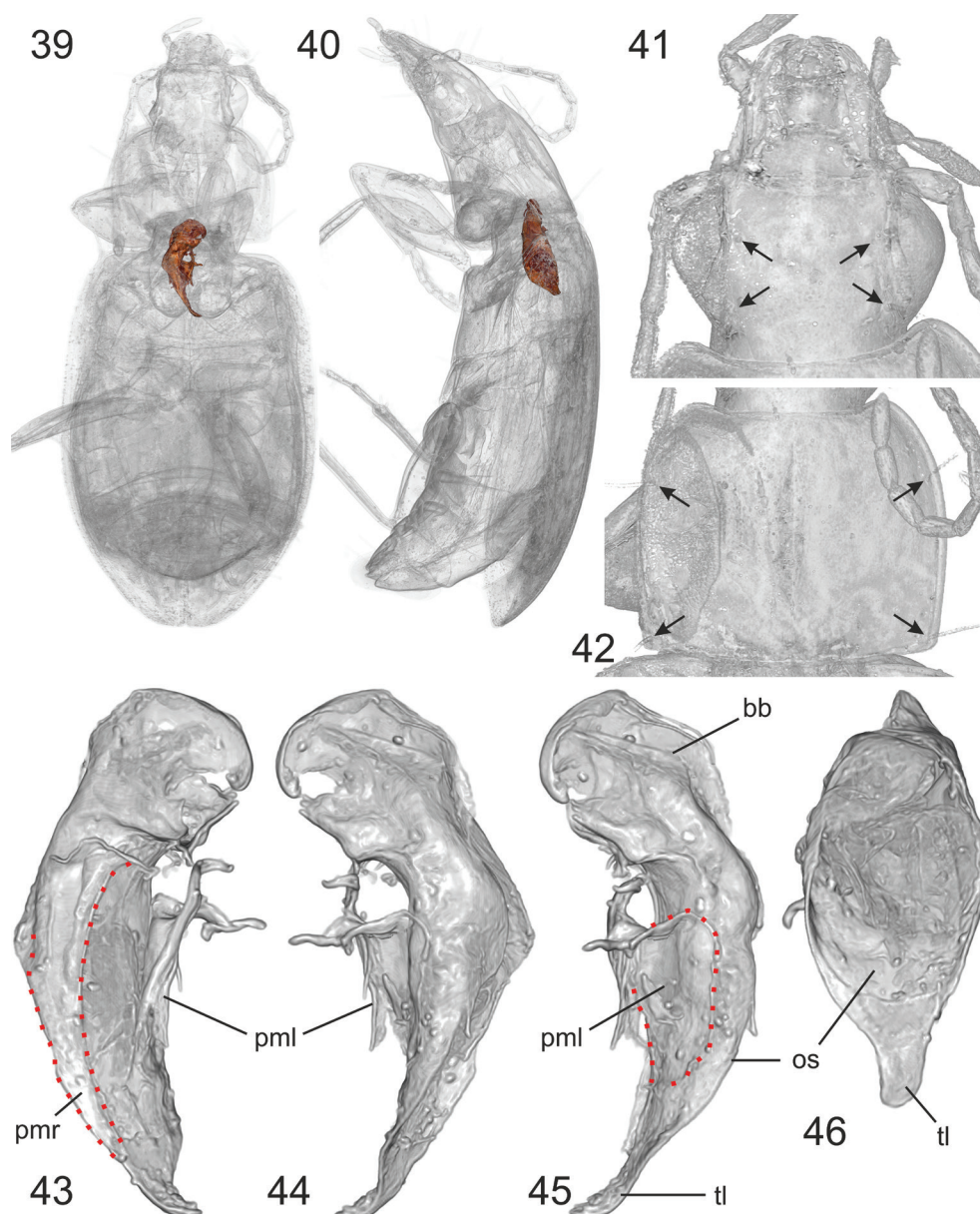
CCHH 952. Female in Baltic amber, with specimen label data “CCHH#952-2”, deposited in the collection of Christel and Hans Werner Hoffeins, Hamburg. Size of the piece approx. $39 \times 15 \times 7$ mm (Fig. 15).

Preservation status: The amber is clear in most parts, a single flowline is attached to the right side of the bee-

tle body, which is clearly visible for most of its length using light microscope (Figs 13, 14); head and abdomen are partly covered by a dirty coating ventrally. The amber was likely altered by autoclaving in order to reduce the milky coating. The results of this process are apparent from the blackened appendages of the beetle that are distinctly deformed (particularly tibiae and tarsi), and from one of the synincluded Nematocera that has a roasted appearance. For details on the effect of autoclaving on amber fossils see Hoffeins (2012). Using micro-CT, the fossilized beetle body yields a contrast so that its external shape could only be coarsely imaged (Fig. 59). This is likewise evidence of prior autoclaving of the piece.

Syninclusions: Two mites, one Brachycera fly, remains of two Nematocera flies, dust particles.

OSAC 265. Male in Baltic amber, with specimen label data “OSAC_2900265”, deposited in the Oregon State University Collection. The original size of the amber piece was $57 \times 16 \times 4$ mm and was separated into three



Figures 39–46. *Quascalathus elpis* (Ortuño and Arillo 2009), volume rendering of specimen “Groehn 7814” using different grey scales of the Amira software. **39.** Dorsal aspect; **40.** Lateral aspect. The displaced aedeagus (highlighted by red colour) was separated by the segmentation function of Amira software in Figures 39 and 40; **41.** Head (the arrows point to the insertions of the supra-orbital setae); **42.** Pronotum (the arrows point to the insertions of the lateral setae); **43–46.** Remains of the aedeagus in right lateral aspect (**43.**); Left lateral aspect (**44.**); Left lateral aspect (**45.**); Dorsal aspect (**46.**). The distal margins of the styloid apophysis of the right paramere in Fig. 43 and the lobate apophysis of the left paramere in Fig. 45 are highlighted by red dotted lines. Abbreviations: **bb** – basal bulb of aedeagal median lobe; **os** – distal ostium; **pml** – left paramere; **pmr** – right paramere; **tl** – terminal lamella of median lobe.

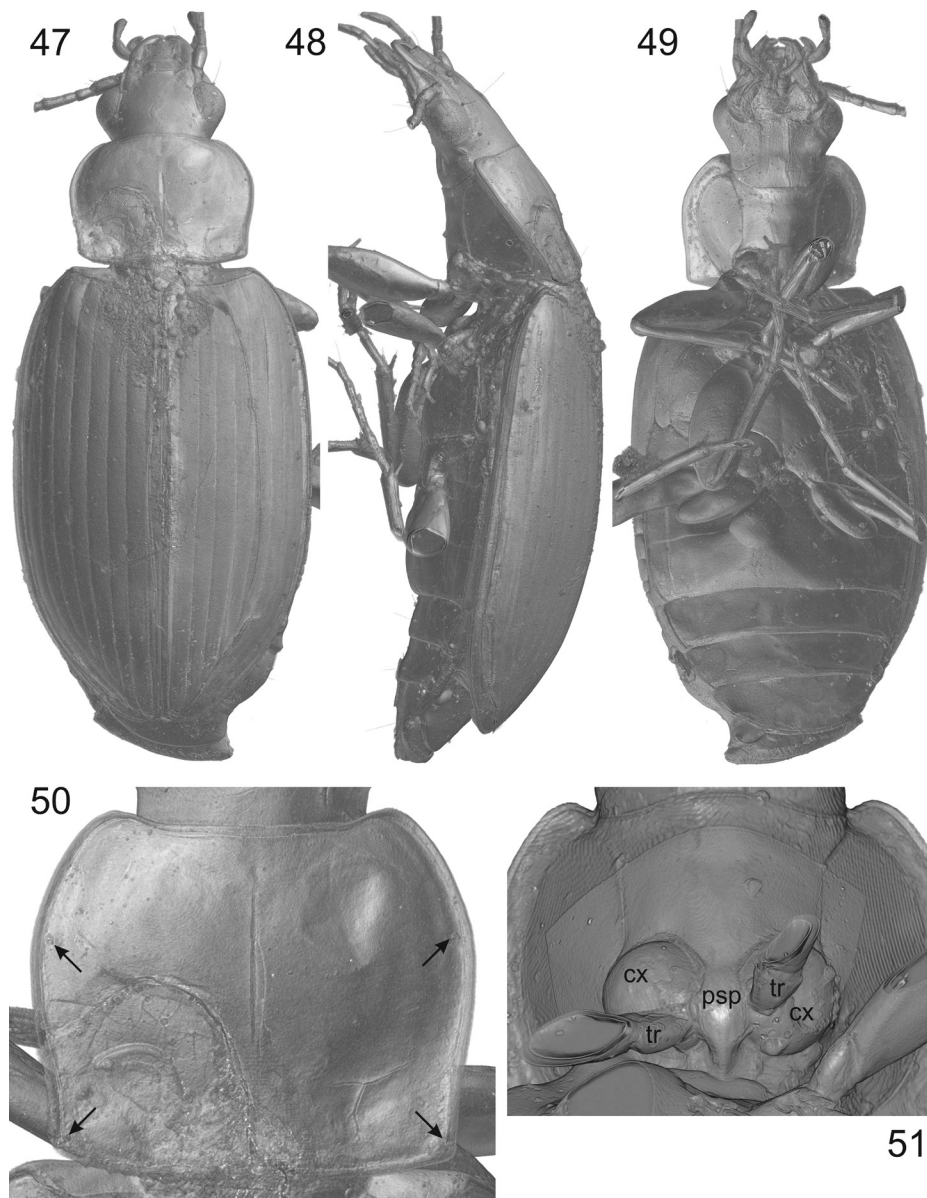
pieces in order to get better micro-CT scanning results. The size of the amber piece bearing the calathine fossil measures approx. $21 \times 9 \times 4$ mm (Fig. 17).

Preservation status: The amber is clear in most parts, some flowlines are attached to the embedded fossil; latter is well visible in most parts of the body using light microscope (Figs 16, 17). Using micro-CT, the fossilized beetle body yields low contrast and therefore, its external shape could only be coarsely imaged (Fig. 60). The aedeagus is not preserved.

Syninclusions: Large number of dust particles in each of the three pieces.

MAIG 76. Female in Baltic amber, with specimen label data “76” deposited in Museum of Amber Inclusions, University of Gdańsk, Poland. Size of the amber piece ca. $33 \times 23 \times 10$ mm, irregularly cut (Fig. 18).

Preservation state: Moderately well preserved due to a large bubble and extensive milky coating attached to the left part of the fossil, resulting in a significant deformation of the beetle body (Fig. 61). A flowline and a corro-



Figures 47–51. *Quasicalathus elpis* (Ortuño and Arillo 2009), volume rendering of specimen “Groehn 7889”. 47. Dorsal aspect; 48. Left lateral aspect; 49. Ventral aspect; 50. Pronotum (the arrows point to the insertions of the lateral setae); 51. Prosternum (for better view the prolegs are partly removed using the clipping plane function of Amira software. Abbreviations: **cx** – procoxa; **psp** – prosternal process; **tr** – protrochanter.

sion crack are attached to the right side of the beetle body; the apex of the right elytron reaches the amber’s external surface due to a small cavity in the amber piece. Because the fossil yields moderately strong contrast during micro-CT scan, details of its external shape could be imaged apart from the ventral side of the head (Figs 61–63). The genitalic segments are not preserved.

Syninclusions: One tiny insect larva; several air bubbles.

GZG 16185. Male in Baltic amber, with specimen label data “GZG BST 16185” and “G633.G636”, deposited in Geoscience Museum, University of Göttingen, Germany (very probably ex coll. Königsberg). Size of the amber piece $15 \times 8.5 \times 6$ mm, originally with seven polished edges, but fragmented into two pieces of about the same

size, with one piece containing most parts of the fossil while the other contains the negative imprint of the left elytron (Fig. 19); the surface of the latter piece bears the inscription “G633.G636”.

Preservation state: Poorly preserved due to amber corrosion; several corrosion cracks pervade the amber surface; amber is markedly darkened with the embedded fossil hardly visible in most views; fossil is partly covered by flowlines, bubbles and milky coating. The fossilized beetle body yields low contrast during micro-CT scan, so that its external shape could only be very coarsely imaged (Fig. 64). The aedeagus is not preserved.

Syninclusions: Stellate hairs, dust particles.

Redescription. Measurements see Table 2.

SBL: 7.5–8.8 mm ($\bar{\text{O}}$ 7.9 mm; n = 7).

Proportions: A3L/HL = 0.40–0.45 ($\bar{\text{O}}$ 0.42; n = 11);

EyL/ HW(-) = 0.65–0.79 ($\bar{\text{O}}$ 0.72; n = 15);

PW/HW(+) = 1.39–1.58 ($\bar{\text{O}}$ 1.50; n = 8);

PW/PL = 1.26–1.33 ($\bar{\text{O}}$ 1.29; n = 8);

PW/PWb = 1.03–1.13 ($\bar{\text{O}}$ 1.10; n = 8);

PWb/PWa = 1.47–1.61 ($\bar{\text{O}}$ 1.52; n = 8);

EW/PW = 1.53–1.64 ($\bar{\text{O}}$ 1.29; n = 7);

EL/EW = 1.51–1.62 ($\bar{\text{O}}$ 1.55; n = 7);

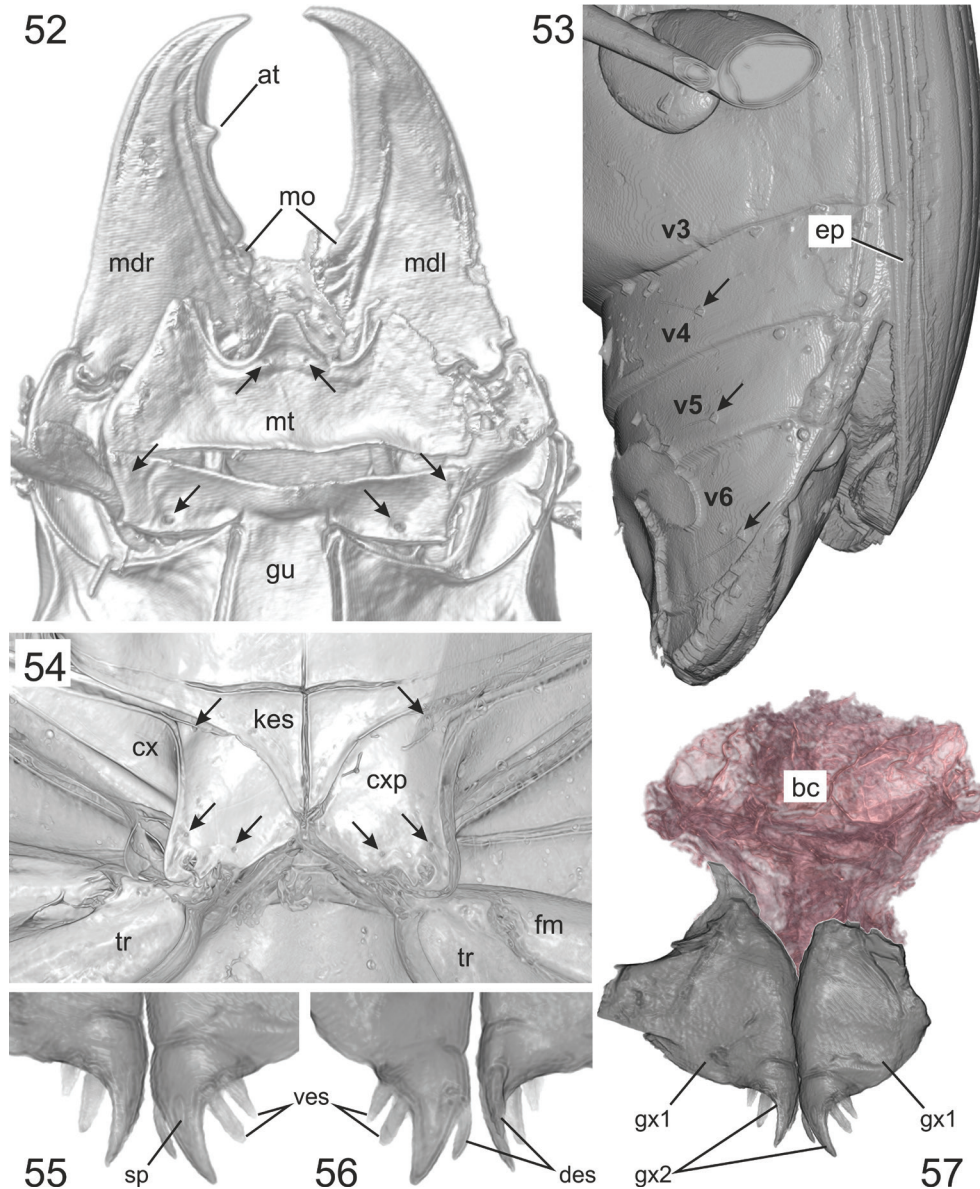
EpL/EpW = 1.47–1.60 ($\bar{\text{O}}$ 1.55; n = 10);

EL/FL = 2.35–2.65 ($\bar{\text{O}}$ 2.53; n = 7);

EL/AedL = 4.05 (n = 1).

Head: Microsculpture on disc consists of very small slightly irregular meshes (magnification 80 \times). In all other characters as described for the new genus, above.

Prothorax: Pronotal lateral margin moderately narrowed toward base, straight or slightly concave before laterobasal angles, angles slightly obtuse (Figs 3, 9, 14, 34, 42, 50, 58–60, 63, 64). Prosternal process with or without apical bead (Figs 37, 38, 51). In all other characters as described for the new genus, above.



Figures 52–57. *Quasicalathus elpis* (Ortuño and Arillo 2009), volume rendering of specimen “Groehn 7889”. **52.** Head, ventral aspect (the arrows point to the insertions of the setae near base of mentum tooth and on submentum); **53.** Abdomen, left lateral aspect (the arrows point to the insertions of the setae on ventrites IV, V, and VI); **54.** Metacoxal area (the arrows point to the insertions of the coxal setae); **55.** Apical gonocoxites, ventral aspect; **56.** Apical gonocoxites, dorsal aspect; **57.** Gonocoxites and remains of the bursa copulatrix (the latter was highlighted by red colour using the segmentation function of Amira software). Abbreviations: **at** – apical tooth of retinacle; **kes** – metathoracic katepisternum; **cx** – metacoxa; **cxp** – metacoxal plate; **des** – dorsal ensiform setae; **ep** – elytral epipleuron; **fm** – metafemur; **gu** – gula; **mdl** – left mandible; **gx1** – basal gonocoxite; **gx2** – apical gonocoxite; **mdr** – right mandible; **mo** – molar; **mt** – mentum; **sp** – sensory pit; **tr** – metatrochanter; **ves** – ventral ensiform setae; **v3**, **v4**, **v5**, **v6** – ventrites III, IV, V, VI.

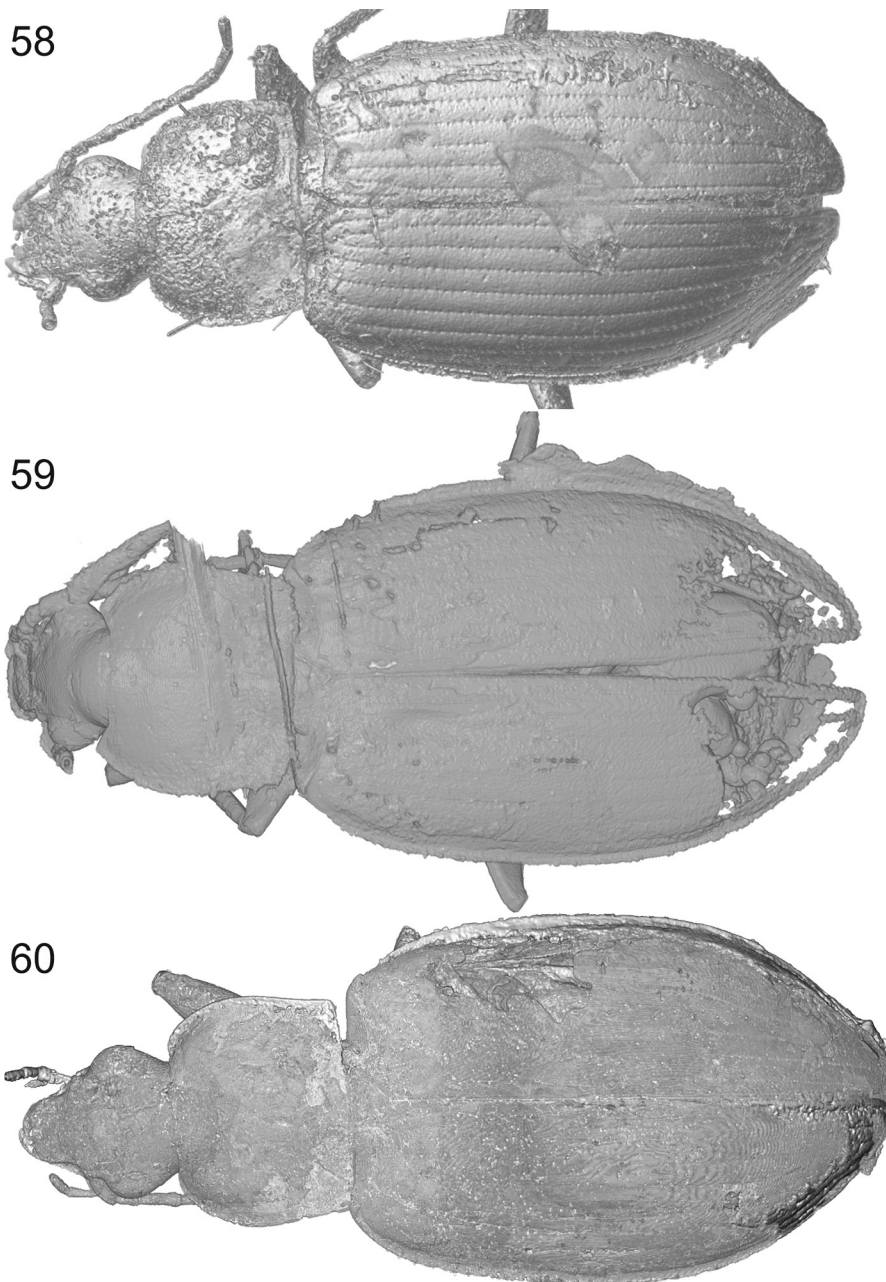
Pterothorax: Elytra with basal margin markedly concave and humerus markedly protruded anteriorly; basal margin forming a slightly obtuse angle ($100\text{--}115^\circ$) with lateral margin (Figs 3, 9, 14, 34, 47, 58–60, 61). Elytral striae moderately deeply engraved, intervals moderately convex. In all other characters as described for the new genus, above.

Female genital: Length of apical gonocoxite about 0.18 mm; shape see Figs 55–57. In all other characters as described for the new genus, above.

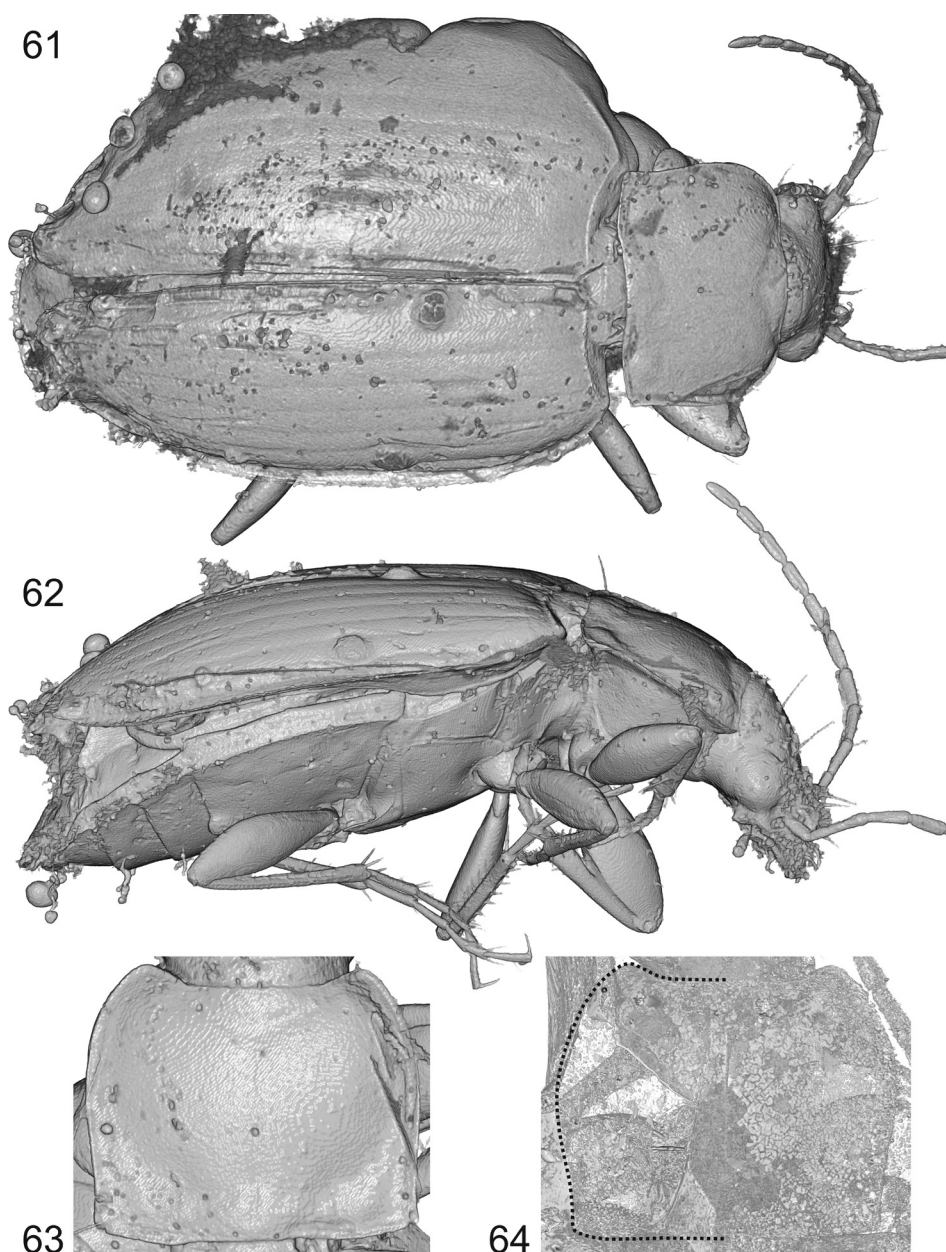
Aedeagus: Length of median lobe about 1.23 mm; median lobe terminal lamella moderately long and more markedly narrowed just behind its base so that its left margin is markedly concave and its apex slender linguulate (Fig. 46); in lateral view, terminal lamella markedly bent

ventrally (Figs 43–45; note that the intensity of ventral bending might also be an artefact of poor preservation). In all other characters as described for the new genus, above.

Differential diagnosis. *Quascalathus elpis* (in sense of this paper) differs from *Q. agonicollis* sp. nov. by larger body (SBL > 7 mm), less obtuse laterobasal angles of pronotum, more concave elytral basal margin, more markedly projected humeri, less obtuse humeral angle ($< 120^\circ$), longer apical gonocoxites and larger aedeagus. It differs from *Q. conservans* sp. nov. by the proportionally smaller aedeagus with terminal lamella bent ventrally (Figs 43–45); the left margin of the terminal lamella in dorsal view is significantly concave in *Q. elpis* (Fig. 46) but almost straight in *Q. conservans* sp. nov. (Fig. 88).



Figures 58–60. *Quascalathus elpis* (Ortuño and Arillo 2009), volume rendering of the dorsal aspects of specimens “Groehn 7962” (58.), “CCHH 952” (59.), and “OSAC 265” (60.).



Figures 61–64. *Quasicalathus elpis* (Ortuño and Arillo 2009), volume rendering of specimens “MAIG 76” (61–63.) and “GZG 16185” (64.); 61. Dorsal aspect; 62. Right lateral aspect; 63, 64. Pronotum (the pronotal outline on left side is highlighted by dotted line in Fig. 64).

***Quasicalathus agonicollis* Schmidt & Will, sp. nov.**

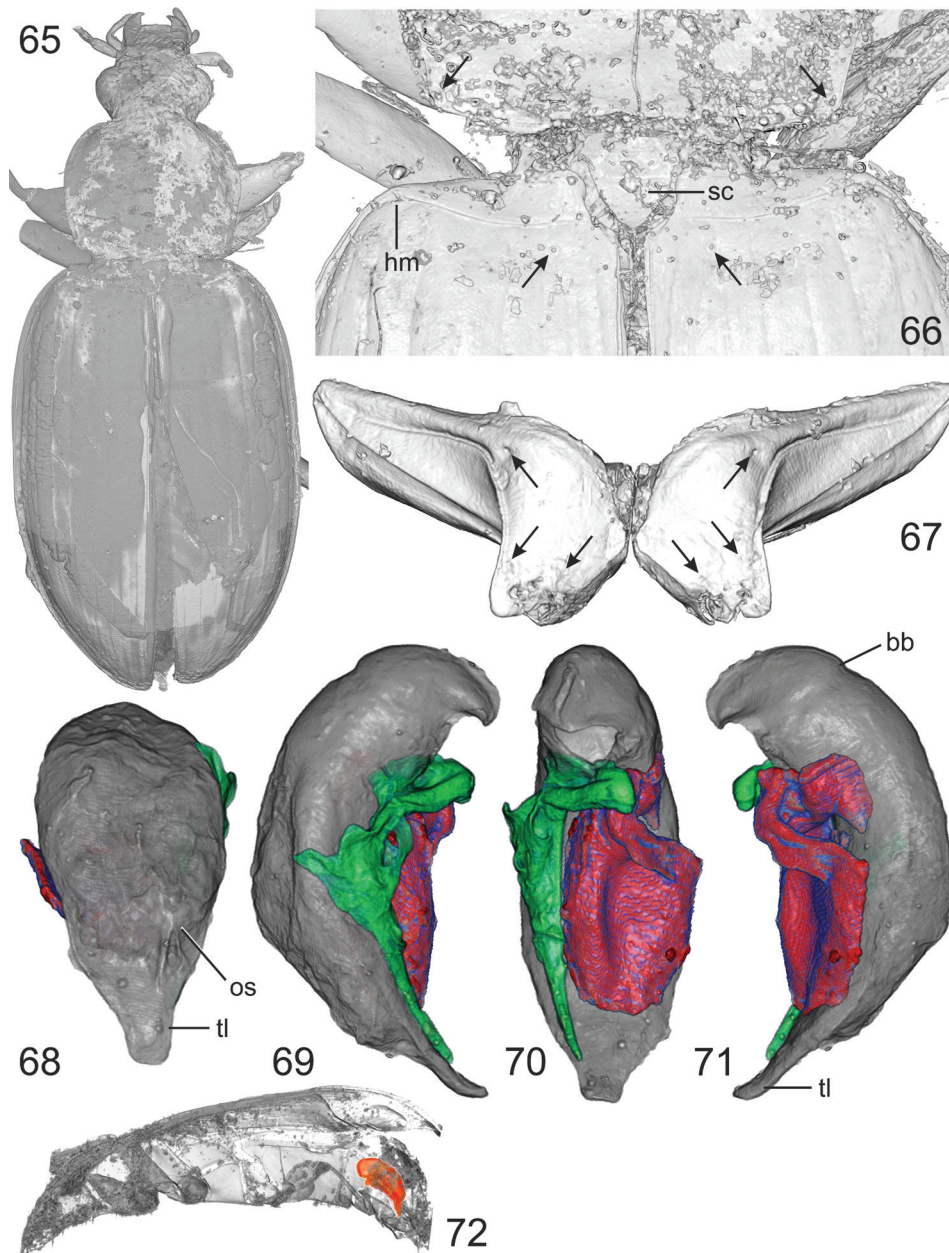
<http://zoobank.org/0555D647-EDC0-4A5F-BDDE-05FA1C5BB140>

Figs 21–31, 65–77

Holotype. Male in Baltic amber, with specimen label data “SDEI-Amb-002528”, deposited in Senckenberg Deutsches Entomologisches Institut, Müncheberg, Germany. The original size of the amber piece was $60 \times 23 \times 7$ mm and was separated into three pieces (SDEI Amb-002528 a, b, c) in order to get better micro-CT scanning results. The size of the amber piece bearing the calathine fossil measures approx. $15 \times 9 \times 4$ mm (Fig. 28).

Preservation status: A clear piece of amber with the embedded carabid fossil well visible, however, exten-

sive flowlines are present in front of the head and on the right side of the beetle body. Several parts of the beetle body are additionally covered by a white coating so that details of the exoskeleton are not visible using light microscopy; this includes the dorsal surface of head and pronotum, lateral parts of the elytra, right side of the ventral surface (Figs 29, 30). The external surface of the fossilized beetle body yields low (head, thorax) or relatively moderate contrast (elytra, abdomen) during micro-CT scan and therefore, the anterior part of the body could only be coarsely imaged (Fig. 65). The aedeagus with median lobe and right paramere is moderately well preserved and could partly be imaged using micro-CT data (Figs 68–72); the left paramere



Figures 65–72. *Quascalathus agonicollis* sp. nov., volume rendering of the holotype using different grey scales of the Amira software. **65.** Dorsal aspect (the negative imprint of the fossil on the inclusion wall is shown); **66.** Basal portion of pronotum and anterior part of elytra (positive of the fossilized beetle is shown; the arrows point to the insertions of the pronotal basolateral setae and the parascutellar setae); **67.** Metacoxa (the arrows point to the insertions of the three coxal setae each side); **68–71.** Aedeagus in dorsal aspect (**68.**), Right lateral aspect (**69.**), Ventral aspect (**70.**), Left lateral aspect (**71.**); The remains of the parameres are coloured (red: left paramere; green: right paramere); **72.** left lateral aspect of beetle body; the aedeagus (highlighted by red colour) was separated by the segmentation function of Amira software. Abbreviations: **bb** – basal bulb of aedeagal median lobe; **hm** – humerus; **os** – distal ostium of median lobe; **sc** – scutellum; **tl** – terminal lamella of median lobe.

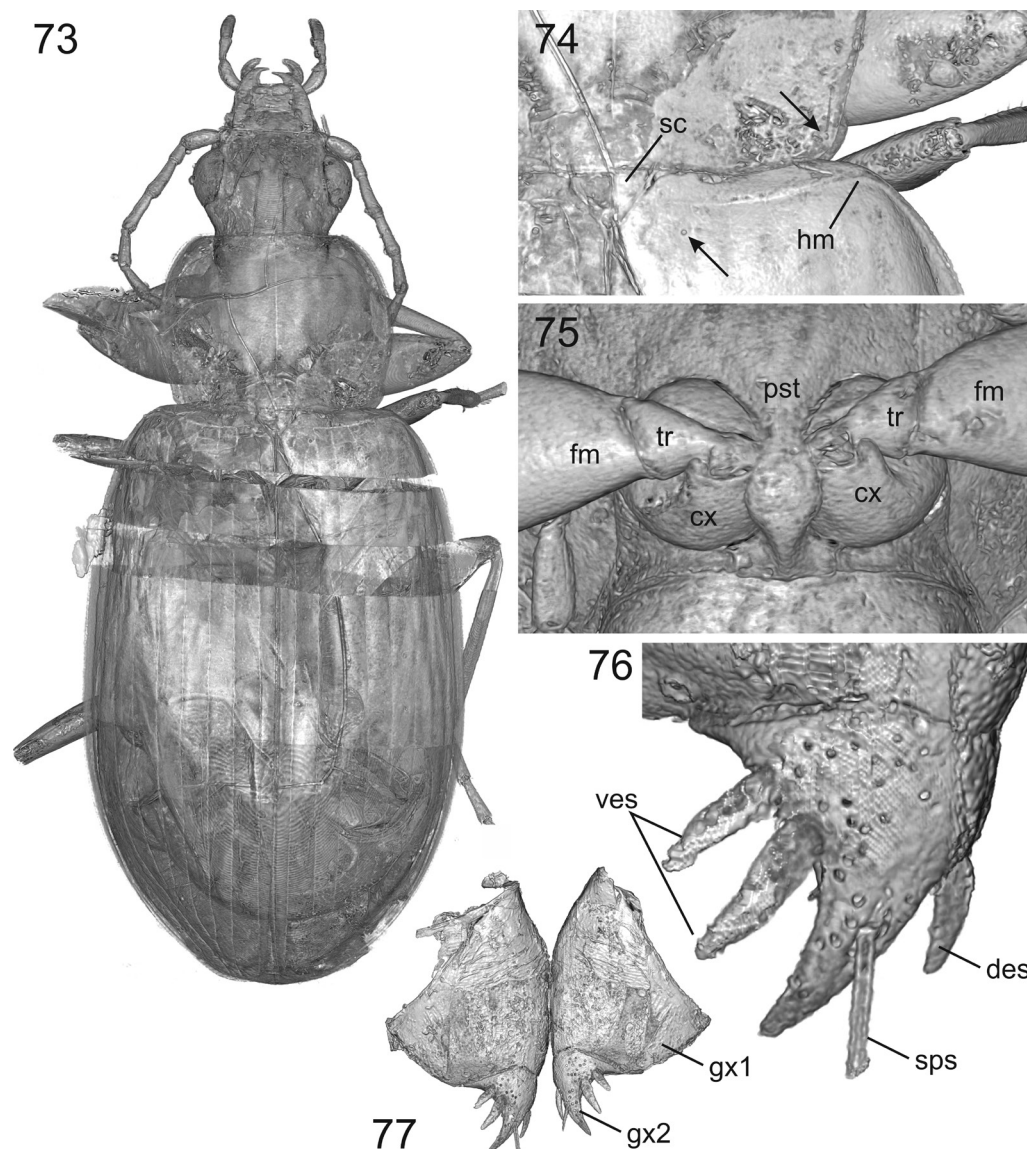
provided contrast during CT scan that was too low for reconstruction.

Syninclusions: SDEI-Amb-002528a: seven very tiny insect larva, dust particles; one mite on the carabid fossil near the beetle’s scutellum. SDEI-Amb-002528b: one Myrmicinae ant, three Nematocera flies, stellate hairs, dust particles. SDEI-Amb-002528c: dust particles.

Additional material. Female in Baltic amber, with specimen label data “GZG BST 16188” and “K2192” (ex

coll. Klebs), deposited in Geoscience Museum, University of Göttingen, Germany. Size of the amber piece approx. $12 \times 7 \times 4$ mm, with seven polished edges (Figs 21, 22); one edge bears the inscription “G644”.

Preservation status: The amber stone is clear in most parts but its surface shows several corrosion cracks (Figs 23, 24); the ventral surface of the fossil is completely covered by a milky coating (Fig. 22). The exoskeleton of the fossil is moderately well preserved and could therefore



Figures 73–77. *Quasicalathus agonicollis* sp. nov., volume rendering of specimen “GZG 16188”. 73. Dorsal aspect; 74. Basal portion of pronotum and anterior part of elytra (right side of body; the arrows point to the insertions of the pronotal basolateral seta and the parascutellar seta); 75. Prosternum with basal portion of prolegs; 76. Left apical gonocoxite, ventral aspect; 77. Gonocoxites, ventral aspect. Abbreviations: **cx** – procoxa; **des** – dorsal ensiform setae; **fm** – profemur; **gx1** – basal gonocoxite; **gx2** – apical gonocoxite; **hm** – humerus; **pst** – prosternum; **sc** – scutellum; **sps** – setae of sensory pit; **tr** – trochanter; **ves** – ventral ensiform setae.

be imaged in most details using micro-CT (Figs 73–75), including the gonocoxites (Figs 76, 77).

Syninclusions: Stellate hairs, dust particles.

Remarks. The specific identity of this second fossil specimen with the holotype of *Q. agonicollis* sp. nov., given the current state is difficult to substantiate. This is due to the poor preservation state of the holotype specimen. In the specimen GZG 16188, the pattern of head microsculpture is quite differently developed from that what we found in *Q. elpis* and the below described *Q. conservans* sp. nov., however, this character state is unknown for the *Q. agonicollis* sp. nov. holotype. Therefore, our decision to identify GZG 16188 as *Q. agonicollis* sp. nov. must be considered provisional. It is based on the following four interspecific diagnostic character states that *Q. agonicollis* sp. nov. holotype

and specimen GZG 16188 share: i) body size small, SBL below 7 mm. ii) pronotal laterobasal angles more markedly obtuse; iii) elytral basal margin moderately concave; iv) humerus slightly protruded with humeral angle more markedly obtuse. Therefore, in the description of *Q. agonicollis* sp. nov. we separate the descriptions of the *Q. agonicollis* sp. nov. holotype and the specimen GZG 16188.

Description of the holotype. Measurements see Table 2.

Standardized body length: 6.7 mm.

Proportions: A3L/HL = 0.45;

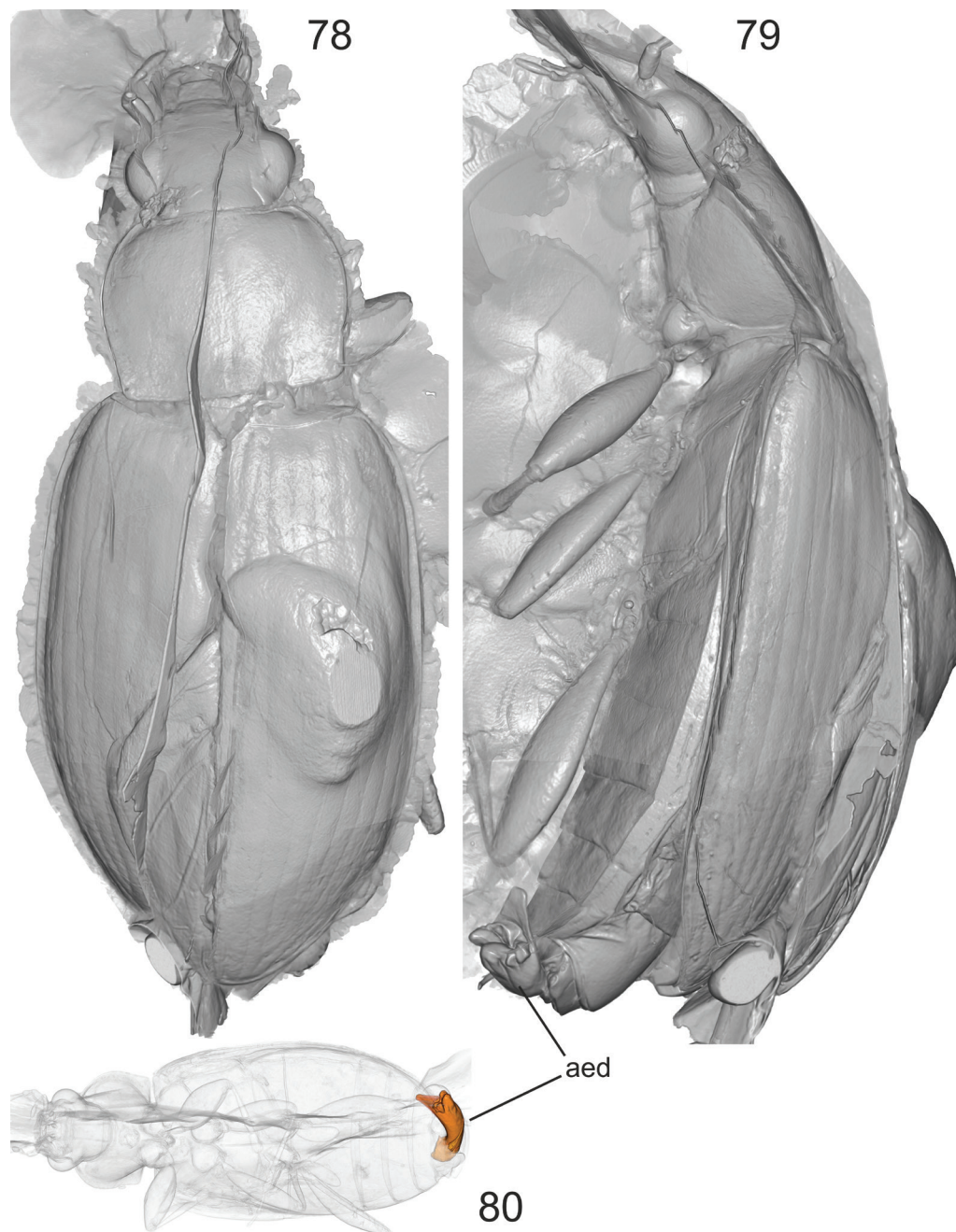
EyL/ HW(-) = 0.62;

PW/HW(+) = 1.45;

PW/PL = 1.26;

PW/PWb = 1.17;

PWb/PWa = not available;



Figures 78–80. *Quasicalathus conservans* sp. nov., volume rendering of the holotype using different grey scales of the Amira software. **78.** Dorsal aspect; **79.** Left lateral aspect (**aed** – aedeagus); **80.** Ventral aspect; the aedeagus (highlighted by red colour) was separated by the segmentation function of Amira software.

EW/PW = 1.60;
 EL/EW = 1.55;
 EpL/EpW = 1.40;
 EL/FL = 2.42;
 EL/AedL = 4.07.

Head: Patterns of microsculpture could not be studied. In all other characters as described for the new genus, above.

Prothorax: Pronotal lateral margin more markedly narrowed toward base than in *Q. elpis*, straight just before laterobasal angles, angles markedly obtuse (Figs 65, 66). Prosternal process with traces of lateral bead evident. In all other characters as described for the new genus, above.

Pterothorax: Elytra with basal margin moderately concave and humerus moderately protruded anteriorly; basal margin forming a more obtuse angle (ca. 125°) with lateral margin (Figs 65, 66). Elytral striae moderately deeply engraved, intervals moderately convex. In all other characters as described for the new genus, above.

Aedeagus: Length of median lobe 1.12 mm. Median lobe terminal lamella almost evenly narrowed from base to apex with side margins almost straight; apex slightly bent ventrally (Fig. 70). In all other characters as described for the new genus, above.

Description of specimen GZG 16188. Measurements see Table 2.

Standardized body length: 6.9 mm.

Proportions: A3L/HL = 0.44;

EyL/ HW(-) = 0.65;

PW/HW(+) = 1.46;

PW/PL = 1.26;

PW/PWb = 1.12;

PWb/PWa = 1.40;

EW/PW = 1.63;

EL/EW = 1.53;

EpL/EpW = 1.62;

EL/FL = 2.55.

Head: Microsculpture consists of moderately large isodiametric sculpticells (Fig. 24). In all other characters as described for the new genus, above.

Prothorax: Pronotal lateral margin almost completely rounded, straight just before laterobasal angles, angles markedly obtuse (Figs 23, 25, 73, 74). Prosternal process with traces of an apical bead (Fig. 75). In all other characters as described for the new genus, above.

Pterothorax: Elytra with basal margin moderately concave and humerus moderately protruded anteriorly; basal margin forming a more obtuse angle (ca. 125°) with lateral margin (Figs 23, 73, 74). Elytral striae shallowly engraved, intervals rather flat. In all other characters as described for the new genus, above.

Female genitalia: Length of apical gonocoxite about 0.15 mm; shape see Figs 76, 77; bursa copulatrix is not preserved. In all other characters as described for the new genus, above.

Differential diagnosis. *Quasicalathus agonicollis* sp. nov. differs from *Q. elpis* and *Q. conservans* sp. nov. by the smaller body (SBL < 7 mm), more obtuse laterobasal angles of the pronotum, less concave elytral basal margin, less projected humeri, a more obtuse humeral angle (> 120°) and relatively smaller aedeagus. Based on specimen GZG 16188, *Q. agonicollis* sp. nov. differs from *Q. elpis* and *Q. conservans* sp. nov. additionally by presence of moderately large isodiametric sculpticells on head disc (small and transverse meshes in *Q. elpis* and *Q. conservans* sp. nov.) and (from *Q. elpis*) by the smaller apical gonocoxite (unknown in *Q. conservans* sp. nov.). Due to the uncertainties in the identification of the *Q. agonicollis* sp. nov. non-type female specimen (see Remarks above), the latter differential characters need confirmation based on additional material. The eyes of the *Q. agonicollis* sp. nov. holotype and the GZG 16188 specimen are found to be proportionally smaller [EyL/ HW(-) = 0.62 resp. 0.65] than in *Q. elpis* (0.72) and the *Q. conservans* sp. nov. holotype (0.72).

***Quasicalathus conservans* Schmidt & Will, sp. nov.**

<http://zoobank.org/1EAF9667-E896-445B-ADED-0DA2B055DF2B>

Material studied. Male in Rovno amber, with specimen label data “SDEI-Amb-002529”, deposited in the Senckenberg Deutsches Entomologisches Institut, Müncheberg, Germany. Size of the amber piece 20 × 10 × 8.5 mm.

Preservation status: The amber is clear but pervaded by numerous small air bubbles and extensive flowlines attached to the embedded fossil that is therefore only partly visible using light microscopy (Figs 32, 33). The exoskeleton of the fossil, including most parts of the aedeagus, is well preserved and, therefore, important diagnostic characters could be reconstructed using micro-CT (Figs 78–89).

Syninclusions: One stellate hair, few tiny dust particles.

Description. Measurements see Table 2.

Standardized body length: 7.3 mm.

Proportions: A3L/HL = 0.44;

EyL/ HW(-) = 0.72;

PW/HW(+) = 1.40;

PW/PL = 1.27;

PW/PWb = 1.11;

PWb/PWa = 1.46;

EW/PW = 1.64;

EL/EW = 1.51;

EpL/EpW = 1.43;

EL/FL = 2.58;

EL/AedL = 3.64.

Head: As described in *Q. elpis*.

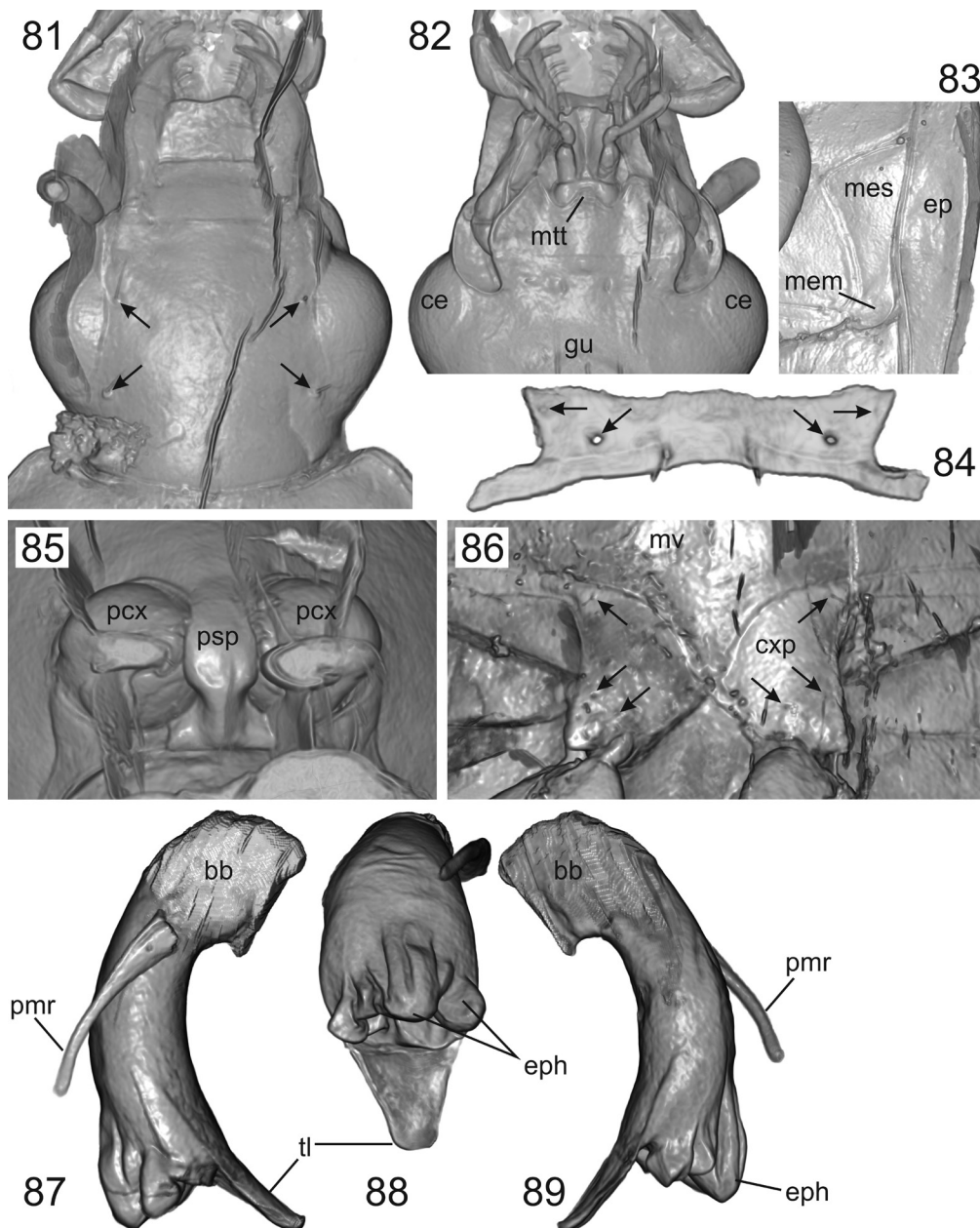
Prothorax: Pronotal lateral margin moderately narrowed toward base, slightly concave before laterobasal angles, angles slightly obtuse (Fig. 78). Prosternal process with traces of a lateral bead (Fig. 85). In all other characters as described for the new genus, above.

Pterothorax: Elytra with basal margin markedly concave and humerus markedly protruded anteriorly; basal margin forming a slightly obtuse angle (ca. 115°) with the lateral margin (Fig. 78). Elytral striae moderately deeply engraved, intervals moderately convex. In all other characters as described for the new genus, above.

Aedeagus: Length of median lobe about 1.33 mm; median lobe terminal lamella moderately long, almost evenly narrowed from base to apex (Fig. 88); terminal lamella almost straight, with tip very slightly bent ventrally (Figs 87, 89). In all other characters as described for the new genus, above.

Differential diagnosis. In external characters, *Q. conservans* sp. nov. appears identical to *Q. elpis*, however, it can be distinguished by the male genitalia. The new species differs by the proportionally larger aedeagus (EL/AedL = 3.64 instead of 4.05 in *Q. elpis*) and by the shape of the median lobe terminal lamella that is nearly evenly narrowed toward the apex if viewed in dorsal aspect and almost straight if viewed laterally (Figs 43, 44 versus 87, 89). *Quasicalathus conservans* sp. nov. differs from the above-described *Q. agonicollis* sp. nov. by larger body (SBL > 7 mm), less obtuse laterobasal pronotal angles, the more markedly concave elytral basal margin, more markedly projected humeri, the less obtuse humeral angle (< 120°), and by the larger aedeagus.

Remarks. *Quasicalathus conservans* sp. nov. and *Q. elpis* are, based on current knowledge,



Figures 81–89. *Quascalathus conservans* sp. nov., volume rendering of the holotype. **81.** Head, dorsal aspect (the arrows point to the insertions of the supraorbital setae); **82.** Head, ventral aspect; **83.** Left external part of metathorax, ventral view; **84.** Submentum (the arrows point to the insertions of the four lateral setae); **85.** Posterior part of prosternum and procoxae; **86.** Posterior part of metasternum and metacoxae; **87–89.** Preserved remains of the aedeagus (**87.** Right lateral aspect; **88.** Dorsal aspect; **89.** Left lateral aspect). Abbreviations: **bb** – basal bulb of aedeagal median lobe; **ce** – compound eye; **cxp** – metacoxal plate; **eph** – partly evaginated lobes of endophallus; **gu** – gula; **mem** – metepimeron; **mes** – metepisternum; **mtt** – mentum tooth; **mv** – metaventricle; **pcx** – procoxa; **pmr** – preserved distal part of right paramere of aedeagal median lobe; **psp** – prosternal process; **sc** – scutellum; **sps** – setae of sensory pit; **tl** – terminal lamella of aedeagal median lobe.

indistinguishable in their external characters but differ clearly in the shape and proportions of the male genitalia. Ball and Nègre (1972) and Schmidt (2018) detailed a similar situation found among many species pairs of Mexican and Himalayan *Calathus* that can only be separated by features of the male genitalia. We hypothesize that *Q. elpis* and *Q. conservans* sp. nov. were most likely allopatric species, distributed in geographically separated parts of the Eocene amber

forests of northern Europe. Under this hypothesis, *Q. elpis* was endemic to the more western part of the Eocene forest and was thus fossilized in Baltic amber, while *Q. conservans* sp. nov. was endemic to the more eastern part of the area and therefore fossilized in Rovno amber. This assumption is consistent with the faunistic data showing that beetle fossils of Baltic and Rovno amber deposits have only few species in common (less than 13%; Matalin et al. 2021).

Conclusions

Sphodrine beetles were present in the Eocene amber producing forest with at least one genus (*Quasicalathus* gen. nov.) including three closely related species that we have identified from Baltic and Rovno amber deposits. However, the presence of the genus *Calathus* and subtribe Calathina in the Eocene forests of Central Europe, as was hypothesized by previous authors, was not substantiated as we found no evidence for this. The systematic limits of our result are due to the fact that apomorphic morphological characters defining Calathina and *Calathus* remain unknown (Schmidt and Will 2020). We propose the new taxon *Quasicalathus* gen. nov. for the *Calathus*-like fossil beetles from Baltic and Rovno amber and place this genus within the “P clade” of Sphodrini (Ruiz et al. 2009), which includes all sphodrine except Atranopsina, but without further affiliation to any of the subtribes. *Quasicalathus* may or may not be a member of Calathina, but it is not representative of Dolichiina, Pristosiina, Sphodrina, or Synuchina due to the absence of their respective group-specific derived characters. As such, *Quasicalathus* could be placed as sister to or a stem-group of any of these subtribes. In order to solve the problem of uncertain taxonomic position of this fossil species group a comprehensive phylogenetic analysis of recent and fossil sphodrine beetles is needed that combines morphological and molecular data in order to present a new basis for understanding character evolution in this group.

In addition to the open question of species-group taxonomy, verifying the true identity and full set of character states of *C. elpis* remains a task for future studies. In the present study, we could not solve this problem simply due to the unavailability of the holotype. Given that *C. elpis* is reported to have two anomalous character states for elytral and metacoxal chaetotaxy as described by Ortuño and Arillo (2009) there is a slight possibility that it represents a fourth fossil species that is not represented in our current material. However, we believe that both the concerning character states—5th elytral interval setose and external posterior seta of metacoxa absent—are simply erroneously attributed to *C. elpis*. This may be resolved when study of the holotype is possible. While the situation is unfortunate at present, our study does show the impact on taxonomic and systematic studies when nomenclatural type specimens are not made available to the scientific community as recommended in The Code (ICZN 1999, Recommendation 72F).

Given that 12 fossil specimens of *Quasicalathus* are now known from Eocene amber deposits, it appears that these beetles were a characteristic element of the amber producing forests of that period. Insect and plant evidence suggests that these amber producing forests grew under warm and humid climatic conditions (Kohlman-Adamska 2001, Alekseev and Alekseev 2016, Sadowski et al. 2017). Taken together, this suggests that the habitat preferences of *Quasicalathus* species were probably like that of the extant Canarian *Lauricalathus* Machado and *Trichocalathus* Bolívar y Pieltain, and the Himalayan *Spinocalathus*

Schmidt. All groups with species adapted to warm, humid forest in the cloud-forest zone of high mountains in lower latitudes (Machado 1992, Schmidt 2018).

Many carabid beetles have denticulate or pectinate tarsal claws including *Abaris* Dejean (Pterostichini), many genera of Lebiini, Cyclosomini, Platynini, and Sphodrini. Denticulate claws probably provide greater grip for movement on irregular and vertical surfaces (Stork 1987) and have been proposed as one of the morphological adaptations to an arboricolous way of life (Erwin 1979, 1985). However, an evolutionary association of pectinate claws and arboreality has been shown to be ambiguous (Ober 2003). Even though there may not be a significant correlation between claw pectination and a fully arboricolous life history, there does seem to be a general tendency for species with pectinate claws to be found in sandy or loose soil habitats if geophilic (e.g., Cyclosomini and *Abaris*) or if more eurytopic, then frequently climbing trunks, rocky cliffs, and herbaceous plants, especially at night, or sheltering under bark (Baehr 1990) during the day. Frequent climbing behaviour would provide an explanation as to how presumably terrestrial beetles that show no evidence of flying at the time of inclusion may have been trapped in tree resin flows in the relatively high numbers observed in *Quasicalathus*. The denticulate tarsal claws found in many sphodrine is considered an apomorphic feature within Sphodrini (Casale 1988) and is proposed as a synapomorphy for the ‘P clade’ of Ruiz et al. (2009). It is possible that the Eocene *Quasicalathus* species represent a group of the ‘P clade’ characterized by propensity to climb, as is known for some extant *Calathus*, *Laemostenus* and *Pristonychus* species (Casale, pers. comm. 2022).

Acknowledgements

We are very grateful to Alexander Gehler (Geoscientific Centre and Museum of the Georg-August-University, Göttingen), Carsten Gröhn (Glinde), and Christel and Hans Werner Hoffeins (Hamburg) for providing amber inclusions for the present study. We thank Achille Casale and Jim Liebherr for their valuable comments that helped us improve the manuscript. The study of JS was supported by the German Research Council (DFG grant SCHM 3005/3-2). The micro-CT machine used at the Rostock University to study the fossil specimens was jointly sponsored by the German Research Council and the country of Mecklenburg-Vorpommern (DFG INST 264/130-1 FUGG).

References

- Alekseev VI, Alekseev PI (2016) New Approaches for Reconstruction of the Ecosystem of an Eocene Amber Forest. *Biology Bulletin* 43: 75–86. <https://doi.org/10.1134/S1062359016010027>
- Bachofen-Echt A (1949) *Der Bernstein und seine Einschlüsse*. Wunderlich Verlag, Straubenhardt, 230 pp. [Reprint 1996] https://doi.org/10.1007/978-3-7091-2303-4_2

- Baehr M (1990) The carabid community living under the bark of Australian eucalypts. In: Stork NE (Ed.) The role of ground beetles in ecological and environmental studies. Intercept, Andover, 3–11.
- Ball GE, Nègre J (1972) The taxonomy of the Nearctic species of the genus *Calathus* Bonelli (Coleoptera: Carabidae: Agonini). Transactions of the American Entomological Society 98: 412–533.
- Bousquet Y (2012) Catalogue of Geadephaga (Coleoptera, Adephaga) of America north of Mexico. Sphodrini – Pseudomorphini. ZooKeys 245(3): 1161–1722. <https://doi.org/10.3897/zookeys.245.3416>
- Casale A (1988) Revisione degli Sphodrini (Coleoptera, Carabidae, Sphodrini). Museo Regionale di Scienze Naturali, Torino, 1024 pp.
- Gomez RA, Will KW, Maddison DR (2016) Are *Miquihuana rhadiniformis* Barr, 1982 and *Pseudamara arenaria* (LeConte, 1847) (Coleoptera, Carabidae) sphodrinids? Phylogenetic analysis of data from next-generation sequencing of museum specimens resolves the tribal-group relationships of these enigmatic taxa. Entomologische Blätter und Coleoptera 112: 149–168.
- Erwin TL (1979) Thoughts on the evolutionary history of ground beetles: hypotheses generated from comparative faunal analyses of lowland forest sites in temperate and tropical regions. In: Erwin TL, Ball GE, Whitehead DR, Halpern AL (Eds) Carabid beetles: their evolution, natural history, and classification. Dr W. Junk, The Hague, 539–592. https://doi.org/10.1007/978-94-009-9628-1_30
- Erwin TL (1985) The taxon pulse: a general pattern of lineage radiation and extinction among carabid beetles. In: Ball GE (Ed.) Taxonomy, phylogeny and zoogeography of beetles and ants. Dr W. Junk, Dordrecht, 437–472.
- Habu A (1978) Fauna Japonica. Carabidae: Platynini. Keigaku Publishing, Tokyo, 447 pp.
- Handlirsch A (1908) Die fossilen Insekten und die Phylogenie der rezenten Formen: Ein Handbuch für Paläontologen und Zoologen, Teil 1. Engelmann, Leipzig, [12 +] 1430 pp. <https://doi.org/10.5962/bhl.title.5636>
- Hoffeins C (2012) On Baltic amber inclusions treated in an autoclave. Polish Journal of Entomology 81: 165–181. <https://doi.org/10.2478/v10200-012-0005-z>
- Hovorka O (2017a) Subtribe Calathina Laporte, 1834. In: Löbl I, Löbl D (Eds) Catalogue of Palearctic Coleoptera, Volume 1. Second edition. Brill Publishers, Leiden, Boston, 760–768.
- Hovorka O (2017b) Subtribe Dolichina Brullé, 1834. In: Löbl I, Löbl D (Eds) Catalogue of Palearctic Coleoptera, Volume 1. Second edition. Brill Publishers, Leiden, Boston, 768–769.
- ICZN [International Commission on Zoological Nomenclature] (1999) International code of zoological nomenclature. 4th edn. International Trust for Zoological Nomenclature, c/o Natural History Museum, London, 306 pp. <https://doi.org/10.5962/bhl.title.50608>
- Jeannel R (1926) Monographie des Trechinae. Morphologie comparée et distribution géographique d'un groupe de Coléoptères (Première livraison). L'Abeille, Paris 32: 221–550.
- Klebs EHR (1910) Über Bernsteineinschlüsse im Allgemeinen und die Coleopteren meiner Bernsteinsammlung. Schriften der Königlichen Physikalisch-ökonomischen Gesellschaft zu Königsberg i. Pr., 51: 217–242.
- Kohlman-Adamska A (2001) A graphic reconstruction of an „amber“ forest. In: Kosmowska-Ceranowicz B (Ed.) The amber treasure trove. Part I. The Tadeusz Giecwicz's collection at the Museum of the Earth, Polish Academy of Sciences, Warsaw, Documentary Studies 18: 15–18.
- Larsson SG (1978) Baltic amber – a palaeobiological study. Entomograph 1: 1–192.
- Lindroth CH (1956) A revision of the genus *Synuchus* Gyllenhal (Coleoptera: Carabidae) in the widest sense, with notes on *Pristosia* Motschulsky (*Eucalathus* Bates) and *Calathus* Bonelli. The Transactions of the Royal Entomological Society of London 108: 485–576. <https://doi.org/10.1111/j.1365-2311.1956.tb01274.x>
- Machado A (1992) Monografía de los carábidos de las Islas Canarias. Instituto de Estudios Canarios, La Laguna, 734 pp.
- Matalin AV, Perkovsky EE, Vasilenko DV (2021) First record of tiger beetles (Coleoptera: Cicindelidae) from Rovno amber, with the description of a new genus and species. Zootaxa 5016(2): 243–256. <https://doi.org/10.11646/zootaxa.5016.2.5>
- Ober K (2003) Arboreality and morphological evolution in ground beetles (Carabidae: Harpalinae): testing the taxon pulse model. Evolution 57(6): 1343–1358. <https://doi.org/10.1111/j.0014-3820.2003.tb00342.x>
- Ober K, Heider TN (2010) Phylogenetic diversification patterns and divergence times in ground beetles (Coleoptera: Carabidae: Harpalinae). BMC Evolutionary Biology 10: e262. <https://doi.org/10.1186/1471-2148-10-262>
- Ortuño VM, Arillo A (2009) Fossil carabids from Baltic amber – A new species of the genus *Calathus* Bonelli, 1810 (Coleoptera: Carabidae: Pterostichinae). Zootaxa 2239: 55–61. <https://doi.org/10.11646/zootaxa.2239.1.5>
- Ruiz C, Jordal B, Serrano J (2009) Molecular phylogeny of the tribe Sphodrini (Coleoptera: Carabidae) based on mitochondrial and nuclear markers. Molecular Phylogenetics and Evolution 50(1): 59–73. <https://doi.org/10.1016/j.ympev.2008.09.023>
- Ruiz C, Jordal BH, Emerson BC, Will KW, Serrano J (2010) Molecular phylogeny and Holarctic diversification of the subtribe Calathina (Coleoptera: Carabidae: Sphodrini). Molecular Phylogenetics and Evolution 55: 358–371. <https://doi.org/10.1016/j.ympev.2009.10.026>
- Ruiz C, Jordal BH, Serrano J (2012) Diversification of subgenus *Calathus* (Coleoptera: Carabidae) in the Mediterranean region – glacial refugia and taxon pulses. Journal of Biogeography 39(10): 1791–1805. <https://doi.org/10.1111/j.1365-2699.2012.02751.x>
- Sadowski E-M, Schmidt AR, Seyfullah LJ, Kunzmann L (2017) Conifers of the ‘Baltic Amber Forest’ and their palaeoecological significance. Stapfia 106: 1–73.
- Schmidt J (2018) Notes on the taxonomy of *Calathus* Bonelli, 1810, with special reference to the *C. heinertzi* group from the Nepal Himalaya (Insecta: Coleoptera: Carabidae: Sphodrini). In: Hartmann M, Barclay MVL, Weipert J (Eds) Biodiversity and Natural Heritage of the Himalaya. Vol. VI. Verein der Freunde und Förderer des Naturkundemuseums Erfurt e.V., Erfurt, 297–318.
- Schmidt J, Belousov I, Michalik P (2016) X-Ray microscopy reveals endophallic structures in a new species of the ground beetle genus *Trechus* Clairville, 1806 from Baltic amber (Coleoptera: Carabidae: Trechini). ZooKeys 614: 113–127. <https://doi.org/10.3897/zookeys.614.9283>
- Schmidt J, Michalik P (2017) The ground beetle genus *Bembidion* Latreille in Baltic amber: Review of preserved specimen and first 3D reconstruction of endophallic structures using X-ray microscopy (Coleoptera: Carabidae: Bembidiini). ZooKeys 662: 101–126. <https://doi.org/10.3897/zookeys.662.12124>
- Schmidt J, Scholz S, Kavanaugh DH (2019) Unexpected findings in the Eocene Baltic amber forests: Ground beetle fossils of the tribe Nebriini (Coleoptera: Carabidae). Zootaxa 4544(1): 103–112. <https://doi.org/10.11646/zootaxa.4701.4.2>

- Schmidt J, Scholz S, Maddison DR (2021) *Balticeler kerneggeri* gen. nov., sp. nov., an enigmatic Baltic amber fossil of the ground beetle subfamily Trechinae (Coleoptera, Carabidae). – Deutsche Entomologische Zeitschrift 68(1): 207–224. <https://doi.org/10.3897/dez.68.66181>
- Schmidt J, Will K (2020) A new subgenus for “*Acalathus*” *advena* (LeConte, 1846) and the challenge of defining Calathina based on morphological characters (Coleoptera, Carabidae, Sphodrini). Zootaxa 4544(4): 581–588. <https://doi.org/10.11646/zootaxa.4722.4.2>
- Sciaky R, Facchini S (1997) *Xestopus cyaneus* new species from China (Coleoptera Carabidae). Bolletino della Società Entomologica Italiana 129(3): 235–240.
- Sciaky R, Wrase DW (1998) Two new genera of Sphodrini Dolichina from China (Coleoptera Carabidae). Bolletino della Società Entomologica Italiana 130(3): 221–232.
- Spahr U (1981) Systematischer Katalog der Bernstein- und Kopal-Käfer (Coleoptera). Stuttgarter Beiträge zur Naturkunde, Serie B, 80: 1–107.
- Standke H (2008) Bitterfelder Bernstein gleich Baltischer Bernstein? – Eine geologische Raum – Zeit – Betrachtung und genetische Schlußfolgerungen. Exkursionsführer und Veröffentlichungen der Deutschen Gesellschaft für Geowissenschaften 236: 11–33.
- Stork N (1987) Adaptations of arboreal carabids to life in trees. Acta Phytopathologica et Entomologica Hungarica 22: 273–291.

Revision of the genus *Woldstedtius* Carlson, 1979 (Hymenoptera, Ichneumonidae, Diplazontinae) from Japan

Shunsuke Morishita¹, Kyohei Watanabe²

¹ Hatchodori 4–9, Toyohashi, Aichi 440–0806, Japan

² Kanagawa Prefectural Museum of Natural History, Iryuda 499, Odawara, Kanagawa 250–0031, Japan

<http://zoobank.org/C402CAE8-14FD-402A-AD05-54646B1493E8>

Corresponding author: Shunsuke Morishita (ezogengoroumodoki4.23@gmail.com)

Academic editor: Jose Fernandez-Triana ♦ Received 15 January 2022 ♦ Accepted 10 March 2022 ♦ Published 4 April 2022

Abstract

Japanese species of the genus *Woldstedtius* Carlson, 1979 are revised. Nine species are recorded from Japan, including two new species, *W. alpicola* sp. nov. and *W. punctatus* sp. nov. *Woldstedtius biguttatus* (Gravenhorst, 1829) is newly recorded from Japan. Taxonomic status of *W. flavolineatus kuroashii* (Uchida, 1957) is changed from the subspecies of *W. flavolineatus* (Gravenhorst, 1829) to a separated species. *Woldstedtius holarcticus* (Diller, 1969) is newly synonymized under *W. kuroashii* (Uchida, 1957). A key to Japanese species of this genus is provided.

Key Words

Asia, fauna, new species, parasitoid wasps, taxonomy

Introduction

The Ichneumonid subfamily Diplazontinae comprises 23 genera and more than 350 species worldwide (Yu et al. 2016). The host range of species in this subfamily appears to be notably narrow, with all confirmed hosts being species of hoverfly (Diptera, Syrphidae). The only exceptions in this regard are two species in the ichneumonid genus *Bioblapsis* Förster (Klopfstein 2014). The genus *Woldstedtius* Carlson, 1979 is a relatively large taxon comprising 44 species distributed in the Australasian, Holarctic, Neotropical, Oceanic, and Oriental regions (Balueva and Lee 2016; Vas 2016; Yu et al. 2016; Johansson 2020). Although the genus has been revised by Klopfstein (2014) for the Western Palearctic species, by Dasch (1964) for the Nearctic species and by Gauld et al. (1997) for the Costa Rican species, members in the Eastern Palearctic region have only been partially studied. Manukyan (2007), for example, provided a key to the six species of this genus known from Far East Russia, and Balueva and Lee (2016) have reviewed the South Korean species. In Japan, seven species have been formally recorded to

date (Yu et al. 2016), however, we have found specimens of some unidentified species and identified a number of unresolved taxonomic problems. Nevertheless, given the large number of previous studies in other regions, this genus may be an adequate taxon for comparison of the fauna with that in other parts of the world.

The purpose of this study was to undertake a taxonomic review of the Japanese species of *Woldstedtius*. We have also produced a key to the Japanese species of this genus, which is presented herein.

Materials and methods

In this study, the dried specimens deposited in the following collections were examined:

- AEIC** American Entomological Institute, Logan, Utah, USA;
KPMNH Kanagawa Prefectural Museum of Natural History, Odawara, Kanagawa, Japan;
MU Meijo University, Nagoya, Aichi, Japan;

NSMT	National Museum of Nature and Science, Tsukuba, Ibaraki, Japan;
SEHU	Systematic Entomology, Hokkaido University, Sapporo, Japan;
TMNH	Toyohashi Museum of Natural History, Toyohashi, Aichi, Japan;
ZSM	Zoologische Staatssammlung München, Germany.

Stereomicroscopes (SMZ745 and SMZ800: Nikon, Tokyo) were used for observation. Photographs (Figs 1, 2, 4–7) were taken by digital camera (TG-4: Olympus, Tokyo) attached to the stereomicroscope (SMZ800). Photographs (Figs 3, 8) were taken by digital camera (CX6: RICOH, Tokyo) attached to the stereomicroscope (SMZ745). Digital images (Figs 1–9) were edited using Adobe Photoshop.

Morphological terminology mainly follows those established by Broad et al. (2018). The following abbreviations are used in description, diagnosis, and remarks: ocello-ocular line (**OOL**), postocellar line (**POL**), diameter of lateral ocellus (**OD**), segments of flagellomeres (**FL**), segments of maxillary palp (**MP**), metasomal tergites (**T**) and holotype (**HT**). The following abbreviations are used in material data: female (**F**), male (**M**), flight interception trap (**FIT**), light trap (**LT**), Malaise trap (**MT**) and yellow pan trap (**YPT**).

Results and discussion

Woldstedtius flavolineatus kuroashii (Uchida 1957) was originally described based on a single female, for which no morphological information, apart from the coloration of mesosoma and legs, is available. Therefore, we examined Japanese specimens of *W. f. kuroashii*, including the holotype, and compared these with the identified European specimens of *W. f. flavolineatus* deposited in ZSM (identified by Diller). On the basis of these comparison, we established that certain character states of *W. f. kuroashii* are clearly different from those of *W. f. flavolineatus*, and accordingly conclude that this subspecies should be treated as a separate species, *W. kuroashii*.

Woldstedtius holarcticus Diller, 1969 resembles *W. kuroashii* in terms of color and body structures. In Japan, Manukyan (2007) recorded this species from Kunashiri Island, although no additional specimens of the species have been recorded elsewhere in Japan. We compared the Japanese specimens of *W. kuroashii*, including holotype, with a paratype of *W. holarcticus* deposited in ZSM. As we detected no clear differences between the two taxa, we propose that *W. holarcticus* should be synonymized under the name *W. kuroashii*. Diller (1969) noted that females of *W. holarcticus* (= *W. kuroashii*) can be distinguished from those of *W. flavolineatus* with respect to coloration of the coxae, the proportions of the hind tibia and tarsus, and surface gloss of the body, and also established that the females of *W. holarcticus* (= *W. kuroashii*) can be

distinguished from those of *W. f. flavolineatus* based on the medially flattened face (medially convex in *W. f. flavolineatus*). We confirmed this character state and established that the face is slightly convex medially in both *W. kuroashii* and *W. f. flavolineatus*, although this feature is weaker in the former than in the latter (Fig. 9A, B). However, given the overlap in the intraspecific variation of this character state, it cannot be reliably used to differentiate the two species. The leg coloration (with the exception of the coxae) of *W. kuroashii* collected from Honshu (including the holotype) is darker compared with that of some Japanese specimens collected from Hokkaido and female paratypes of *W. holarcticus* (blackish-brown to black) (orange to brown in some Japanese specimens collected from Hokkaido and the paratype of *W. holarcticus*). As a consequence of these comparisons, we detected no significant differences with respect to other character states of these specimens, and accordingly conclude that the observed variation is intraspecific variation within a single species.

In this study, we identified specimens of *W. biguttatus* from Japan for the first time. This species closely resembles *W. flavolineatus*, and indeed, some *W. biguttatus* specimens have been incorrectly recorded as *W. flavolineatus* e.g., Konishi et al. (2014) and Morishita et al. (2021). In contrast, we were unable to find any specimens of *W. flavolineatus* that have been collected in Japan. Given that some of the voucher specimens of the previous studies could not be reliably identified owing to inadequate labeling, we have certain reservations as to the Japanese distribution records of *W. flavolineatus*, and accordingly recommend a further re-examination of the distribution of this species.

On the basis of the aforementioned taxonomic treatments, we conclude that a total of nine species in the genus *Woldstedtius* have been found in Japan to date.

Taxonomy

Subfamily Diplazontinae Viereck, 1918

Genus *Woldstedtius* Carlson, 1979

Type. *Bassus biguttatus* Gravenhorst, 1829: 332. Original designation.

Diagnosis. According to Klopstein (2014), this genus can be distinguished from other genera by the following combination of character states: antenna without tyloids in males; mesoscutum without notauli; fore wing areolet absent; hind tibia usually black with a white base, in males with light coloration often extending to half the length of the tibia, rarely hind tibia all dark or yellow or orange with a dark apex; ovipositor sheaths transversely truncate and open towards apex; very even, weakly coriaceous microsculpture.

Remarks. Japanese species can be identified by the following key.

Key to Japanese species of *Woldstedtius* (males of *W. takagii* and *W. yokohamensis* are unknown)

- 1 Hind coxa white with a brown dorsal stripe in females (Fig. 4A). Face blackish-brown to black with a white median spot, this spot connected with white clypeus in females (Fig. 4B), entirely white in males (Fig. 4F). Scutellum with large white marking (Fig. 4C). Latero-median carina of T I short, along less than basal 0.3 of T I (Fig. 9H) *W. karafutensis* (Uchida, 1957) (female and male)
- Above combination of character states lacking. Hind coxa entirely black or entirely orange in females (Figs 1A, 2A, 3A, 5A, 6A, 7A, 8A). Coloration of face various in females. Scutellum entirely black or black with a whitish-yellow to yellow apical spot (Figs 1C, 2C, 3C, 5C, 6C, 7C, 8C). Latero-median carina of T I long, along more than basal 0.4 of T I (Fig. 9E–G, I–K) 2
- 2 Hind coxa entirely black in both sexes (Figs 1A, 5A, 6A, E, 7A, 8A) 3
- Hind coxa entirely orange in females (Figs 2A, 3A), entirely or largely yellow to reddish-yellow and usually with a blackish-brown dorsal stripe in males (Figs 1E, 2E, 3E, 5E) 7
- 3 Inner orbits divergent downward (Figs 7B, 9C). Face 2.6–2.9 × as broad as high. Basal 0.2 of propodeum weakly protruded in lateral view (Fig. 9D). Yellow shoulder marks of mesoscutum absent (Fig. 7A) *W. takagii* (Uchida, 1957) (female)
- Inner orbits almost parallel (Figs 1B, 5B, 6B, 8B). Face less than 2.5 × as broad as high. Basal 0.2 of propodeum not protruded in lateral view. Yellow shoulder marks of mesoscutum present (Figs 1A, 5A, 6A, 8A) 4
- 4 Scutellum coarsely and densely punctate (separated by ca. 0.8–1.3 × their diameter) and entirely black (Fig. 6C). Propodeum rugulose (Fig. 6D) *W. punctatus* sp. nov. (female and male)
- Scutellum finely and sparsely punctate (separated by ca. 1.5–2.5 × their diameter) and black with a whitish-yellow to yellow apical spot (Figs 1C, 5C, 8C). Propodeum coriaceous or at least finely rugulose 5
- 5 Face black with a pair of yellow spots along inner orbits (Fig. 8B). Scutellum finely and densely punctate (separated by ca. 1.0 × their diameter) *W. yokohamensis* (Uchida, 1957) (female)
- Face black with a whitish-yellow to yellow median spot (Figs 1B, 5B). Scutellum finely and sparsely punctate (separated by ca. 1.5–2.5 × their diameter) (Figs 1C, 5C) 6
- 6 T I 1.4–1.5 × as long as maximum width. Propodeum finely rugulose (Fig. 1D). Hind trochanter black (Fig. 1A). Pleural carina of propodeum entirely present *W. alpicola* sp. nov. (female)
- T I 1.1–1.25 × as long as maximum width. Propodeum coriaceous (Fig. 5D). Hind trochanter white (Fig. 5A). Pleural carina of propodeum absent posteriorly *W. kuroashii* (Uchida, 1957) (female)
- 7 Inner orbits divergent downward. Antenna with 19–21 (rarely 22) flagellomeres. Metasoma entirely black or black with some orange markings in females *W. citropectoralis* (Schmiedeknecht, 1926) (female and male)
- Inner orbits almost parallel in females (Figs 2B, 3B), weakly divergent downward in males (Figs 1F, 2F, 3F, 5F). Antenna with 22–25 flagellomeres. Metasoma entirely black in females 8
- 8 Mesoscutum without yellow shoulder marks in females (Fig. 2A). Face entirely black or black with a small median yellow or brown spot in females (Fig. 2B). Mesopleuron with a yellow ventral marking (Fig. 2E) in males. Mesosternum black in males (Fig. 2E) *W. biguttatus* (Gravenhorst, 1829) (female and male)
- Mesoscutum with yellow shoulder marks in females (Fig. 3A). Face black with a large yellow median spot in females (Fig. 3B). Mesopleuron with a large whitish-yellow to yellow marking; it is enlarged anteriorly in males (Figs 1E, 3E, 5E). Mesosternum yellow in males (Figs 1E, 3E, 5E) 9
- 9 Propodeum finely rugulose (e.g., Fig. 1D), with a complete pleural carina. Bases of T IV to T VII each with a transverse yellow band *W. alpicola* sp. nov. (male)
- Propodeum coriaceous (e.g., Figs 3D, 5D), with a pleural carina absent posteriorly in both sexes. Coloration of T IV to T VII various in males 10
- 10 Bases of T III and T IV each with a transverse yellow basal band in males. T I entirely coriaceous *W. flavolineatus* flavolineatus (Gravenhorst, 1829) (female and male)
- T III with a pair of whitish-yellow apical spots (sometimes these spots connected each other). T IV and T V each with a transverse whitish-yellow apical band. T I coriaceous, with irregular rugae laterally *W. kuroashii* (Uchida, 1957) (male)

***Woldstedtius alpicola* sp. nov.**

<http://zoobank.org/E030CAC0-73B1-4BDC-BD63-F5E6BD3BAC4B>
Figs 1A–F, 9E

Type series. *Holotype*: F, Japan, Honshu, Mie Pref., Inabe City, Mt. Fujiwaradake, 1 Jun 2021, S. Morishita leg. (KPMNH). *Paratypes*: Japan: [Honshu] 1 F, Yamanashi Pref., Kosu City, Mt. Daibosatsu, Kaminikkawa-toge,

16 Jun 2007, K. Watanabe leg. (TMNH); 1 M, Kanagawa Pref., Yamakita Town, Mt. Oomuroyama–Mt. Kanyuudousan, 15 Jun 2008, H. Kawai leg. (KPMNH); 1 F, Nagano Pref., Otaki Vil., Mt. Ontakesan, 13–25 Jul 2015, S. Shimizu leg. (MT) (KPMNH).

Description. Female (n = 3). Body length 8.5–9.2 (HT: 8.5) mm, polished, coriaceous and covered with silver setae.

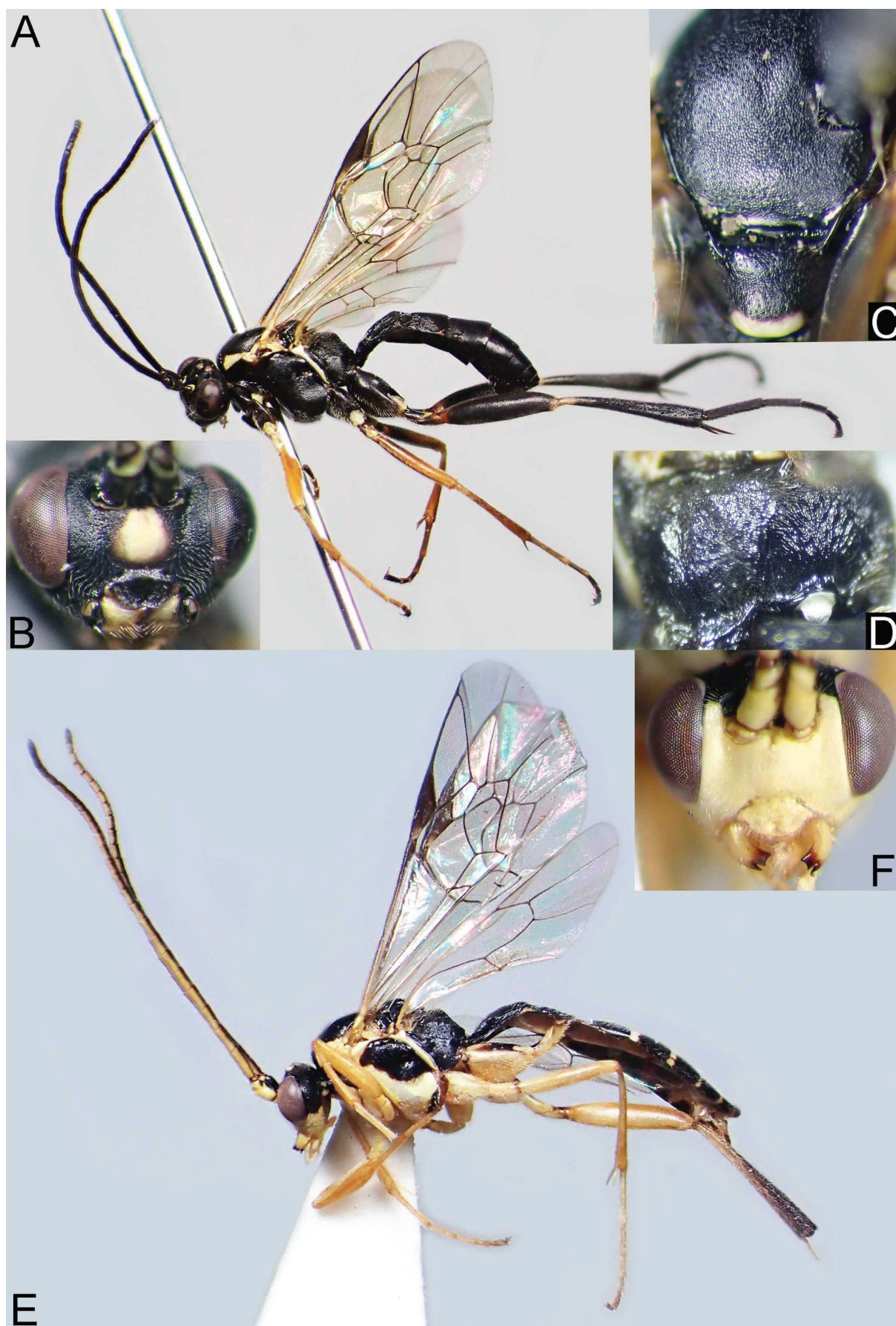


Figure 1. *Woldstedtius alpicola* sp. nov. (A–D. female, holotype; E, F. male, paratype) — A, E. Habitus; B, F. Head, frontal view; C. Mesonotum, dorsal view; D. Propodeum, dorsal view.

Head 0.51–0.54 (HT: 0.53) × as long as wide. Clypeus 2.0–2.35 (HT: 2.0) × as broad as high, slightly convex basally in lateral view. Face 2.1–2.4 (HT: 2.4) × as broad as high, densely punctate, convex medially in lateral view and separated from clypeus by shallow clypeal sulcus. Inner orbits almost parallel (Fig. 1B). Length of malar space 0.9–1.15 (HT: 0.9) × as long as basal mandibular width. POL 1.9–2.1 (HT: 1.9) × as long as OD. OOL 0.9–1.18 (HT: 0.9) × as long as OD. POL 1.86–1.95 (HT: 1.86) × as long as OOL. Antenna with 24–25 (HT: 24) flagellomeres. FL I 1.29–1.35 (HT: 1.35) × as long as FL II. MP IV 1.42–1.53 (HT: 1.53) × as long as MP V.

Mesosoma. Lateral aspect of pronotum strigose anteriorly. Mesoscutum finely and densely punctate (separated by ca. 1.0 × their diameter) (Fig. 1C). Scutellum finely and sparsely punctate (separated by ca. 1.5–2.5 × their diameter) (Fig. 1C). Anterior part and lower half of mesopleuron coarsely and densely punctate. Speculum smooth. Sternaulus weakly impressed. Propodeum finely rugulose (Fig. 1D), rounded in lateral view and pleural carina entirely present. Fore wing length 7.4–8.5 (HT: 7.4) mm. Nervellus intercepted below middle. Hind femur 4.7–5.3 (HT: 4.7) × as long as maximum depth in lateral view. Hind tibia 7.5–8.0 (HT: 8.0) × as long as maximum depth in lateral view. Ratio of length of hind first to fifth tarsomeres 1.0: 0.6: 0.4: 0.2: 0.2–0.3 (HT: 0.2).

Metasoma. T I rectangular in dorsal view (Fig. 9E), 1.4–1.5 (HT: 1.4) × as long as maximum width, irregular rugulose laterally, sometimes striate between latero-median carinae. Latero-median carina present basal ca. 0.5 of T I (Fig. 9E). T II 0.6–0.73 (HT: 0.73) × as long as maximum width, striate anteriorly and strigose laterally.

Coloration (Fig. 1A–D). Body (excluding wings and legs) black. Face with a large yellow spot medially. Palpi, subtegular ridge and mesepisternum yellow. Mandible yellow, except for apex and base. Lateral aspect of pronotum with a yellow spot posteriorly. Mesoscutum with yellow shoulder marks. Tegula tinged with yellow anteriorly. Scutellum with a yellow spot apically. Wings hyaline. Veins and pterostigma blackish-brown except for yellowish-brown wing base. Legs blackish-brown to black. Fore trochanter, trochantellus, apex of hind femur and base of hind tibia tinged with white. Fore femur, tibia and tarsomeres orange to brown. Apex of hind trochantellus and base of hind femur tinged with reddish-brown.

Male (n = 1). Similar to female. Body length (excluding antennae) 8.1 mm. Face 2.5 × as broad as high. Length of malar space 0.8 × as long as basal mandibular width. POL 2.2 × as long as OD. OOL 1.2 × as long as OD. POL 2.1 × as long as OOL. Inner orbits weakly divergent downward (Fig. 1F). Fore wing length 6.3 mm.

Coloration (Fig. 1E, F). Body (excluding wings and legs) black. Clypeus, palpi, face, ventral surface of antenna, malar space, propleuron, epicnemium, mesosternum, tegula, subtegular ridge and mesepisternum yellow. Gena tinged with yellow ventrally. Mandible yellow, except for apex. Lateral aspect of pronotum tinged with yellow ventrally and posteriorly. Mesopleuron with a large yellow

marking, it enlarged anteriorly. Scutellum with a yellow spot apically. T IV to T VII with a transverse yellow band posteriorly. Wings hyaline. Veins and pterostigma brown to blackish-brown except for yellow wing base. Legs yellow to yellowish-brown. Hind coxa and trochanter each with a blackish-brown stripe dorsally. Hind trochantellus and tibia tinged with blackish-brown.

Distribution. Japan (Honshu).

Bionomics. Host unknown. Adults were collected in broad-leaved forest at altitudes of ca. 1,000–2,000 meters.

Etymology. The species name refers that this species inhabits alpine region.

Remarks. This species resembles *W. kuroashii* but can be distinguished from the latter by the following combination of character states: pleural carina of propodeum entirely present in both sexes (absent posteriorly in both sexes of *W. kuroashii*); propodeum finely rugulose in both sexes (coriaceous in both sexes of *W. kuroashii*); T I 1.4–1.5 × as long as maximum width in both sexes (1.1–1.25 in females, 1.14–1.26 in males of *W. kuroashii*). This species also resembles a Korean species, *W. pallidus* Balueva & Lee, 2016 (male is unknown), but can be distinguished by the following combination of character states in females: a large yellow median spot of face present (absent in *W. pallidus*); antenna with 24–25 flagellomeres (22–23 in *W. pallidus*); scutellum finely and sparsely punctate on coriaceous background (entirely coriaceous in *W. pallidus*); propodeum finely rugulose (coriaceous in *W. pallidus*).

Woldstedtius biguttatus (Gravenhorst, 1829)

Figs 2A–F, 9F

Bassus biguttatus Gravenhorst, 1829: 332.

Bassus rufipes Gravenhorst, 1829: 337. Name preoccupied.

Bassus confusus Woldstedt, 1874: 63. Synonymized by Morley (1906).

Syrphoctonus flavolineatus: Konishi et al. 2014: 491. Misident (at least in part).

Woldstedtius flavolineatus: Morishita et al. 2021: 53. Misident.

Materials examined. JAPAN: [Hokkaido] 1 F, Hokkaido, Nemuro, Shibetsu, Rubesu, 25–28 Aug 1971, K. Yamagishi leg. (MU); 1 F, Hokkaido, Sapporo, 20 May 1967, K. Kusigemati leg. (SEHU). [Honshu] 1 F, Gunma Pref., Katashina Vil., Marunuma, Yuzawa, 2 Jul 2008, K. Watanabe leg. (KPMNH); 1 F, Saitama Pref., Honjo City, Okubo-yama, 1 Apr 2001, N. Shimizu leg. (KPMNH); 1 F, Saitama Pref., Sate City, Makinoji, 6 Apr 2009, S. Yoshizawa leg. (KPMNH); 2 F, Tokyo, Chiyoda, Imperial Palace, Fukiagegyoen 20 May–19 Jun 1996, K. Konishi leg. (MT) (NSMT); 1 F, Tokyo, Chiyoda, Imperial Palace, Fukiagegyoen, Kajuen, 17–24 Sep 2009 (MT) (NSMT); 1 F & 1 M, ditto, 14–21 Oct 2009 (MT) (NSMT); 1 M, ditto, 13–20 Apr 2010 (MT) (NSMT); 1 F, ditto, 11–18 May 2010 (MT) (NSMT); 1 M, Tokyo, Chiyoda, Imperial Palace, Fukiagegyoen, Otakinagare, 29 Mar–6 Apr 2009 (MT) (NSMT); 1 F, ditto, 12–17 May 2011 (MT) (NSMT); 1 F, ditto, 17–24 May 2011 (MT)

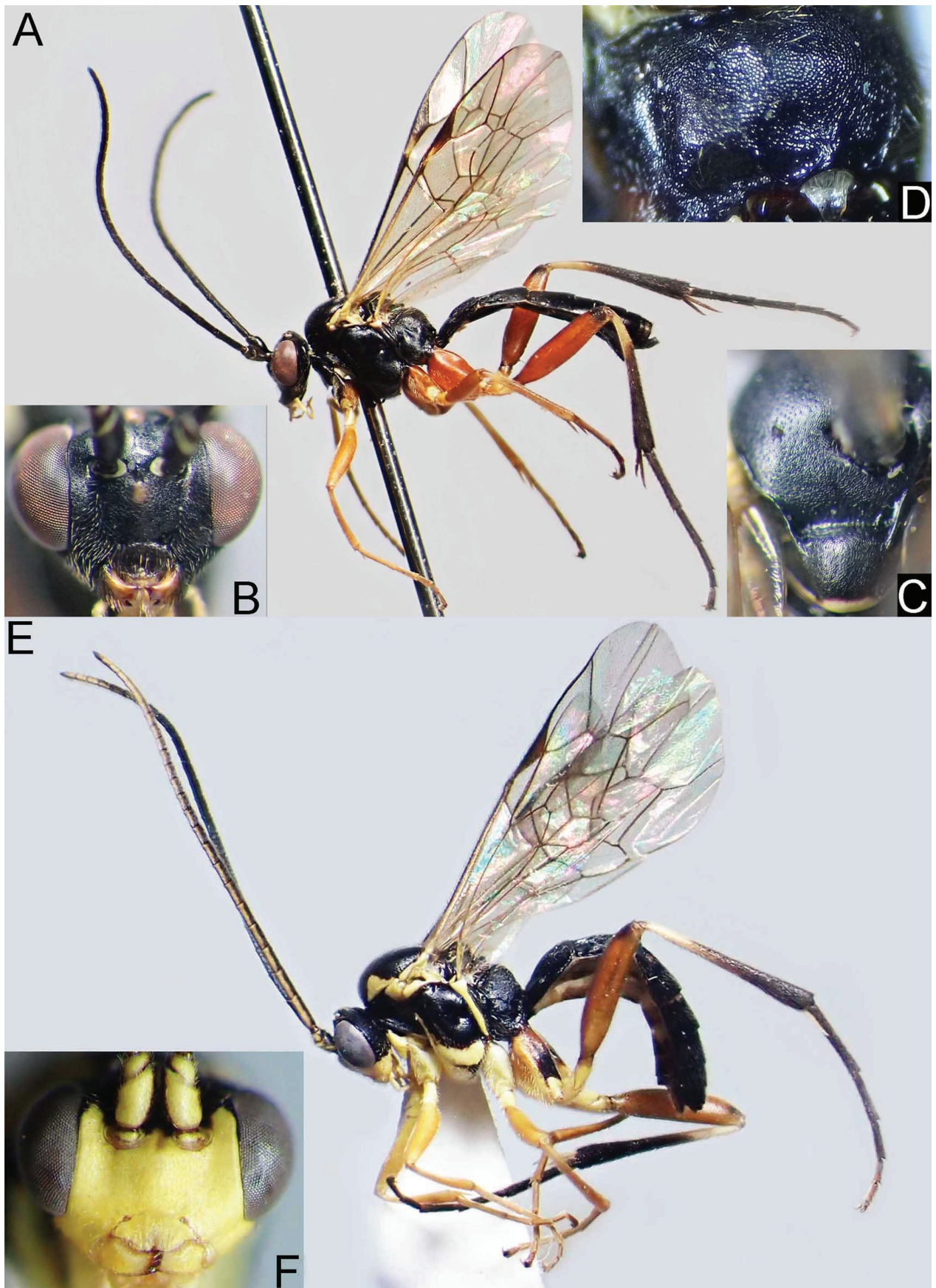


Figure 2. *Woldstedtius biguttatus* (Gravenhorst, 1829) (A–D. female; E, F. male) — A, E. Habitus; B, F. Head, frontal view; C. Mesonotum, dorsal view; D. Propodeum, dorsal view.

(NSMT); 1 F, Tokyo, Chiyoda, Imperial Palace, Biol. Inst., nr. Paddy field, 12–17 May 2011 (MT) (NSMT); 1 F, Tokyo, Chiyoda, Imperial Palace, Dokan-shinmichi, 7–14 Oct 2009 (MT) (NSMT); 1F & 1 M, ditto, 21–28 Oct 2009 (MT) (NSMT); 4 F & 1 M, ditto, 28 Oct–4 Nov 2009 (MT) (NSMT); 2 F & 1 M, ditto, 11–18 Nov 2009 (MT) (NSMT); 1 M, ditto, 18–24 Nov 2009 (MT) (NSMT); 1 F & 4 M, ditto, 24 Nov–7 Dec 2009 (MT) (NSMT); 1 M, ditto, 3–17 Mar 2010 (MT) (NSMT); 3 M, ditto, 29 Mar–6 Apr 2010 (MT) (NSMT); 2 F, ditto, 6–13 Apr 2010 (MT) (NSMT); 1 F, ditto, 27 Apr–4 May 2010 (MT) (NSMT); 3 F, ditto, 4–11 May 2010 (MT) (NSMT); 6 F & 2 M, ditto, 25 May–1 Jun 2010 (MT) (NSMT); 1 M, Tokyo, Chiyoda, Imperial Palace, Dokan-bori, 23 Mar 2010, K. Watanabe leg. (MT) (NSMT); 2 M, Tokyo, Ome City, Mt. Otsukayama, 1 Jun 2008, M. Irie leg. (KPMNH); 3 M, Tokyo, Ome City, Mt. Mitakesan, 1 Jun 2008, M. Gunji leg. (KPMNH); 1 F, Kanagawa Pref., Fujisawa City, Ishikawa, 11 May 2001, I. Waki leg. (NSMT); 1 F, Kanagawa Pref., Ebina City, Sagamigawa, 13 Apr 2006, M. Ooishi & R. Watanabe leg. (YPT) (KPMNH); 1 F, Kanagawa Pref., Chigasaki City, Serizawa, 10 May 2013, K. Watanabe leg. (KPMNH); 1 F, Kanagawa Pref., Atsugi City, Funako, Tokyo University of Agriculture, 6 May–7 Jun 2016, Y. Kato & S. Koizumi leg. (MT) (KPMNH); 1 M, ditto, 22 Apr–16 May 2016, Y. Kato & S. Koizumi leg. (MT) (KPMNH); 1 M, Kanagawa Pref., Atsugi City, Tokyo University of Agriculture, 2 Apr 2009, H. Katahira leg. (KPMNH); 1 M, Kanagawa Pref., Oiso Town, Koma, Komayama, 16 Apr 2016, K. Watanabe leg. (KPMNH); 4 M, Kanagawa Pref., Nakai Town, Zoushiki, 16 Apr 2019, K. Watanabe leg. (KPMNH); 1 F, Kanagawa Pref., Kiyokawa Vil., 4 Oct 2008, Y. Oogane leg. (KPMNH); 2 F, Kanagawa Pref., Hadano City, Koubouyama, 1 May 2016, K. Watanabe & H. Utsugi leg. (KPMNH); 2 M, ditto, 18 Apr 2010, K. Watanabe leg. (KPMNH); 1 F, Kanagawa Pref., Hadano City, Chimura, Mt. Zukkoyama, 16 Apr 2017, K. Watanabe leg. (KPMNH); 1 M, ditto, 7 May 2017, K. Watanabe leg. (KPMNH); 1 F, Kanagawa Pref., Tennoujione, 29 Jun 2013, (FIT) (KPMNH); 3 M, Kanagawa Pref., Kaisei Town, Kanaishima, 22 Mar 2016, K. Watanabe leg. (KPMNH); 1 F, Kanagawa Pref., Odawara City, Kuno, 24 Mar 2014, K. Watanabe leg. (KPMNH); 1 M, ditto, 24 Mar 2014, K. Watanabe leg. (KPMNH); 1 F, Kanagawa Pref., Odawara City, Kamisoga, 29 Apr 2017, K. Watanabe leg. (KPMNH); 1 F, Kanagawa Pref., Yamakita Town, Hinokiboramaru, 6 Aug 2014, T. Taniwaki leg. (KPMNH); 1 F, Kanagawa Pref., Yamakita Town, Mt. Oomuroyama–Mt. Kanyuudousan, 15 Jun 2008, H. Kawai leg. (KPMNH). 1 F, Yamanashi Pref., Kosu City, Enzanushioku, Sagashio, 12 Jun 2010, K. Watanabe leg. (KPMNH); 1 F, Yamanashi Pref., Hokuto City, Masutomi, Biwakubo-sawa, 28 Jul 2007, K. Watanabe leg. (KPMNH); 1 F, Yamanashi Pref., Yamanakako Vil., Hirano, Mikuni-toge, 8 Aug 2020, S. Morishita leg. (TMNH); 3 F, Shizuoka Pref., Shizuoka City, Umegashima, 3 Jun 2001, T. Sugiyama leg. (YPT) (MU); 2 F, ditto, 18 Jun 2001, T. Sugiyama leg. (YPT) (MU); 2 F, ditto, 18 Jun–2 Jul 2001, T. Sugiyama leg. (MT) (MU); 1 F, ditto, 17 Jul–5 Aug 2001, T. Sugiyama leg. (MT) (MU); 1 F, Aichi Pref., Shitara Town, Tsuguhonsawa, 7 May–26 Jun 2020, S. Morishita leg. (MT) (TMNH); 1 F, ditto, 17 Jun 2019, S. Morishita leg. (TMNH); 1 F, ditto, 5 Jul 2019, S. Morishita leg. (TMNH); 1 F, Aichi Pref., Shinshiro City, Tsukudeiwanami, 17 May 2019, S. Morishita leg. (TMNH); 1 M, ditto, 2 May 2019, S. Morishita leg. (TMNH); 3 F & 4 M, Aichi Pref., Toyohashi City, Hosoya, Kitahosoya, 6 Apr 2019, S. Morishita leg. (TMNH); 1 F, Aichi Pref., Toyohashi City, Unoya, Nabeyamashita, 10 Apr 2019, S. Morishita leg. (TMNH); 1 F & 1 M, ditto, 30 Apr 2019, S. Morishita leg. (TMNH); 2 M, Aichi Pref., Toyohashi City, Oiwa, Taimatsu-toge, 6 Apr 2021, S. Morishita leg. (TMNH); 1 F, Aichi Pref., Toyohashi City, Imure, Takayama, 2 Jun–6 Jun 2019, S. Morishita leg. (MT) (TMNH); 1 F, Aichi Pref., Toyohashi City, Nishiiwata, 12 Jul 2018, S. Morishita leg. (TMNH); 1 M, ditto, 3 May 2019, S. Morishita leg. (TMNH); 3 M, Aichi Pref., Toyokawa City, Mikami-cho, 15 Sep 2019, S. Morishita leg. (TMNH); 1 M, Aichi Pref., Kasugai City, Takagi, 19 May 2017, M. Sugiura leg. (MU); 2 F, Aichi Pref., Toyota City, Sanage, 30 Apr–6 May 2002, M. Kiyota leg. (MT) (MU); 1 F, Aichi Pref., Asuke Town, Tanoshiri, 15–24 May 2005, Y. Nishimura leg. (MT) (MU); 1 F, ditto, 15–21 Jun 2005, Y. Nishimura leg. (MT) (MU); 1 F, ditto, 15–21 Jun 2005, J. Yamagiwa leg. (MT) (MU); 1 F, ditto, 13–19 Jul 2005, Y. Nishimura leg. (MT) (MU); 1 F, Aichi Pref., Nisshin City, Komenogi, 28 May–3 Jun 2011, H. Seo leg. (MT) (MU); 1 F, Aichi Pref., Nisshin City, Nokata, 28 May–3 Jun 2011, H. Seo leg. (MT) (MU); 1 F, Aichi Pref., Ichinomiya City, 14–20 Oct 2006, C. Ueshima leg. (MT) (MU); 1 M, Gifu Pref., Kani City, Katabira 3–9 Apr 2004, K. Ito leg. (MT) (MU); 1 M, ditto, 10–16 Apr 2004, K. Yamagishi leg. (MT) (MU); 2 F, ditto, 17–23 Apr 2004, K. Ito leg. (MT) (MU); 1 M, ditto, 1–7 May 2004, K. Ito leg. (MT) (MU); 1 M, ditto, 15–21 May 2004, K. Ito leg. (MT) (MU); 1 F, Nagano Pref., Kawakami Vil., Azusayama, 14 Jun 2015, K. Watanabe leg. (KPMNH); 1 F, Nagano Pref., Nagawa Town, Daimon, 27 Aug 2011, S. Fujie leg. (KPMNH); 1 F, Nagano Pref., Otaki Vil., Mt. Ontakesan, Hakkaisan, 8 Aug 2010, K. Watanabe leg. (KPMNH); 1 F, ditto, 25 Jun–15 Jul 2015, S. Shimizu leg. (MT) (KPMNH); 1 F, Toyama Pref., Mt. Jodosan, 7 Jun 1972, M. Watanabe leg. (KPMNH); 1 M, Toyama Pref., Toyama City, Inonedani, 7–14 Jul 2009, M. Watanabe leg. (MT) (KPMNH); 1 M, ditto, 8–15 Sep 2009, M. Watanabe leg. (MT) (KPMNH); 1 M, ditto, 15–22 Sep 2009, M. Watanabe leg. (MT) (KPMNH); 1 M, Toyama Pref., Toyama City, Kamegai, 1–8 Sep 2009, M. Watanabe leg. (MT) (KPMNH); 1 M, ditto, 8–15 Sep 2009, M. Watanabe leg. (MT) (KPMNH); 1 M, Toyama Pref., Toyama City, Jurodani, 7–14 Jul 2009, M. Watanabe leg. (MT) (KPMNH); 1 M, Toyama Pref., Nanto City, Kamimomose, 11–18 Aug 2009, M. Watanabe leg. (MT) (KPMNH); 1 M, ditto, 1–8 Sep

2009, M. Watanabe leg. (MT) (KPMNH); 4 M, ditto, 15–29 Sep 2009, M. Watanabe leg. (MT) (KPMNH); 2 F, Ishikawa Pref., Nomi City, Mitsukuchi, 30 Apr–13 May 2011, R. Ishiguro leg. (MT) (MU); 1 F, ditto, 6–21 Oct 2011, H. Fukutomi leg. (MT) (MU); 1 F, Ishikawa Pref., Hakusan City, Sannomiya, 17–23 May 2009, H. Fukutomi leg. (MT) (MU); 1 F, ditto, 24–30 May 2009, H. Fukutomi leg. (MT) (MU); 1 F & 1M, Mie Pref., Taiki Town, Takihara, 20–31 May 2019, T. Nishimura leg. (MT) (MU); 1 M, Kyoto Pref., Yawata City, Yawatahayashinomoto, 15 May 2015, K. Watanabe leg. (KPMNH); 2 F, Osaka Pref., Chihayaakasaka Vil., Mt. Kongosan, 7–15 Jul 2012, S. Fujie leg. (MT) (KPMNH); 1 F, Hyogo Pref., Kobe City, Motoyama Town, Hokura-jinja, 5 May 2012, K. Watanabe leg. (KPMNH); 1 F, Tottori Pref., Wakasa Town, Mt. Hyonosen, 17 Jul 2011, K. Watanabe leg. (KPMNH). [Shikoku] 1 F & 1 M, Tokushima Pref., Zennyuji-toh, 13–22 May 2003, H. Otsuka leg. (MT) (MU). [Kyushu] 1 F, Kagoshima Pref., Sakurajima, 13 May 1973, K. Kusigemati leg. (SEHU); 1 F, Kagoshima Pref., Terayama, 19 Apr 1973, K. Kusigemati leg. (SEHU); 1 F, Kagoshima Pref., Uearata, 18 Oct 1973, K. Kusigemati leg. (SEHU). BULGARIA: 1 M, Batak, 20 Jul 1966 (ZSM). GERMANY: 1 M, Stolzenau, 8 Aug 1945 (ZSM). RUSSIA: 1 F, Altay, Lake Telezkoe, Chulishman, 6 Aug 1989, A. Tereshkin leg. (ZSM).

Description. Female (n = 100). Body length 4.5–7.2 mm, weakly polished, coriaceous and covered with silver setae.

Head 0.5–0.54 × as long as wide. Clypeus 2.0–2.2 × as broad as high, slightly convex basally in lateral view. Face 2.0–2.35 × as broad as high, densely punctate, convex medially in lateral view, separated from clypeus by shallow clypeal sulcus. Inner orbits almost parallel (Fig. 2B). Length of malar space 1.0–1.1 × as long as basal mandibular width. POL 1.8–2.3 × as long as OD. OOL 1.0–1.3 × as long as OD. POL 1.7–2.1 × as long as OOL. Antenna with 22–25 flagellomeres. FL I 1.25–1.33 × as long as FL II. MP IV 1.25–1.33 × as long as MP V.

Mesosoma. Lateral aspect of pronotum rugulose anteriorly. Mesoscutum finely and sparsely punctate (separated by ca. 1.5–3.0 × their diameter) (Fig. 2C). Scutellum finely and sparsely punctate (separated by ca. 1.5–2.5 × their diameter) (Fig. 2C). Anterior and lower parts of mesopleuron coarsely and sparsely punctate. Sternaulus weakly impressed. Propodeum rounded in lateral view, without rugae (Fig. 2D), without carinae except for anterior part of pleural carina. Fore wing length 3.8–6.5 mm. Nervellus intercepted below middle. Hind femur 4.22–4.5 × as long as maximum depth in lateral view. Hind femur 8.0–8.5 × as long as maximum depth in lateral view. Ratio of length of hind first to fifth tarsomeres 1.0: 0.6: 0.4–0.5: 0.2–0.3: 0.3.

Metasoma. T I rectangular in dorsal view (Fig. 9F), 1.0–1.2 × as long as maximum width, rugulose laterally. Latero-median carina present basal ca. 0.5 of T I. T II 0.66–0.88 × as long as maximum width, striate anteriorly and strigose laterally.

Coloration (Fig. 2A–D). Body (excluding wings and legs) black. Face sometimes with a small yellow or brown median spot. Palpi, tegula and upper part of mesepisternum yellow. Mandible yellow, except for apex and base. Lateral aspect of pronotum with a yellow spot posteriorly. Subtegular ridge tinged with yellow anteriorly. Scutellum with a yellow spot apically. Wings hyaline. Veins and pterostigma brown to blackish-brown except for yellowish-brown wing base. Legs orange. Apex of fore coxa and apex of hind femur tinged with black. Trochanters and trochantelli yellow. Hind tibia and tarsomeres black. Base of hind tibia tinged with white.

Male (n = 71). Similar to female. Inner orbits weakly divergent downward (Fig. 2F). Length of malar space 0.83–1.0 × as long as basal mandibular width.

Coloration (Fig. 2E, F). Body (excluding wings and legs) black. Clypeus, palpi, face, ventral surface of antenna, malar space, propleuron, epicnemium, tegula, subtegular ridge and mesepisternum yellow. Gena tinged with yellow ventrally. Mandible yellow, except for apex. Lateral aspect of pronotum with a yellow spot ventrally and posteriorly. Mesoscutum with yellow shoulder marks. Mesopleuron with a yellow marking ventrally. Scutellum with a yellow spot apically. T III and T IV each with a pair of yellow spots anteriorly (sometimes these spots united into a single spot). Wings hyaline. Veins and pterostigma brown to blackish-brown except for yellowish-brown wing base. Legs yellow. Fore and mid femora, tibiae and tarsi orange. Hind coxa with a blackish-brown stripe dorsally. Hind femur brown to blackish-brown. Base of hind trochantellus tinged with blackish-brown. Hind tibia and tarsomeres black. Base of hind tibia tinged with whitish-yellow.

Distribution. Japan (Hokkaido, Honshu, Shikoku, and Kyushu). Outside Japan, this species is widely distributed in Palearctic region (Yu et al. 2016).

Bionomics. Host unknown in Japan. Outside of Japan, the following three hoverfly species have been recorded as hosts: *Eupeodes lapponicus* (Zetterstedt, 1838); *Neocnemodon fulvimanus* (Zetterstedt, 1843); *Sphaerophoria scripta* (Linnaeus, 1758) (Yu et al. 2016). *Anthonomus pomorum* (Linnaeus, 1758) and *Loxostege sticticalis* (Linnaeus, 1761) have also been recorded as hosts (Yu et al. 2016), but are considered doubtful records. Most adults were collected from various open habitats (e.g., grasslands, meadows and paddy fields).

Remarks. This is the first record of this species from Japan. This species resembles *W. flavolineatus*, but can be distinguished from the latter by the following combination of character states: face entirely black or black with a small yellow or brown median spot in females (black with a large yellow median spot in females of *W. flavolineatus*); pronotum black with yellow ventral corner in males (black with yellow ventral and hind parts in males of *W. flavolineatus*); yellow shoulder marks absent in females (present in females of *W. flavolineatus*); mesopleuron with a yellow marking ventrally in males (with a large yellow marking; it is enlarged anteriorly in males of *W. flavolineatus*).

***Woldstedtius citropeccatoralis* (Schmiedeknecht, 1926)**

Bassus abductor Bridgman, 1886: 336. Name preoccupied.

Homocidus citropeccatoralis Schmiedeknecht, 1926: 3412.

Material examined. No specimens available.

Distribution. Japan (Kunashiri Is.). Outside Japan, this species is widely distributed in Holarctic region (Yu et al. 2016).

Remarks. This species was recorded from Japan by Manukyan (2007), but no additional specimens were found in this study.

***Woldstedtius flavolineatus* (Gravenhorst, 1829)**

Remarks. This species is divided into two subspecies, *W. flavolineatus flavolineatus* and *W. f. nigroscutellatus* (Habermehl, 1925). The latter subspecies has been recorded from Germany and Netherlands (Habermehl 1925; Teunissen 1948). Klopstein (2014) noted this subspecies could not be examined by her because type specimens were not available. Judging from the original description of the latter (Habermehl 1925), this subspecies could readily be synonymized under the former.

***Woldstedtius flavolineatus flavolineatus* (Gravenhorst, 1829)**

Figs 3A–F, 9G

Bassus flavolineatus Gravenhorst, 1829: 337.

Homocidus flavolineatus Uchida, 1957: 251.

Bassus interruptus Holmgren, 1858: 359. Synonymized by Thomson (1890).

Bassus bimaculatus Holmgren, 1858: 360. Synonymized by Thomson (1890).

Bassus agilis Cresson, 1868: 111. Synonymized by Dasch (1964).

Bassus frontalis Cresson, 1868: 111. Synonymized by Dasch (1964).

Mesoleius junctus Provancher, 1883: 10. Synonymized by Dasch (1964).

Materials examined. Italy: 1 F Sud-tirol, Coltina d'Ampezzo, 29 Jul 1933, E. Bauer leg. (ZSM). Bulgaria: 1 M Vitoscha, 24 Jul 1966 (ZSM).

Diagnosis. Body weakly polished. Inner orbits almost parallel in females, weakly divergent downward in males. Antenna with 22–24 flagellomeres in females, 22–25 in males. Propodeum without rugae (Fig. 3D), without carinae except for anterior part of pleural carina. T I entirely coriaceous, rectangular in dorsal view (Fig. 9G). Latero-median carina of T I present basal ca. 0.5 of T I. Face black with a large yellow median spot in females (Fig. 3B), entirely yellow in males (Fig. 3F). Lateral aspect of pronotum black with ventral and posterior yellow spots in females (Fig. 3A), black with yellow ventral and posterior areas in males (Fig. 3E). Mesopleuron entirely black in females (Fig. 3A), black with a large yellow marking, it enlarged anteriorly in males (Fig. 3E). Shoul-

der marks of mesoscutum yellow in both sexes (Fig. 3C, E). Scutellum black with an apical yellow spot in both sexes (Fig. 3C). Hind coxa entirely orange in females (Fig. 3A), yellow with brown base in males (Fig. 3E). Hind trochanter yellow in females (Fig. 3A), yellow with a brown dorsal spot in males (Fig. 3E). Metasoma entirely black in females, bases of T III and T IV each with a transverse yellow band in males.

Distribution. Japan (Hokkaido, Honshu, Shikoku, and Kyushu). Outside Japan, this species is widely distributed in Holarctic, Oriental, Oceanic, and Neotropical region (Yu et al. 2016).

Bionomics. In Japan, one hover fly species, *Episyrphus balteatus* (De Geer, 1776) is recorded as a host (Uchida 1957).

Remarks. No additional specimen of this species from Japan was found in this study. Some or all previous records of this species from Japan may be based on misidentification of *W. biguttatus*.

***Woldstedtius karafutensis* (Uchida, 1957)**

Figs 4A–F, 9H

Homocidus karafutensis Uchida, 1957: 252.

Materials examined. Type series: RUSSIA: 1 F (*holotype*), Sakhalin Is., Tarandomari, 25 Jul 1934, C. Watanabe & T. Inoue leg. (SEHU); JAPAN: [Hokkaido] 1 F (*paratype*), Hokkaido, Sapporo, 6 Jul 1954, Townes family leg. (SEHU). **Non-types:** JAPAN: [Honshu] 1 F, Fukushima Pref., Showa Vil., Mt. Hakase, 24 Aug–19 Sep 1998, T. Muroi leg. (MT) (MU); 1 F, Yamagata Pref., Mamurogawa Town, Azusayama, 5 Sep 2009, Y. Matsubara & K. Fukuda leg. (MT) (KPMNH); 2 F, Shizuoka Pref., Shizuoka City, Umegashima, 3 Jun–16 Jul 2001, T. Sugiyama leg. (MT) (MU); 2 F, ditto, 17 Jul–5 Aug 2001, T. Sugiyama leg. (MT) (MU); 1 M, Shizuoka Pref., Honkawane Town, Yamainudan, 14 Jun 2008, K. Watanabe leg. (KPMNH); 2 F, Gifu Pref., Kani City, Katabira, 8–14 May 2004, K. Yamagishi leg. (MT) (MU); 1 F, Toyama Pref., Nanto City, Togamura, Kamimomose, 4–11 Aug 2009, M. Watanabe leg. (MT) (KPMNH); 1 F, Ishikawa Pref., Kaga City, Mt. Kariyasuyama, 7–18 Jul 2002, K. Esaki leg. (MT) (TMNH); 1 F, Ishikawa Pref., Hakusan City, Sannomiya, 6–18 Sep 2009, H. Fukutomi leg. (MT) (MU); 1 M, Ishikawa Pref., Hakusan City, Togadani, 18 May–4 Jun 2010, H. Fukutomi leg. (MT) (MU); 1 F, Hyogo Pref., Kami Town, Ojira-ku, Niiya, Mikata-kogen, 26 Jun–18 Jul 2011, S. Fujie leg. (MT) (KPMNH).

Description. Female (n = 14). Body length 4.1–6.0 mm, polished, coriaceous, covered with silver setae.

Head 0.5 × as long as wide. Clypeus 2.1–2.4 × as broad as high, flat in lateral view. Face 1.88–2.2 × as broad as high, densely punctate, convex medially in lateral view, separated from clypeus by shallow clypeal sulcus. Inner orbits almost parallel (Fig. 4B). Length of malar space 1.1–1.15 × as long

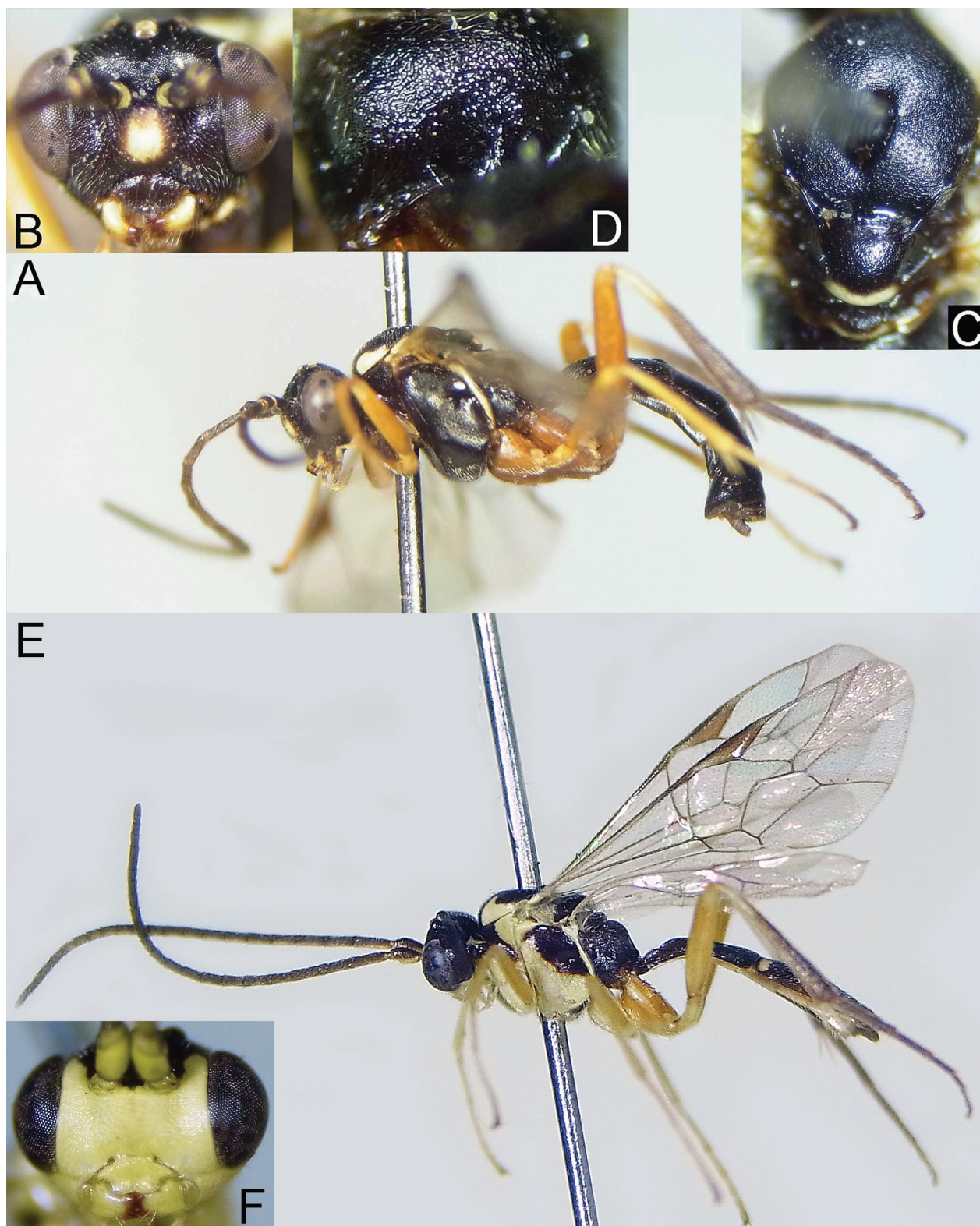


Figure 3. *Woldstedtius flavolineatus flavolineatus* (Gravenhorst, 1829) (A–D. female; E, F. male) — A, E. Habitus; B, F. Head, frontal view; C. Mesonotum, dorsal view; D. Propodeum, dorsal view.

as basal mandibular width. POL 2.0–2.1 × as long as OD. OOL 1.0–1.2 × as long as OD. POL 2.0–2.2 × as long as OOL. Antenna with 20–21 flagellomeres. FL I 1.15–1.35 × as long as FL II. MP IV 1.45–1.66 × as long as MP V.

Mesosoma. Lateral aspect of pronotum rugulose anteriorly. Mesoscutum densely punctate (separated by ca.

0.5–1.0 × their diameter) (Fig. 4C). Scutellum finely and sparsely punctate (separated by ca. 1.5–2.0 × their diameter). Lower part of mesopleuron coarsely and sparsely punctate. Sternaulus indistinct. Propodeum without rugae and carinae (Fig. 4D), rounded in lateral view. Fore wing length 4.0–5.0 mm. Nervellus intercepted below middle.

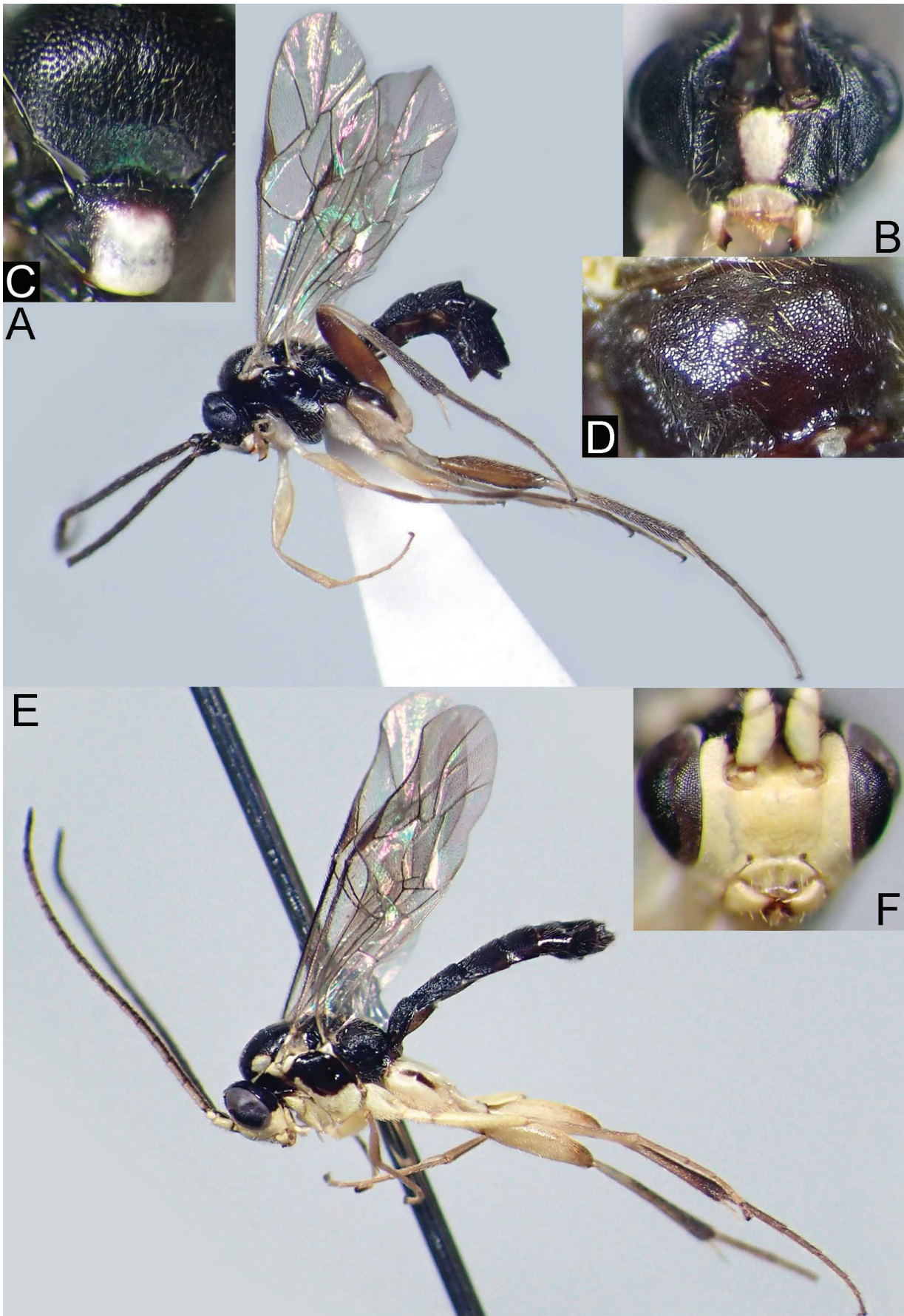


Figure 4. *Woldstedtius karafutensis* (Uchida, 1957) (A–D. female; E, F. male) — A, E. Habitus; B, F. Head, frontal view; C. Mesonotum, dorsal view; D. Propodeum, dorsal view.

Hind femur 3.75–4.0 × as long as maximum depth in lateral view. Hind tibia 8.0–9.5 × as long as maximum depth in lateral view. Ratio of length of hind first to fifth tarsomeres 1.0: 0.6: 0.5: 0.3: 0.25–0.3.

Metasoma. T I square in dorsal view (Fig. 9H), 1.0–1.1 × as long as maximum width, rugulose laterally. Latero-median carina present basal ca. 0.3 of T I (Fig. 9H). T II 0.86–1.0 × as long as maximum width, strigose except for posterior margin smooth.

Coloration (Fig. 4A–D). Body (excluding wings and legs) black to blackish-brown. Face with a large white median spot (this spot connected with white clypeus). Clypeus, palpi, tegula, subtegular ridge, upper mesepisternum and scutellum white. Mandible white, except for apex and base. Lateral aspect of pronotum with a white spot posteriorly. Antenna brown. Veins and pterostigma yellowish-brown to brown. Legs whitish-yellow. Hind coxa with a dorsal blackish-brown stripe. Hind femur brown. Hind tibia and tarsomere black. Base of hind tibia tinged with white.

Male (n = 2). Similar to female. Inner orbits weakly divergent downward (Fig. 4F).

Coloration (Fig. 4E, F). Body (excluding wings and legs) black to blackish-brown. Clypeus, palpi, face, ventral surface of antenna, malar space, propleuron, epicnemium, mesosternum, tegula, subtegular ridge, upper mesepisternum and scutellum white. Gena tinged with white ventrally. Mandible white except for apex. Lateral aspect of pronotum tinged with white ventrally and posteriorly. Mesoscutum with white shoulder marks. Mesopleuron with a large white marking; it is enlarged anteriorly. Wings hyaline. Veins and pterostigma yellowish-brown to brown. Legs white. Fore and mid tarsi, apex of hind trochantellus, base and apex of hind femur and hind tarsomeres brown. Hind coxa with a dorsal brown stripe. Hind tibia tinged with brown.

Distribution. Japan (Hokkaido and Honshu). Outside Japan, this species has been recorded from Russia and South Korea (Balueva and Lee 2016 and Yu et al. 2016).

Bionomics. Host unknown.

Remarks. This is the first record of this species from Honshu.

Woldstedtius kuroashii (Uchida, 1957)

Figs 5A–F, 9B, I

Homocidus flavolineatus var. *kuroashii* Uchida, 1957: 251.

Syrphoctonus holarcticus Diller, 1969: 548. Syn. nov.

Materials examined. Type series: JAPAN: [Honshu] 1 F (*holotype* of *H. flavolineatus* var. *kuroashii*), Nagano Pref., Mt. Norikura, 30 Jul 1954, Townes family leg. (AEIC). GERMANY: 1 F (*paratype* of *S. holarcticus*), Ober-Bayern, Garmisch, 21 Jul 1926, E. Bauer leg. (ZSM). **Non-types:** JAPAN: [Hokkaido] 4 F, Hokkaido, Hidaka Town, Uenzaru-gawa, 10 Jul–1 Aug 2007,

A. Ueda leg. (MT) (KPMNH); 1 M, Hokkaido, Sapporo City, Mt. Soranumadake, 14 Jun–4 Jul 2007, A. Ueda leg. (MT) (KPMNH); 1 F, Hokkaido, Kamikawa Town, Ginsendai, 1 Aug 2021, K. Watanabe leg. (TMNH). [Honshu] 1 F, Fukushima Pref., Kitakata City, Yamato, Zouriduka–Mt. Iide, 11 Jul 2013, K. Yoshiga leg. (KPMNH); 1 M, Tochigi Pref., Kuriyama Vil., Yamato, Kinunuma, 1–14 Jul 2004, H. Makihara leg. (MT) (KPMNH); 3 F, Gunma Pref., Tsumagoi Vil., Kanbara, Takaminekogen, 3 Sep 2015, K. Watanabe leg. (KPMNH); 1 M, Niigata Pref., Nagaoka City, Suyoshi, Mt. Nokogiriyama, 7 Jun 2014, S. Shimizu leg. (KPMNH); 1 F, Tokyo, Chiyoda, Imperial Palace, Fukiagegyoen, Otakinagare, 14–26 Apr 2011 (MT) (NSMT); 2 M, Tokyo, Ome City, Mt. Mitakesan, 1 Jun 2008, M. Gunji leg. (KPMNH); 1 M, Kanagawa Pref., Fujino Town, Mt. Jinbayama, 7 Jun 2008, K. Watanabe leg. (KPMNH); 1 M, Kanagawa Pref., Hadano City, Chimura, Mt. Zukkoyama, 16 Apr 2017, K. Watanabe leg. (KPMNH); 1 M, Kanagawa Pref., Hakone Town, Mt. Kamiyama, 21 Jun 2010, M. Takakuwa leg. (KPMNH); 1 M, Kanagawa Pref., Yamakita Town, Mt. Komotsurusuiyama, 23 Jul 2014, T. Taniwaki leg. (KPMNH); 1 M, Kanagawa Pref., Yamakita Town, Mt. Hinokiboramaru, 17 Jul 2014, T. Taniwaki leg. (KPMNH); 1 F, Yamanashi Pref., Fujiyoshida City, Takizawarindo, 7–11 Sep 2017 A. Owaki leg. (MT) (KPMNH); 1 F, Yamanashi Pref., Narusawa Vil., Fujirindo, 5 Sep 2015 K. Watanabe leg. (KPMNH); 1 F, Shizuoka Pref., Shizuoka City, Mt. Tyausudake, 28 Jul 1970, H. Takizawa leg. (SEHU); 1 F, Shizuoka Pref., Honkawane Town, Yamainudan, 14 Jun 2008, K. Watanabe leg. (KPMNH); 6 M, ditto, 14 Jun 2008, K. Watanabe leg. (KPMNH); 1 M, Gifu Pref., Kani City, Katabira, 17–23 Apr 2004, K. Ito leg. (MT) (MU); 2 F, Nagano Pref., Otaki Vil., Mt. Ontakesan, Tanohara, 8 Aug 2007, K. Watanabe leg. (KPMNH); 1 M, Nagano Pref., Otaki Vil., Mt. Ontakesan, Hakkaisan, 6 Aug 2010, K. Watanabe leg. (TMNH); 1 F, ditto, 7 Aug 2010, K. Watanabe leg. (TMNH); 1 F, ditto, 5–9 Aug 2010, K. Watanabe leg. (MT) (KPMNH); 7 M, ditto, 5–9 Aug 2010, K. Watanabe leg. (MT) (KPMNH); 1 F, Toyama Pref., Toyama City, Inonedani, 21–28 Jul 2009, M. Watanabe leg. (MT) (KPMNH); 1 F, ditto, 11–16 Aug 2009, M. Watanabe leg. (MT) (KPMNH); 1 F, ditto, 1–8 Sep 2009, M. Watanabe leg. (MT) (KPMNH); 1 F, ditto, 8–15 Sep 2009, M. Watanabe leg. (MT) (KPMNH); 6 F, ditto, 15–22 Sep 2009, M. Watanabe leg. (MT) (KPMNH); 1 F, Toyama Pref., Toyama City, Jurodani, 11–16 Aug 2009, M. Watanabe leg. (MT) (KPMNH); 1 M, Ishikawa Pref., Hakusan City, Sannomiya, 15 Oct–6 Nov 2009, H. Fukutomi leg. (MT) (MU); 1 F, Ishikawa Pref., Hakusan City, Yawata, 7–24 Oct 2009, H. Fukutomi leg. (MT) (MU); 1 M, Fukui Pref., Ikeda Town, Mizuumi, Mt. Hekosan, 18 Jun 2016, S. Shimizu leg. (KPMNH); 1 F, Hyogo Pref., Sasayama City, Mt. Koganegadake, 14 May 2014, Y. Ueyama leg. (KPMNH)

Description. Female (n = 33). Body length 5.5–8.5 mm, polished, coriaceous. covered with silver setae.

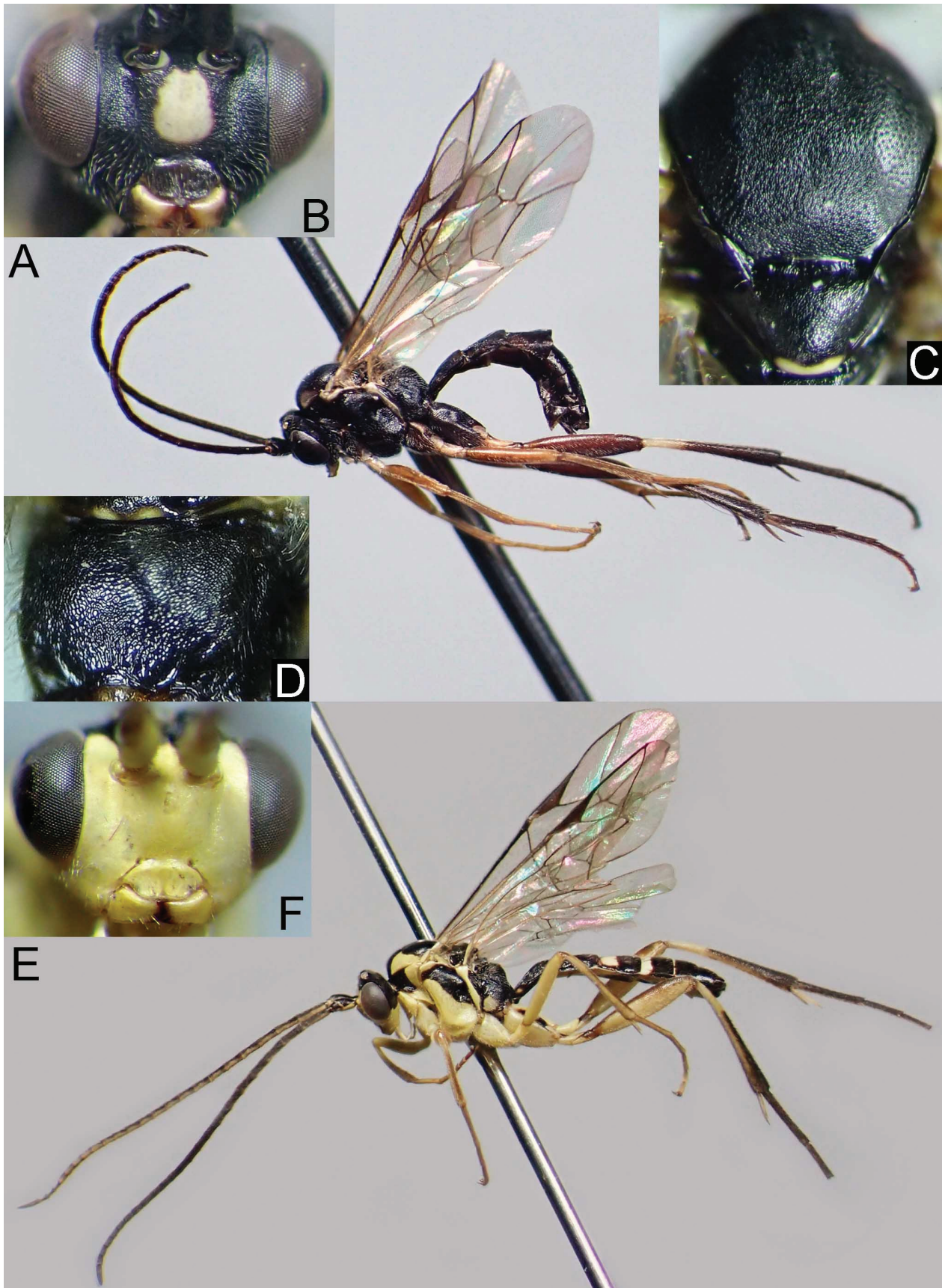


Figure 5. *Woldstedtius kuroashii* (Uchida, 1957) (A–D. female; E, F. male) — A, E. Habitus; B, F. Head, frontal view; C. Mesonotum, dorsal view; D. Propodeum, dorsal view.

Head 0.5–0.53 × as long as wide. Clypeus 2.0–2.3 × as broad as high, convex basally in lateral view. Face 2.2–2.3 × as broad as high, densely punctate, convex medially in lateral view (Fig. 9B), separated from clypeus by shallow clypeal sulcus. Inner orbits almost parallel (Fig. 5B). Length of malar space 1.0–1.2 × as long as basal mandibular width. POL 2.16–2.3 × as long as OD. OOL 1.0–1.38 × as long as OD. POL 1.86–2.1 × as long as OOL. Antenna with 23–25 flagellomeres. FL I 1.25–1.3 × as long as FL II. MP IV 1.2–1.29 × as long as MP V.

Mesosoma. Lateral aspect of pronotum rugulose or rarely strigose anteriorly. Mesoscutum finely and densely punctate (separated by ca. 1.0 × their diameter) (Fig. 5C). Scutellum finely and sparsely punctate (separated by ca. 1.5–2.5 × their diameter) (Fig. 5C). Mesopleuron coarsely and sparsely punctate except for speculum. Sternaulus weakly impressed. Propodeum rounded in lateral view, without rugae (Fig. 5D), without carinae except for anterior part of pleural carina. Fore wing length 5.8–6.9 mm. Nervellus intercepted below middle. Hind femur 4.0–4.5 × as long as maximum depth in lateral view. Hind tibia 7.8–8.4 × as long as maximum depth in lateral view. Ratio of length of hind first to fifth tarsomeres 1.0: 0.6: 0.4–0.5: 0.3: 0.2–0.3.

Metasoma. T I rectangular in dorsal view (Fig. 9I), 1.1–1.25 × as long as maximum width, rugulose laterally. Latero-median carina present on basal ca. 0.5 of T I (Fig. 9I). T II 0.65–0.8 × as long as maximum width, striate anteriorly and strigose laterally.

Coloration (Fig. 5A–D). Body (excluding wings and legs) black. Face with a large whitish-yellow median spot (this spot rarely obscured). Palpi, tegula, subtegular ridge and mesepisternum yellow. Mandible whitish-yellow except for apex and base. Lateral aspect of pronotum with a whitish-yellow spot posteriorly. Mesoscutum with whitish-yellow shoulder marks (these marks rarely disappeared). Scutellum with a whitish-yellow spot apically. Veins and pterostigma brown to blackish-brown except for yellow wing base. Legs blackish-brown to black. Apex of fore coxa and base of hind tibia tinged with white. Trochanters and trochantelli white. Femora, fore and mid tibiae and tarsi sometimes (including paratype of *W. holarcticus*) orange to brown. Fore and mid coxae each with a white stripe dorsally (this stripe often obscured). Base of hind femur tinged with reddish-brown.

Male (n = 26). Similar to female. Inner orbits weakly divergent downward (Fig. 5F). Antenna with 22–25 flagellomeres. Punctures on mesoscutum weaker than female. T I 1.14–1.26 × as long as maximum width. T II 0.83–0.93 × as long as maximum width.

Coloration (Fig. 5E, F). Body (excluding wings and legs) black. Clypeus, palpi, face, ventral surface of antenna, malar space, propleuron, epicnemium, mesosternum, tegula, subtegular ridge and mesepisternum whitish-yellow. Gena tinged with whitish-yellow ventrally. Mandible whitish-yellow, except for apex. Lateral aspect of pronotum tinged with whitish-yellow ventrally and posteriorly. Mesopleuron with a large whitish-yellow marking, it enlarged anteriorly. Scutellum with a whitish-yellow

spot apically. T III with a pair of whitish-yellow spots anteriorly (sometimes these spots united into a single spot). T IV and T V each with a transverse whitish-yellow band anteriorly. Wings hyaline. Veins and pterostigma brown to blackish-brown except for yellow wing base. Legs yellow to yellowish-brown. Hind coxa and trochanter each with a dorsal blackish-brown stripe. Hind trochantellus and tibia tinged with blackish-brown.

Distribution. Japan (Hokkaido and Honshu). Outside Japan, this species is widely distributed in the Holarctic and Oriental regions (Yu et al. 2016).

Bionomics. Host unknown. Most adults were collected from the treetops of broad-leaved trees.

Remarks. This is the first record of this species from Hokkaido.

***Woldstedtius punctatus* sp. nov.**

<http://zoobank.org/4934EAC1-4504-45A8-9848-B1F7BF26301B>

Figs 6A–F, 9J

Type series. Holotype: F, Japan, Honshu, Kanagawa Pref., Nakai Town, Zoushiki, 16 Apr 2019, K. Watanabe leg. (KPMNH). **Paratypes:** Japan: [Honshu] 1 M, Niigata Pref., Nagaoka City, Joganji Town, Mt. Happoudai, 24 May 2014, S. Shimizu leg. (KPMNH); 1 M, Saitama Pref., Urawa City, Tajima, 21 Apr 1999, T. Nambu leg. (KPMNH); 1 F, Kanagawa Pref., Kamakura City, Nikaidou, Zuisenji, 24 Apr 1955, H. Nagase leg. (KPMNH); 1 M, Kanagawa Pref., Oiso Town, Koma, Komayama, 16 Apr 2016, K. Watanabe leg. (KPMNH); 1 F, Kanagawa Pref., Mt. Hinokiboramaru, 16 May 2013, (FIT) (KPMNH); 1 M, Kanagawa Pref., Mt. Komotsurushiyama, 16 Jun 2013, (FIT) (KPMNH); 1 F, Kanagawa Pref., Yamakita Town, Nakagawa, Mt. Hinokiboramaru, 16 Jun 2015, K. Watanabe leg. (KPMNH); 1 F, Nagano Pref., Otaki Vil., Ontakekyuukamura, 8 Jul 2011, M. Ito leg. (LT) (TMNH); 5 M, Fukui Pref., Ikeda Town, Mizuumi, Mt. Hekosan, 18 Jun 2016, S. Shimizu leg. (KPMNH); 2 M, ditto, 18 Jun 2016, T. Tokuhira leg. (TMNH); 1 F, Osaka Pref., Higashiosaka City, Hirao-ka-park, 19 Apr 2020, Y. Yamamoto leg. (KPMNH).

Description. Female (n = 6). Body length 7.5–10.7 (HT: 7.5) mm, polished, coriaceous, covered with silver setae.

Head 0.5–0.53 (HT: 0.5) × as long as wide. Clypeus 1.9–2.0 (HT: 1.92) × as broad as high, slightly convex basally in lateral view. Face 2.3–2.5 (HT: 2.4) × as broad as high, densely punctate, convex medially in lateral view and separated from clypeus by shallow clypeal sulcus. Inner orbits almost parallel (Fig. 6B). Length of malar space 1.0–1.2 (HT: 1.1) × as long as basal mandibular width. POL 2.1–2.3 (HT: 2.1) × as long as OD. OOL 0.88–1.0 (HT: 1.0) × as long as OD. POL 2.1–2.5 (HT: 2.3) × as long as OOL. Antenna with 23–25 (HT: 24) flagellomeres. FL I 1.3–1.4 (HT: 1.3) × as long as FL II. MP IV 1.25–1.5 (HT: 1.25) × as long as MP V.

Mesosoma. Lateral aspect of pronotum strigose anteriorly. Mesoscutum finely and densely punctate (separated by ca. 1.0 × their diameter) (Fig. 6C). Scutellum coarse-

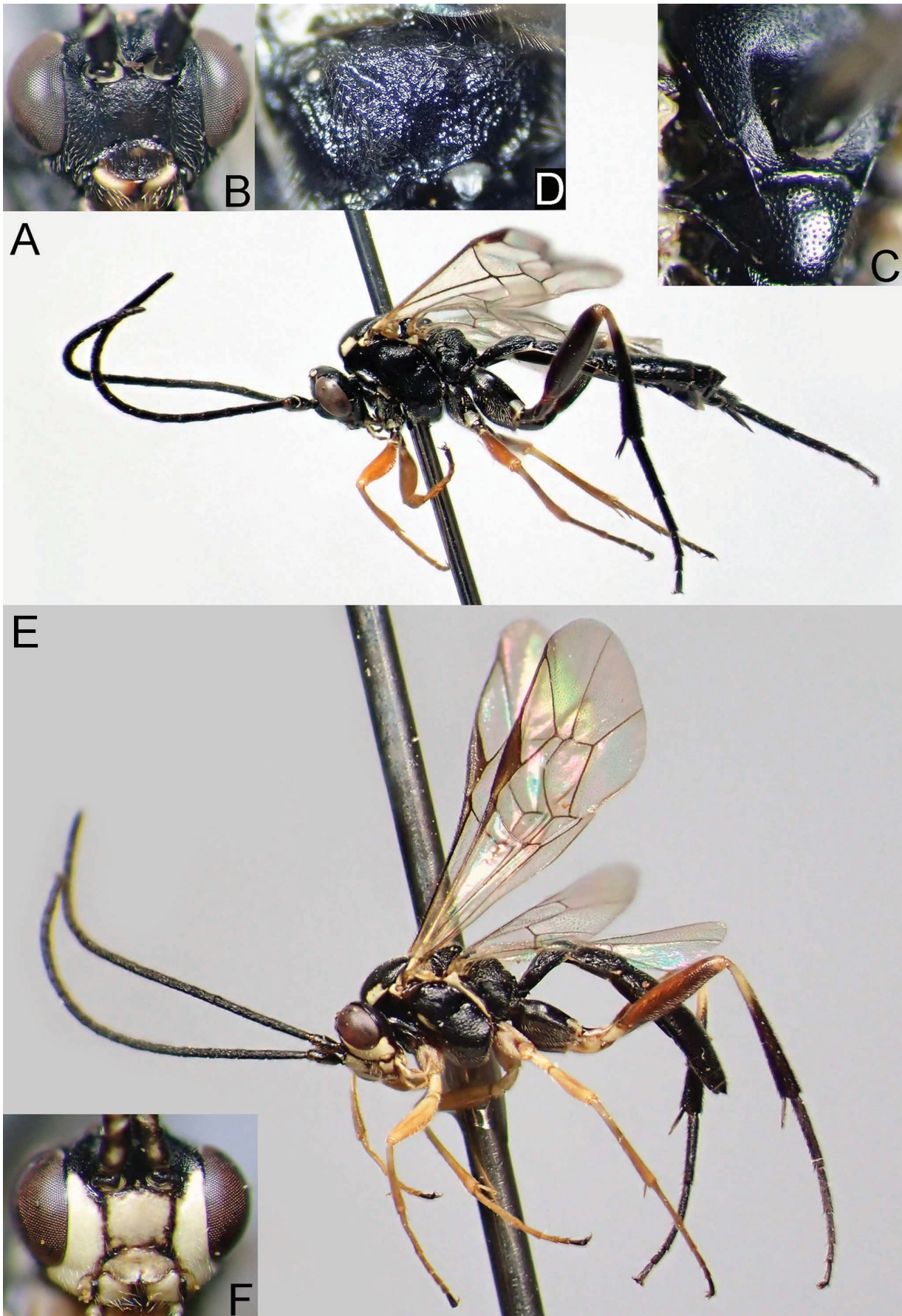


Figure 6. *Woldstedtius punctatus* sp. nov. (A–D. female, holotype; E, F. male, paratype) — A, E. Habitus; B, F. Head, frontal view; C. Mesonotum, dorsal view; D. Propodeum, dorsal view.

ly and densely punctate (separated by ca. $0.8\text{--}1.3 \times$ their diameter) (Fig. 6C). Mesopleuron coarsely and sparsely punctate except for speculum. Sternaulus weakly impressed. Propodeum rounded in lateral view, rugulose (Fig. 6D), without carinae except for pleural carina. Fore wing length $6.9\text{--}8.9$ (HT: 7.0) mm. Nervellus intercepted below middle. Hind femur $4.25\text{--}4.5$ (HT: 4.25) \times as long as maximum depth in lateral view. Hind tibia $7.1\text{--}7.7$ (HT: 7.1) \times as long as maximum depth in lateral view. Ratio of length of hind first to fifth tarsomeres 1.0: 0.6: 0.4: 0.25: 0.3.

Metasoma. T I rectangular in dorsal view (Fig. 9J), $1.2\text{--}1.26$ (HT: 1.25) \times as long as maximum width, rugulose laterally. Latero-median carina present basal ca. 0.5 of T I (Fig. 9J). T II $0.6\text{--}0.75$ (HT: 0.6) \times as long as maximum width, strigose anteriorly and laterally.

Coloration (Fig. 6A–D). Body (excluding wings and legs) black. Sometimes face with a small brown spot medially. Palpi and upper mesepisternum yellow. Mandible yellowish-brown except for apex and base. Lateral aspect of pronotum with a yellow spot posteriorly. Mesoscutum with small yellow shoulder marks. Tegula tinged with yellow anteriorly. Wings hyaline. Veins and pterostigma blackish-brown except for yellowish-brown wing base. Legs black. Apex of fore and mid trochanters, base of fore trochantellus and base of hind tibia tinged with white. Fore and mid femora, tibiae and tarsi orange. Apex of hind trochantellus and base of hind femur tinged with reddish-brown.

Male (n = 11). Similar to female. Body length (excluding antennae) $5.5\text{--}9.8$ mm. Length of malar space $0.9\text{--}1.1$ \times as long as basal mandibular width. Inner orbits weakly divergent downward (Fig. 6F). Fore wing length $5.0\text{--}8.0$ mm.

Coloration (Fig. 6E, F). Body (excluding wings and legs) black. Face with a large whitish-yellow spot medially and whitish-yellow longitudinal stripes along inner orbits. Clypeus, palpi, malar space, ventral surface of antenna and mesepisternum whitish-yellow. Mandible whitish-yellow except for apex. Lateral aspect of pronotum with a whitish-yellow spot posteriorly. Mesoscutum with whitish-yellow shoulder marks. Tegula tinged with whitish-yellow anteriorly. Subtegular ridge brown. Epicnemium with a small whitish-yellow spot. Wings hyaline. Veins and pterostigma brown to blackish-brown except for yellowish-brown wing base. Legs whitish-yellow to yellow. Fore and mid coxae tinged with black basally. Hind coxa, tibia and tarsomeres black. Hind trochanter, trochantellus, apex of hind femur and base of hind tibia tinged with white. Hind femur brown.

Distribution. Japan (Honshu).

Bionomics. Host unknown. Most adults were collected in broad-leaved forests of mountainous regions. One paratype collected from the Nagano Prefecture was collected by light trap.

Etymology. The species name refers to the scutellum having coarse punctures.

Remarks. This species can be easily distinguished from any other species by the entirely black scutellum

and the coarse and dense punctures on scutellum (separated by ca. $0.8\text{--}1.3 \times$ their diameter).

Woldstedtius takagii (Uchida, 1957)

Figs 7A–D, 9C, D, K

Homocidus yokohamensis var. *takagii* Uchida, 1957: 251

Materials examined. Type series: JAPAN: [Hokkaido] 1 F (*holotype*), Hokkaido, Sapporo, 15 Jul 1955, S. Takagi leg. (SEHU). **Non-types:** JAPAN: [Honshu] 1 F, Yamanashi Pref., Kosu City, Mt. Daibosatsu, Kaminikawa-toge, 16 Jun 2007, K. Watanabe leg. (KPMNH); 1 F, Toyama Pref., Nanto City, Togamura, Kamimomose, 25 Aug–1 Sep 2009, M. Watanabe leg. (MT) (KPMNH).

Description. Female (n = 3). Body length $7.7\text{--}7.9$ mm, polished, coriaceous, covered with silver setae.

Head $0.47\text{--}0.52$ \times as long as wide. Clypeus $1.78\text{--}2.0$ \times as broad as high, convex basally in lateral view. Face $2.6\text{--}2.9$ \times as broad as high, densely punctate, convex medially in lateral view, separated from clypeus by shallow clypeal sulcus. Inner orbits strongly divergent downward (Figs 7B, 9C). Length of malar space $1.0\text{--}1.1$ \times as long as basal mandibular width. POL $2.0\text{--}2.15$ \times as long as OD. OOL $1.05\text{--}1.25$ \times as long as OD. POL $1.8\text{--}1.9$ \times as long as OOL. Antenna with 25–26 flagellomeres. FL I $1.2\text{--}1.33$ \times as long as FL II. MP IV $1.25\text{--}1.4$ \times as long as MP V.

Mesosoma. Lateral aspect of pronotum strigose anteriorly. Mesoscutum finely and densely punctate (separated by ca. $0.8\text{--}1.0 \times$ their diameter) (Fig. 7C). Scutellum finely and densely punctate (separated by ca. $0.8\text{--}1.0 \times$ their diameter) (Fig. 7C). Mesopleuron coarsely and densely punctate except for the areas on and below speculum. Sternaulus weakly impressed. Propodeum weakly protruded basal 0.2 in lateral view (Fig. 9D), rugulose (Fig. 7D), without carinae except for pleural carina. Fore wing length $6.5\text{--}7.4$ mm. Nervellus intercepted below middle. Hind femur $4.2\text{--}4.3$ \times as long as maximum depth in lateral view. Hind tibia 7.5 \times as long as maximum depth in lateral view. Ratio of length of hind first to fifth tarsomeres 1.0: 0.6–0.7: 0.4: 0.2–0.3: 0.3.

Metasoma. T I nearly square in dorsal view (Fig. 9K), $0.95\text{--}1.05$ \times as long as maximum width, rugulose laterally. Latero-median carina present basal ca. 0.5 of T I (Fig. 9K). T II $0.65\text{--}0.75$ \times as long as maximum width, striate anteriorly.

Coloration (Fig. 7A–D). Body (excluding wings and legs) black. Face with a large yellow spot medially (this spot sometimes obscured). Palpi, tegula and mesepisternum yellow (mesepisternum sometimes darkened ventrally). Mandible yellow except for apex and base. Lateral aspect of pronotum with a yellow spot posteriorly. Scutellum with a yellow spot apically. Subtegular ridge often tinged with yellow. Wings hyaline. Veins and pterostigma blackish-brown except for yellowish-brown wing base. Legs yellow to

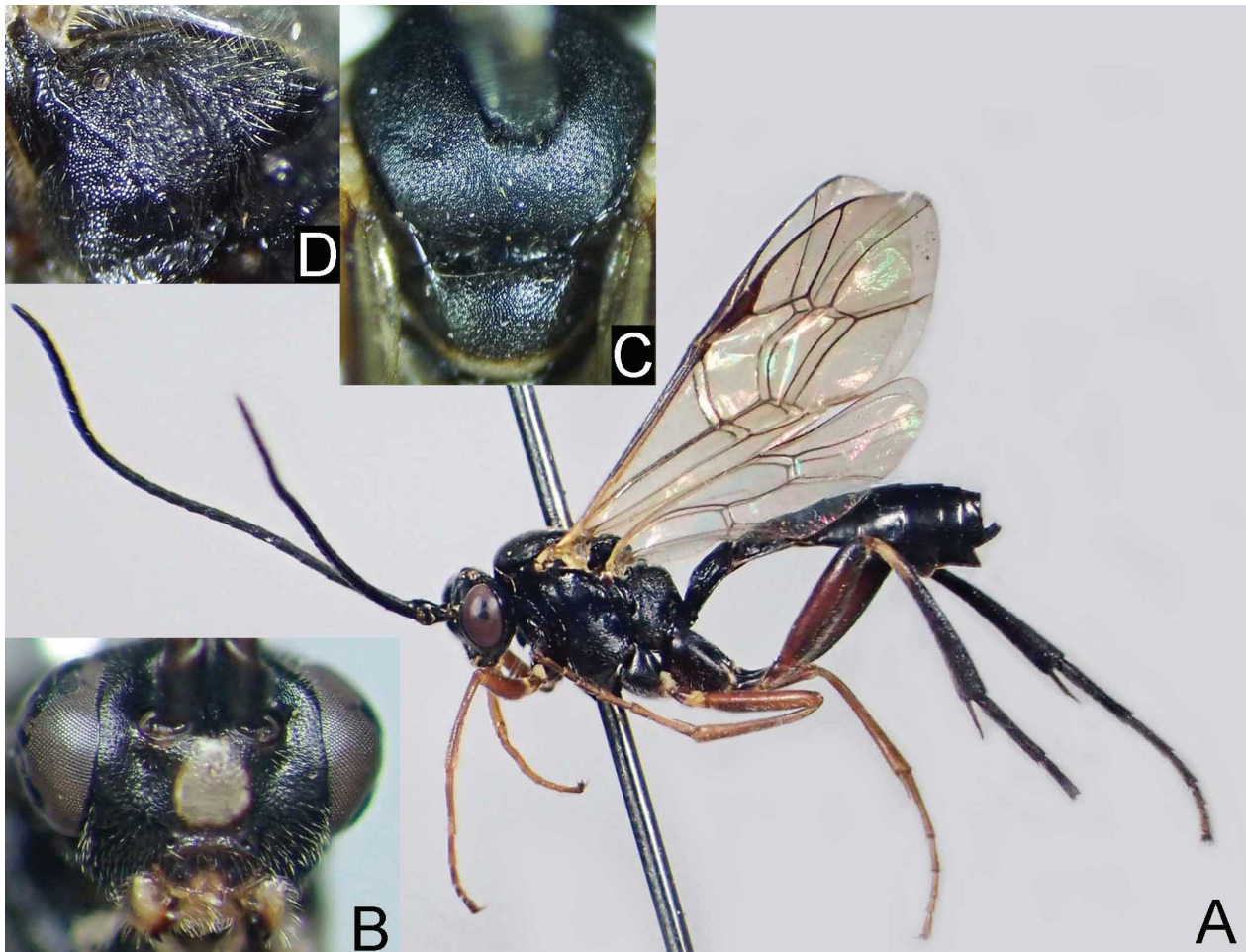


Figure 7. *Woldstedtius takagii* (Uchida, 1957) (A–D. female) — A. Habitus; B. Head, frontal view; C. Mesonotum, dorsal view; D. Propodeum, dorsal view.

brown. Fore and mid trochanters often tinged with black. Coxae, hind trochanter, hind tibia and hind tarsomeres black. Hind trochantellus and femur reddish-brown to blackish-brown. Base of hind tibia tinged with white.

Male. Unknown.

Distribution. Japan (Hokkaido and Honshu).

Bionomics. Host unknown. Adults were collected in broad-leaved forests of mountainous regions.

Remarks. This species resembles *W. kuroashii*, but can be distinguished from the latter by the following combination of character states in females: inner orbits divergent downward (almost parallel in *W. kuroashii*); propodeum weakly protruded basal 0.2 in lateral view (rounded in *W. kuroashii*); yellow shoulder marks of mesoscutum absent (present in *W. kuroashii*).

Woldstedtius yokohamensis (Uchida, 1930)

Fig. 8A–D

Homocidus yokohamensis Uchida, 1930: 258

Materials examined. Type series: JAPAN: [Honshu] 1 F (*holotype*), Yokohama, 26 Apr 1928, K. Sato leg. (SEHU).

Description. Female (n = 1: holotype). Body length 9.1 mm, polished, coriaceous, covered with silver setae.

Head 0.5 × as long as wide. Clypeus 2.0 × as broad as high, convex basally in lateral view. Face 2.0 × as broad as high, finely and densely punctate, convex medially in lateral view, separated from clypeus by shallow clypeal sulcus. Inner orbits almost parallel (Fig. 8B). Length of malar space 1.1 × as long as basal mandibular width. POL 2.1 × as long as OD. OOL 1.25 × as long as OD. POL 2.0 × as long as OOL. Antenna with 26 flagellomeres. FL I 1.35 × as long as FL II. MP IV 1.33 × as long as MP V.

Mesosoma. Lateral aspect of pronotum strigose anteriorly. Mesoscutum finely and densely punctate (separated by ca. 1.0 × their diameter) (Fig. 8C). Scutellum finely and densely punctate (separated by ca. 1.0 × their diameter). Mesopleuron finely rugulose and densely punctate except for the areas on and below speculum. Sternaulus very weakly impressed. Propodeum rounded in lateral view, rugulose (Fig. 8D), without carinae except for pleural carina. Fore wing length 7.1 mm. Nervellus intercepted below middle. Hind femur 4.4 × as long as maximum depth in lateral view. Hind tibia 8.5 × as long as maximum depth in lateral view. Ratio of length of hind first to fifth tarsomeres 1.0: 0.7: 0.4: 0.2: 0.26.

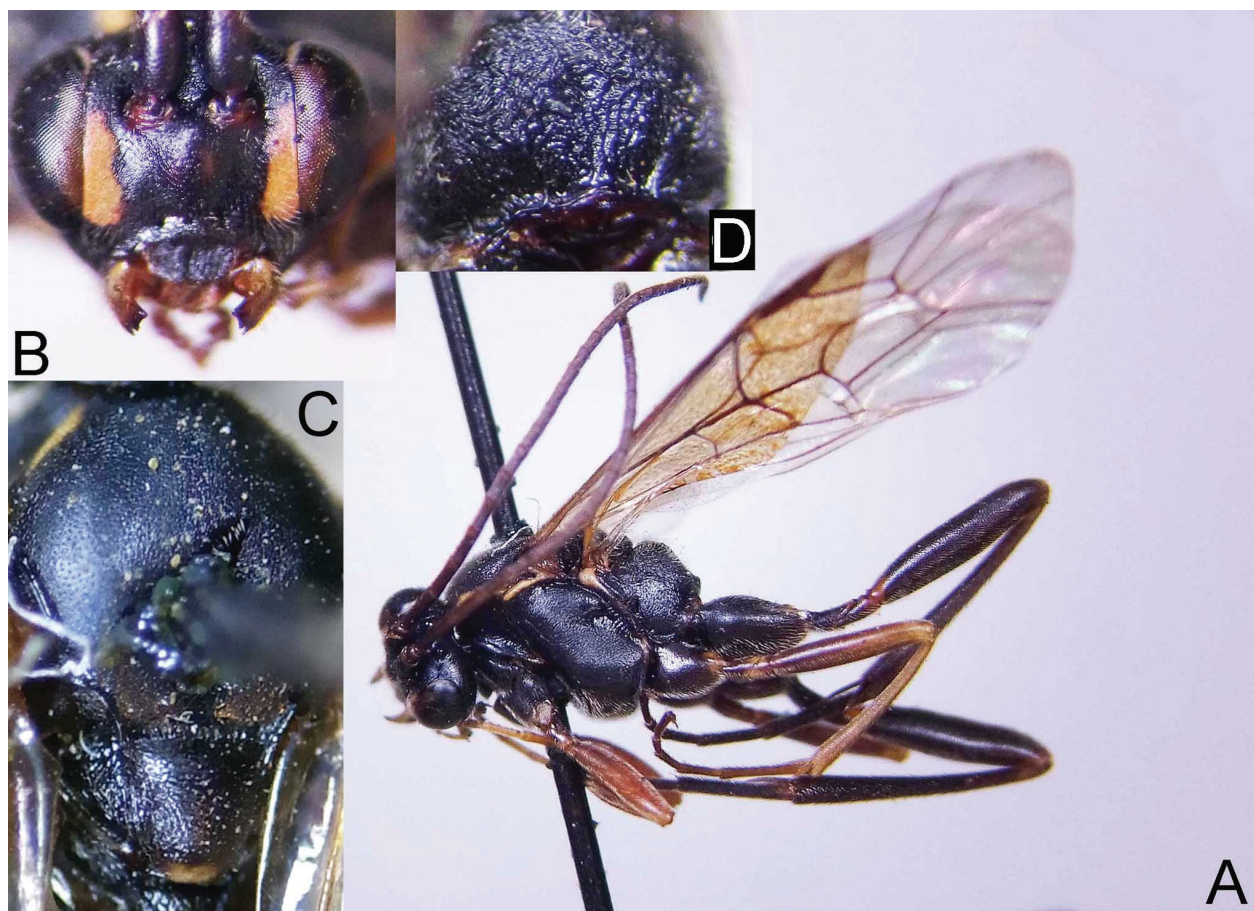


Figure 8. *Woldstedtius yokohamensis* (Uchida, 1930) (A–D. female, holotype) — A. Habitus; B. Head, frontal view; C. Mesonotum, dorsal view; D. Propodeum, dorsal view.

Metasoma. T I rectangular in dorsal view, $1.3 \times$ as long as maximum width. Latero-median carina present basal ca. 0.5 of T I. T II $0.72 \times$ as long as maximum width, striate anteriorly and strigose laterally.

Coloration (Fig. 8A–D). Body (excluding wings and legs) black. Face with a pair of yellow spots along inner orbits. Palpi, subtegular ridge and upper mesepisternum yellow. Mandible yellow except for apex. Lateral aspect of pronotum with a yellow spot posteriorly. Mesoscutum with yellow shoulder marks. Scutellum with a yellow spot apically. Wings hyaline. Veins and pterostigma blackish-brown except for yellowish-brown wing base. Legs black. Fore and mid trochantelli, femora, tibiae and tarsi yellowish-brown to brown. Apex of hind trochantellus and base of hind femur tinged with reddish-brown. Base of hind tibia tinged with brown.

Male. Unknown.

Distribution. Japan (Honshu). Outside Japan, this species has been recorded from South Korea (Balueva and Lee 2016).

Bionomics. Unknown.

Remarks. This species may be rare in Japan. We could only examine the holotype. No additional specimen of this species from Japan was found.

Notes on the distribution and habitat of Japanese *Woldstedtius*

In the Japanese Diplazontinae, the proportion of the species with holarctic distribution shows a strong bias by genus (e.g., 44% in *Diplazon*, 14% in *Promethes* and 17% in *Sussaba*). Our findings revealed that 33% (three of nine species) of Japanese *Woldstedtius* are also distributed in the Holarctic region. In addition, given that *W. karafutensis* and *W. yokohamensis*, which were previously known only from Japan, have subsequently been recorded in Korea by Balueva and Lee (2016), we speculate that the currently known Japanese endemics, namely, *W. alpicola*, *W. punctatus*, and *W. takagii*, may also be distributed in other parts of the Eastern Palearctic Region.

Woldstedtius biguttatus is the most commonly collected species of *Woldstedtius* in Japan, and is typically found in different types of open habitat (e.g., grasslands, meadows, and paddy fields). In contrast, those species characterized by black coxae, namely, *W. alpicola*, *W. kuroashii*, *W. punctatus*, and *W. takagii*, are generally collected from the canopies of broad-leaved trees, and compared with *W. biguttatus*, fewer specimens of these species have been collected. We specu-

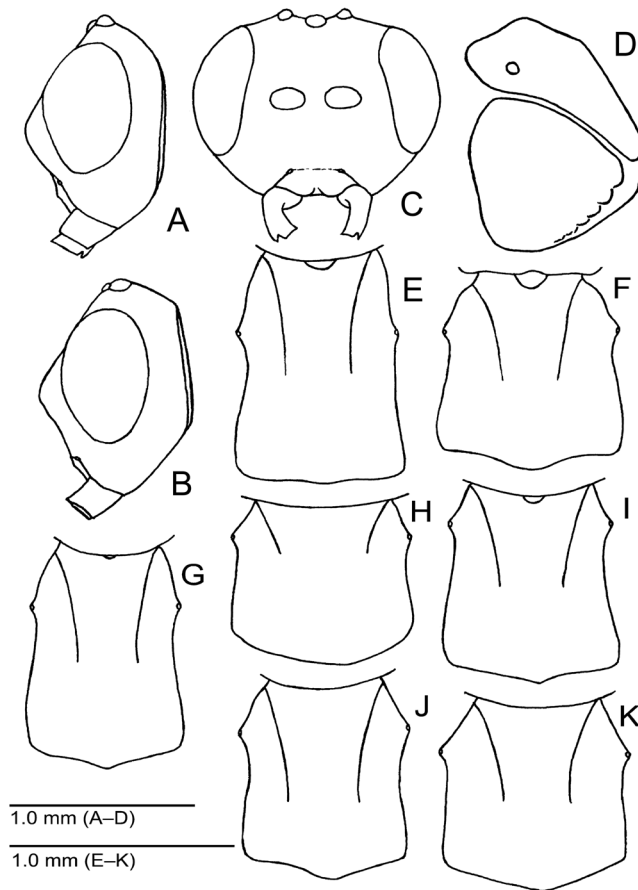


Figure 9. Japanese *Woldstedtius* **A, G.** *W. f. flavolineatus* (Gravenhorst, 1829); **B, I.** *W. kuroashii* (Uchida, 1957); **C, D, K.** *W. takagii* (Uchida, 1957); **E.** *W. alpicola* sp. nov.; **F.** *W. biguttatus* (Gravenhorst, 1829); **H.** *W. karafutensis* (Uchida, 1957); **J.** *W. punctatus* sp. nov. (**E, J.** holotype; **B, I.** paratype) — **A, B.** head, lateral view; **C.** head, frontal view; **D.** propodeum, lateral view; **E–K.** T I, dorsal view.

late that these differences in habitat usage could be attributable to the habitat requirements of the respective host species.

Acknowledgements

The authors wish to express their cordial thanks to David Wahl (AEIC), Kenzo Yamagishi (MU), Masahiro Ohara (SEHU), and Michiaki Hasegawa (TMNH), for their kind support in researching the collections and also to Tatsuya Ide (NSMT) and Stefan Schmidt (ZSM) for the generous loan of valuable specimens. This study was partly supported by the Grant-in-Aid for JSPS KAKENHI Grant numbers 19H00942 for KW.

References

- Balueva EN, Lee JW (2016) Study of the genus *Woldstedtius* Carlson (Hymenoptera: Ichneumonidae: Diplazontinae) with description of three new species in South Korea. *Journal of Asia-Pacific Entomology* 19(2): 387–397. <https://doi.org/10.1016/j.aspen.2016.04.012>
- Bridgman JB (1886) Further additions to the Rev. T.A. Marshall's catalogue of British Ichneumonidae. *The Transactions of the Entomological Society of London* 1886: 335–373. <https://doi.org/10.1111/j.1365-2311.1886.tb01631.x>
- Broad GR, Shaw MR, Fitton MG (2018) Ichneumonid Wasps (Hymenoptera: Ichneumonidae): their classification and biology. *Handbooks for the Identification of the British Insects* 7(12): 1–418. [+ vi]
- Carlson RW (1979) Family Ichneumonidae. Stephanidae. In: Krombein KV, Hurd PDJ, Smith DR, Burks BD (Eds) *Catalog of Hymenoptera in America north of Mexico*. Smithsonian Institution Press, Washington, 315–741.
- Cresson ETJ (1868) A list of the Ichneumonidae of North America, with descriptions of new species. *Transactions of the American Entomological Society* 2: 89–114. <https://doi.org/10.2307/25076198>
- Dasch CE (1964) Ichneumon-flies of America north of Mexico 5: Subfamily Diplazontinae. *Memoirs of the American Entomological Institute* 3: 1–304.
- Diller EH (1969) Beitrag zur Taxonomie der Gattung *Syrphoctonus* Foerster mit Beschreibung einer neuen holarktischen Art (Hymenoptera, Ichneumonidae). *Acta Entomologica Musei Nationalis Pragae* 38: 545–552.
- Gauld ID, Wahl D, Bradshaw K, Hanson WS (1997) The Ichneumonidae of Costa Rica, 2. *Memoirs of the American Entomological Institute* 57: 1–485.
- Gravenhorst JLC (1829) *Ichneumonologia Europaea. Pars III. Sumtibus auctoris, Vratislaviae, 1097 pp.* <https://doi.org/10.5962/bhl.title.65750>

- Habermehl H (1925) Beiträge zur Kenntnis der palaearktischen Ichneumonidenfauna. *Konowia* 4: 264–276.
- Holmgren AE (1858) Försök till uppställning och beskrifning af de i Sverige funna Tryphonider (Monographia Tryphonidum Sueciae). Kongliga Svenska Ventenskapsakademiens Handlingar Neue Folge 1(2): 305–394.
- Johansson N (2020) Additions to the Swedish fauna of Diplazontinae (Hymenoptera: Ichneumonidae) with the descriptions of five new species. *European Journal of Taxonomy* 724: 70–92. <https://doi.org/10.5852/ejt.2020.724.1159>
- Klopfstein S (2014) Revision of the Western Palaearctic Diplazontinae (Hymenoptera, Ichneumonidae). *Zootaxa* 3801(1): 1–143. <https://doi.org/10.11646/zootaxa.3801.1.1>
- Konishi K, Matsumoto R, Yoshida T, Watanabe K (2014) Ichneumonidae and Trigonalidae (Hymenoptera) collected by faunal survey of the Imperial Palace, Tokyo. *Memoirs of the National Science Museum* 50: 485–497. [In Japanese]
- Manukyan AR (2007) Diplazontinae. In: Lelej AS (Ed.) Neuropteroidea, Mecoptera, Hymenoptera. Pt 5. Dalnauka, Vladivostok, 718–732. [in Russian]
- Morishita S, Watanabe K, Yamauchi T (2021) Records of ichneumonid wasps collected by Malaise traps in Toyama Prefecture, Japan (part 2). *Tsunekibachi* 36: 47–57. [In Japanese]
- Morley C (1906) On the Ichneumonidous group Tryphonides schizodonti, Holmgr., with descriptions of new species. *Transactions of the Royal Entomological Society of London* 4: 419–438. <https://doi.org/10.1111/j.1365-2311.1906.tb02460.x>
- Provancher L (1883) Faune Canadienne. Hyménoptères. Additions et corrections. *Naturaliste Canadien* 14: 3–20.
- Schmiedeknecht O (1926) *Opuscula Ichneumonologica*. V. (Fasc. XLII–XLIII.) Tryphoninae. Blankenburg in Thüringen, 3283–3442.
- Teunissen HGM (1948) Naamlijst van inlandse sluipwespen (Fam. Ichneumonidae I). *Tijdschrift voor Entomologie* 89: 10–38.
- Thomson CG (1890) XLIII. Öfversigt af arterna inom släktet Bassus (Fab.). *Opuscula Entomologica*. Lund XIV: 1459–1525.
- Uchida T (1930) Vierter Beitrag zur Ichneumoniden-Fauna japans. *Journal of the Faculty of Agriculture, Hokkaido University* 25: 243–298.
- Uchida T (1957) Beitrage zur kenntnis der Diplazoninen fauna japans und seiner umgegenden (hymenoptera, Ichneumonodae). *Journal of the Faculty of Agriculture, Hokkaido University* 50: 226–265.
- Vas Z (2016) *Woldstedtius merkli* sp. n. from Hungary (Hymenoptera: Ichneumonidae). *Folia Entomologica Hungarica* 77: 57–65. <https://doi.org/10.17112/FoliaEntHung.2016.77.57>
- Yu DS, van Achterberg K, Horstmann K (2016) World Ichneumonoidea 2015. Taxonomy, biology, morphology and distribution. [Database on flash drive]. Taxapad, Vancouver.

Identity of *Zorotypus juninensis* Engel, 2000, syn. nov. revealed: it is conspecific with *Centrozoros hamiltoni* (New, 1978) (Zoraptera, Spiralizoridae)

Petr Kočárek¹, Ivona Horká¹

¹ Department of Biology and Ecology, University of Ostrava, Chittussiho 10, CZ-710 00 Ostrava, Czech Republic

<http://zoobank.org/561646B1-FB8F-4126-91EA-9B67F76215BE>

Corresponding author: Petr Kočárek (petr.kocarek@osu.cz)

Academic editor: Susanne Randolf ♦ Received 5 March 2022 ♦ Accepted 19 May 2022 ♦ Published 8 June 2022

Abstract

Zorotypus juninensis Engel, 2000, was previously diagnosed based on the external morphology of female and male specimens without description of the male copulatory organ, which is an important character for classification in Zoraptera. Based on a detailed morphological study of the *Zorotypus juninensis* Engel, 2000 type collections deposited in the American Museum of Natural History in New York, and based on the comparison with the holotype male of *Centrozoros hamiltoni* (New, 1978), we have determined that these two species are conspecific. We therefore formally synonymize *Zorotypus juninensis* Engel, 2000, **syn. nov.** with *Centrozoros hamiltoni* (New, 1978). Morphological characters and phylogenetic relationships of *Centrozoros* Kukalova-Peck & Peck, 1993 are also discussed in this report.

Key Words

Neotropical region, Peru, Polyneoptera, synonymy, taxonomy

Introduction

Zoraptera is one of the smallest and least known of the insect orders (Mashimo et al. 2014b). The extant diversity of Zoraptera is much lower than that of almost all other groups of Hexapoda, with only 44 described species (Mashimo et al. 2014b; Choe 2018; Kočárek et al. 2020) that are distributed mainly in tropical regions (Hubbard 1990; Choe 2018). Zoraptera show extreme uniformity in general body morphology, and this has led to the persistence of a conservative classification of extant Zoraptera with only a single nominotypical genus in a single family for > 100 years (Mashimo et al. 2014b; Kočárek et al. 2020). All known extant species were described within a single genus, *Zorotypus* Silvestri, 1913 (Kočárek et al. 2020). Kukalova-Peck and Peck (1993) were the first to propose a classification of Zoraptera into seven genera based on wing venation, and Chao and Chen (2000) subsequently introduced a new genus, *Formosozoros*, based on a single

apomorphic species from Taiwan. Engel and Grimaldi (2000) critically revised the supraspecific classification of Zoraptera and concluded that the proposed generic characters concerning wing venation are either continuous across taxa or variable within a given species. In contrast to the external uniformity in Zoraptera, there are repeatedly documented conspicuous differences in the reproductive system (Dallai et al. 2012, 2014, 2015). These observations suggested the existence of deep evolutionary lineages within Zoraptera, although at the time, not enough information was available to reconstruct the phylogeny (Kočárek et al. 2020).

Matsumura et al. (2020) and Kočárek et al. (2020) conducted the first molecular phylogenetic studies using a combination of nuclear and mitochondrial markers. Both independent analyses revealed two major phylogenetic lineages with maximal statistical support. These two lineages were classified by Kočárek et al. (2020) as families (Zorotypidae Silvestri, 1913 and Spiralizoridae Kočárek, Horká

& Kundera, 2020), and each of them was divided into two robustly supported subclades, i.e. subfamilies (Kočárek et al. 2020). The recognition of two families and four subfamilies is supported by synapomorphies in the structure and shape of the male genitalia and other taxonomically valuable characters. Striking differences in the structure of male genitalia within the recovered monophyletic clades illustrate deep divergences of these old evolutionary lineages.

The classification proposed by Kočárek et al. (2020) comprises two families, four subfamilies, and nine genera, and is based mainly on a molecular phylogenetic analysis in combination with an analysis of the morphology of the male reproductive system. Unfortunately, researchers described some species based solely on immature or female specimens or provided insufficient information on male genitalia (Kočárek et al. 2020). Altogether, 9 species could not be properly assigned to a supraspecific rank and therefore remain *incertae sedis* until males are described or molecular phylogenetic studies are conducted. One of these species is *Zorotypus juninensis* Engel, 2000, for which the original diagnosis was based on female and male specimens without available information about the male reproductive system, i.e., without information required for generic classification.

In this contribution, we present the results of morphological analysis of the type series of *Zorotypus juninensis* Engel, 2000 which led to the clarification of the taxonomical status of this species.

Materials and methods

The type specimens of *Zorotypus juninensis* Engel, 2000, which were stored in 96% ethanol, were studied and photographed with a Leica Z16 APO macroscope equipped with a CANON 6D Mark II camera; a slide-mounted type specimen of *Centrozoros hamiltoni* (New, 1978) and genitalia of *Z. juninensis* were observed and documented with an Olympus CX41 microscope equipped with a Canon D1000 camera. Micrographs of 20 to 30 focal layers of the same specimen were combined with Helicon Focus software and finally processed with Adobe Photoshop CS6 Extended (version 13). Coiled flagella were measured with Corel Draw software. For observation of genital armature, the armature was placed in a 10% KOH solution at room temperature for 1 h before it was washed with distilled water and returned to 96% ethanol for observation and storage.

The classification and nomenclature are based on the study by Kočárek et al. (2020); abdominal morphology follows Mashimo et al. (2014a).

Total genomic DNA was isolated from the tissue of the paratype female of *Z. juninensis* (AMNH: IZS00343398) with courtesy of the museum. The isolation was performed with a QIAamp DNA Micro Kit (QIAGEN, Hilden, Germany) following the manufacturer's protocol. The mitochondrial markers, 16S rRNA and the cytochrome c oxidase subunit I (COI), and the nuclear marker, 18S rRNA, were amplified by PCR with minor modification of previously reported thermal cycling conditions (Kočárek et al.

2020). Partial segments of these markers were amplified using the primers listed in Kočárek et al. (2020).

Depositories for type specimens are abbreviated as follows: AMNH (American Museum of Natural History, New York, USA); BMNH (The Natural History Museum, London, United Kingdom); ZMH (Zoological Museum Hamburg, Germany). Classification and nomenclature follow Kočárek et al. (2020).

In addition to investigating the type material of *C. hamiltoni* (New, 1978) and *Z. juninensis* Engel, 2000 (see the next section), we compared the material with the following museum specimens of *Centrozoros neotropicus* (Silvestri, 1916): COSTA RICA · 1 ♂; San José; 14 Nov 1935; leg. F. Nevermann; coll. ZMH; COSTA RICA · 1 ♀; Farm Hamburg am Ravantazon; 4 Feb 1934; leg. F. Nevermann; coll. ZMH.

Taxonomy

Centrozoros hamiltoni New, 1978

Figs 1, 2

Zorotypus juninensis Engel, 2000 syn. nov.

Note. New 1978: 365–368 (description, illustration, keyed); Hubbard 1990: 52 (catalog of world species); Choe 1989: 150 (distribution map); Choe 1992: 250 (distribution map); Engel 2000: (description of *Z. juninensis*, syn. nov.); Choe 2018: 200 (distribution); Mashimo et al. 2019: 753 (distribution); Matsumura et al. 2020: 352–357 (distribution, phylogenetic relationships); Kočárek et al. 2020: 11–12, 14–15 (male genitalia, classification).

Studied type material. *Centrozoros hamiltoni* (New, 1978) – **Holotype:** COLOMBIA · 1 apterous ♂; nr. Purace, Marenberg, Huila; 30 Mar 1976; leg. W.D. Hamilton; coll. BMNH; *Zorotypus juninensis* Engel, 2000, syn. nov. – **Holotype:** PERU · 1 apterous ♀; Agueas Mellizas, Estancia Naranjal San Ramon, Dep. Junin; 1 500 m; July 1965; leg. P. & B. Wygodzinsky; coll. AMNH: IZS00343397; **Paratypes:** 1 apterous ♀; 1 apterous ♂: same locality data as in Holotype (AMNH: IZS00343398).

Diagnosis. Dark-brownish black Zoraptera, with anterior regions of abdominal tergites darker than posterior regions; antennal segment nine, and apex of segment eight pale. Body length ranges from 2.9 to 3.6 mm; antennal length ranges from 1.45 to 1.63 mm. Ventral side of metafemur with row of 8 to 10 thickened setae situated in the distal two-thirds of the femur; proximal third with several (5–8) slender setae (Fig. 1A, B). Metafemur of females with the same arrangement of setae with less pronounced thickening. Abdominal tergites T5–T8 (Fig. 2A–D) each with a single posterior row of 10 to 14 setae and 1 or 2 more anterior setae near each lateral border. Abdominal tergite T9 with group of 6 to 8 thickened setae on each side of the midline (Fig. 2A, D). Tergite T10+11 membranous medially (Fig. 2A, C, D), with about 20 short setae each side of the midline and a median insert bearing a short dorsally curved extension (mating hook).

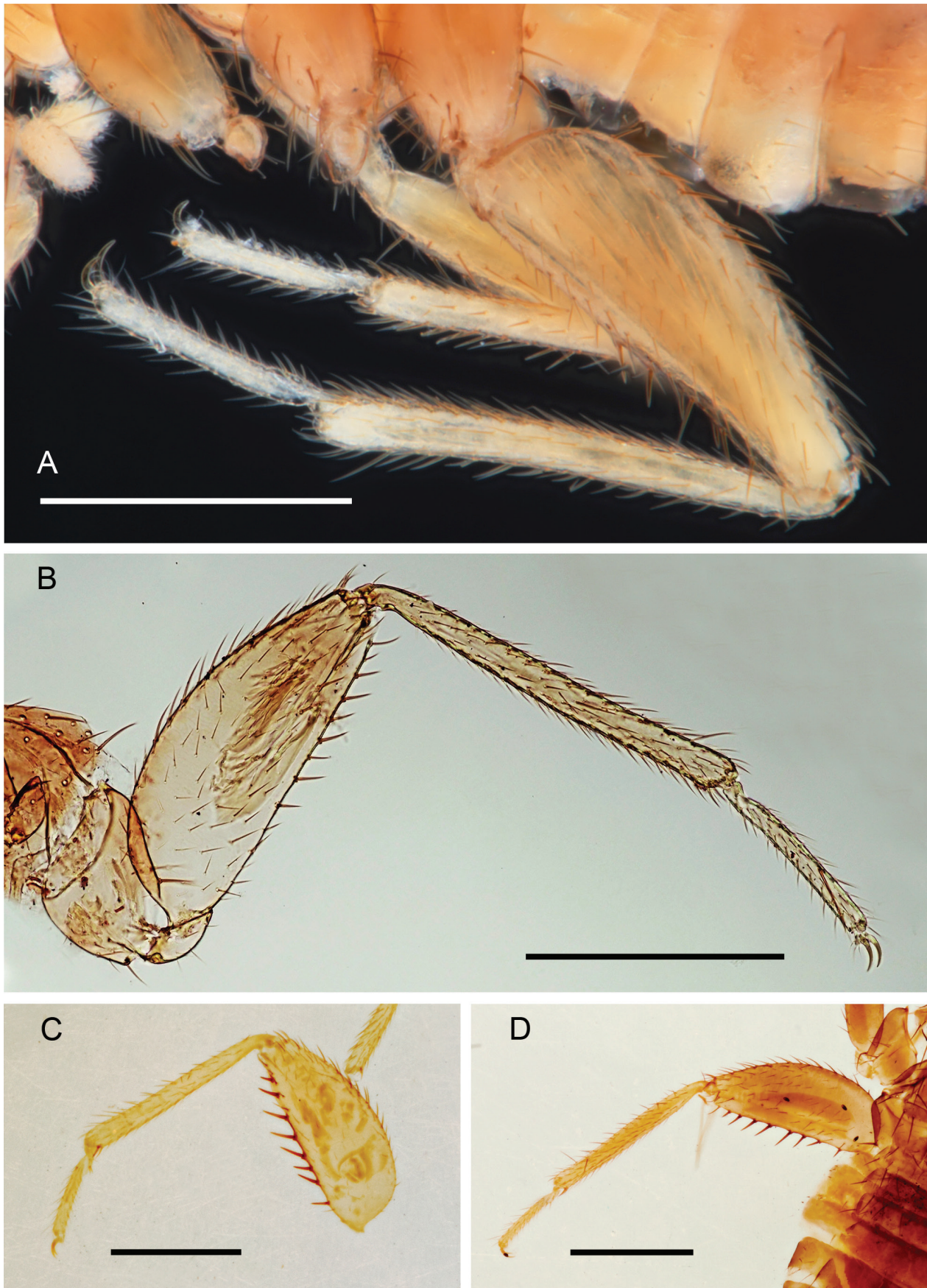


Figure 1. A. Hind legs of the paratype male of *Zorotypus juninensis* Engel, 2000 syn. nov.; B. Hind leg of the holotype male of *Centrozoros hamiltoni* (New, 1978); C. Hind leg of a male of *Centrozoros neotropicus* (Silvestri, 1916); D. Hind leg of a female of *C. neotropicus*. Scale bars: 0.5 mm.

Cerci (Fig. 2A–D) slightly longer than wide, tapered, with several long apical setae. Male genitalia symmetrical (Fig. 2E, F). Basal plate flat, 0.5 mm long, sclerotized, with an anterior conical process, and posteriorly bifurcated; flagellum sclerotized, coiled, and 1.4 mm long.

Taxonomic comments. The studied paratype male of *Z. juninensis* fully agrees with the holotype male of *C. hamiltoni* in external characters as well as in morphology of male genital armature. The spiral of the coiled flagellum is more open in paratype of *Z. juninensis* (Fig. 2E) than in *C. hamiltoni* (Fig. 2F); the less open flagellum of *C. hamiltoni* is probably an artefact of preparation. We measured the lengths of both flagella, and these were nearly identical (1.382 mm for *Z. juninensis* vs. 1.375 mm for *C. hamiltoni*).

Centrozoros hamiltoni (New, 1978) is morphologically similar to *C. manni* (Caudell, 1923), *C. neotropicus* (Silvestri, 1916), *C. cramptoni* (Gurney, 1938), and *C. gurneyi* (Choe, 1989). *C. manni* is known only from female specimens. Engel and Grimaldi (2000) reported that *C. hamiltoni* (*sensu* this study) differed from *C. manni* in lacking a medial cleft on the apex of S8 in females and in its broadly separated basal processes on S9 in females, its S9 setation pattern on females, its medial field of minute spicules on the cerci, and its long, sinuous setae on the cerci. *Centrozoros neotropicus* (Silvestri, 1916) is another species similar to *C. hamiltoni* in external morphology, including the setation and arrangement of abdominal tergites/sternites. This species is known only from Costa Rica (Silvestri 1916; Gurney 1938; Choe 1992; Kočárek et al. 2020), and it differs from *C. hamiltoni* in the arrangement of its metafemur setae (Fig. 1C, D), which are composed of 5–9 thick setae of similar length (as noted earlier, *C. hamiltoni* has 8–10 thickened setae in the distal two-thirds of its femurs and 5–8 slender and shorter setae in the basal one-third of its femurs). The morphology of only females has been described in literature (Silvestri 1916). We also studied the single male specimen of *C. neotropicus* deposited in the ZMH collections, but the permanent slide did not enable the detailed study of the copulatory organs necessary for clear species diagnosis. The validity of this species was verified molecularly (Kočárek et al. 2020), but the diagnosis should be augmented by the description of male genitalia after the next specimens of males are found. *Centrozoros cramptoni* and *C. gurneyi* seem to be most closely related to *C. hamiltoni* based on their similar morphology of male genital armature. The proximal part of the basal plate of both species has a conical shape as does the plate in *C. hamiltoni*, but the corners of the bifurcated basal part are continually divergent in *C. cramptoni* (Gurney, 1938) in contrast to the convergent tips of corners in *C. hamiltoni* (Fig. 2E, F); in the case of *C. gurneyi*, the bifurcated part regularly narrows towards the end, and the tips of the arms are narrower than the midregion of the basal plate (Choe 1989). These three species also differ in the arrangement of metafemur setae and in the setation of abdominal tergite T9. Like sternite 8 in *C. manni* females, sternite S8 in the females of *C. gurneyi* have an emarginated tip (in contrast to *C. hamiltoni* and *C. neotropicus* with not emarginated distal margin of S8). Relative to *C. hamiltoni*, *C. gurneyi* and *C. cramptoni*,

the other two *Centrozoros* species (*C. snyderi* (Caudell, 1920) and *C. mexicanus* (Bolivar y Pieltain, 1940)) differ substantially in the morphology of male genitals in that they have a broad rather than a conical basal plate (Gurney 1938; Bolivar y Pieltain 1940). *Centrozoros snyderi* and *C. mexicanus* appear to be closely related.

Molecular identification. For unequivocal species identification, we attempted to obtain a DNA barcode from the *Z. juninensis* paratype (AMNH: IZS00343398). For DNA isolation, we used the QIAamp DNA micro kit designed for a small amount of tissue. According to the voucher, the specimen was preserved in pure ethanol and was almost 60 years old when we examined it. Although we have attempted to amplify the DNA several times, our attempts to obtain partial sequences of 16S RNA, COI, and 18S RNA have failed.

Distribution. *Centrozoros hamiltoni* (New, 1978) was originally reported from Colombia (New 1978), and was additionally documented from Colombia by Villamizar and González-Montana (2018). The morphological characters of a single male from Barbados mentioned by New (1978) were similar to all of the characters described for *C. hamiltoni* except that basal plate was a little narrower and shorter on the Barbados male than on the *C. hamiltoni* males; Matsumura et al. (2020) described a specimen from Ecuador that they tentatively identified as *C. hamiltoni*. *Zorotypus juninensis* Engel, 2000 has been described from Junin Province in Peru (Engel and Grimaldi 2000), and was later reported from Peru by Matsumura et al. (2020). Published records indicate that the distribution of *C. hamiltoni* includes western Amazonia (Colombia, Peru, Ecuador), but the record from Barbados suggests a potentially wider distribution in the Neotropical region. Further studies are needed to clarify the distribution of *C. hamiltoni*.

Discussion

The genus *Centrozoros* (Kukalova-Peck & Peck, 1993) has been described based only on the wing venation of *C. gurneyi* (Choe, 1989). Engel and Grimaldi (2000) synonymized this genus with *Zorotypus* Silvestri, 1913 based on the variability of characters used for the generic diagnosis. Kočárek et al. (2020) reinstated the genus based on molecular phylogeny relationships and a critical evaluation of morphological characters. The genus *Centrozoros* (Kukalova-Peck & Peck, 1993) *sensu* Kočárek et al. (2020) includes species that are distributed in the Neotropical region and whose males have an enlarged basal plate with a coiled intromittent organ and an anterior tongue-like process that is not dilated anteriorly (Kočárek et al. 2020). *Centrozoros hamiltoni*, *C. cramptoni*, and *C. gurneyi* share a similar basic morphological plan of the male genitalia, and these three species probably compose a monophyletic group in *Centrozoros* along with *C. mexicanus* and *C. snyderi*. The remaining *Centrozoros* species are known only from females, and their taxonomic relationships are therefore unclear. *Centrozoros hamiltoni* fully fits the diagnostic characters of *Centrozoros*, and the

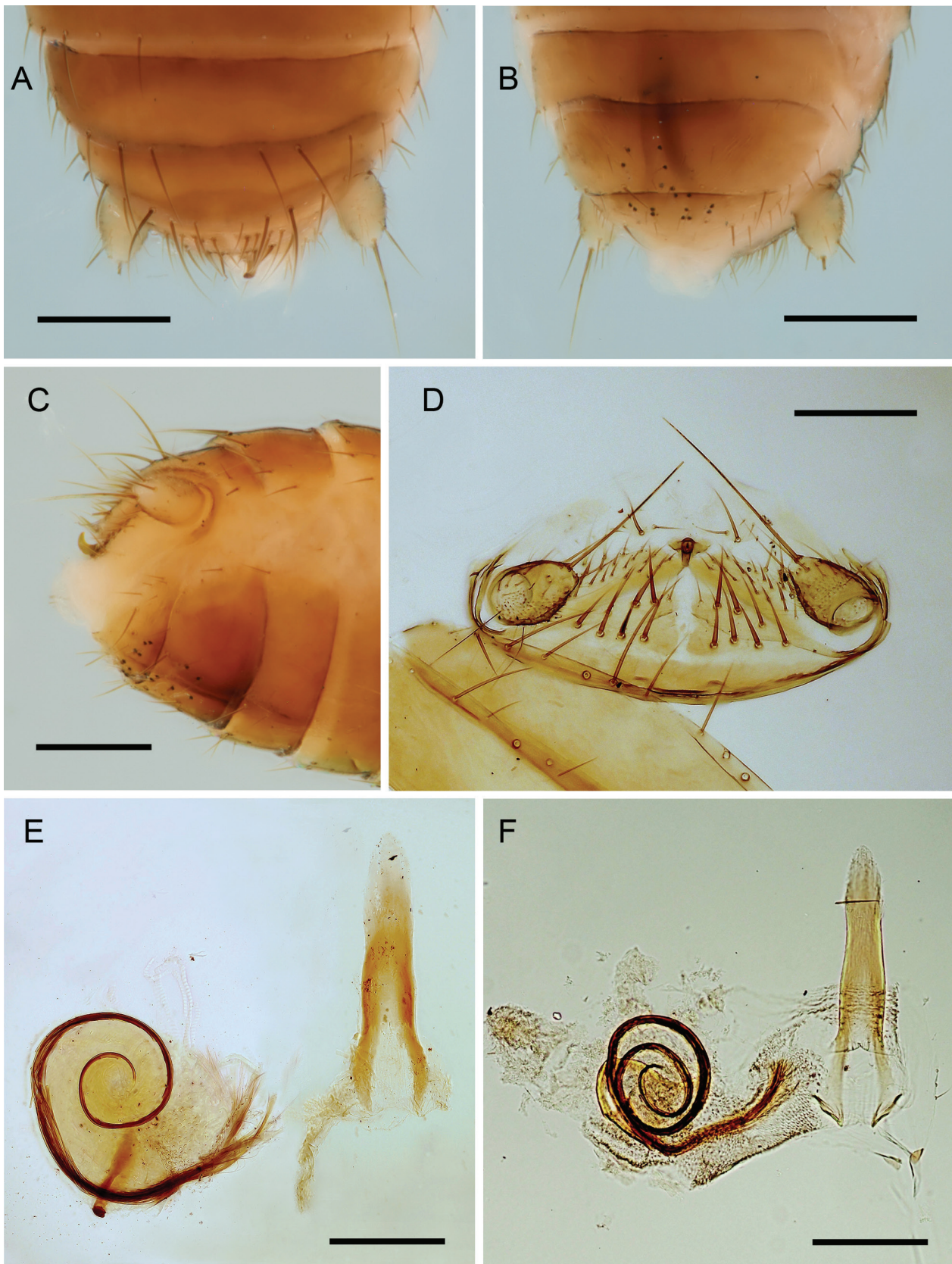


Figure 2. *Centozoros hamiltoni* (New, 1978). **A, B, C, E.** The paratype male of *Zorotypus juninensis* Engel, 2000, syn. nov.; **D, F.** The holotype male of *C. hamiltoni*. **A.** Tip of the male abdomen of *C. hamiltoni*, dorsal view; **B.** Tip of the male abdomen of *C. hamiltoni*, ventral view; **C.** Tip of the male abdomen of *C. hamiltoni*, ventro-lateral view; **D.** Tip of the male abdomen of *C. hamiltoni*, dorsal view; **E.** Male genital armature of the *Z. juninensis* paratype; **F.** Male genital armature of the *C. hamiltoni* holotype. Scale bars: 0.2 mm.

placement to *Centrozoros* has been proved also by molecular phylogeny studies of Matsumura et al. (2020), with *C. manni*, *C. mexicanus* and *Z. juninensis* (= *C. hamiltoni*) included.

To date, molecular characterizations have been published for four of the seven described species of *Centrozoros*, i.e., for *C. manni*, *C. mexicanus*, *C. hamiltoni*, and *C. neotropicus* (Kočárek et al. 2020; Matsumura et al. 2020). However, both Matsumura et al. (2020) and Kočárek et al. (2020) reported several molecularly different, undescribed species of *Centrozoros*. It is therefore evident that the genus is more diverse than previously thought and requires extensive taxonomic revision. Because of the high level of external uniformity in Zoraptera (and supposed parthenogenetic reproduction in some species of *Centrozoros*), it is important to clarify the species identity by DNA barcodes, ideally extracted from the type specimens or at least from the type locality or from a locality that is geographically near the type locality.

Acknowledgements

We thank the following curators for loans of Zoraptera material from the collections under their care: Paul A. Brown and Maxwell V. L. Barclay (Natural History Museum, London, United Kingdom), Jessica L. Ware and Ruth Salas (American Museum of Natural History, New York, USA), and Thure Dalsgaard (Zoological Museum Hamburg, Germany). The research was supported by project GACR 22-05024S (Evolution of angel insects (Zoraptera): from fossils and comparative morphology to cytogenetics and transcriptomes). We would like to thank Bruce Jaffee (University of California at Davis, Davis, CA, USA) for linguistic and editorial suggestions.

References

- Bolivar y Pieltain C (1940) Estudio de un nuevo Zoraptero de Mexico. *Anales. Escuela Nacional de Ciencias Biologicas (Mexico)* 1(3–4): 513–523.
- Chao RF, Chen CS (2000) *Formosozoros newi*, a new genus and species of Zoraptera (Insecta) from Taiwan. *The Pan-Pacific Entomologist* 76: 24–27. <https://www.biodiversitylibrary.org/part/268683>
- Choe JC (1989) *Zorotypus gurneyi*, new species, from Panama and redescription of *Z. barberi* Gurney (Zoraptera: Zorotypidae). *Annals of the Entomological Society of America* 82(2): 149–155. <https://doi.org/10.1093/aesa/82.2.149>
- Choe JC (1992) Zoraptera of Panama with a review of the morphology, systematics, and biology of the order. In: Quintero D, Aiello A (Eds) *Insects of Panama and Mesoamerica, Selected Studies*, Oxford University Press, Oxford, UK, 249–256.
- Choe JC (2018) Biodiversity of Zoraptera and their little-known biology. In: Footitt RG, Adler PH (Eds) *Insect Biodiversity: Science and Society*. John Wiley & Sons Ltd., New York, NY, USA, Volume 2: 199–217. <https://doi.org/10.1002/9781118945582.ch8>
- Dallai R, Mercati D, Gottardo M, Dossey AT, Machida R, Mashimo Y, Beutel RG (2012) The male and female reproductive systems of *Zorotypus hubbardi* Caudell, 1918 (Zoraptera). *Arthropod Structure & Development* 41(4): 337–359. <https://doi.org/10.1016/j.asd.2012.01.003>
- Dallai R, Gottardo M, Mercati D, Machida R, Mashimo Y, Matsumura Y, Rafael JA, Beutel RG (2014) Comparative morphology of spermatzoa and reproductive systems of zorapteran species from different world regions (Insecta, Zoraptera). *Arthropod Structure & Development* 43(4): 371–383. <https://doi.org/10.1016/j.asd.2014.03.001>
- Dallai R, Gottardo M, Mercati D, Rafael JA, Machida R, Mashimo Y, Matsumura Y, Beutel RG (2015) The intermediate sperm type and genitalia of *Zorotypus shannoni* Gurney: Evidence supporting infraordinal lineages in Zoraptera (Insecta). *Zoomorphology* 134(1): 79–91. <https://doi.org/10.1007/s00435-014-0244-5>
- Engel MS, Grimaldi DA (2000) A winged *Zorotypus* in Miocene amber from the Dominican Republic (Zoraptera: Zorotypidae), with discussion on relationships of and within the order. *Acta Geologica Hispanica* 35: 149–164. <https://revistes.ub.edu/index.php/ActaGeologica/article/view/4741/6165>
- Gurney AB (1938) A synopsis of the order Zoraptera, with notes on the biology of *Zorotypus hubbardi* Caudell. *Proceedings of the Entomological Society of Washington* 40: 57–87. <https://archive.org/details/biostor-244799/page/n1/mode/2up>
- Hubbard MD (1990) A catalog of the order Zoraptera (Insecta). *Insecta Mundi* 4: 49–66. <https://digitalcommons.unl.edu/cgi/viewcontent.cgi?article=1392&context=insectamundi>
- Kočárek P, Horká I, Kundrata R (2020) Molecular Phylogeny and Infraordinal Classification of Zoraptera (Insecta). *Insects* 11(1): 51. <https://doi.org/10.3390/insects11010051>
- Kukalova-Peck J, Peck SB (1993) Zoraptera wing structures: Evidence for new genera and relationship with the blattoid orders (Insecta: Blattellodea). *Systematic Entomology* 18(4): 333–350. <https://doi.org/10.1111/j.1365-3113.1993.tb00670.x>
- Mashimo Y, Beutel RG, Dallai R, Lee CY, Machida R (2014a) Postembryonic development of the ground louse *Zorotypus caudelli* Karny (Insecta: Zoraptera: Zorotypidae). *Arthropod Systematics & Phylogeny* 72(1): 55–71. https://www.senckenberg.de/wp-content/uploads/2019/08/05_asp_72_1_mashimo_55-71.pdf
- Mashimo Y, Matsumura Y, Machida R, Dallai R, Gottardo M, Yoshizawa K, Friedrich F, Wipfler B, Beutel RG (2014b) 100 years Zoraptera—A phantom in insect evolution and the history of its investigation. *Insect Systematics & Evolution* 45(4): 371–393. <https://doi.org/10.1163/1876312X-45012110>
- Mashimo Y, Mueller P, Beutel RG (2019) *Zorotypus pecten*, a new species of Zoraptera (Insecta) from mid-Cretaceous Burmese amber. *Zootaxa* 4651(3): 565–577. <https://doi.org/10.11646/zootaxa.4651.3.9>
- Matsumura Y, Beutel RG, Rafael JA, Yao I, Câmara JT, Lima SP, Yoshizawa K (2020) The evolution of Zoraptera. *Systematic Entomology* 45(2): 349–364. <https://doi.org/10.1111/syen.12400>
- New TR (1978) Notes on Neotropical Zoraptera, with descriptions of two new species. *Systematic Entomology* 3(4): 361–370. <https://doi.org/10.1111/j.1365-3113.1978.tb00005.x>
- Silvestri F (1916) Diagnosi preliminare di una nuova specie di *Zorotypus* (Insecta, Zoraptera) di Costa Rica. *Bollettino del Laboratorio di Zoologia Generale e Agraria della R. Scuola Superiore d'Agricoltura in Portici* 10: e120.
- Villamizar G, González-Montana LA (2018) Morphological description of an alate female of *Zorotypus hamiltoni* New (Zoraptera: Zorotypidae) from Colombia. *Caldasia* 40(2): 255–261. <https://doi.org/10.15446/caldasia.v40n2.71887>

Taxonomic revision of the African and Southwest Asian species of *Platyderus* Stephens, subg. *Eremoderus* Jeanne (Coleoptera, Carabidae, Sphodrini)

Borislav Guéorguiev¹, David W. Wrase², Thorsten Assmann³, Jan Muilwijk⁴, Patrice Machard⁵

¹ National Museum of Natural History, Bulgarian Academy of Sciences, 1 Blvd. Tsar Osvoboditel, 1000 Sofia, Bulgaria

² Oderstr. 2, 15306, Gusow-Platow, Germany

³ Leuphana University Lüneburg, Institute of Ecology, Universitätsallee 1, 21335 Lüneburg, Germany

⁴ Department of Entomology, Naturalis Biodiversity Centre, Darwinweg 2, 2333 CR Leiden, Netherlands

⁵ 29 Chemin de Champigny, Molineuf, F-41190 Valencisse, France

<http://zoobank.org/7DEB0587-A373-4B06-BAAD-CA6102EC6581>

Corresponding author: Borislav Guéorguiev (gueorguiev@nmnhs.com)

Academic editor: James Liebherr ♦ Received 15 March 2022 ♦ Accepted 11 May 2022 ♦ Published 13 June 2022

Abstract

Species of the subgenus *Eremoderus* Jeanne, 1996, genus *Platyderus* Stephens, 1827, occurring in continental Africa (excluding Macaronesia) and southwest Asia, are taxonomically revised. The following new species groups and species are defined and described, “*weiratheri*” group: *Platyderus* (*Eremoderus*) *chatzakiae*, **sp. nov.** (type locality: Greece, Kalymnos Island, near Stimenia Village); “*iranicus-vanensis*” group: *Platyderus* (*Eremoderus*) *felixa*, **sp. nov.** (type locality: Iran, Chahar Mahal va Bakhtiari Province, 10 km west of Naghan Town); *Platyderus* (*Eremoderus*) *iranicus*, **sp. nov.** (type locality: Iran, Chahar Mahal va Bakhtiari Province, 7 km NE Naghan Town); *Platyderus* (*Eremoderus*) *vanensis*, **sp. nov.** (type locality: Turkey, Van Province, Gevaş Town); *Platyderus* (*Eremoderus*) *vrabeci*, **sp. nov.** (type locality: Turkey, Nemrut Dağı); “*lassallei*” group: *Platyderus* (*Eremoderus*) *lassallei*, **sp. nov.** (type locality: Iran, Mazandaran Province, between Nur City and Lavij Village); “*davatchii*” group: *Platyderus* (*Eremoderus*) *klapperichi*, **sp. nov.** (type locality: Iran, Mazandaran Province, Damavand, 2000 m); “*afghanisticus*” group: *Platyderus* (*Eremoderus*) *afghanisticus*, **sp. nov.** (type locality: Afghanistan, “Habatah”); “*languidus*” group: *Platyderus* (*Eremoderus*) *arabicus*, **sp. nov.** (type locality: Saudi Arabia, “Hedjaz”); *Platyderus* (*Eremoderus*) *brunki*, **sp. nov.** (type locality: Republic of Yemen, Thula District, between Kaukaban and Shibam); *Platyderus* (*Eremoderus*) *irakensis*, **sp. nov.** (type locality: Iraq, Ar Rutba District, 115 km E Ar-Rutbah Town); *Platyderus* (*Eremoderus*) *jordanensis*, **sp. nov.** (type locality: Jordan, Al-Betrā’ District, Little Petra). Six previously described species — *P. brunneus* Karsch, *P. insignitus* Bedel, *P. languidus* Reiche & Saulcy, *P. ledouxi* Morvan, *P. taghizadehi* Morvan, and *P. weiratheri* Mařan — are redescribed based on type and/or non-type material. *P. davatchii* Morvan placed as a member of the subgenus was not treated due to the lack of material available for study. The following new nomenclature acts are proposed: *Platyderus brunneus* Karsch, 1881, **stat. rev.**, is removed from synonymy with *Feronia languida* Reiche & Saulcy, 1855; *Platyderus elegans* Bedel, 1900, **syn. nov.**, is proposed as junior synonym of *Platyderus brunneus* Karsch, 1881; *Platyderus ferrantei* Reitter, 1909 is proposed as subspecies *Platyderus brunneus ferrantei* Reitter, 1909, **stat. nov.** In order to preserve the stability of nomenclature, lectotypes are designated for: *Feronia languida* Reiche & Saulcy, *Platyderus brunneus* Karsch, and *Platyderus weiratheri* Mařan. Keys to identification of the male and female specimens of the species from the regions studied are provided.

Key Words

Afghanistan, Egypt, Greece (Dodecanese), Iran, Iraq, Israel, Jordan, Libya, Morocco, *Platyderus*, Saudi Arabia, taxonomy, Tunisia, Turkey, Yemen

Introduction

The Palaearctic genus *Platyderus* Stephens, 1827 belongs to the subtribe Atranopsina Baehr, 1982, of tribe Sphodrini Laporte, 1834, and includes 111 species that are arranged in two subgenera (Hovorka 2017; Machard 2017; Machard 2020). Most representatives of this genus, especially members of *Platyderus* (s. str.), prefer shaded and humid habitats. In Europe and Anatolian Peninsula, they are found usually in shaded habitats near brooks or rivers during the summer, or in subterranean environment. In the southern margins of the generic range many species live in humid ravines and are active in the winter and early spring seasons because of the humid microhabitat conditions (Anichtchenko 2005; Ruiz-Tapiador and Anichtchenko 2007). Some taxa are partly depigmented and exhibit a moderate morphological specialization to a semi-hypogean mode of life because of the xeric conditions in occupied habitats (Lagar Mascaró 1978; Anichtchenko 2005; Ortuño and Gilgado 2010; authors' observations). All *Platyderus* taxa hitherto examined possess reduced metathoracic wings. As a consequence of flight loss and habitat selection species of this genus exhibit a tendency toward geographic isolation and differentiation into various localized forms (Ruiz-Tapiador and Anichtchenko 2007), especially in the southern Palaearctic Region and at higher altitudes. Based on longstanding taxonomic studies in Spain, Anichtchenko (2011) proposed that the true generic diversity is likely to be twice higher than presently described, and that ignorance regarding diversity is due mostly to the rarity of material in collections, due to prior use of ineffective collecting methods.

Platyderus-species possess a median protrusion of the anterior margin of the pronotum provided with a vertex underneath covered with a microsculpture of transverse granulae. This peculiar, diagnostic structure representing a stridulatory organ was first described by Lindroth (1956). The structure in question is considered a synapomorphic feature in subtribe Atranopsina including *Platyderus* (Casale, 1988: 126) but excluding the Macaronesian genus *Amaroschema* Jeannel, 1943 (see Machado 1992).

Because external morphology of the closely related species is rather uniform (especially in *Platyderus* s. str.), and many species exhibit infraspecific variation, in many instances no stable characters exist to provide reliable identification. For example, the shape of the pronotum, extent of punctation (if present) on the pronotal base, and position and number of the elytral discal pores often vary among individuals of a given species (Guéorguiev 2009; Anichtchenko 2012).

The subgenus *Eremoderus* Jeanne, 1996 was proposed by Jeanne (1996: 398) for *Platyderus* species with four or more setiferous punctures on the anterior side of the ventral margin of the mesofemur (in original: "Mésosfémurs avec quatre soies (parfois cinq ou six) près du bord postérieur de leur face inférieure"). The type species of *Eremoderus* was designated as

Feronia languida Reiche & Saulcy, 1855. In the same work (ibid.), Jeanne refers to the new subgenus two species groups, the group of *P. insignitus* and the group of *P. languidus*. Because this author has never discussed the species included in each of these groups, respectively the internal structure of the subgenus, one may conclude that only two species were then included in *Eremoderus*. Some authors like Serrano (2003, 2013) and Azadbakhsh and Nozari (2015) who respectively treated the Iberian and Iranian representatives of *Platyderus* as belonging to the nominotypical subgenus, accepted Jeanne's division of the genus into two subgenera (see also Hovorka and Sciaky 2003; Hovorka 2017; Machard 2017; 2019). Other authors, however, treated *Platyderus* s. str. and *Eremoderus* as subjective synonyms (Lorenz 1998, 2005) or expressed support for such a view (Guéorguiev 2009; Schmidt 2009). According to the most recent view (Hovorka 2017), the subgenus in question includes five species, *P. alticola* Wollaston, 1864 and *P. lancerottensis* Israelson, 1990 from Canary Islands, *P. insignitus* Bedel, 1902 from Morocco, the supposedly widespread *P. languidus* (Reiche & Saulcy, 1855), and *P. haberhaueri* Heyden, 1889 from Uzbekistan and Tajikistan.

The aim of the present study is to revise the known taxa of *Eremoderus* from Africa (excluding Macaronesia) and Southwestern Asia, to classify a set of recently collected specimens morphologically close to *P. insignitus* and *P. languidus*, and, as a consequence of these tasks to estimate if the rank of the subgenus given by Jeanne (1996) is justified.

Materials and methods

We have examined 195 individuals representing 18 species and one undefined form, with 141 of them measured to obtain data for sizes and ratios. Even though no specimens of *P. davatchii* were available to us this taxon is referred to *Eremoderus* on account of its habitus and general morphology (see Morvan 1970: 194–195 and fig. 6) with both *P. taghizadehi* and *P. ledouxi*.

Examination methods

Dissections and preparations of male genitalia were performed following Hanley and Ashe (2003). After processing, genitalia were preserved by embedding in Euparal Medium or a mixture of polyvinylpyrrolidone, glycerol and sorbitol on a microplastic card for future studies. The microplastic card has been added on the pin under the dissected specimen. Examinations and measurements of morphological details as well as color images were taken with an Olympus SZX 10 stereo microscope. Line drawings were performed using a drawing tube on Carl Zeiss Jena Amplitval microscope.

We recorded data for variation in two measurements and eight ratios to obtain body proportions on the dorsal

surface of specimens (Tables 1–3); for this purpose we measured ten male and ten female specimens, if available. A ninth ratio, MA/MI was taken after gauging the left metepisternum of five specimens, if available.

The maps were generated through the online tool SimpleMappr (Shorthouse 2010).

Abbreviations to measurements and ratios

BL	body length from the apex of the longer mandible to the apex of the longer elytron;
EL	length of elytra (measured along the length of stria 1 from the basal margin to the apex of the left elytron);
EW	maximum width of elytra (= BW: body width) measured as maximum distance across elytra;
HW	maximum linear distance across the head including eyes;
MA	length of anterior margin of metepisternum.
MI	length of interior margin of metepisternum (excl. metepimeron);
PA	width of pronotal apex between the tips of the anterior angles;
PB	width of pronotal base between the tips of the posterior angles;
PL	length of pronotum along median line.
PW	maximum width of pronotum.

The length of the median lobe of aedeagus was measured between base and apex when the lobe is in ventral position.

Abbreviations used for the depositories of the examined material

HNHM	Hungarian Natural History Museum, Budapest, Hungary (Otto Merkl, Győző Szél);
HMIM	Hayk Mirzayans Insect Museum, Tehran, Iran (Sayeh Serri);
MFNB	Museum für Naturkunde Berlin, Germany (Johannes Frisch, Bernd Jaeger);
MHNG	Muséum d'Histoire Naturelle, Geneva, Switzerland (Julio Cuccodoro);
MIZ	Museum and Institute of Zoology, Warszawa, Poland (Tomasz Huflejt);
MMBC	Moravske Museum, Brno, Czech Republic (Petr Baňar);
MNHN	Muséum National d'Histoire Naturelle, Paris, France (Thierry Deuve, Azadeh Taghavian);
NHMC	Natural History Museum of Crete, Greece (Apostolos Trichas);
NHMUK	Natural History Museum, London, United Kingdom (Maxwell Barclay, Beulah Garner);
NME	Naturkundmuseum Erfurt, Germany (Matthias Hartmann);

NMNHS	National Museum of Natural History, Sofia, Bulgaria (Borislav Guéorguiev);
NMPC	National Museum (Natural History), Prague, Czech Republic (Jiří Hájek);
NMW	Naturhistorisches Museum Wien, Vienna, Austria (Harald Schillhammer);
SMNH-TAU	Steinhardt Museum of Natural History, Tel Aviv University, Tel Aviv, Israel (Laibale Friedman);
cASL	working collection of Thorsten Assmann, Lüneburg, Germany (part of Zoologische Staatssammlung, München);
cBRU	collection of Ingo Brunk, Dresden, Germany;
cDOS	collection of Alexander Dostal, Vienna, Austria;
cFEL	collection of Ron Felix, Berkel Enschede, The Netherlands;
cHAJ	collection of Evžen and Patrik Hajdaj, Ježov, Czech Republic;
cKME	collection of Rudolf Kmeco, Litovel, Czech Republic;
cLAS	collection of Bernard Lassalle, Boissy-les-Perche, France;
cMAC	collection of Patrice Machard, Molineuf, France;
cMUI	collection of Jan Muilwijk, Bilthoven, The Netherlands;
cPTZ	collection of Andreas Pütz, Eisenhüttenstadt, Germany;
cREU	collection of Christoph Reuter, Hamburg, Germany;
cWEI	collection of Patrick Weill, Pau, France;
cWR	working collection David W. Wrase, Gusow-Platkow, Germany (part of Zoologische Staatssammlung, München);
cZIEG	collection of Wolfgang Ziegler, Rondeshagen, Germany.

The total number of specimens examined, counted for each species, is represented by the abbreviation TME. The total number of specimens with genitalia examined, counted for each species, is indicated by the abridgment TGE.

Labelling

Exact label data are cited for all material. Labels of type specimens were cited as originally given, with the author's remarks and comments enclosed in square brackets. Specimens of the newly described species are provided with one red printed label "HOLOTYPE, or PARATYPE / name of taxon sp. nov. / Guéorguiev, Wrase, Assmann, Muilwijk, Machard year". Specimens for lectotype designation are provided with one red printed label "LECTOTYPE or PARALECTOTYPE / name of taxon, author(s) name(s) year / des. Guéorguiev, Wrase, Assmann, Muilwijk, Machard year".

Separate label lines are indicated by a slash (/), and separate labels are noted by a double slash (//). Abbreviation ‘h’ stands for handwritten, ‘h&p’ for mixed handwritten and printed, ‘o’ for orange, ‘p’ for printed, ‘pn’ for pink, ‘r’ for red, ‘tl’ for teal (medium blue-green), ‘tq’ for turquoise (light blue-green), ‘w’ for white, and ‘y’ for yellow.

Taxonomic treatment

Genus *Platyderus* Stephens, 1827

Type species. *Harpalus depressus* Audinet-Serville, 1821

Subgenus *Eremoderus* Jeanne, 1996

Type species. *Feronia languida* Reiche & Saulcy, 1855

Diagnosis. Within *Platyderus*, the members of *Eremoderus* are separated by the following set of distinctive characters: ventral sclerite of median lobe of aedeagus narrow and long (best seen at ventral view, Figs 10A–I, 11A–G); seminal canal and receptaculum of comparable lengths (Figs 13A–F, 14A–C, E, F, 15A–F); ventral margin of anterior side of mesofemur with four or more, rarely three (specimens of *P. taghizadehi* and *P. weiratheri*) setiferous punctures ventrally (Fig. 5A–I); proximal margin, i.e. the “apex” of urite IX symmetrical or nearly symmetrical (Fig. 7A–M).

Description. Microsculpture and micropunctuation. Dorsal surface of head with regular isodiametric to slightly transverse sculpticells that are more or less reduced on posterior half of clypeus and disc (most species) or with complete microreticulation of isodiametric sculpticells (taxa of “*languidus*” group), labrum with coarser such sculpticells than remainder of head. Elytral microreticulation distinct, usually more engraved and larger than on head and pronotum, represented by regular isodiametric sculpticells (some specimens of *P. vanensis* sp. nov. without micropunctuation on elytral intervals 1–5). Dorsal surface of head and pronotum with scattered micropunctuation hardly visible below magnification 90×, elytra with coarser, more distinct micropunctuation, visible at magnification below 90× (micropunctuation absent on dorsal surface of head and elytra in most taxa of “*languidus*” group, except for head of *P. languidus*). **Punctuation.** Basal foveae of pronotum and adjacent lateral areas moderately punctate, punctures at sides usually not reaching anterior half (*P. weiratheri*, taxa of “*lassallei*” and “*davatchii*” groups), coarsely and densely punctate as punctures at sides usually reaching anterior half (*P. chatzakiae* n.sp., taxa of “*iranicus-vanensis*” group), or scarcely punctate to impunctate (*P. afghanisticus* sp. nov., taxa of “*languidus*” group). Prosternum laterally and proepisternum moderately (most species) to coarsely, densely and deeply punctate (taxa of “*iranicus-vanensis*” group) or finely, sparsely and

shallowly punctate to impunctate (taxa of “*languidus*” group). Prosternum medially and metasternum medially smooth. Mesepisternum, metasternum laterally and metepisternum indistinctly (*P. afghanisticus*, taxa of “*languidus*” groups) or clearly punctate (taxa of resting species groups, as in *P. vanensis* sp. nov. more coarsely than in other species). Abdominal ventrite 1 punctate and/or wrinkled, sometimes impunctate, ventrites 2–3 wrinkled, punctate or impunctate at sides, smooth medially, ventrites 4–5 mostly impunctate and smooth, but sometimes finely wrinkled at sides, 6 usually impunctate and smooth in whole (ventrites 1–4 coarsely punctate at sides in eastern populations of *P. vanensis* sp. nov.). **Chaetotaxy.** Labrum with six equidistant setae, lateral two longer than medial four. Clypeus with two long anterolateral setae. Two supraorbital setae each side. Stipes with anterior and posterior setae, former about half the length of latter. Pair of long setae on apical margin of ligula. Penultimate labial palpomere with two long setae on internal margin and 2–4 rather short apical setae; terminal labial palpomere with some scattered, very short and fine hairs. Mentum with two short and fine paramedial setae (sometimes broken off). Submentum with two long medial setae and two very short and fine lateral setae (occurring in most species but often broken off) or without lateral setae (*P. klapperichi* sp. nov.). Pronotum with one lateral seta at second quarter and one basal seta near posterior angles. Elytron with parascutellar seta at junction of angular base of stria 1, puncture small; interval 3 with three (rarely two) discal setiferous punctures (in *P. vanensis* sp. nov., punctures hardly discernible because of coarse and deep macropunctuation of interval), first one adjoining stria 3 (rarely in midst of interval 3 – *P. chatzakiae* sp. nov., adjoining stria 2 – *P. irakensis* sp. nov. or absent – in most specimens of “*iranicus-vanensis*” group), second and third punctures adjoining stria 2, first puncture situated in anterior third, second puncture in medial third or third quarter, and third puncture (lacking in *P. chatzakiae* sp. nov.) in posterior third to fifth; apical portion of stria 7 with two setiferous punctures, as posterior one situated closer to lateral gutter than to suture; umbilicate series consists of 16–17 (rarely 15 or 18 on one elytron) uniform punctures, not forming compact groups, anterior three punctures on lateral gutter, remaining ones on stria 8. Posterior side of profemur with three (most species) or more (*P. brunneus*, *P. irakensis*, *P. jordanensis*, *P. languidus*) long setae, one to two in basal third, one to two in medial third (near ventral edge), and one in proximal fifth (near knee). Anterior side of mesofemur ventrally usually with four or more setae, rarely with three setae; mesocoxa surface vaguely (most species) or densely pubescent (taxa of “*languidus*” group), with one posteromedial seta and one (most species) or one to four lateral setae (taxa of “*weiratheri*” and “*languidus*” groups); mesotrochanter with seta. Anterior side of metafemur ventrally mostly with one seta in basal third and one in medial third (additional setae existing in specimens of taxa from “*languidus*” group). Abdominal

ventrites 3–5 with ambulatory setae; last ventrite with two setae in male and female. **Head.** Eyes subconvex, long, each with length little exceeding length of scapus; tempora oblique, straight or convexly converging to neck. Labrum as long as or slightly shorter than clypeus. Clypeus slightly concave in front, rarely straight (*P. afghanisticus* sp. nov.). Mentum and submentum separate by distinct labial suture; mentum wide, short, deeply emarginate, without paramedial pits, median tooth, prominent, rounded anteriorly and bordered at base, epilobes well-exceeding median tooth in front, with posterior border medially concave. **Thorax.** Disc of pronotum barely to moderately convex; median line well-impressed, long but not reaching anterior and posterior margin; base with one sublateral fovea each side, impressed on basal third, foveae well-impressed (most species) or shallowly impressed (taxa of “*languidus*” group); anterior margin narrower than posterior margin, slightly concave each side, median projection covering *pars stridens* (stridulatory organs); anterior bead narrow, present laterally, impressed, present, lacking or indistinctly impressed in medial eighth to tenth; anterior angles well-projecting, rounded at tip; sides convex, straight or concave to base, lateral beads fine, complete to posterior angles; posterior margin concave in middle, slightly convex near angles; basal bead present laterally, present or reduced medially; posterior angles obtuse, projecting or not projecting laterally, rounded at tip. Prosternal process bordered, subovate, rounded at apex. Metepisternum narrowed behind, its internal margin as long as, or longer than, anterior margin. **Elytra.** Elytra coalesced along suture, widest at middle third or third quarter. Disc convex; humeri widely rounded. Basal bead arcuate medially, reaching or almost reaching scutellum, laterally forming obtuse angle with lateral margin and no denticle at humerus. Sides from basal margin towards middle third smoothly widened, from there to apex roundly narrowed. Parascutellar striole, if present, short, joining (rarely) or not joining (mostly) with stria 1; striae 1–6 usually reaching or almost reaching basal bead, 7 reaching or not reaching to it; base of stria 8 ending at third umbilicate puncture; striae 1, 7 and 8 apically separately joining lateral gutter; striae 1 and 2 mostly fused shortly before apex and reaching lateral gutter (if stria 2 not joining stria 1, it ends before lateral gutter); pairs of striae 3–4 and 5–6 fused before apex but neither joined stria reach lateral gutter (joined stria of pair 3–4 ending more apically than that of pair 5–6; in two specimens of *P. felixi* sp. nov., following aberration exists: striae 3 and 4 posteriorly, each of them fusing separately with stria 2 and joined stria reaching lateral gutter); parascutellar striola and striae 1–8 impunctate or finely punctate, shallow (taxa of “*languidus*” group), finely to moderately punctate and impressed (most species), or coarsely punctate and impressed (*P. vanesis* sp. nov.). Intervals subconvex (most species) to nearly flat (taxa of “*languidus*” group). Metathoracic wings reduced, scales-like, or absent. **Abdomen.** Ventrites 2 and 3 coalesced, suture between them mostly present, rarely lacking. **Legs.**

Moderately to considerably long and slender. Tarsomeres 1–5 convex and smooth (most species; Fig. 6D, E) or partly flattened and slightly longitudinally grooved (*P. brunneus*, *P. irakensis*; Fig. 6A–C) on dorsal side, with two rows of setae on ventral side; male protarsomeres 1–3 distinctly dilated, with biseriolate adhesive vestiture ventrally; mesotarsomeres 1–3 and metatarsomeres 1–3 laterally grooved or ungrooved. **Male genitalia.** Urite IX suboval, with proximal margin not or slightly asymmetrical (Fig. 7A–M). Median lobe of aedeagus in lateral view curved ventrally, with basal bulb protruding dorsally and having a well-developed, thick aileron and apex straight or turned up (Figs 8A–I, 9B–H); same in ventral view straight, subcylindrical, with long shaft (part restricted between basal bulb and apical lamella) and apical lamella more or less symmetrical (Figs 10A–I, 11A–G). Internal sac well-differentiated, containing two sclerites, a less sclerotized (reticulate), globular dorsal sclerite and a more sclerotized, elongate ventral sclerite (respectively, light grey colored and dark grey colored on Figs 8–11); in lateral view dorsal sclerite rounded (often a denser, saddle-shaped structure at proximal position is distinguished), and ventral sclerite is drop-shaped, both sclerites hardly distinctive to each other in lateral position than in ventral position; in ventral view dorsal sclerite is laterally rounded (forming one or two short curves from left side and one long curve from right side), and ventral sclerite is long and more or less narrow, with distal end straight or nearly straight (taxa of most species groups) or curved to left (“*lassallei*” and “*davatchii*” groups) and a position within internal sac parallel to longitudinal axis of median lobe (most species) or oblique to it (“*weiratheri*” group). Right paramere short, thin, more or less concave ventrally (Fig. 12A–N). **Female genitalia** (Figs 13A–F, 14A–C, E, F, 15A–F). Basal gonocoxite large to very large (five to ten times larger than apical gonocoxite), unsetose. Apical gonocoxite small, short, with narrow, falcate apex (mostly pointed, rarely blunt or rounded), one (taxa of “*languidus*” group, except for *P. brunki* sp. nov.) or two large dorsolateral ensiform setae (taxa of “*weiratheri*”, “*iranicus-vanensis*”, “*lassallei*”, “*davatchii*” group plus *P. brunki* sp. nov.), one large dorsomedial ensiform seta, and two long and fine apical nematiform setae in sensory pit (nematiform setae not found only in *P. jordanensis* sp. nov. and *P. languidus*). Bursa copulatrix small to moderately large, subconical or subquadrate, one-chambered in most species, two-chambered in *P. irakensis* sp. nov. Spermatheca relatively long, moderately differentiated, formed by seminal canal and receptaculum of similar length, seminal canal narrower, somewhat curved, receptaculum wide and straight; spermathecal gland very large, subelongate to round, with well-differentiated atrium; spermathecal canal short, connected in apical second fourth of spermatheca, either in basal third (taxa of “*languidus*” group, except *P. brunki* sp. nov. and *P. insignitus*) or medial third of receptaculum (two foregoing species plus taxa of remaining species groups).

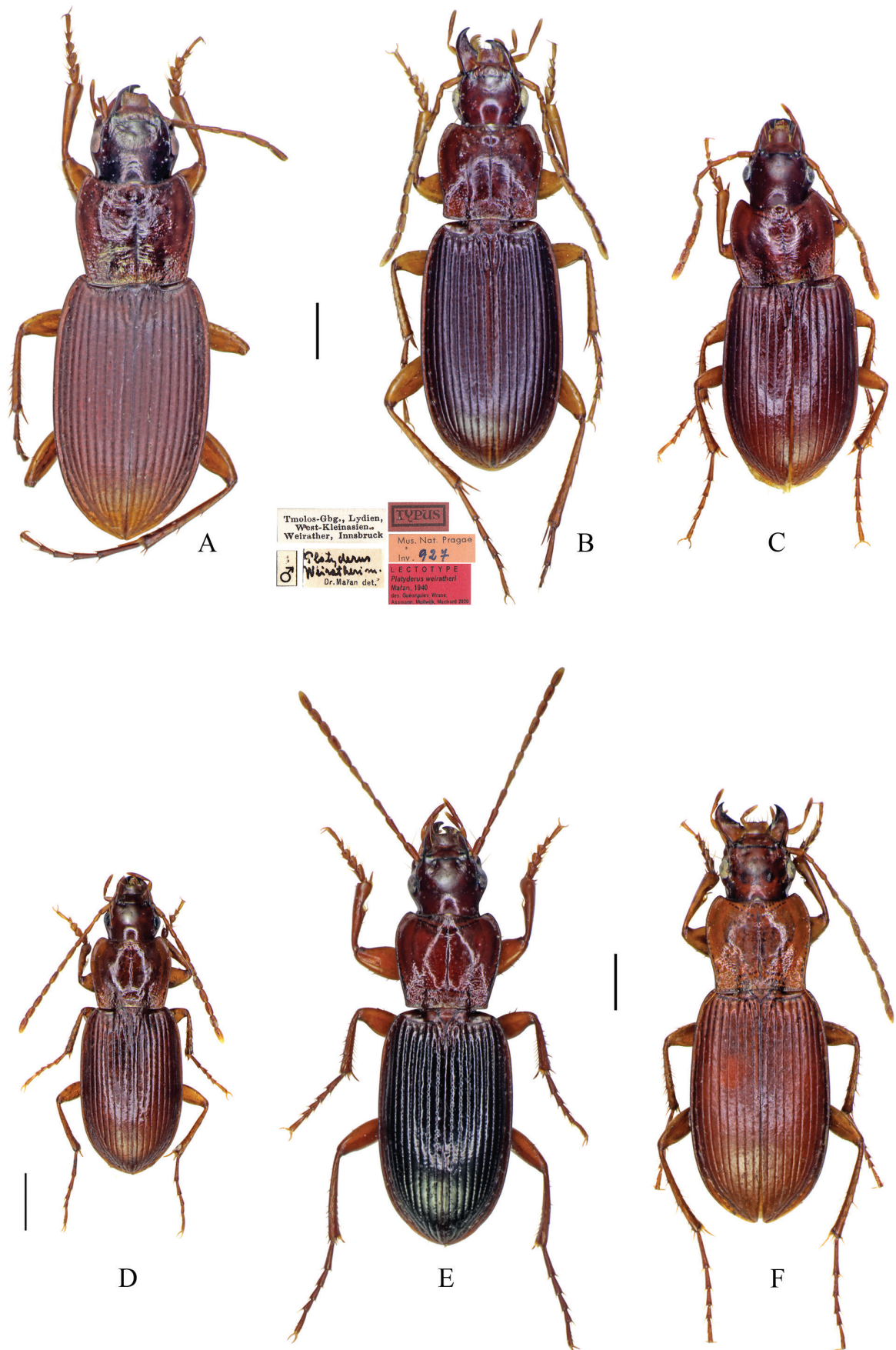


Figure 1. Dorsal habitus. **A.** *Platyderus (Eremoderus) chatzakiae*, sp. nov., holotype; **B.** *P. (E.) weiratheri* Mařan, 1940, lectotype and its labels; **C.** *P. (E.) felixi*, sp. nov., holotype; **D.** *P. (E.) iranicus*, sp. nov., male paratype, Cheri pass 20 km W Samsami, Chahar Mahal va Bakhtiari Province, Iran; **E.** *P. (E.) vanensis*, sp. nov., holotype; **F.** *P. (E.) vrabeci*, sp. nov., holotype. Scale bars: 1 mm.

“*weiratheri*” species group

Diagnosis. Representatives of this group share one trait, the ventral sclerite of internal sac obliquely situated with respect to the main axis of the median lobe in the ventral view and distinctly bent in middle in lateral view (Fig. 10A, B). Species from the other groups of *Eremoderus* have a ventral sclerite parallel to the main axis of the median lobe in ventral view and straight in the lateral view (Fig. 10C–I). This trait divides the subgenus into two groups that may separate, one including the taxa of the “*weiratheri*” group, and another – taxa of the remaining species groups.

Notes. The group includes *P. weiratheri* from South-west Turkey and *P. chatzakiae* sp. nov. from Kalymnos Island (Greece, Dodecanese; see Fig. 16). The first species inhabits high altitudes in the western Toros Range, whereas the second one is a dweller of Mediterranean scrub habitat at lower altitudes.

1. *Platyderus (Eremoderus) chatzakiae*, sp. nov.

<http://zoobank.org/65B653A0-F02D-4F08-B697-41D5DE8E7B79>

Figs 1A, 7A, 8A, 10A, 12A, 16, Table 1

Type locality. Greece, Kalymnos Island, Stimenia Cave.

Note on type locality. The Stimenia Cave is situated in the northeastern part of the Vathi Valley, in an area called St. Nikolas, on the Kalymnos Island, belonging to the Dodecanese.

Type material. *Holotype* ♂, ‘8422, KALYMNOS Stimenia, end / road st18 9/6/2005, Lg Chatzaki’ (NHMC).

TME: 1 specimen. TGE: 1♂.

Etymology. Latinized eponym based on the surname of Maria Chatzaki (Democritus University of Thrace, Komotini, Greece), a Greek arachnologist, who collected the holotype.

Diagnosis. *P. chatzakiae* sp. nov. differs from *P. weiratheri* in wider body (BW: 2.85 mm, vs. 2.35–2.60 mm), more coarsely punctate disc of head (vs. finely punctate or nearly smooth disc of head), anterior elytral discal puncture situated in midst of interval 3 (vs. anterior discal puncture adjoining stria 3), and elytra both in relation to elytra width narrower (EL/EW= 1.60, vs. 1.63–1.71) and in relation to pronotum length shorter (EL/PL= 2.49, vs. 2.55–2.83).

Description. *Habitus.* Large size for *Platyderus* species (BL: 8.05 mm; BW: 2.85 mm), with elongate, moderately convex body (Fig. 1A). **Measurements and ratios.** See Table 1. **Color and lustre.** Body dorsally and ventrally red-brown, head, pronotum and ventral surface slightly darker than elytra, appendages (antennae, palpi and legs) and elytral epipleura slightly lighter than elytra. Head, pronotum, and ventral surface rather shiny, elytra much less shiny. **Microsculpture and punctuation.** Pronotum without regular microreticulation even on anterolateral and posterolateral parts. Elytral intervals, scutellum and basal margin with distinct isodiametric sculpticells; lateral gutter without

microsculpture. Ventral surface with scarcely-visible isodiametric sculpticells (proepisternum) or with sculpticells slightly transverse (abdominal ventrites at sides) to not apparent. Head punctate and wrinkled on disc and posterior part of clypeus, labrum impunctate, without wrinkles, anterior part of clypeus and vertex sparsely punctate, without wrinkles. Pronotum coarsely and densely punctate in basal part and laterally, finely and sparsely punctate on disc and anterior part medially. Elytra with scanty micropunctuation. Abdominal ventrite 1 moderately wrinkled, ventrites 2–6 smooth. **Head.** One-third narrower than pronotum wide (PW/HW= 1.34). Eyes almost flat. Labrum subrectangular, as long as clypeus, with anterior margin rather concave. Frontoclypeal suture distinct in middle, indistinct at sides. Frontal furrows subfoveolate, shallow. Paraorbital sulci straight, moderately deep, ended posteriorly after level of posterior margin of eye and slightly before level of posterior supraorbital pore. **Thorax.** Pronotum slightly wider than long (PW/PL= 1.19), with widest point at second quarter. Anterior and posterior transverse impressions slightly distinct medially, lacking laterally. Sides sinuate, convex medially and anteriorly, slightly concave posteriorly; anterior border distinctly beaded laterally, indistinctly in medial 1/15; posterior margin finely beaded. Metepisternum as long as wide, MA/MI= 0.97–1.03. **Elytra.** Elongate, less than one and two thirds as long as wide (EL/EW= 1.60), two and a half times as long as pronotum (EL/PL= 2.49), and about a third as wide as pronotum (EW/PW= 1.31), with widest point at medial third. Parascutellar striole and striae well-impressed, slightly punctate; parascutellar striole short, not joining stria 1; striae 1–3 (and 4 on right elytron) reaching basal bead, 5–7 not reaching it. Interval 3 with three discal setiferous punctures on left elytron and two on right elytron, first pair of large, foveolate punctures in midst of interval 3, second pair of smaller, punctiform punctures adjoining stria 2, third pair of punctures lack, instead an additional large, foveolate puncture present in midst of interval 3 of left elytron between first and second punctures. Umbilicate setiferous series with 17 punctures on left elytron and 16 punctures on right elytron. **Legs.** Posterior side of profemur with one seta in basal third and one seta in medial third. Anterior side of left mesofemur ventrally with five, right one with four equidistant setiferous punctures. Anterior side of metafemur ventrally with two long setae, one in basal third and one in medial third. **Male genitalia.** Urite IX suboval, with proximal margin slightly asymmetrical and pointed (Fig. 7A). Median lobe of aedeagus in lateral view, with short basal bulb, long and broad shaft moderately constricted proximally, and a short, straight apex; median lobe in ventral view straight, about 3.5 times longer than wide; apical lamella (dorsal view) short, symmetrical, subacuminate at tip, with sides straight. Internal sac in lateral view (Fig. 8A) with ventral sclerite partly visible (as a short plate); same in ventral view (Fig. 10A), with dorsal sclerite situated proximally and surrounding ventral sclerite from behind, ventral sclerite obliquely situated, broadened distally. Right paramere less concave ventrally (Fig. 12A). **Female genitalia.** Unknown.

Habitat. The holotype was collected in a pitfall trap that was set (3 May–9 June 2005) at the end of a street leading to Stimenia Cave, west of Vathys Village (Maria Chatzaki pers. comm.). The habitat where the specimen was found consists of a homogenous degraded phrygana (Mediterranean open scrubland and grass community at low altitude). Approximate GPS coordinates of the location are: 36.9975 26.9607.

Distribution. Kalymnos Island (Greece, Dodecanese; Fig. 16).

2. *Platyderus (Eremoderus) weiratheri* Mařan, 1940

Figs 1B, 5A, 7B, 8B, 10B, 12B, 13A, 16, Table 1

Platyderus Weiratheri Mařan, 1940: 25 (type locality: “Lydien in montibus Tmolos” [= Bozdağlar], Turkey).

Note on type locality. The mount Bozdağlar (Ancient Greek name: Tmōlos), with maximal elevation 2159 m a.s.l., is situated in the southwestern part of the Anatolian Peninsula.

References. *Platyderus weiratheri*: Jedlička 1963: 22; Lorenz 1998: 375; Hovorka and Sciaky 2003: 523; Lorenz 2005: 396; Hovorka 2017: 760.

Type material. Should consist of two male and three female specimens (Mařan *ibid.*) all of them syntypes according to Art. 73.2.1. (ICZN 1999). From these specimens, we found only one male syntype with extracted genitalia, here designated as lectotype. This specimen and its genitalia (with missing urite) are glued on two separate white cards on the same pin. The specimen designated herewith as lectotype is labelled as follows: ‘♂ [w, p] // Tmolos-Gbg., Lydien, / West-Klainsien. / Weirather, Innsbruck [w, p] // TYPUS [r, p] // Mus. Nat. Pragae / Inv. 927 [o, h/p] // *Platyderus Weiratheri* m. Dr. Mařan det. [w, h&p] // lectotype label’ [NMPC]. The depositories and present state of remaining four type specimens remain unknown.

Other material examined. Turkey: Bozdağlar (= Mount Tmolus) situated on territories of districts of İzmir, Manisa and Aydın: 1♂, ‘Tmolos-Gbg., Lydien, / West-Kleinasien. / Weirather, Innsbruck // *Platyderus* spec. ? det. J. Müller (vergl. mit cyprius !) // Coll. Mus. / Vindob.’ (NMW); 1♂, 1♀, ‘Tmolos-Gbg., Lydien, / West-Kleinasien. / Weirather, Innsbruck // Coll. Mus. / Vindob.’ (NMW); 2♂♂, 1♀, ‘Tmolos-Gbg., Lydien, / West-Kleinasien. / Weirather, Innsbruck’ (NMW); 1♂, ‘Boz dağ, vt N / 1150–1200 m / 5–5–1995 // TURQUIE / Izmir / C. JEANNE // Collection / Machard’ (cMAC); 3♀♀, ‘TURKEY, vil. Izmir, Boz / dağlari, Boz dağ köy env. / 1500–1700 m a.s.l. / 30.5.–3.6.03, R.Lohaj lgt.’ (NMNHS, cWR).

TME: 11 specimens. TGE: 2♂♂, 1♀.

Diagnosis. See “Diagnosis” of *P. chatzakiae* sp. nov.

Redescription. **Habitus.** Specimens of large size for *Platyderus* species (BL: 7.00–8.10 mm; BW: 2.35–2.60 mm), with rather elongate, moderately convex body (Fig. 1B). **Measurements and ratios.** See Table 1. **Color**

and lustre. Body dorsally and ventrally dark reddish, head and pronotum mostly lighter than elytra, appendages (antennae, palpi and legs) rufous, lighter colored than dorsal surface. Integument moderately shiny, head and pronotum slightly shinier than elytra. **Microsculpture and punctuation.** Pronotum without regular microreticulation. Elytral intervals and scutellum with distinct isodiametric sculpticells; basal margin and lateral gutter with such sculpticells less evident or without microsculpture. Ventral surface with hardly visible isodiametric (proepisternum) or slightly transverse sculpticells (abdominal ventrites at sides) or mostly sculpticells not apparent. Head with some punctures and wrinkles only clypeus and frons, labrum, disc and vertex without punctures and wrinkles. Pronotum in basolateral part coarsely and sensely punctate, basal punctures reaching or not reaching the anterior half laterally, disc and anteroapical part mostly smooth, anterior third medially finely punctate and wrinkled. Elytral intervals mostly with a row of punctures, rarely without punctation. Abdominal ventrites 1–5 wrinkled at sides. **Head.** One-third or narrower than pronotum wide (PW/HW= 1.32–1.44). Eyes slightly convex. Labrum subrectangular, slightly shorter than clypeus, with anterior margin concave. Frontoclypeal suture distinct in middle, indistinct at sides. Frontal furrows barely distinct, small and shallow. Paraorbital sulci straight, moderately deep, ending backwards slightly before level of posterior supraorbital pore. **Thorax.** Pronotum about one eighth to one quarter wider than long (PW/PL= 1.13–1.27), with widest point at second quarter. Anterior and posterior transverse impressions slightly distinct medially. Sides sinuate, convex medially and anteriorly, slightly to hardly concave posteriorly; anterior border lack in medial 1/10. Metepisternum about as long as wide, MA/MI= 0.95–1.02. **Elytra.** Elongate, about two thirds longer than wide (EL/EW= 1.63–1.71), two and a half times or longer than pronotum (EL/PL= 2.55–2.83), and a third wider than pronotum (EW/PW= 1.29–1.40), with widest point at medial third or third quarter. Parascutellar striae and striae well-impressed, more coarsely punctate than in *P. chatzakiae* sp. nov. and less coarsely than in *P. vanensis* sp. nov.; striae short, not joining stria 1; striae 1–6 reaching or almost reaching basal bead, 7 reduced before. Interval 3 with three discal setiferous punctures on each elytron. Umbilicate setiferous series consisting of 15–16 (rarely 17) punctures on each elytron. **Legs.** Posterior side of profemur with one seta in basal third and one seta in medial third. Anterior side of mesofemur ventrally mostly with 4 equidistant setiferous punctures, rarely with 3 or 5 punctures (Fig. 5A). Anterior side of metafemur ventrally with two long setae, one in basal third and one in medial third. **Male genitalia.** Urite IX with proximal margin almost asymmetrical (Fig. 7B). Median lobe of aedeagus in lateral view as in *P. chatzakiae*, with shaft little longer (Fig. 8B); median lobe in ventral view straight, about 3.5 times longer than wide (Fig. 10B); apical lamella (dorsal view) as in *P. chatzakiae*. Internal sac as in *P. chatzakiae*, only ventral sclerite narrowed toward both proximal and

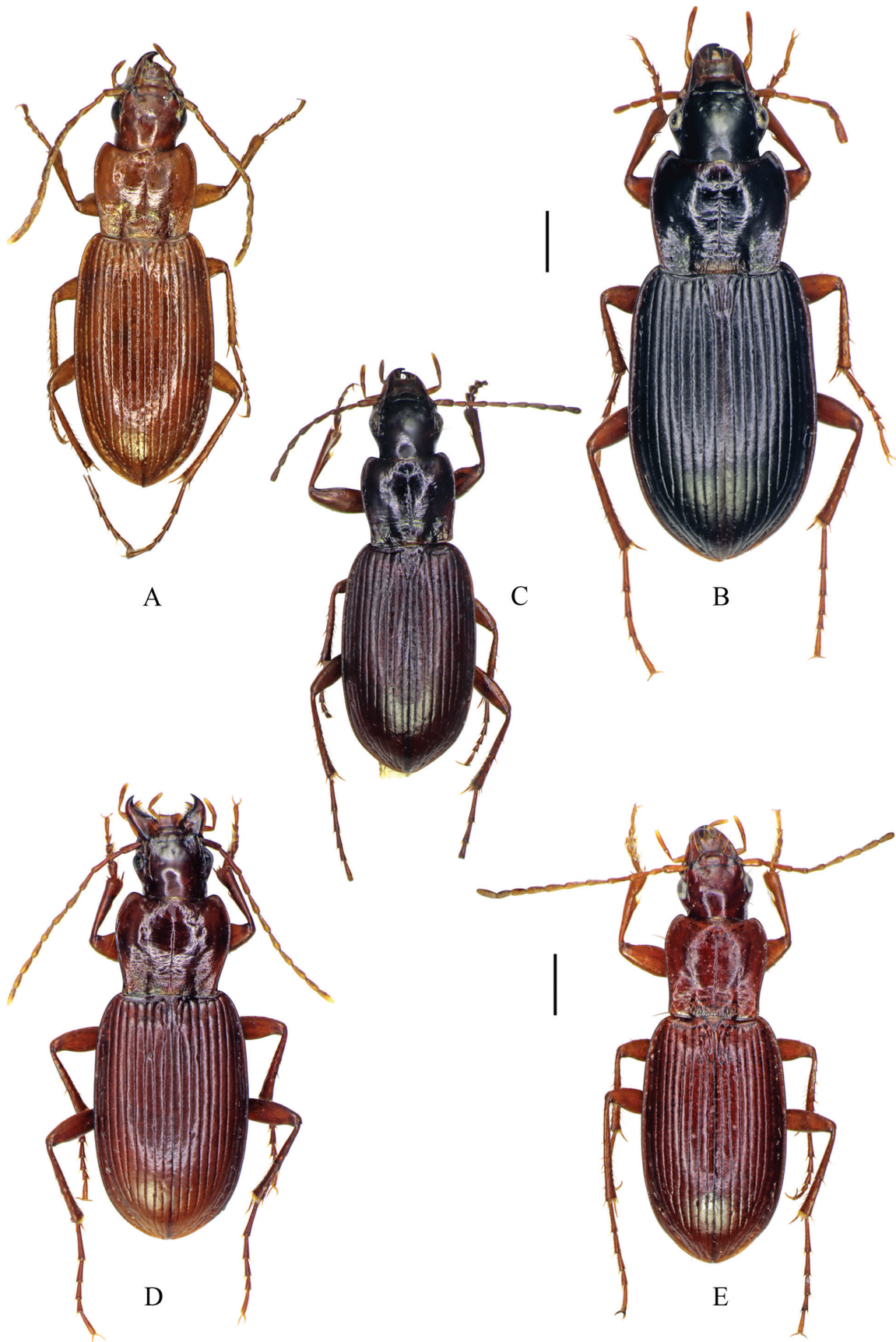


Figure 2. Dorsal habitus. **A.** *Platyderus (Eremoderus)* sp., female specimen, Karabet Pass, Turkey; **B.** *P. (E.) lassallei*, sp. nov., female paratype, E Qolqol, Mazandaran Province, Iran; **C.** *P. (E.) klapperichi*, sp. nov., holotype; **D.** *P. (E.) ledouxi* Morvan, 1974, male specimen, 10 km S Hasan Keif, Mazandaran Province, Iran; **E.** *P. (E.) taghizadehi* Morvan, 1974, male specimen, Tochal, Tehran Province, Iran. Scale bars: 1 mm.

distal ends, with widest point in middle (Fig. 10B). Right paramere on Fig. 12B. **Female genitalia** (Fig. 13A). Apical gonocoxite with pointed apex and two dorsolateral ensiform setae. Spermathecal canal connected in medial third of receptaculum.

Habitat. Nothing is known about bionomics of this species.

Distribution. Apparently endemic to the mountains of the Bozdağlar Mountain, in Southwest Turkey (Fig. 16).

“*iranicus-vanensis*” group

Diagnosis. Includes species with basal foveae of pronotum and adjacent lateral areas coarsely and densely punctate with punctures at sides usually reaching anterior half. The prosternum laterally and proepisternum also coarsely and densely punctate. The ventral sclerite of internal sac of median lobe in ventral view is elongate, relatively wide, with straight distal end; the same in lateral view is significantly widened anteriorly having maximum width at the distal third about three or more times larger than width at the proximal third (Figs 8C–F, 10C–F). Most specimens lack also the first elytral discal puncture and have apical gonocoxite with proximal dorsolateral ensiform seta finer than the distal seta.

In addition, the Iranian congeners of the “*iranicus-vanensis*” group differ from those of the “*davatchii*” group in: (1) sides of pronotum nearly straight to the posterior angles (vs. sides of pronotum concave to the posterior angles) and (2) pronotum appreciably wider than long (PW/PL >1.20, vs. PW/PL <1.20). For further differences between taxa of the group dealt with here and *P. lassallei* see “Diagnosis” under the “*lassallei*” species group.

Habitat. The habitats of the *Eremoderus*-species in the Zagros (Iran) consist mostly of subalpine slopes, partly near snowfields, and seldom of cultivated grasslands and small orchards. Outside the cultivated grasslands along the rivers and streams the vegetation is xerophilic. The altitude of the area where *P. felixi* sp. nov. was collected is appreciably lower than that of the localities of *P. iranicus* sp. nov.

“*iranicus*” subgroup

Notes. This complex includes two allopatric, high altitudinal species, *P. felixi* and *P. iranicus* with parascutellar striae, striae 1–8 scarcely punctate and moderately impressed and quite short and crooked right parameres (Fig. 12C, D).

3. *Platyderus (Eremoderus) felixi* sp. nov.

<http://zoobank.org/17C88C87-FE7B-46B8-8602-F57CC6318FD0>

Figs 1C, 5B, 7C, 8C, 10C, 12C, 13B, 17, Table 1

Type locality. Iran, Chahar Mahal va Bakhtiari Province, 10 km W Naghan Town, 31.9410, 50.6014, 1492–1505 m.

Notes on type locality. The distance from Naghan Town to the type locality is about 10 km in straight line

and the direction is to the west of the town. The GPS coordinates and height indicated are more or less correct as they well correspond to the river that flows towards the village of Do Polan. In fact, the type locality is closer to the last village than to Naghan Town.

Type material. **Holotype** ♂, ‘IRAN, / Chahār Mahāll vā Bachtīārī / 10km W Naghan Town / 31°56'27"N, 050°36'05.5"E / 1492–1505m, 02.04.2007 / leg. Jan Muilwijk’ (HMIM). Paratypes: 4♀♀, labeled as holotype (cMUI); 1♂, ‘IRAN, / Chahār Mahāll vā Bachtīārī / 10km W Naghan Town / 31°56'27"N, 050°36'05.5"E / 1492–1505m, 02.04.2007 / leg. R.F.F.L. Felix’ (cFEL).

TME: 6 specimens. TGE: 2♂♂, 1♀.

Etymology. Latinized patronym name after Ron Felix (Berkel-Enschot, Netherlands), an enthusiastic coleopterologist working on the taxonomy of carabid beetles, with great collecting skills, who collected part of the type series of the new species.

Diagnosis. It is distinct from *P. iranicus* sp. nov. in the pronotum significantly wider than head (PW/HW ≥1.45, vs. PW/HW ≤1.45) and elytra noticeably less wide in relation to length (EL/EW ≤1.55, vs. EL/EW ≥1.55). In addition, median lobe of aedeagus (lateral view) of the new species is larger, with shaft broader and apex barely bent up (*P. iranicus* has significantly narrower shaft and apex more distinctly bent up; Fig. 8C, D).

Description. **Habitus.** Specimens of moderate size for *Platyderus* species (BL: 6.00–7.00 mm; BW: 2.20–2.50 mm), with relatively short, moderately convex body (Fig. 1C). **Measurements and ratios.** See Table 1. **Color and lustre.** Integument uniformly reddish-brown, appendages somewhat lighter than body. Surface moderately shiny. **Microsculpture and punctation.** Disc of head with less distinct microsculpture. Pronotum with regular isodiametric sculpticells posterolaterally and slightly stretched isodiametric sculpticells anterolaterally, microsculpture faint to absent in middle. Ventral surface (excl. gula) microsculptured, sculpticells isodiametric (mentum, submentum, pro-, mes-, and metepisternum, prosternum and abdominal ventrites laterally) or slightly stretched isodiametric (genae, medial surface of prosternum, metasternum, abdominal ventrites medially and legs). **Head.** As wide as a half of pronotum (mean PW/HW= 1.49). Eyes moderately convex. Labrum subrectangular, as long as clypeus, with anterior margin straight. Frontoclypeal suture distinct in middle but very fine, lacking at sides. Frontal furrows shallow, punctiform. Paraorbital sulci moderately deep, ending slightly before or at level of posterior supraorbital pore. **Thorax.** Pronotum distinctly wider than long (mean PW/PL= 1.31), with widest point at second quarter. Anterior and posterior transverse impressions indistinct. Anterior bead present medially, very fine. Sides convex anteriorly, nearly straight posteriorly. Metepisternum slightly longer than wide, MA/MI= 0.90–0.95. **Elytra.** Cylindrical, one and a half time as long as wide (mean EL/EW= 1.52), wider and quite longer than pronotum (mean EW/PW= 1.31; mean EL/PL= 2.62). Parascutellar striae and striae

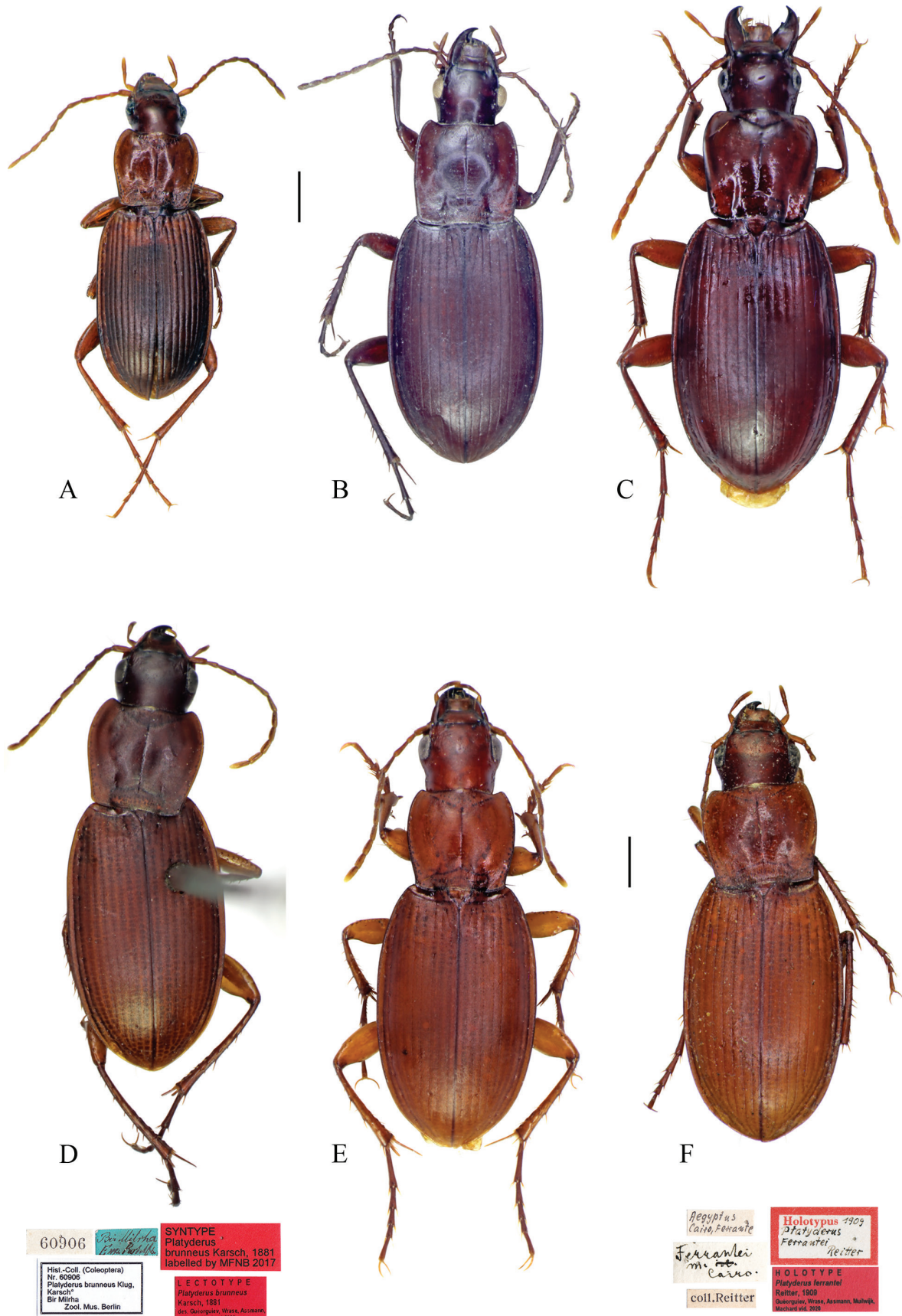


Figure 3. Dorsal habitus. **A.** *Platyderus (Eremoderus) afghanisticus*, sp. nov., holotype; **B.** *P. (E.) arabicus*, sp. nov., holotype; **C.** *P. (E.) brunki*, sp. nov., holotype; **D.** *P. (E.) brunneus brunneus* Karsch, 1881, lectotype and its labels; **E.** *P. (E.) brunneus brunneus* Karsch, 1881, male specimen, 50 km W of Ben Gardane, Medenine Governorate, Tunisia; **F.** *P. (E.) brunneus ferrantei* Reitter, 1909, lectotype and its labels. Scale bars: 1 mm.

Table 1. Morphometric data for species of the ‘*weiratheri*’ and ‘*iranicus-vanensis*’ groups of *Platyderus*.

Species (number of samples)	BL/mm	BW/mm	PW/HW	PW/PL	PW/PA	PW/PB	PA/PB	EL/EW	EW/PW	EL/PL
<i>P. weiratheri</i> Mañan (6♂♂, 5♀♀)	7.00–8.10	2.35–2.60	1.32–1.44	1.13–1.27	1.32–1.41	1.09–1.19	0.81–0.89	1.63–1.71	1.29–1.40	2.55–2.83
<i>P. weiratheri</i> Mañan (mean)	7.52	2.50	1.38	1.20	1.37	1.15	0.84	1.67	1.32	2.64
<i>P. chatzakii</i> (1♂)	8.05	2.85	1.34	1.19	1.36	1.19	0.88	1.60	1.31	2.49
<i>P. felixi</i> sp. nov. (2♂♂, 4♀♀)	6.00–7.00	2.20–2.50	1.45–1.52	1.25–1.34	1.33–1.43	1.10–1.13	0.79–0.83	1.48–1.55	1.29–1.35	2.60–2.66
<i>P. felixi</i> sp. nov. (mean)	6.58	2.40	1.49	1.31	1.39	1.11	0.80	1.52	1.31	2.62
<i>P. iranicus</i> sp. nov. (19♂♂, 16♀♀)	4.30–6.65	1.50–2.30	1.32–1.45	1.21–1.31	1.30–1.42	1.10–1.24	0.82–0.93	1.55–1.69	1.24–1.34	2.50–2.77
<i>P. iranicus</i> sp. nov. (mean)	5.67	1.95	1.40	1.26	1.36	1.18	0.87	1.60	1.29	2.59
<i>P. vanensis</i> sp. nov. (11♂♂, 11♀♀)	6.85–8.40	2.25–2.70	1.30–1.43	1.13–1.24	1.32–1.41	1.14–1.29	0.82–0.95	1.61–1.73	1.22–1.36	2.52–2.74
<i>P. vanensis</i> sp. nov. (mean)	7.53	2.45	1.36	1.19	1.36	1.20	0.88	1.68	1.30	2.60
<i>P. sp.</i> (1♀, Karabet Pass)	7.05	2.25	1.34	1.12	1.34	1.18	0.88	1.76	1.36	2.67
<i>P. vrabeci</i> sp. nov. (1♂, 1♀)	7.30–7.45	2.40–2.50	1.38–1.42	1.21–1.25	1.41–1.42	1.17–1.21	0.83–0.85	1.63–1.66	1.32	2.63–2.71
<i>P. vrabeci</i> sp. nov. (mean)	7.38	2.45	1.40	1.23	1.42	1.19	0.84	1.65	1.32	2.67

For abbreviations in line 1, see “Abbreviations to measurements and ratios” (section “Material and methods”).

moderately impressed, wide; striole short, not joining stria 1; striae 1–6 reaching basal bead, 7 reduced before. Following aberration exists in two specimens, striae 3 and 4 posteriorly, each of them fusing separately with stria 2 and joined stria reaches lateral gutter, otherwise striae posteriorly as in subgeneric description. Interval 3 with three or two minute discal setiferous punctures situated as follows: anterior puncture (in most specimens missing on one or both elytron) adjoining stria 2, in middle of interval 3 or adjoining stria 3, remaining two punctures adjoining stria 2. Umbilicate setiferous series mostly consists of 16 punctures on elytron, rarely with 17 punctures. **Legs.** Posterior side of profemur with one seta in basal third and one in medial third. Mesofemur with four setiferous punctures on anterior side ventrally (Fig. 5B). Anterior side of metafemur ventrally with two long setae, one in basal third and one in medial third. **Male genitalia.** Urite IX small, oval, with proximal margin slightly asymmetrical and rounded (Fig. 7C). Median lobe of aedeagus curved in lateral view, with short basal bulb, long and broad shaft moderately constricted proximally, and apex hardly reversely turned up; median lobe in ventral view straight, ca. 3.7 times longer than wide; apical lamella more or less asymmetrical. Internal sac in lateral view (Fig. 8C) with ventral sclerite distinctly broadened and rounded distally; same in ventral view (Fig. 10C), with dorsal sclerite forming a concave left protuberance and a convex right curve, and ventral sclerite narrow and completely straight. Right paramere rather short and crooked (Fig. 12C). **Female genitalia** (Fig. 13B). Apical gonocoxite with pointed apex and two dorsolateral ensiform setae. Spermathecal canal connected in medial third of receptaculum.

Comparisons. The new species lives in sympatry with *Platyderus* (s. str.) *umbratus* (Ménétriés, 1832). However, *P. felixi* has pronotum more coarsely punctate in basolateral parts with punctures almost reaching the lateral margin, mesotibia with four setiferous punctures on its anterior side ventrally, and short urite with apex more symmetrical (Fig. 7C), whereas *P. umbratus* possesses pronotum shallowly punctate in base with punctures mostly limited to the basal impressions, mesotibia with two setiferous punctures on its anterior side ventrally, and long urite with apex curved to left (as in Fig. 7O).

Habitat. The specimens were hand collected by R. Felix and J. Muilwijk close to the village Do Polan along the river course. The vegetation there consisted of (over)-grazed grassland, fields and small orchards; characteristic of a cultivated landscape.

Distribution. Southwest Iran: Central Zagros Mountain Chains (Chahar Mahal va Bakhtiari Province, Kiar County; Fig. 17).

4. *Platyderus (Eremoderus) iranicus* sp. nov.

<http://zoobank.org/3C731C6C-346E-4E8A-B5F3-D2D0B3E27D97>

Figs 1D, 5C, 8D, 10D, 12D, 13C, 17, Table 1

Type locality. Iran, Chahar Mahal va Bakhtiari Province, 7 km NE Naghan Town, 31.97472, 50.77694, 2400 m.

Type material. **Holotype** 1♂, ‘IRAN, / Chahār Mahāll vā Bachtīārī / 7km NE Naghan Town / 31°58'29"N, 050°46'37"E 2400m / 03.04.2007, leg. Jan Muilwijk’ (HMIM). Paratypes: 1♀, labelled as holotype (cMUI); 1♀, ‘IRAN (Chahār Mahāll vā Bachtīārī) / Zagros Mts. / Boldaghi vill. (nr Choghaklor lake) / 3 km S Sibak, 2600–2700 m / 31°51'47"N, 50°55'24" E / (subalpine slopes with snowfields / under stones) / 20.IV.2018 Wrase & Laser [07]’ (cWR); 1♂, ‘IRAN (Chahār Mahāll vā Bachtīārī) / Zagros Mts., Zard Koh Mt. / Cheri pass 20 km W Samsami / 2775 m, 32°09'55"N/ 50°10'37"E / (subalpine slopes/under stones) / 21.IV.2018 Wrase & Laser [08]’ (cWR); 5♂♂, 1♀, ‘IRAN, Zagros Mts., P: / Chahar Mahal va / Bakhtiari, Zard Koh Mt. / pass, subalpine slope // 2770m, 21.IV.2018 / 32°09'55"N/ 50°10'37"E / leg. M. Hartmann’ (cNME); 10♂♂, 5♀♀, 32°09'55"N, 50°10'37"E Iran / Zagros Mts., p. Chahār Mahāll / vā Bachtīārī, Zard Koh Mts., pass / 20km W Samsami, subalpine / slopes 21.IV.2018 2.775m NN / leg.: Schnitter IR49’ (NME); 12♂♂, 2♀♀, ‘IRAN: Zagros Mts., p.Chahār Mahāll / vā Bachtīārī, Zard Koh Mts.,pass 20km / W Samsami, 32°09'55"N, 50°10'37"E / 2775m, 21.IV.2018, subalp. slopes / leg. A.Weigel #49’ (NME); 1♀, ‘IR Chaharmahal and / Bakhtiari Cheri pass / 4.vi.2018 3000m / 32°09'31"N, 50°10'47"E / Muilwijk J.’ (cMUI); 1♂, ‘IR Chaharmahal and / Bakhtiari Cheri pass / 5.vi.2018 2450m / 32°10'36"N, 50°10'06"E / Muil-

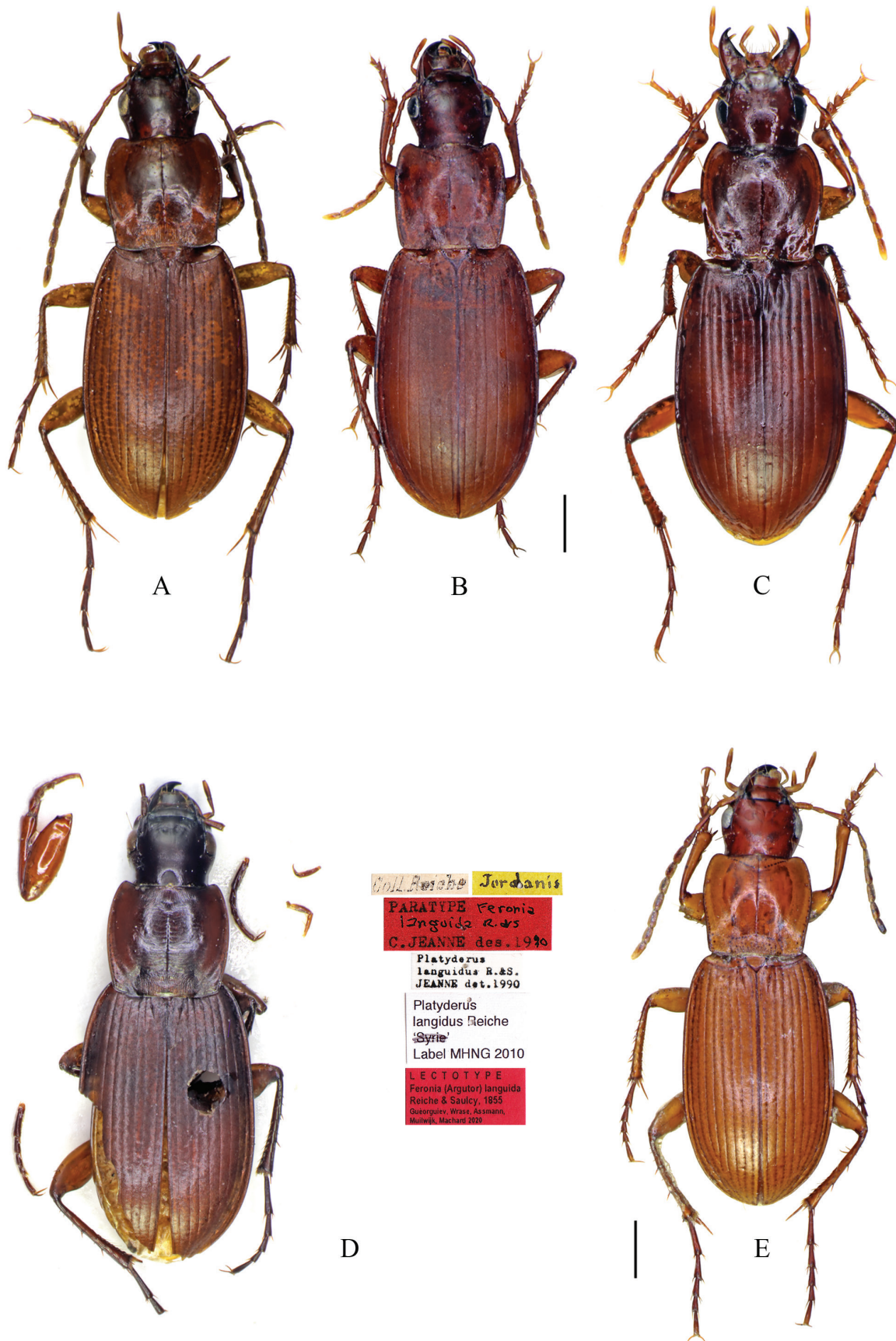


Figure 4. Dorsal habitus. **A.** *Platyderus (Eremoderus) insignitus insignitus* Bedel, 1902, male specimen, SW Tiznit, Sous-Massa Region, Morocco; **B.** *P. (E.) irakensis*, sp. nov., holotype; **C.** *P. (E.) jordanensis*, sp. nov., holotype; **D.** *P. (E.) languidus* (Reiche & Saulcy, 1855), lectotype and its labels; **E.** *P. (E.) languidus* (Reiche & Saulcy, 1855), male specimen, “Jerusalem Syria”, Jerusalem District, Israel. Scale bars: 1 mm.

wijk J.' (cMUI); 9♀♀, 'IR Chahar Mahaal Va / Bakhtiari Chery pass / 31.v.2019 Muilwijk J. / 2950–3260 m / 32°10'51"N, 50°09'59"E (cMUI, HMIM); 1♂, 2♀♀, 'IRAN (Chahār Mahāll vā Bachtīārī) / Zagros Mts., 5 km SW Asad Abad / 32°20'30"N / 50°32'59"E / ca 2400 m (subalpine slopes/ / under stones) / 19.IV.2018 Wrase & Laser [03]' (cWR); 3♂♂, 32°20'30"N, 50°32'59"E Iran / Zagros Mts., p. Chahār Mahāll / vā Bachtīārī, Asad Abad 5 km SW / snow field, high pasture / 19.IV.2018 2.500–2.770m NN / leg.: Schnitter IR 44' (NME); 1♂ (genitalia lost after study), 3♀♀, 'IRAN Zagros Mts., P: Chahar / Mahall va Bakhtiari, Asad / Abad 5 km SW, 32°20'30"N, / 50°32'59"E snow field, high / pasture, 19.IV.2018, 2.500– / 2.770m, leg. A. Weigel #18–04' (NME); 3♂♂, 'IRAN: Zagros Mts., p.Chahār Mahāll / vā Bachtīārī, Asad Abad 5 km SW, / 19.IV.2018, 32°20'30"N, 50°32'59"E / 2500–2770m, snow field, high / pasture leg. A. Weigel #44' (NME); 1♂, 'IRAN, Zagros Mts., P: / Chahar Mahal va / Bakhtiari, Asad Abad / 5 km SW, 2500–2770m // 19.IV.2018, snow field / high pasture, 32°20'N / 30", 50°32'59"E / leg. M. Hartmann, #3/18' (NME); 4♂♂, 3♀♀, 'IR Esfahan Kamran Pass / 1.vi.2019 Muilwijk J. / 3000–3300m / 32°45'49"N, 50°02'34"E' (cMUI); 1♂, 'IR Esfahan Pashadagan / 2.vi.2019 / Muilwijk J. 3000–3300m / 32°45'48"N, 49°59'52"E' (cMUI).

TME: 72 specimens. TGE: 16♂♂, 3♀♀.

Etymology. Adjective, derived from the name of the country where the species was collected.

Diagnosis. See "Diagnosis" under *P. felixi* sp. nov.

Description. Habitus. Specimens of small size for *Platyderus* species (BL: 4.30–6.65 mm; BW: 1.50–2.30 mm), with relatively short, moderately convex body (Fig. 1D). **Measurements and ratios.** See Table 1. **Color and lustre.** Integument uniformly yellow-brown to reddish-brown, appendages somewhat lighter than body. Surface moderately shiny. **Microsculpture and punctation.** Clypeus, vertex and disc of head with reduced microsculpture. Pronotum with regular isodiametric sculpticells posterolaterally and scarcely-visible to absent microsculpture in middle and anteriorly. Ventral surface with microsculpture and dorsal punctation as in *P. felixi* sp. nov. **Head.** About two thirds as wide as pronotum (mean PW/HW= 1.37). Eyes moderately convex. Labrum subrectangular, as long as or slightly shorter than clypeus, with anterior margin straight. Frontoclypeal suture and frontal furrows as in *P. felixi* sp. nov. Paraorbital sulci moderately deep, ending before level of posterior supraorbital pore. **Thorax.** Pronotum wider than long (mean PW/PL= 1.27), with widest point at second quarter. Anterior and posterior transverse impressions indistinct. Anterior bead lacking in medial 1/10 to 1/8. Sides convex anteriorly, straight posteriorly. Metepisternum somewhat longer than wide, MA/MI= 0.9–1.0. **Elytra.** Cylindrical, one and a half times or more as long as wide (mean EL/EW= 1.61), wider than pronotum and relatively long in relation to pronotum length (mean EW/PW= 1.31; mean EL/PL= 2.66). Parascutellar striole and striae as in *P. felixi* sp. nov. Interval 3 with two or three minute discal setiferous punctures, anterior puncture being mostly

absent. Umbilicate setiferous series consisting mostly of 15 or 16 punctures. **Legs.** Posterior side of profemur with one seta in basal third and one in medial third. Anterior side of mesofemur ventrally with four setiferous punctures (Fig. 5C). Anterior side of metafemur ventrally with two long setae, one in basal third and one in medial third. **Male genitalia.** Median lobe of aedeagus in lateral view as in *P. felixi* sp. nov., but significantly narrower, with shaft less protruding dorsally and more constricted proximally (Fig. 8D); median lobe in ventral view straight, ca. 3.7 times longer than wide; apical lamella nearly symmetrical (Fig. 10D). Internal sac in lateral view as in *P. felixi* sp. nov., but with ventral sclerite truncate distally; same in ventral view as in *P. felixi* sp. nov. Right paramere as that of *P. felixi* sp. nov. but somewhat finer (Fig. 12D). **Female genitalia** (Fig. 13C). Apical gonocoxite with blunt apex and two dorsolateral ensiform setae. Spermathecal canal connected in medial third of receptaculum.

Habitat. The holotype and one female paratype were collected along an artificial lake situated in a valley northwest of village Aliabad. They were caught at grassland with lots of stones situated along this lake. The vegetation there consisted of grassland, fields and small orchards – as a whole a cultivated landscape. Other ground beetles collected at this place, together with the new species, were *Carabus maurus osculatii* Villa, 1844, *Poecilus festinus* (Chaudoir, 1868) and *Amblystomus niger* (Heer, 1841).

Cheri Pass environments were represented by overgrazed grasslands with rocks and stones at lower altitudes and stone slopes with sparse vegetation and snow fields at higher altitudes. Similarly, Kamran Pass habitats were consisted of overgrazed grasslands at lower altitude and of stony (sub)alpine slopes with sparse vegetation and snow fields at higher altitudes.

Habitats around Asad Abad represent grasslands on subalpine slopes; specimens there were collected under stones, sometimes near edges of snowfields.

Distribution. Southwest Iran: Central Zagros Mountain Chains. So far, four isolated populations are known: (1) Borujen County; (2) Kuhrang County (type locality); (3) Shahr-e Kord County (locality southwest Asad Abad); (4) Fereydunshahr County (Kamran Pass), the first three in Chahar Mahal va Bakhtiari Province, the fourth one in Isfahan Province (near border area with Chahar Mahal va Bakhtiari Province).

Notes. The two specimens collected 7 km northeast of Naghan Town represent the nearest population of *P. iranicus* sp. nov. to the type locality of *P. felixi* sp. nov., ca. 17 km in a straight line (Fig. 17). The specimen from the environments of the Choghaklor Lake was collected together with three specimens of *Platyderus* (s. str.) *umbratus* (Men.).

The distance between the population from the type locality (near Cheri Pass) and that one southwest of Asad Abad is ca. 45 km in a straight line. On the other hand, the distance between Cheri Pass and locality northeast of Naghan Town is ca. 62 km in a straight line. Respectively, the distance between the locality southwest of Asad Abad and that one northeast of Naghan Town is about 47 km

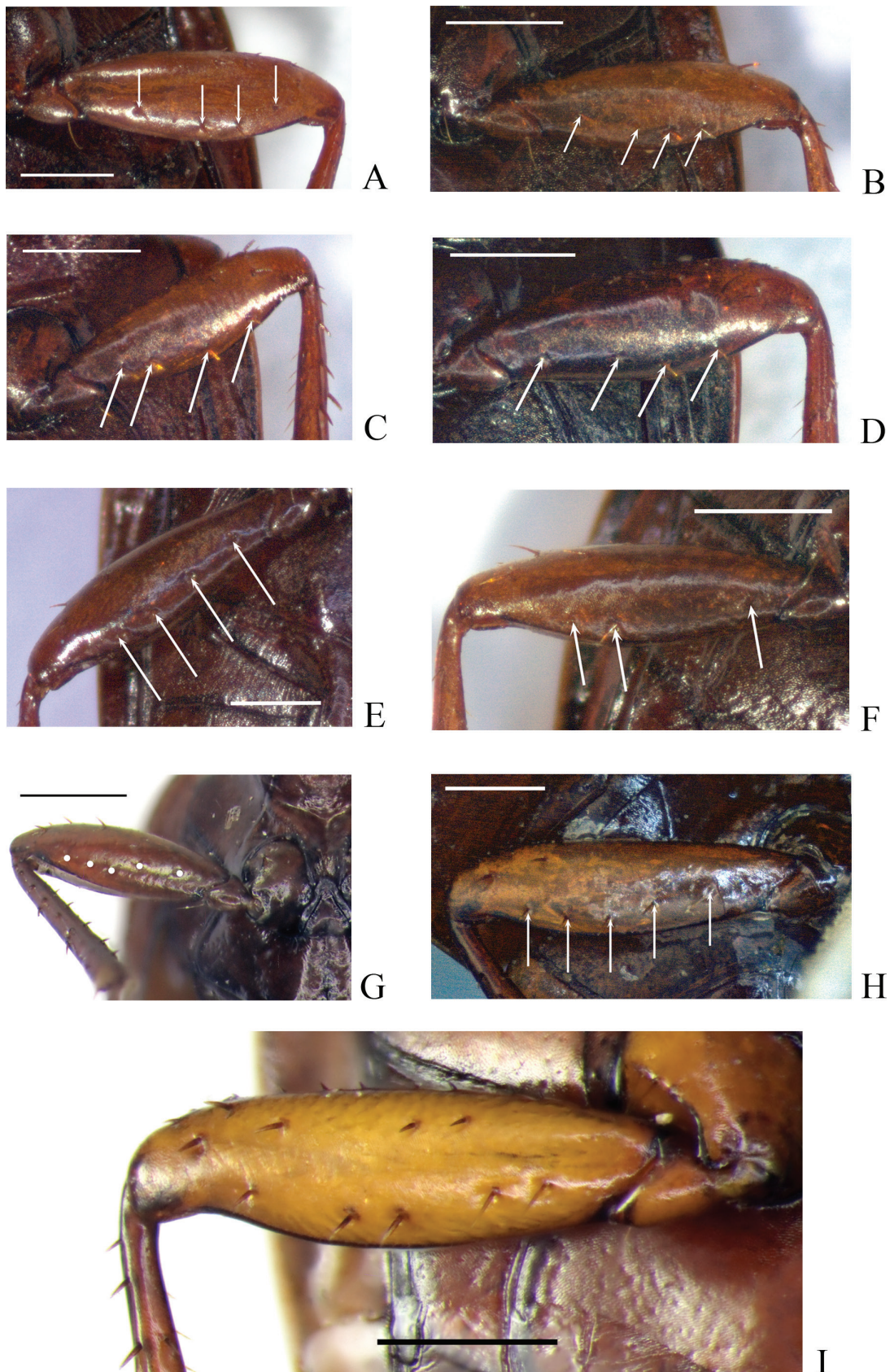


Figure 5. Mesofemora, anterior side (A–D: left mesofemur, E–I: right mesofemur; white arrows and dots indicate position of setiferous punctures). **A.** *Platyderus (Eremoderus) weiratheri* Mařan, 1940, female specimen, Boz dađ ky env., Izmir District, Turkey; **B.** *P. (E.) felixi*, sp. nov., topotype female paratype; **C.** *P. (E.) iranicus*, sp. nov., topotype female paratype; **D.** *P. (E.) lassallei*, sp. nov., female paratype, Iran, Mazandaran Province, E Qolqol; **E.** *P. (E.) klapperichi*, sp. nov., holotype; **F.** *P. (E.) taghizadehi* Morvan, 1974, male specimen, Tochal, Tehran Province, Iran; **G.** *P. (E.) afghanisticus*, sp. nov., holotype; **H.** *P. (E.) brunneus ferrantei* Reitter, 1909, lectotype; **I.** *P. (E.) languidus* (Reiche & Saulcy, 1855), female specimen, Netanya 1.3.97, Central District, Israel. Scale bars: 0.5 mm.

in a straight line. The distance between the type locality (near Cheri Pass) and the locality of Kamran Pass is about 67 km in a straight line (the same distance is between the populations from the Kamran Pass and that of Asad Abad). The distance between the Kamran Pass (Ferey-dunshahr County) and the locality northeast of Naghan Town is about 112 km in a straight line.

“*vanensis*” subgroup

Notes. By its parascutellar striole and striae 1–8 more coarsely and densely punctate and more deeply impressed, the species from Eastern Turkey differ from those of the “*iranicus*” subgroup.

5. *Platyderus (Eremoderus) vanensis* sp. nov.

<http://zoobank.org/5DAEBFAF-5211-4ED1-83DE-822DD8402705>

Figs 1E, 8E, 10E, 13D, E, 16, Table 1

Type locality. Turkey, Van Province, Gevaş Town environs.

Note on type locality. Gevaş Town is situated on the southern shore of Van Lake. The holotype was perhaps collected in vicinities of the town.

Type material. Holotype: 1♂, ‘TURCIA or. Van / Gevas 29.6.1993 / lgt. J. Růžička // *Platyderus* / cf. / punctiger / (REICHE & SAULCY) / WRASE det. 2008’ (cWR). **Paratypes:** 1♀, ‘TURKEY OR. / GEVAS env., 2100–2600m / (CADIR DAGI) / 1993–06–29, Klíma lgt. // *Platyderus* / cf. / punctiger / (REICHE & SAULCY) / WRASE det. 2008’ (NMNHS); 1♂, 1♀, ‘Resadiye 1900m / TR: Bitlis 6.91 / coll. B. Lassalle’ (cLAS); 1♀, ‘CE TURKEY, prov. Bitlis / 38°37’N, 42°16’E 2290m / Şentepe env. / Nemrut Mt. – crater / 24.VI.08 lgt. E.Hajdaj // COLL. / E. & P. HAJDAJ / JEŽOV / Czech Republic’ (cHAJ); 5♂♂, 2♀♀, ‘TR, Bitlis, Yelkenli / Van lake, ca. 1800 m / ~ 38°28’N, 42°32’E / 21.IV.–20.V.2014 / pitfall, leg. C. Reuter’ (NMNHS, cREU, cWR); 1♀, ‘col de Buglan 1500m / TR Mus 6.88 / col. B. Lassalle’ (cLAS); 1♂, ‘E Turkey, Mus / 8km SE Solhan, Buglan / Gec., 1700–1800m / 38°56’N, 41°08’E 18. – / 20.VI.05 lgt. E.&P.Hajdaj’ (cHAJ); 3♂♂, 5♀♀, ‘TR, Bingöl / Muş / Buğlan Geçidi, 1640 m / 21.IV. – 11.V.2014 / pitfall, leg. C. Reuter’ (NMNHS, cREU, cWR).

TME: 22 specimens. TGE: 4♂♂, 2♀♀.

Etymology. An adjective derived from the geographical name Van.

Diagnosis. The new species is most closely related to *P. vrabeci* sp. nov., but easily differs from it by the apical lamella of the median lobe (dorsal and ventral view) that is less symmetrical and shorter (Fig. 10E), conical shape of bursa copulatrix (Fig. 13D, E), darker coloration of the integument, elytral striae and striole more coarsely punctate and smaller value PW/PA (1.32–1.41, vs. 1.41–1.42).

Description. Habitus. Specimens of middle size for *Platyderus* species (BL: 6.85–8.40 mm; BW: 2.25–2.70 mm), with subelongate, slender body (Fig. 1E). **Measurements and ratios.** See Table 1. **Color and lustre.**

Body dorsally and ventrally mostly reddish-brown, appendages (antennae, palpi and legs) lighter colored than body, some specimens from Buğlan Geçidi with elytra almost black, and head, pronotum and ventral surface reddish-brown. Integument rather shiny. **Microsculpture and punctuation.** Pronotum and elytral intervals 1–5 (rarely also 6–7) without distinct sculpticells or with very faint ones, intervals 6–9 mostly (all specimens from Yelkenli) with distinct isodiametric sculpticells. Ventral surface mostly without visible sculpticells, sometimes with scarcely-visible isodiametric meshes. Pronotum coarsely and densely punctate in basal third and adjacent lateral areas, punctures at sides often reaching medial third. Abdominal ventrites 1–4 punctate at sides. **Head.** About two thirds as wide as pronotum (PW/HW= 1.30–1.43). Antennae long, with last three antennomeres exceeding base of pronotum. Eyes long, subconvex. Labrum subrectangular, with anterior margin slightly concave. Frontal furrows shallow, subfoveolate. Paraorbital sulci moderately deep, ending slightly before level of posterior supraorbital pore. **Thorax.** Pronotum wider than long (PW/PL= 1.13–1.24), widest point at anterior third. Anterior transverse impression barely distinct, posterior one distinct medially. Sides sinuate, convex anteriorly, concave posteriorly; anterior bead reduced in medial 1/10. Metepisternum slightly longer than wide, MA/MI= 0.87–0.93. **Elytra.** Elongate, about one and two thirds as long as wide (EL/EW= 1.61–1.73), two and a half times as long as pronotum (EL/PL= 2.52–2.74), and one third wider than pronotum (EW/PW= 1.22–1.36), with widest point at medial fifth. Parascutellar striole and striae deeply impressed (specimens from Buğlan Geçidi with striae 7–8 less impressed than others); parascutellar striole short, not connected with stria 1. Interval 3 with three discal setiferous punctures. Umbilicate setiferous punctures consisting of 16–17 (rarely 18) each side. **Legs.** Posterior side of profemur with one seta in basal third and one in medial third. Mesofemur with three or four setiferous punctures (three specimens with two on one side) on anterior side ventrally. Anterior side of metafemur ventrally with two long setae, one in basal third and one in medial third. **Male genitalia.** Median lobe of aedeagus in lateral view, with elongate basal bulb, long and broad shaft moderately constricted proximally, and short, straight apex; median lobe in ventral view straight, about 3.4 times longer than wide; apical lamella (dorsal view) short, symmetrical, rounded at tip, with sides straight or slightly convex. Internal sac in lateral view (Fig. 8E) with ventral sclerite distinctly broadened and rounded distally; same in ventral view (Fig. 10E), with dorsal sclerite forming a slightly sclerotized and short left-sided protuberance and a convex and long right-sided curve, and ventral sclerite narrow and nearly straight (only just scarcely bent to left). **Female genitalia** (Fig. 13D, E). Apical gonocoxite with semi-pointed apex and two dorsolateral ensiform setae. Spermathecal canal connected in medial third of receptaculum.

Habitat. Christoph Reuter (CR) and Bernard Lassalle (BL) kindly provided us with information on habitat

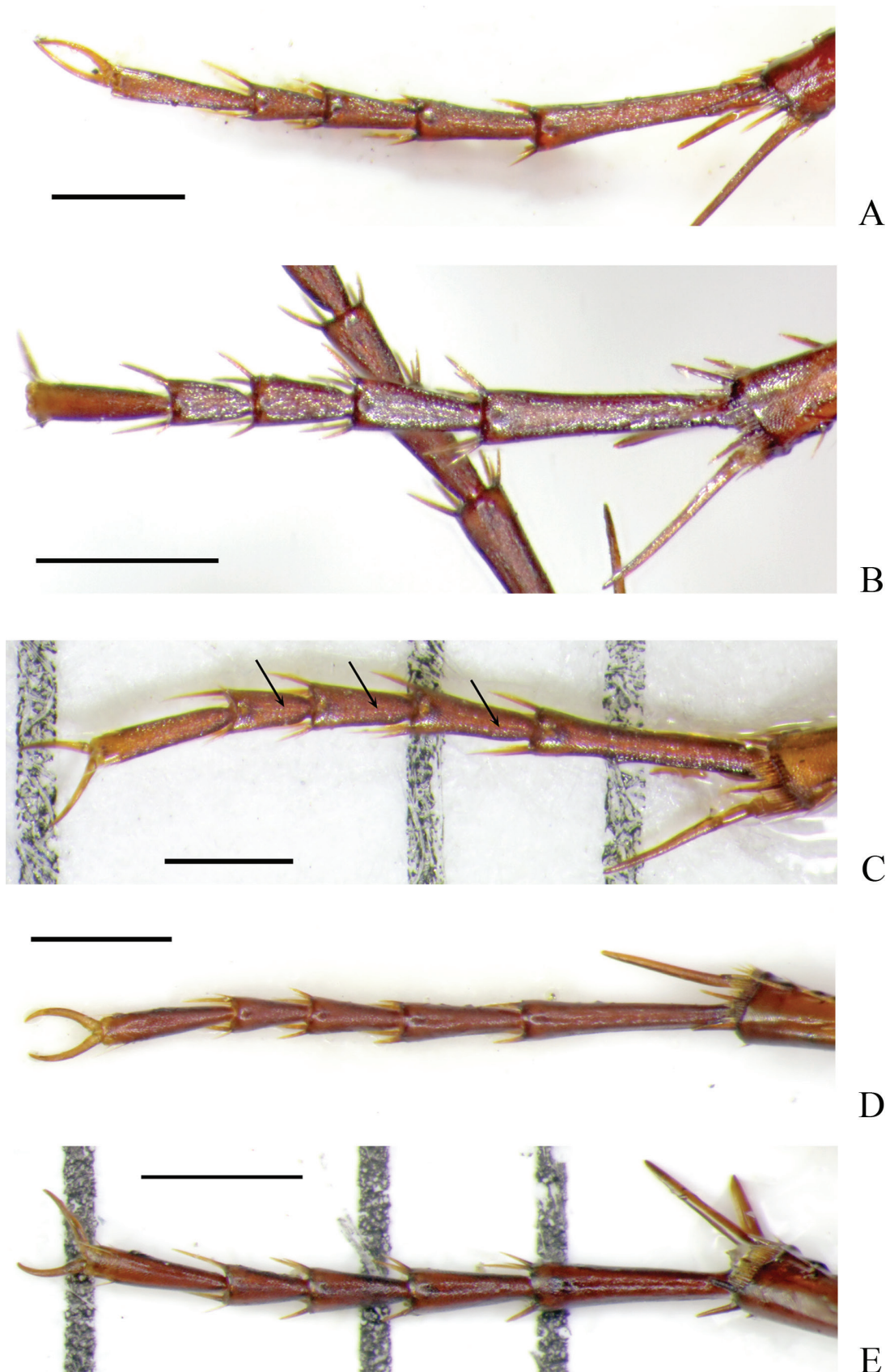


Figure 6. Metatarsus, dorsal view. **A.** *Platyderus (Eremoderus) brunneus brunneus* Karsch, 1881, left metatarsus, female specimen, Aziziyah, Jafara District, Libya; **B.** *P. (E.) brunneus ferrantei* Reitter, 1909, left metatarsus, female specimen, Holot Haluza, Southern District, Israel; **C.** *P. (E.) irakensis*, sp. nov., left metatarsus (black arrows indicate longitudinal grooves on metatarsomeres 2, 3 and 4), holotype; **D.** *P. (E.) jordanensis*, sp. nov., right metatarsus, holotype; **E.** *P. (E.) languidus* (Reiche & Saulcy, 1855), right metatarsus, male specimen, Nahal Prat, Judea and Samaria Area, Israel. Scale bars: 0.5 mm.

preferences. The specimens found by CR near Yelkenli were collected in a stunted oak forest. Underground is karst rock, in the middle of the tiny valley flows a small stream that still carries water, at least in spring. The series found by CR at Buğlan Geçidi, 1640 m, was collected in a semi-open landscape with a low, sparse oak forest of rather small, thin trees, a lot of scrubland, in between meadows, at least in some places, again karst rock, weathered rocks, and a lot of foliage. BL declare that he found a female specimen at Buğlan Geçidi, 1500 m, in “oak bushes”; same stated that, in Resadiye one male and one female of the new species was collected in small oak grove in a little valley.

Distribution. Turkey (provinces of Bingöl and Muş: Buğlan Geçidi; Bitlis Province; Van Province; Fig. 16). In Bitlis Province, the species inhabits the Nemrut volcanic massif west of Bitlis Town and the mountain region south of the Yelkenli (= Reşadiye) Bucağı. In Van Province, *P. vanensis* sp. nov. lives around Gevaş Town and in the Çadir Dağı, a massif situated south of the town aforementioned. In the border area of provinces of Bingöl and Muş, it lives along the pass Buğlan Geçidi.

Platyderus (Eremoderus) sp.

Fig. 2A, Table 1

Material examined. TURKEY: 1♀, ‘Col. Karabet 3000m / TR. Van / 18 VII 84 Machard / Collection Machard’ (cMAC).

TME: 1 specimen. TGE: 0.

Diagnostic features. It is distinct from individuals of *P. vanensis* sp. nov. by flatter elytral intervals and less coarsely punctate elytral striae. Measurements and ratios shown on Table 1.

Habitat and bionomic notes. The specimen was collected by PM just before the pass Karabet Pass (eastern slope), on the road coming from Yukari-Narlica köyü village towards the pass. There is a large cirque on the left with many snowfields and streams descending from them; it was found in gravel between the rivulets, at an altitude of about 2800 m.

Distribution. Karabet Pass [= Karabet Geçidi] (Turkey, Eastern Anatolia Region, Van Province).

Notes. The single female remains unidentified due to the lack of a male specimen. In addition, the characters of the elytral intervals and striae are not sufficiently diagnostic to propose a new name for this form.

6. *Platyderus (Eremoderus) vrabeci* sp. nov.

<http://zoobank.org/E82E9976-9F7E-4BE7-A545-FA359CEBCCF6>

Figs 1F, 7D, 8F, 10F, 12E, 13F, 16, Table 1

Type locality. Turkey, Adiyaman Province, Nemrut Dağı, NE of Adiyaman.

Notes on type locality. The Nemrut Dağı, a mount in Southeastern Anatolia, elevated over 2150 m a.s.l., not far from the upper reaches of the Euphrates. It belongs to

the Taurus Mountains and lies 86 kilometers northeast of Adiyaman in the province of the same name.

The GPS coordinates indicated on original labels are imprecise. They were taken from a map after the time of collecting (V. Vrabec, pers. comm.).

Type material. *Holotype* ♂, ‘S Turkey: NEMRUT DAGI / (NE from Adiyaman), UTM: DC60 / 38.00N/38.35E, 1700–1900 m / mount. pastures, stone fields / 27.–28.IV.1997, V. Vrabec lgt.’ (cWR). Paratype: 1♀, labelled as holotype (NMNHS).

TME: 2 specimens. TGE: 1♂, 1♀.

Etymology. Patronymic, named after Vladimír Vrabec, an entomologist interested in beetles and butterflies, who collected the type series of the new species.

Diagnosis. It differs from *P. vanensis* sp. nov. by the uniformly lighter coloration of the body, by the elytra and striae much less coarsely and deeply punctate, and by slightly higher value of ratio PW/PA (1.41–1.42, vs. 1.32–1.41). The apical lamella in *P. vrabeci* sp. nov. is also more symmetrical and elongate (Fig. 10F) and the bursa copulatrix is rounded (Fig. 13F).

Description. Habitus. Specimens of relatively large size for *Platyderus* species (BL: 7.30–7.45 mm; BW: 2.40–2.50 mm), with elongate, moderately convex body (Fig. 1F). **Measurements and ratios.** See Table 1.

Color and lustre. Body and appendages rusty red, head slightly darker than pronotum and elytra. Integument moderately shiny, head and pronotum shinier than elytra.

Microsculpture and punctuation. Pronotum without microreticulation. Elytral intervals and scutellum with distinct isodiametric sculpticells, basal margin and lateral gutter of elytra without evident microsculpture. Ventral surface largely with sculpticells not apparent or with scarcely-visible isodiametric (proepisternum, abdominal ventrites 1–5 laterally) or slightly transverse sculpticells (abdominal ventrite 6). Head with punctures and wrinkles only on posterior part of clypeus and areas in and around frontal furrows, rest of dorsal surface smooth. Pronotum coarsely punctate in basal third, with some punctures at sides reaching medial third; disc and apical third smooth. Elytral intervals with a row of irregular punctures. Abdominal ventrites smooth to very finely wrinkled at sides. **Head.** One-third or less as wide as pronotum (PW/HW= 1.38–1.42). Eyes moderately convex. Labrum subrectangular, as long as clypeus, with anterior margin slightly concave. Frontoclypeal suture distinct, impressed in middle, less distinct to obliterate at sides. Frontal furrows moderately distinct and impressed, subfoveolate. Paraorbital sulci straight, moderately deep, backward barely reaching posterior margin of eye, not reaching level of posterior supraorbital pore. **Thorax.** Pronotum about a quarter wider than long (PW/PL= 1.21–1.25), with widest point at second quarter. Anterior and posterior transverse impressions barely distinct. Sides sinuate, convex medially and anteriorly, concave posteriorly; bead of anterior border present throughout, rather fine; bead of posterior border present laterally and submedially, reduced to lacking at medial 1/10.

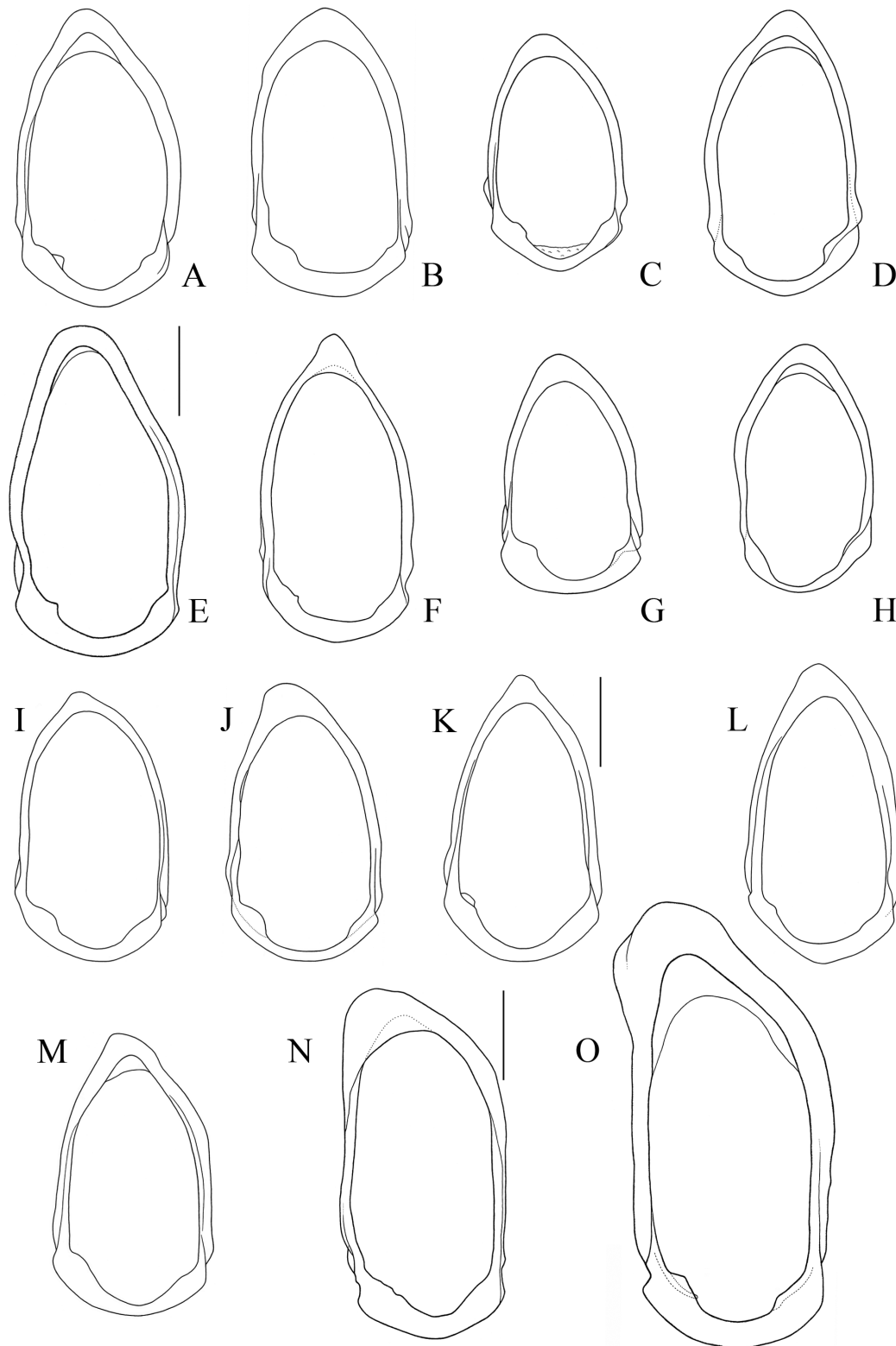


Figure 7. Urite, ventral view. **A.** *Platyderus (Eremoderus) chatzakiae*, sp. nov., holotype; **B.** *P. (E.) weiratheri* Mařan, 1940, E: topotype male specimen; **C.** *P. (E.) felixi*, sp. nov., holotype; **D.** *P. (E.) vrabeci*, sp. nov., holotype; **E.** *P. (E.) lassallei*, sp. nov., holotype; **F.** *P. (E.) ledouxi* Morvan, 1974, male specimen, 10 km S Hasan Keif, Mazandaran Province, Iran; **G.** *P. (E.) taghizadehi* Morvan, 1974, male specimen, Tochal, Tehran Province, Iran; **H.** *P. (E.) afghanisticus*, sp. nov., holotype; **I.** *P. (E.) brunneus brunneus* Karsch, 1881, male specimen, 50 km W of Ben Gardane, Medenine Governorate, Tunisia; **J.** *P. (E.) brunneus ferrantei* Reitter, 1909, male specimen, Holot Haluza, Southern District, Israel; **K.** *P. (E.) jordanensis*, sp. nov., holotype; **L.** *P. (E.) languidus* (Reiche & Saulcy, 1855), lectotype; **M.** *P. (E.) languidus* (Reiche & Saulcy, 1855), male specimen, Naħal Prat, Judea and Samaria Area, Israel; **N.** *P. (Platyderus)* sp., male specimen, Boz Dağlar Mtn., Turkey; **O.** *P. (P.) reticulatus* (Chaudoir), male specimen, Tashehzeh, Nowshahr County, Mazandaran Province, Iran. Scale bars: 0.5 mm.

Metepisternum as long as wide, MA/MI= 0.95–1.01. **Elytra.** Elongate, about two thirds as long as elytra wide (EL/EW= 1.63–1.66), two times and two thirds as long as pronotum (EL/PL= 2.63–2.71), and one and a third as wide as pronotum (EW/PW= 1.32), with widest point at beginning of third quarter. Parascutellar striole and striae well-impressed, moderately punctate (less coarsely than *P. weiratheri* and *P. vanensis* sp. nov.); parascutellar striole short, not joining stria 1; striae 1–6 reaching basal bead, 7 shortened a little before. Interval 3 with three discal setiferous punctures, as first lack on left elytron of paratype. Umbilicate setiferous series with 16 punctures on each side in holotype, with 17 punctures on left elytron and 15 ones on right elytron in paratype. **Legs.** Posterior side of profemur with one seta in basal third and one in medial third. Mesofemur with 3–4 setiferous punctures on anterior side ventrally. Anterior side of metafemur ventrally with two long setae, one in basal third and one in medial third. **Male genitalia.** Urite IX suboval, with proximal margin slightly asymmetrical and pointed (Fig. 7D). Median lobe of aedeagus in lateral view similar to that of *P. vanensis*, but slightly narrower and with apex a little longer (Fig. 8F); same in ventral view straight, about 3.2–3.3 times longer than wide (Fig. 10F); apical lamella (dorsal view) less symmetrical and more elongate than in *P. vanensis* sp. nov. Internal sac in lateral view (Fig. 8F) with ventral sclerite distinctly broadened and rounded distally; same in ventral view (Fig. 10F), with ventral sclerite somewhat more broadened distally than that of *P. vanensis* sp. nov. Right paramere on Fig. 12E. **Female genitalia** (Fig. 13F). Apical gonocoxite with semi-pointed apex and two dorsolateral ensiform setae. Spermathecal canal connected in medial third of receptaculum.

Habitat. Slopes with pastures and stone fields covered with snow patches at the time of collecting at an altitude of 1700–1900 m. Several trees in poor condition and a few flowering wild representatives of *Hyacinthus* spp. were observed around the place of collecting (V. Vrabec, pers. comm.).

Distribution. Nemrut Dağı (Turkey, Southeastern Anatolia, Province of Adıyaman; Fig. 16).

“lassallei” species group

Notes. The species of the “lassallei” and the “davatchii” group share a synapomorphy, the distal end of the ventral sclerite of the median lobe is curved to the left (ventral view).

7. *Platyderus (Eremoderus) lassallei* sp. nov.

<http://zoobank.org/8A300B91-AAEF-4283-8EDF-314FF907E684>

Figs 2B, 5D, 7E, 8G, 10G, 12F, 14A, 17, Table 2

Type locality. Iran, Mazandaran Province, Nur County, between Nur City and Lavij Village, 500–1300 m.

Notes on type locality. Bernard Lassalle (pers. comm.) stated that the holotype was caught with soil traps in the period 8–25 June 2000. The place of the exposition of

traps was: “south of Nur, on the road between Nur and Lavij, in a mixed forest, between 500–1300 m”. However, having in mind that the northern outskirts of Lavij Village are situated at about 600 m altitude, we consider that the real altitude at which the specimen was caught is between 500 and 600 meters.

Type material. **Holotype** ♂, ‘sud Nur 500–1300m / IR:Mazandaran 6.00 / coll. B.Lassalle’ (cLAS). Paratypes: 1♂, ‘IRAN, Prov. Mazandaran / [IR08–01] Sari County, / Mohammadabad, Elburz Mts., / N-Slope, NE Sangdeh, 1533m, / 36°04'06.6"N, 53°09'57.8"E, / Fagus forest, leaves debris, / sifted, 29.V.2008, leg. A. Pütz’ (cWR); 1♀, ‘IRAN, Prov. Mazandaran / [IR08–03A] Sari County, / Mohammadabad Elburz Mts., / N-Slope, E Qolqol, / 36°10'26.7"N, 53°16'29.2"E, / 916m, sifted, 30.V.2008, / leg. A. Pütz’ (cPTZ); 1♂, 2♀♀, ‘N.IRAN-Mazandaran prov. / Maji to Vemzela rd. 1360 m / 36°07'10.8"N, 53°11'50.9"E / 1–5.VI.2018, Václav Čutka leg.’ (NMNHS); 1♂, 1♀, ‘N.IRAN-Mazandaran prov. / Sári-Talarem env, 36°13'21"N, 53°15'49.6"E, 965m, forest / 1–5.VI.2018, Václav Čutka leg.’ (cKME); 1♂, ‘N.IRAN-Mazandaran prov. / Galugah-Niala env. 1390 m / 36°37'38.8"N, 53°50'15.6"E / 4.VI.2018, Václav Čutka leg.’ (cKME).

TME: 9 specimens. TGE: 5♂♂, 1♀.

Etymology. Latinized patronym based on the surname of Bernard Lassalle (Boissy-les-Perche, France), whose assiduous efforts in the field contributed substantial numbers of Carabid beetles that are very interesting or new to science.

Diagnosis. This species is distinct from the other species of the subgenus in the following set of characters: (1) large size of body (8.00–8.50 mm, Table 2); (2) deep black color of body and reddish-brown appendages; (3) dorsal surface of head and pronotum basal foveae with more extensive punctation (incl. micropunctation); (4) median lobe of aedeagus (lateral view) less noticeably curved basally, with apex not turned up.

In addition to the aforementioned characters, the new species differs from species of the “davatchii” group (which together with *P. lassallei* are the only *Eremoderus*-representatives that inhabit Alborz Range) in the wider pronotum (PW/PL > 1.20, vs. PW/PL < 1.19) with sides to base more convex, the less long elytra (EL/EW < 1.58–1.60, vs. EL/EW > 1.60), and the larger and longer median lobe (1.4 mm long and 4.3–4.4 times longer than wide, measurements taken ventrally). The median lobes of *P. ledouxi* and *P. taghizadehi* are proportionally smaller and less long (1.1–1.3 mm long and 3.7–3.9 times longer than wide) more clearly curved basally, with apex somewhat turned up (lateral view).

Description. **Habitus.** Specimens of large size for *Platyderus* species (BL: 8.05–8.50 mm; BW: 2.95–3.05 mm), with suboval and subconvex body (Fig. 2B). **Measurements and ratios.** See Table 2. **Color and lustre.** Head, pronotum and elytra black, ventral part of body dark brown, appendages distinctly lighter than body, reddish-brown. Integument moderately shiny. **Microsculpture**

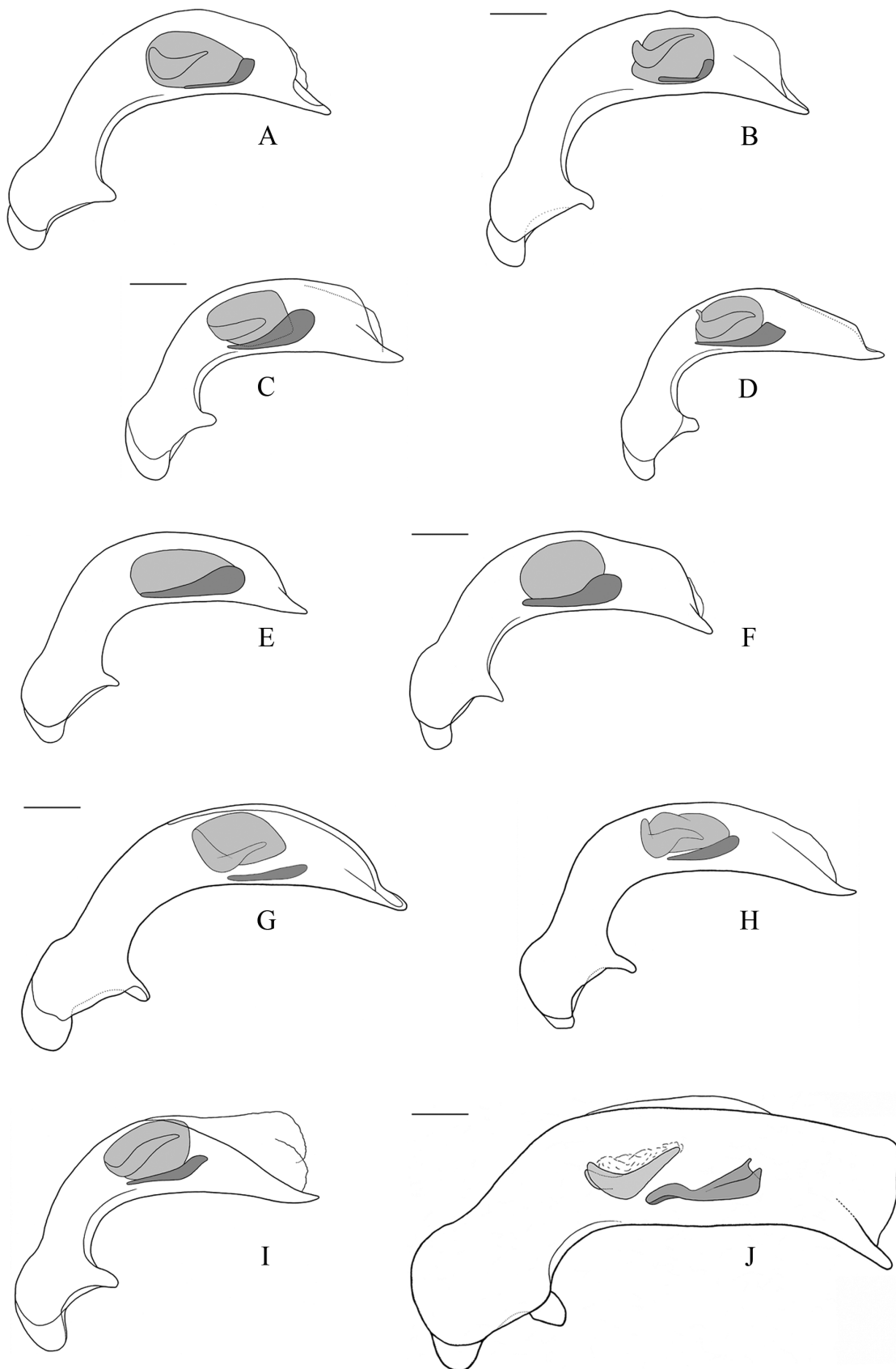


Figure 8. Median lobe of aedeagus, left lateral view. **A.** *Platyderus (Eremoderus) chatzakiae*, sp. nov., holotype; **B.** *P. (E.) weiratheri* Mařan, 1940, lectotype; **C.** *P. (E.) felixi*, sp. nov., holotype; **D.** *P. (E.) iranicus*, sp. nov., holotype; **E.** *P. (E.) vanensis*, sp. nov., holotype; **F.** *P. (E.) vrabeci*, sp. nov., holotype; **G.** *P. (E.) lassallei*, sp. nov., holotype; **H.** *P. (E.) ledouxi* Morvan, 1974, male specimen, 10 km S Hasan Keif, Mazandaran Province, Iran; **I.** *P. (E.) taghizadehi* Morvan, 1974, male specimen, Tochal, Tehran Province, Iran; **J.** *P. (Platyderus)* sp., male specimen, vicinity of Izmir City, Turkey. Scale bars: 0.2 mm.

and punctuation. Disc of head with reduced sculpticells. Pronotum with regular isodiametric sculpticells posterolaterally and stretched isodiametric sculpticells anterolaterally, microsculpture very faint to absent on disc. Ventral surface largely with obsolete microsculpture, slightly stretched isodiametric sculpticells present on mentum, submentum and sternal parts laterally, slightly transverse sculpticells present on sternal part medially; gula, abdominal ventrites and legs without microreticulation. Prosternum laterally punctate. **Head.** About two thirds as wide as pronotum (mean PW/HW= 1.39). Antennae long, with last three antennomeres exceeding base of pronotum. Eyes large and convex. Labrum subrectangular, with anterior margin slightly concave. Frontal furrows slightly impressed, subfoveolate. Paraorbital sulci moderately deep, ending slightly before level of posterior supraorbital pore. **Thorax.** Pronotum distinctly wider than long (mean PW/PL= 1.23), widest at second quarter. Anterior transverse impressions barely distinct to indistinct, posterior one well-distinct medially. Sides convex anteriorly, slightly to barely concave posteriorly; bead of anterior margin present laterally, reduced in medial 1/10; bead of posterior margin present throughout (in one paratype reduced to absent in medial 1/8). Metepisternum as long as wide, MA/MI about 1.0. **Elytra.** Suboval, one-and-a-half times as long as wide (mean EL/EW= 1.51), wider and much longer in relation to pronotum (mean EW/PW= 1.38; mean EL/PL= 2.58). Stria 7 reaching or ending before. Elytral interval 3 with three discal setiferous punctures, anterior puncture adjoining stria 3, remaining two punctures adjoining stria 2. Umbilicate setiferous series of 16 punctures on each elytron. **Legs.** Posterior side of profemur with one seta in basal third and one in medial third. Anterior side of mesofemur ventrally (Fig. 5D) mostly with three–four setiferous punctures (one specimen with five punctures on one mesofemur, whereas another with two such also on one mesofemur). Anterior side of metafemur ventrally with two long setae, one in basal third and one in medial third. **Male genitalia.** Urite IX large, with right shoulder straight to apex and proximal margin widely rounded (Fig. 7E). Median lobe of aedeagus in lateral view arcuate ventrally, with apex almost straight; same in ventral view straight, ca. 4.3–4.4 times longer than wide, with apical lamella symmetrical. Internal sac in lateral view well-differentiated, with ventral sclerite long and narrow (Fig. 8G), in ventral view with dorsal sclerite forming a short left-sided curve and a long right-sided curve, and ventral sclerite straight, narrow, with distal end curved to left (Fig. 10G). Right paramere relatively large, rather concave ventrally (Fig. 12F). **Female genitalia** (Fig. 14A). Apical gonocoxite with semi-pointed apex and two dorsolateral ensiform setae. Spermathecal canal connected in medial third of receptaculum.

Comparisons. By dorsal coloration, form of pronotum and elytra, the new species is similar to *P. reticulatus* (Chaudoir, 1842), the only member of the nominotypical subgenus that lives in sympatry with *P. lassallei* on north slopes of the Alborz Range. However, the latter has the anterior

side of mesofemur ventrally mostly with three–four setae (vs. two such setae in *P. reticulatus*) as well as completely different shapes of the urite and median lobe of aedeagus.

Habitat. According to the label data, the species occurs on northern slopes in *Fagus orientalis* or mixed forests in altitudes of about 500–1600 m a.s.l. Specimens were collected by sifting leaves debris or with pitfall traps.

Distribution. North Iran: Central Alborz Range (Fig. 17). The three records known until today come from three counties of the Province of Mazandaran, Nur County, Sary County and Galugah County. The areas between these counties are probably also populated by *P. lassallei* sp. nov.

“*davatchii*” species group

Diagnosis. This group includes *P. davatchii*, *P. ledouxi*, *P. taghizadehi* and *P. klapperichi* sp. nov., which are adapted to inhabit higher altitudes and open habitats in the Alborz Range (Fig. 17). Compared with *P. lassallei* sp. nov., the species in question have a more elongate and parallel body of smaller size and lighter color of the integument (see also “Diagnosis” under “*lassallei*” species group).

The species from the “*davatchii*” group differs from those of the “*iranicus*” subgroup, in: (1) the sides of pronotum are clearly concave toward the posterior angles (vs. sides of pronotum hardly concave or straight toward the posterior angles), (2) PW/PL < 1.20 (vs. PW/PL > 1.22), and (3) EL/EW ≥ 1.63 (vs. EL/EW ≤ 1.63).

Habitat. The habitat of the species of the “*davatchii*” group is similar to that of the two Iranian species from the Zagros Mountains (see “Habitat” under “*iranicus-vanensis*” species group). In the high mountain zone of Elburz the *Eremoderus*-species were collected in natural mountain pastures, covered with snow in winter.

Notes. Having not been able to examine the type material of Pierre Morvan, we treated *P. davatchii* Morvan, 1970, *P. taghizadehi* Morvan, 1974 and *P. ledouxi* Morvan, 1974 as valid species. Based on original descriptions and new material at hand, we were able to ascertain the identity of the last two species. Without available material for study, the identity of *P. davatchii* remains unknown for the time being.

8. *Platyderus (Eremoderus) davatchii* Morvan, 1970

Fig. 17

Platyderus davatchii Morvan, 1970: 194 (type locality: “l’Elburz, environs d’Alamut ; alt. 2 700 m...près d’un torrent, versant nord”).

Notes on type locality. The type locality in the Iranian province of Qazvin, in Qazvin County, in the vicinities of Alamut Castle, 2700 m, may conditionally confine to the high area of the Central Alborz Range situated northward of the upper current of Shāh Rūd River, eastward of the Ovan Lake and westward of the upper currents of Seh Hazar River. It may concern the area situated north–north-east of ruins of the Alamut Castle.

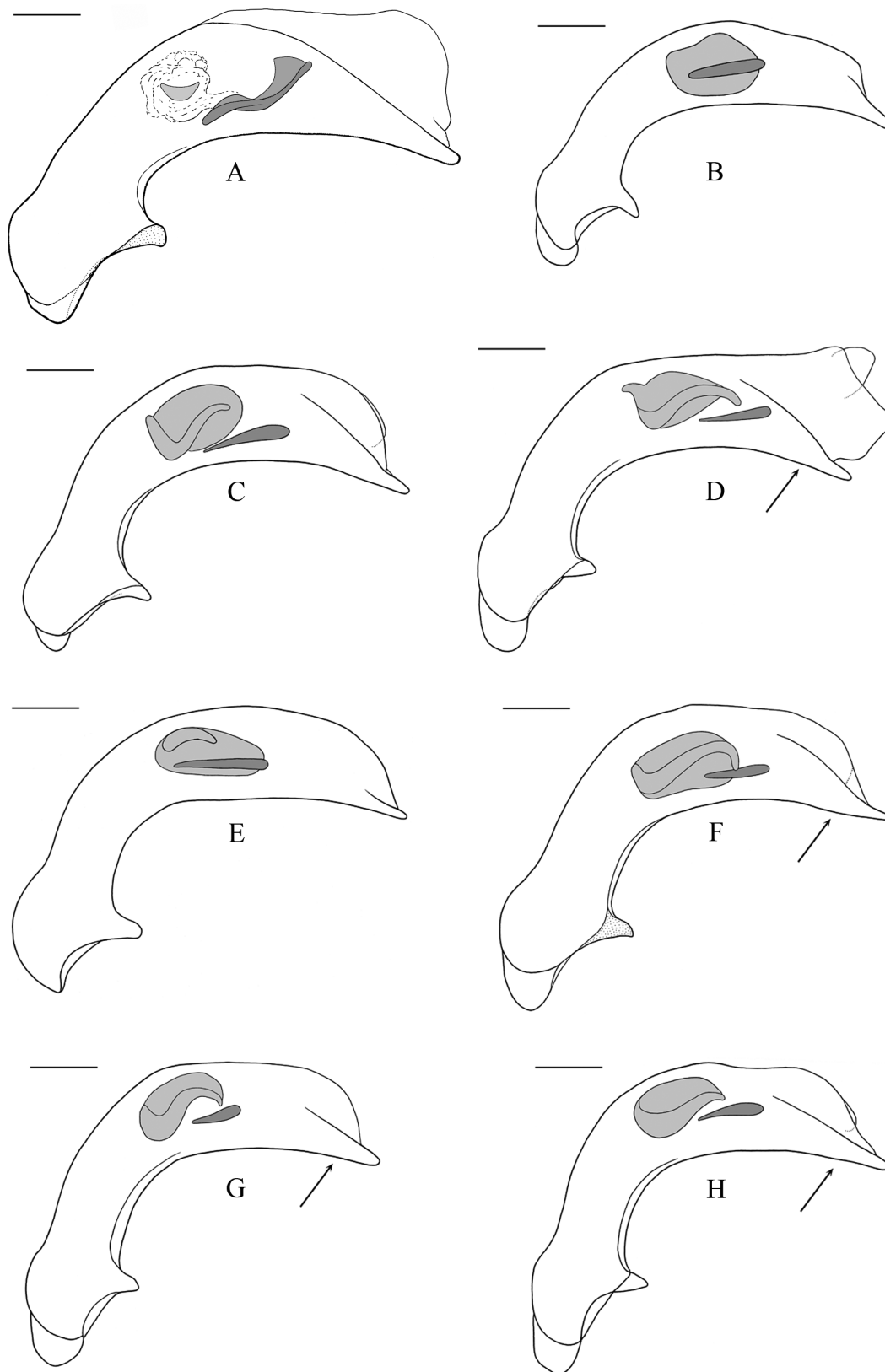


Figure 9. Median lobe of aedeagus, left lateral view (black arrows on D, F–H indicate convexity of ventral margin of apex of median lobe). **A.** *Platyderus (Platyderus)* sp., male specimen, Boz Dağlar Mtn., Turkey; **B.** *P. (Eremoderus) afghanisticus*, sp. nov., holotype; **C.** *P. (E.) brunneus brunneus* Karsch, 1881, male specimen, 50 km W of Ben Gardane, Medenine Governorate, Tunisia; **D.** *P. (E.) brunneus ferrantei* Reitter, 1909, male specimen, Holot Haluza, Southern District, Israel; **E.** *P. (E.) insignitus insignitus* Bedel, 1902, male specimen, SW Tiznit, Sous-Massa Region, Morocco; **F.** *P. (E.) jordanensis*, sp. nov., holotype; **G.** *P. (E.) languidus* (Reiche & Saulcy, 1855), lectotype; **H.** *P. (E.) languidus* (Reiche & Saulcy, 1855), male specimen, Nahal Prat, Judea and Samaria Area, Israel. Scale bars: 0.2 mm.

References. *Platyderus davatchii*: Morvan 1970: Morvan 1974: 149; Lorenz 1998: 375; Hovorka and Sciaky 2003: 522; Lorenz 2005: 395; Azadbakhsh and Nozari 2015: 84; Hovorka 2017: 757.

Type material. *Holotype* ♀ preserved in private collection Pierre Morvan (Carentoir, France). Not examined.

Other material examined. None.

Habitat. The holotype was collected under a large stone near a stream, on a north slope at ca. 2700 m altitude.

Distribution. Only known from type location in North Iran: Central Alborz Range (Fig. 17).

Notes. Based on the habitus drawing and features noted in the original description (Morvan 1970: 194, fig. 6), *P. davatchii* is without doubt an *Eremoderus*-species. For the time being, it is the westernmost and the least known representative of the “*davatchii*” species group. Study of the holotype or topotypical male specimens of *P. davatchii* is a key issue that can help to decide whether its closest neighbor, *P. ledouxi*, is a separate species or its synonym. The distance between the population from Alamut Region (Qazvin County), referred to the former species, and the population south of Kelārdascht [= Hasankif; = Rudbarak] (Chalus County: Kelārdascht District), referred to the latter species is about 40–50 km in straight line.

The record about *P. davatchii* from “10 km S Hasan Keif” (Lohaj and Mlejnek 2007) actually concerns *P. ledouxi*.

9. *Platyderus (Eremoderus) klapperichi* sp. nov.

http://zoobank.org/8CA1EB54-9BEA-4E30-83C6-BF3B49C83A13
Figs 2C, 5E, 17, Table 2

Type locality. Iran, Alborz Mountains, Damavand, 2000 m.

Notes on type locality. The locality is situated in the Province of Tehran, in the Damavand County (Central Alborz Range). Data on the label are insufficient to locate whether the holotype has been collected in the surrounding area of the Damavand City or in foothills of the Mount Damavand.

Type material. *Holotype* ♂, ‘IRAN, Demavand / 2000 m, Elbursggeb. / 2.VI.1960 / leg. J. Klapperich’ (HNHM). TME: 1 specimen. TGE: 0.

Etymology. The species is named in honor of the German entomologist and collector of insects Johann Friedrich Klapperich (1913–1987), famous by its very successful expeditions to Southern China, the near and Middle East, and who collected the holotype of this new species.

Diagnosis. It differs from other representatives of the “*davatchii*” group by very small size of body (BL < 7 mm) and pronotum less wide in relation to head (PW/HW = 1.27). In addition, it differs from *P. taghizadehi* by anterior side of mesofemur ventrally with four setiferous punctures (vs. three setiferous punctures in *P. taghizadehi*).

Description. *Habitus.* Specimen of small size for *Platyderus* species, with elongate and convex body (Fig. 2C). *Measurements and ratios.* See Table 2. *Color and lustre.* Body uniformly dark brown (castaneous), antennae, palpi and legs reddish-brown. Integument moder-

ately shiny. **Microsculpture and punctuation.** Microsculpture of head faint to absent on clypeus and frons, present on vertex. Pronotum with isodiametric sculpticells only posterolaterally, remaining surface without distinct microsculpture. Lateral parts of pro- and metasternum, pro-, mes-, and metepisternum, abdomen and legs with slightly stretched isodiametric sculpticells; ventral part of head, prosternum and metasternum medially without or with reduced sculpticells. Pronotum basal half with several transverse wrinkles. **Head.** Narrower than pronotum (PW/HW = 1.27). Frontal furrows slightly impressed, shapeless, wrinkled. Paraorbital sulci moderately deep, ending at level close to posterior supraorbital pore. Frons behind frontal furrows wrinkled. **Thorax.** Pronotum barely wider than long (PW/PL = 1.09), with widest point at second quarter. Anterior transverse impression distinct, posterior transverse one indistinct between adjacent wrinkles. Sides moderately curved apicad and basad, convexly anteriorly, concavely posteriorly; beads of anterior margin and posterior margin present laterally, very faint to reduced in medial 1/8. Metepisternum somewhat longer than wide, MA/MI about 0.8. **Elytra.** Cylindrical, about one and two thirds as long as wide (EL/EW = 1.70), wider and considerably longer than pronotum (EW/PW = 1.40; EL/PL = 2.60). Stria 7 ending at first umbilicate puncture on left elytron or after reaching first forming a kink connecting with the basal rim on the right elytron. Two or three discal setiferous punctures, anterior puncture near stria 3 on left elytron, and lacking on right elytron, remaining two punctures adjoining stria 2. Umbilicate setiferous series of 15 setiferous punctures on left elytron, with 16 punctures on right elytron. **Legs.** Posterior side of profemur with one seta in basal third and one in medial third. Anterior side of mesofemur ventrally with four setiferous punctures (Fig. 5E). Anterior side of metafemur ventrally with two long setae, one in basal third and one in medial third. **Male genitalia.** Unknown (see “Notes”). **Female genitalia.** Unknown.

Comparisons. The species can be easily distinguished from *P. lassallei* by characters noted in section “Diagnosis” (under *P. lassallei*).

Habitat. Like other representatives of the “*davatchii*” group, *P. klapperichi* inhabits high-mountain meadows around and above 2000 m a.s.l.

Distribution. North Iran, Central Alborz Range, most likely in vicinities of Damavand City (Fig. 17).

Notes. The aedeagus with attached parameres and urite IX were lost after the extraction.

10. *Platyderus (Eremoderus) ledouxi* Morvan, 1974

Figs 2D, 7F, 8H, 10H, 12G, 14B, 17, Table 2

Platyderus ledouxi Morvan, 1974: 149 (type locality: “l’Elburz, province du Mazandaran, massif du Soleyman, Roudbarak, alt: 1800 m, en forêt de *Fagus*”).

Notes on type locality. The Takht-e Soleyman Massif, a subrange of the Central Alborz Range, is located in the Province of Mazandaran (Chalus County, Keraldasht

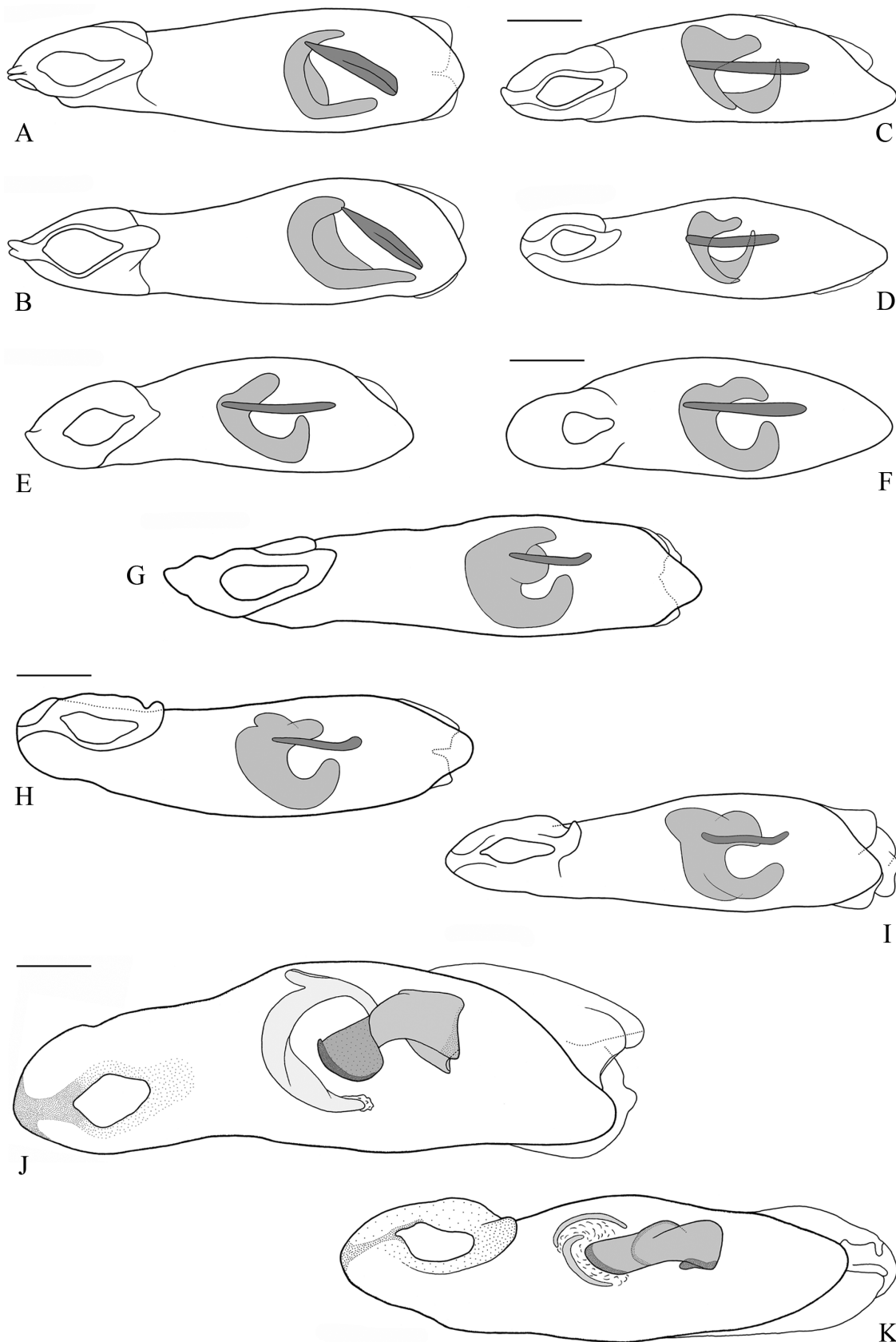


Figure 10. Median lobe of aedeagus, ventral view. **A.** *Platyderus (Eremoderus) chatzakiae*, sp. nov., holotype; **B.** *P. (E.) weiratheri* Mařan, 1940, lectotype; **C.** *P. (E.) felixi*, sp. nov., holotype; **D.** *P. (E.) iranicus*, sp. nov., holotype; **E.** *P. (E.) vanensis*, sp. nov., holotype; **F.** *P. (E.) vrabeci*, sp. nov., holotype; **G.** *P. (E.) lassallei*, sp. nov., holotype; **H.** *P. (E.) ledouxi* Morvan, 1974, male specimen, 10 km S Hasan Keif, Mazandaran Province, Iran; **I.** *P. (E.) taghizadehi* Morvan, 1974, male specimen, Tochal, Tehran Province, Iran; **J.** *P. (Platyderus) sp.*, male specimen, vicinity of Izmir City, Turkey; **K.** *P. (P.) sp.*, male specimen, Boz Dađlar Mtn., Turkey. Scale bars: 0.2 mm.

Table 2. Morphometric data for species of the ‘*lassallei*’, ‘*davatchii*’ and ‘*afghanisticus*’ groups of *Platyderus*.

Species (number of samples)	BL/mm	BW/mm	PW/HW	PW/PL	PW/PA	PW/PB	PA/PB	EL/EW	EW/PW	EL/PL
<i>P. lassallei</i> sp. nov. (2♂♂, 1♀)	8.05–8.50	2.95–3.05	1.37–1.41	1.23–1.24	1.39–1.40	1.16–1.18	0.83–0.84	1.49–1.55	1.36–1.41	2.51–2.62
<i>P. lassallei</i> sp. nov. (mean)	8.27	3.00	1.39	1.23	1.40	1.17	0.84	1.51	1.38	2.58
<i>P. ledouxi</i> Morvan (2♂♂, 1♀)	7.35–7.90	2.45–2.55	1.43–1.51	1.13–1.16	1.43–1.49	1.23–1.28	0.84–0.88	1.63–1.69	1.32–1.34	2.50–2.59
<i>P. ledouxi</i> Morvan (mean)	7.53	2.52	1.48	1.15	1.46	1.25	0.86	1.67	1.33	2.55
<i>P. taghizadehi</i> Morvan (1♂, 1♀)	7.10–7.20	2.40	1.31–1.33	1.06–1.12	1.34–1.36	1.13–1.22	0.83–0.91	1.65–1.68	1.41–1.42	2.47–2.67
<i>P. taghizadehi</i> Morvan (mean)	7.15	2.40	1.32	1.09	1.35	1.18	0.87	1.67	1.42	2.57
<i>P. klapperichii</i> sp. nov. (1♂)	6.60	2.20	1.27	1.09	1.38	1.15	0.83	1.70	1.40	2.60
<i>P. afghanisticus</i> sp. nov. (1♂)	6.80	2.25	1.40	1.24	1.49	1.24	0.83	1.63	1.37	2.78

For abbreviations in line 1, see “Abbreviations to measurements and ratios” (section “Material and methods”).

District). For the type locality Morvan indicated as biotope a beech forest in the vicinity of Rudbarak village, situated at ca. 1800 m altitude. This site lies in the upper valley of the Sardabrud River, northeast of the Takht-e Suleyman Massif.

References. *Platyderus davatchii*: Morvan 1970: Lohaj and Mlejnek 2007: 12. *P. ledouxi*: Lorenz 1998: 375; Hovorka and Sciaky 2003: 522; Lorenz 2005: 396; Azadbakhsh and Nozari 2015: 84; Hovorka 2017: 758.

Type material. *Holotype* ♂ in MNHN, not examined; paratype ♀ in private collection Pierre Morvan (Carentoir, France), not examined.

Other material examined. **Iran:** Mazandaran Province: 1♂, ‘N Iran p. Mazandarán / 10 km S Hasan Keif / 2300m 3625N 5102E [36°25'N, 51°02'E] / 17.VI.2000 lgt. Hajdaj E.P. // Collectio / Hajdaj // *Platyderus* / cf. / *davatchii* Morv. / D.W. Wrase det. 01’ (cHAJ); 1♂, 1♀, ‘IR Mazandaran 10km SW / Rudbarak 36°24'00.1"N, 51°2'07.5"E 2500m / 16.06.17 Seiedy/Muilwijk’ (cMUI).

TME: 3 specimens. TGE: 2♂♂, 1♀.

Diagnosis. Similar to *P. taghizadehi*, but differs from it in pronotum much wider than head (PW/HW > 1.40), with apex more constricted compared with widest point (PW/PA > 1.40), elytra in relation to pronotum narrower (EW/PW < 1.38), and anterior side of mesofemur ventrally with four setiferous punctures. Male specimens of *P. ledouxi* can be additionally distinguished from males of *P. taghizadehi* by median lobe at lateral view larger (1.2–1.3 mm, vs. 1.1–1.2 mm, with a longer shaft (Fig. 8H).

Redescription (based on non-type material). **Habitus.** Specimens of moderate size for *Platyderus* species (BL: 7.35–7.90 mm; BW: 2.45–2.55 mm), with elongate and subconvex body (Fig. 2D). **Measurements and ratios.** See Table 2. **Color and lustre.** Integument uniformly dark brown, appendages barely lighter than body. Surface moderately shiny. **Microsculpture and punctuation.** Pronotum with regular isodiametric sculpticells posterolaterally and slightly transverse ones anterolaterally, microsculpture faint to absent in middle. Ventral surface (excluding gula) microsculptured, mentum, submentum and proepisternum with regular isodiametric microsculpture, abdominal ventrites and femora with slightly stretched isodiametric sculpticells. **Head.** Significantly narrower than pronotum (mean PW/HW = 1.48). Antennae long, with last three antennomeres exceeding base of pronotum. Eyes long, subconvex. Labrum subrectangular, with anterior

margin slightly concave. Frontal furrows small, shallow, subfoveolate. Paraorbital sulci moderately deep, ending at level of posterior supraorbital pore or lightly before.

Thorax. Pronotum slightly wider than long (mean PW/PL = 1.15), widest at second quarter. Anterior and posterior transverse impressions indistinct. Sides rather convex anteriorly, fairly concave posteriorly; mean PW/PA = 1.46, mean PW/PB = 1.25; bead of anterior margin present laterally, reduced in medial 1/8 to 1/10; bead of posterior margin reduced to absent in medial 1/8. Metepisternum slightly longer than wide, MA/MI about 0.9. **Elytra.** Long, cylindrical, about one and two thirds as long as wide (mean EL/EW = 1.67), one time and a third as wide as pronotum (mean EW/PW = 1.33; mean EL/PL = 2.55). Stria 7 reaching basal margin. Three elytral discal setiferous punctures in interval 3 (one specimen with four punctures on one elytron, as an additional puncture exists at fourth sixth, between second and third normal punctures), anterior puncture usually adjoining stria 3 (in two specimens adjoining stria 2 on one elytron), remaining two punctures adjoining stria 2 (in specimens from Rudbarak env., right elytron with medial pore adjoining stria 3). Umbilicate setiferous series of 16–17 punctures on each elytron (one specimen with 18 punctures on one elytron). **Legs.** Posterior side of profemur with one seta in basal third and one seta in medial third. Anterior side of mesofemur ventrally with four setiferous punctures. Anterior side of metafemur ventrally with two long setae, one in basal third and one in medial third. **Male genitalia.** Urite IX elongate, suboval, with proximal margin rather pointed (Fig. 7F). Median lobe of aedeagus in lateral view with shaft longer than in *P. taghizadehi*, and significantly more curved than in *P. lassallei*, and with apex turned up; median lobe in ventral view straight, ca. 3.85 times longer than wide, with apical lamella nearly symmetrical. Internal sac in lateral view (Fig. 8H) with ventral sclerite elongate, widened medially and distally; same in ventral view (Fig. 10H) with dorsal sclerite forming two left-sided protuberances and a large right-sided curve, and ventral sclerite narrow, straight, with distal end curved to left. Right paramere thin, concave ventrally (Fig. 12G). **Female genitalia** (Fig. 14B). Apical gonocoxite with blunt apex and two dorsolateral ensiform setae. Spermathecal canal connected in medial third of receptaculum.

Habitat. All specimens above examined were collected in open places at high altitudes between 2300 m and

2700 m a.s.l. The specimens collected by JM in June 2017 have been caught under stones in a high-mountain meadow covered with lots of flowers, without bushes or trees. The place was definitely not dry during the time of visiting and perhaps covered with snow a few weeks before.

The type series of *P. (Eremoderus) ledouxi* and *P. (Platyderus) chodjii* Morvan, 1974 were collected together (cfr. Morvan 1974), demonstrating that the two species occur sympatrically.

Distribution. North Iran: the Central Alborz Range, in area of the upper valley of Sardabrud River, northeast of the Takht-e Suleyman Subrange (Fig. 17).

Notes. Although not able to study the holotype, based on the original description of *P. ledouxi* and the illustrations of the median lobe of aedeagus and internal sac (Morvan 1974: 148–149, figs 17–24), we have no doubt that the material examined belongs to this species.

See also “Notes” under *P. davatchii* Morvan.

11. *Platyderus (Eremoderus) taghizadehi* Morvan, 1974

Figs 2E, 5F, 7G, 8I, 10I, 12H, 14C, 17, Table 2

Platyderus taghizadehi Morvan, 1974: 147 (type locality: “l’Elburz, massif du Sutak-kuh, Dizine 3500 m”).

Notes on type locality. The Mount Sutak Kuh is situated in the province of Mazandaran (southwestern part of Nur County), and lies in the Central Alborz Range, at ca. 3500 m altitude. Its approximate GPS coordinates are 36.153, 51.456, referring to a point situated ca. 300 m higher than the height Morvan mentioned (ibid.). The type locality locates somewhere between the Sutak Kuh Peak, in the north, and the Dīzīn Ski Resort, in the south. Roughly, it may be defined as a site in the plot Kando-vān Tunnel – Āzād Kuh Peak – Kholeno Lake – Dīzīn Ski Resort. Spatially, it is a point geographically situated midway between the type localities of *P. ledouxi* (vicinities of Rudbarak) and *P. klapperichi* sp. nov. (vicinities of Damavand City).

References. *Platyderus taghizadehi*: Lorenz 1998: 375; Hovorka and Sciaky 2003: 523; Lorenz 2005: 396; Azadbakhsh and Nozari 2015: 84; Hovorka 2017: 759.

Type material. *Holotype* ♂ in private collection Pierre Morvan (Carentoir, France). Not examined.

Other material examined. Iran: Tehran Province: 1♀, ‘IR Alburz Dizin / 36°2'00.6"N, 51°26'00.5"E / 3300–3600m 10.06.17 / Muilwijk J // *Platyderus taghizadehi* / Morvan / Muilwijk 2017’ (cMUI); 1♂, ‘IR Tehran Tochal / 35°53'26.2"N, 51°24'25.1"E / 3550m 27.06.17 / Seiedy/Muilwijk // *Platyderus taghizadehi* / Morvan / Muilwijk 2017’ (cMUI).

TME: 2 specimens. TGE: 1♂, 1♀.

Diagnosis. A species of medium size for *Platyderus*, with anterior side of mesofemur ventrally with three setiferous punctures. It is distinct from the closely related *P. ledouxi* by pronotum about a third wider than head (PW/HW= 1.31–1.33), with apex compared with widest point

less constricted (PW/PA <1.40), and elytra in relation to pronotum significantly wider (EW/PW >1.38). See also “Diagnosis” under *P. ledouxi*.

Redescription (based on non-type material). **Habitus.** Moderately large-sized specimens for *Platyderus* species (BL: 7.10–7.20 mm; BW: 2.40 mm), with elongate and slender body (Fig. 2E). **Measurements and ratios.** See Table 2. **Color and lustre.** Integument of body orange-brown, appendages slightly lighter than body. Surface moderately shiny. **Microsculpture and punctuation.** Pronotum largely with reduced sculpticells or without microsculpture, traces of isodiametric sculpticells present only laterally. Ventral surface (excluding gula and prosternal process) microsculptured, genae, mentum, submentum, proepisternum and ventrites 2–3 medially with regular isodiametric meshes, abdominal ventrites laterally and legs with slightly stretched isodiametric sculpticells. Prosternum scarcely punctate. **Head.** Two thirds as wide as pronotum (mean PW/HW= 1.32). **Head.** Significantly narrower than pronotum (mean PW/HW= 1.48). Antennae long, with last three antennomeres exceeding base of pronotum. Eyes long, little convex. Labrum subrectangular, with anterior margin concave. Frontal furrows small, subfoveolate. Paraorbital sulci moderately deep, ending slightly before level of posterior supraorbital pore. **Thorax.** Pronotum sub-quadrate, barely wider than long (mean PW/PL= 1.09), widest at second quarter. Anterior and posterior transverse impressions indistinct. Sides rather sinuate, convex anteriorly, concave posteriorly; mean PW/PA= 1.35, mean PW/PB= 1.18; bead of anterior margin present laterally, reduced in medial 1/6; bead of posterior margin reduced to absent in medial 1/5 to 1/3. Metepisternum longer than wide, MA/MI about 0.9. **Elytra.** Long, cylindrical, one and two thirds as long as wide (mean EL/EW= 1.67), wider and much longer than pronotum (mean EW/PW= 1.42; mean EL/PL= 2.57). Stria 7 not reach basal margin. Elytral interval 3 with three discal setiferous punctures (specimen from Dizin with four punctures on left elytron, as an additional one between second and third normal puncture) located as follows: anterior puncture adjoining stria 2, stria 3 or in middle of interval 3, medial puncture adjoining stria 2 or in midst of interval 3, posterior puncture adjoining stria 2. Umbilicate setiferous series consisting of 16 punctures on each elytron in specimen from Tochal, and with 15 punctures on each elytron in specimen from Dizin. **Legs.** Posterior side of profemur with one seta in basal third and one in medial third. Mesofemur with three setiferous punctures on anterior side ventrally (Fig. 5F), but one specimen has two punctures on one mesofemur. Anterior side of metafemur ventrally with two long setae, one in basal third and one in medial third. **Male genitalia.** Urite IX small, suboval, with proximal margin slightly asymmetrical (Fig. 7G). Median lobe of aedeagus in lateral view with shaft shorter than that in *P. ledouxi* and more curved than that in *P. lassallei* sp. nov., and with apex turned up; median lobe in ventral view straight, ca. 3.7 times longer than wide, with apical lamella slightly asymmetrical. Internal sac

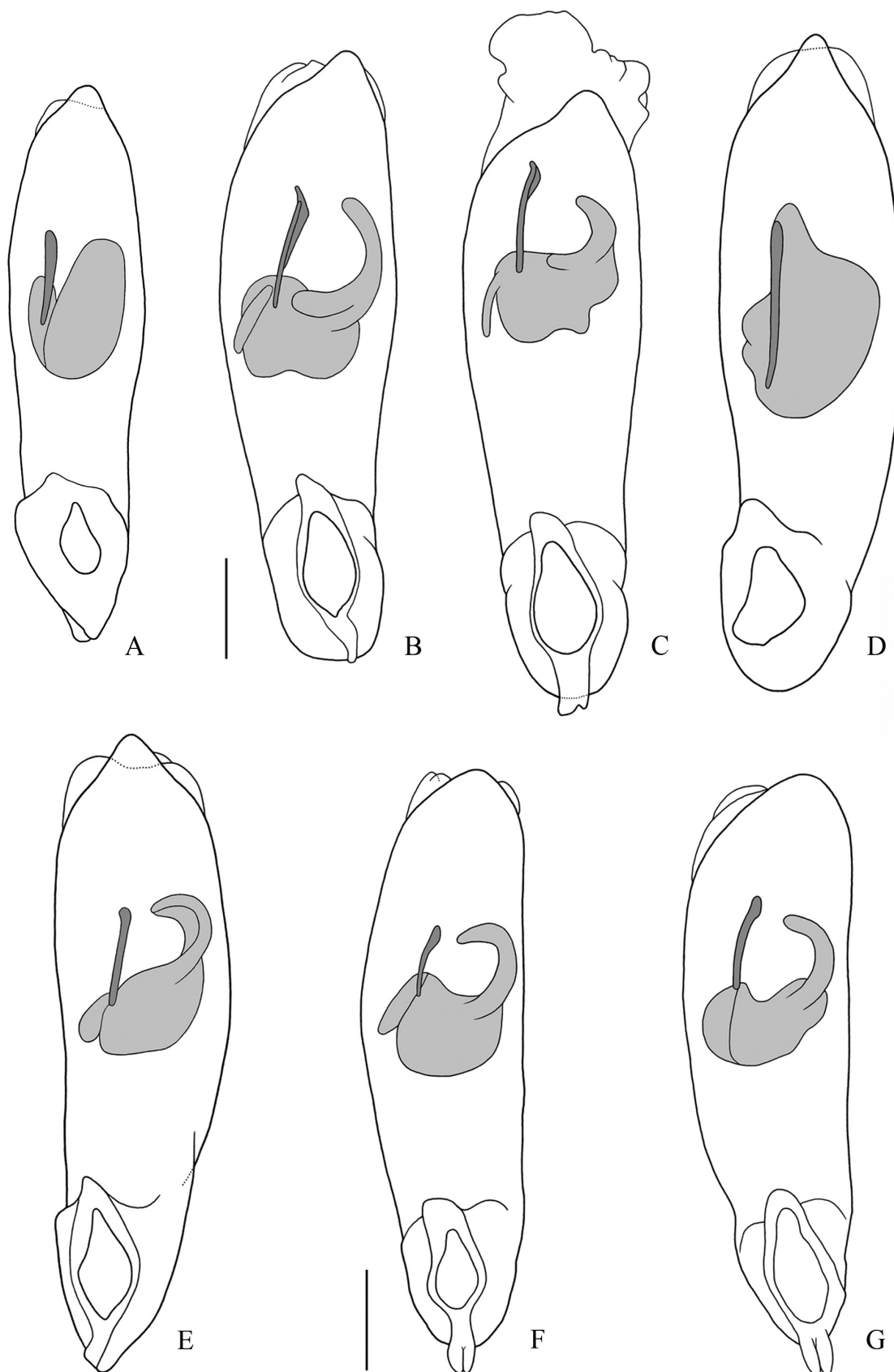


Figure 11. Median lobe of aedeagus, ventral view. **A.** *Platyderus (Eremoderus) afghanisticus*, sp. nov., holotype; **B.** *P. (E.) brunneus brunneus* Karsch, 1881, male specimen, 50 km W of Ben Gardane, Medenine Governorate, Tunisia; **C.** *P. (E.) brunneus ferrantei* Reitter, 1909, male specimen, Holot Haluza, Southern District, Israel; **D.** *P. (E.) insignitus insignitus* Bedel, 1902, male specimen, SW Tiznit, Sous-Massa Region, Morocco; **E.** *P. (E.) jordanensis*, sp. nov., holotype; **F.** *P. (E.) languidus* (Reiche & Saulcy, 1855), lectotype; **G.** *P. (E.) languidus* (Reiche & Saulcy, 1855), male specimen, Nahal Prat, Judea and Samaria Area, Israel. Scale bars: 0.2 mm.

of same structure as in *P. ledouxi*, but dorsal sclerite in ventral view with left-sided protuberances somewhat larger. Right paramere shorter and more crooked than that of *P. ledouxi* (Fig. 12H). **Female genitalia** (Fig. 14C). Apical gonocoxite with pointed apex and two dorsolateral ensiform setae. Bursa copulatrix smaller than that of *P. ledouxi*. Spermathecal canal connected in medial third of receptaculum.

Habitat. All specimens hitherto known were found in open places at high altitudes between 3300 m and 3600 m. The two specimens collected by JM in June 2017 were caught from under stones in rather steep green mountain meadows (without bushes or trees). At the time of its collection the place was not dry, probably due to the thaw just a few weeks before and to some water streamed down.

Distribution. North Iran, Central Alborz Range (Fig. 17). The species occurs in the area where three Iranian provinces, Mazandaran, Alborz and Tehran, are touching each other.

Notes. Three metric measurements made by Morvan (1974: 147), i.e. width (1.15 mm), length (1.13 mm) of pronotum and length of elytra (2.1 mm), are certainly wrong. If these are correct, then we should have a total length of the pronotum and elytra 3.23 mm, but then the length of head should be at least 4 mm as far as the holotype of *P. taghizadehi* has length of body 7.5 mm (ibid.: 147).

Being a male specimen, the holotype of *P. taghizadehi* (or topotypic males) must be studied for two reasons. Firstly, this investigation can support the current taxonomic affinity with *P. ledouxi* because the distance in a straight line between the population of *P. ledouxi* southwest of Rudarbak and the type locality of *P. taghizadehi* is only about 50 kilometers and it is unclear whether the Chalus River acts as a biogeographical barrier. Furthermore, it is necessary to confirm the conspecificity of the populations from Sutak Kuh Peak and Tochal Peak (here last referred to as *P. taghizadehi*), so that the two local forms of *P. taghizadehi* can be distinguished from *P. klapperichi* sp. nov. (from Damavand County).

“afghanisticus” species group

12. *Platyderus (Eremoderus) afghanisticus*, sp. nov.

<http://zoobank.org/6600933A-0719-49DA-B7EE-B268433A3815>

Figs 3A, 5G, 7H, 9B, 11A, 12I, 17, Table 2

Type locality. “Afghanistan, Habatah, 1.300 m”.

Notes on type locality. The precise location remains unestablished as far as several possibilities for the name “Habatah” exist: Haybatay Ghar; Haibatai Ghundey [= Haibatai Ghundey]; and Haybati. Given the altitude of 1300 m a.s.l. pointed on the label, a quite possible location may be the upper course of Gomal River, Afghan Province of Paktika (see Fig. 17).

Type material. *Holotype* ♂, ‘Afghanistan’ [w, p] // Habatah / 1.300m 17.6.1964 / leg. Kullman [w, h] // genus

/ ? / det. Ing. Jedlička [w, h&p] // Collectio / Moravské museum, / Brno [w, p]’ (MMBC).

TME: 1 specimen. TGE: 1♂.

Diagnosis. This species is distinguished from all other members of the subgenus by: (1) yellow-brown color of body; (2) ventral surface largely impunctate; (3) pronotum with posterior angles not projecting laterally and basal bead complete; (4) metepisternum as long as wide; and (5) ventral sclerite of median lobe in lateral view not appreciably broadened distally (Fig. 9B).

Description. Habitus. Specimens of small size for *Platyderus* (BL: 6.80 mm; BW: 2.25 mm), with oblong, moderately convex body (Fig. 3A). Measurements and ratios. See Table 2. **Color and lustre.** Body dorsally and ventrally, including appendages yellow-brown. Head, pronotum and ventral surface moderately shiny, elytra less shiny than dorsal surface of head and pronotum.

Microsculpture and punctation. Pronotum with isodiametric sculpticells on posterolateral parts and slightly transverse ones on anterior third, with disc having scarcely visible microsculpture. Ventral surface with scarcely-visible regular isodiametric (proepisternum, ventrites laterally) or slightly transverse sculpticells (metacoxae, ventrites medially), or microsculpture not apparent (remaining part). Pronotum almost impunctate, with a few large punctures near posterior angles and several longitudinal wrinkles on anterior transverse impression. Ventral surface, including mesepisternum, metepisternum and abdominal ventrites impunctate; prosternum medially, proepisternum and metasternum laterally with shallow punctures; abdominal ventrites 1–2 wrinkled submedially.

Head. More than one-third narrower than pronotum wide (PW/HW= 1.40). Antennae long, with last three antennomeres exceeding base of pronotum. Eyes slightly convex. Labrum subrectangular, with anterior margin straight. Frontal furrows short, shallow. Paraorbital sulci shallow, narrow, ending before level of posterior supraorbital pore. **Thorax.** Pronotum about a quarter wider than long (PW/PL= 1.24), widest at second quarter. Anterior transverse impressions distinct, posterior one well-impressed laterally reaching basal foveae. Sides not sinuate, convex anteriorly, nearly straight posteriorly; anterior bead present laterally, absent in medial 1/10; lateral and basal beads present throughout. Metepisternum nearly as long as wide, MA/MI= 0.95–0.97. **Elytra.** Elongate, about one and two thirds as long as elytra width (EL/EW= 1.63), two and three quarters as long as pronotum (EL/PL= 2.78), and one third as wide as pronotum (EW/PW= 1.36), with widest point at medial third. Striae moderately punctate and impressed; parascutellar striole nearly connected with stria 1; base of stria 1 very short, joining stria 2 and reaching parascutellar pore; striole and basal portion of stria 1 slightly impressed, remaining part of stria 1 and other striae well-impressed. Interval 3 with three discal setiferous punctures each side. Umbilicate setiferous punctures 16 each side. **Legs.** Posterior side of profemur with one seta in basal third and one in medial third. Anterior side of right mesofemur ventrally with five

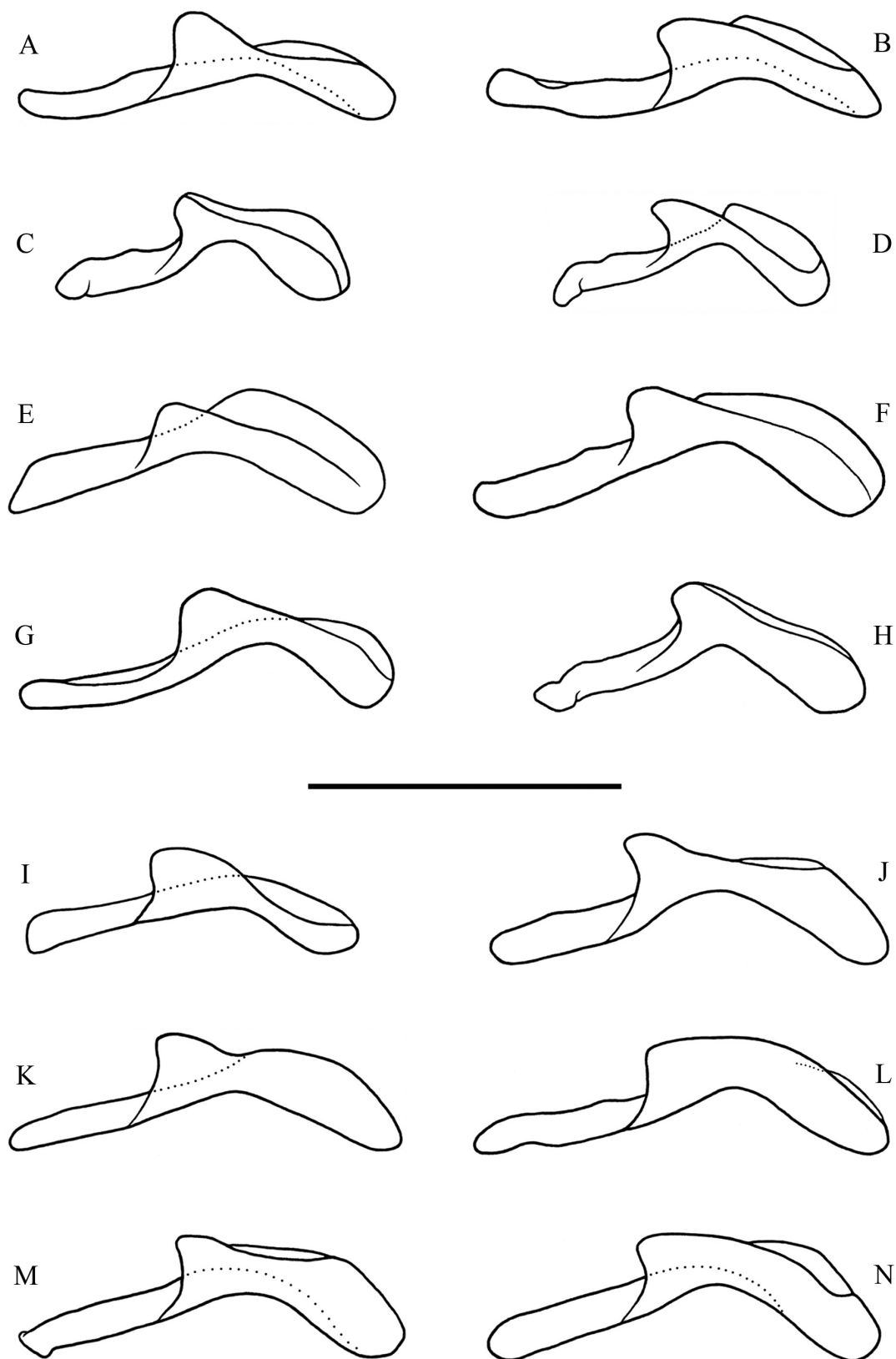


Figure 12. Right paramere, external face. **A.** *Platyderus (Eremoderus) chatzakiae*, sp. nov., holotype; **B.** *P. (E.) weiratheri* Mařan, 1940, lectotype; **C.** *P. (E.) felixi*, sp. nov., holotype; **D.** *P. (E.) iranicus*, sp. nov., holotype; **E.** *P. (E.) vrabeci*, sp. nov., holotype; **F.** *P. (E.) lassallei*, sp. nov., holotype; **G.** *P. (E.) ledouxi* Morvan, 1974, male specimen, 10 km S Hasan Keif, Mazandaran Province, Iran; **H.** *P. (E.) taghizadehi* Morvan, 1974, male specimen, Tochal, Tehran Province, Iran; **I.** *P. (E.) afghanisticus*, sp. nov., holotype; **J.** *P. (E.) brunneus brunneus* Karsch, 1881, male specimen, 50 km W of Ben Gardane, Medenine Governorate, Tunisia; **K.** *P. (E.) brunneus ferrantei* Reitter, 1909, male specimen, Holot Haluza, Southern District, Israel; **L.** *P. (E.) jordanensis*, sp. nov., holotype; **M.** *P. (E.) languidus* (Reiche & Saulcy, 1855), lectotype; **N.** *P. (E.) languidus* (Reiche & Saulcy, 1855), male paralectotype, “Syria”. Scale bars: 0.5 mm.

(Fig. 5G), left one with four setiferous punctures. Anterior side of metafemur ventrally with two long setae, one in basal third and one in medial third. **Male genitalia.** Urite IX small, oval, with proximal margin nearly symmetrical (Fig. 7H). Median lobe of aedeagus in lateral view slender, with narrow basal bulb, broad shaft with proximal part slightly constricted, and short, straight apex (Fig. 9B); median lobe in ventral view straight, about 4 times as long as wide; apical lamella (dorsal view) short, symmetrical, rounded at tip, with sides straight to very slightly convex. Internal sac in lateral view (Fig. 9B) with ventral sclerite broad and nearly equally wide in its length; same in ventral view (Fig. 11A), with dorsal sclerite seemingly separated from ventral sclerite, and ventral sclerite narrow, widened distally. Right paramere fine, moderately concave ventrally (Fig. 12I). **Female genitalia.** Unknown.

Distribution. Afghanistan (? “Habatah”); Fig. 17.

“*languidus*” species group

Diagnosis. Species are distinct from those of the other *Eremoderus* species groups by: (1) dorsal surface of body with complete or nearly complete microreticulation of isodiametric sculpticells, with transverse sculpticells lacking or highly restricted; (2) basal foveae of pronotum shallowly impressed, foveae and adjacent lateral areas impunctate or scarcely punctate; (3) basal bead of pronotum reduced to absent in basal 1/3 to 1/2; (4) elytral striae scarcely impressed, impunctate or slightly punctate, and elytral intervals rather flat; (5) mesocoxa with two to four long lateral setae, rarely one seta (polysetose state of character shared only by taxa of “*weiratheri*” group).

In addition, the species have anterior side of the mesofemur ventrally with five to seven (rarely four) setiferous punctures. In addition, all taxa save *P. brunki* sp. nov. share apical gonocoxite with one dorsomedial ensiform seta.

Notes. This group includes seven species, *P. languidus* (Reiche & Saulcy, 1855), *P. brunneus* Karsch, 1881, *P. insignitus* Bedel, 1902, *P. arabicus* sp. nov., *P. brunki* sp. nov., *P. irakensis* sp. nov. and *P. jordanensis* sp. nov. (Figs 18, 19). Most probably, the Macaronesian species *P. alticola* Wollaston, 1864 and *P. lancerottensis* Israelson, 1990 also belong to this group (see Israelson 1990: 166, fig. 4).

13. *Platyderus (Eremoderus) arabicus*, sp. nov.

<http://zoobank.org/20D0899F-1E9F-41EB-8247-EBA911C8DEFE>
Figs 3B, 14E, 19, Table 3

Type locality. Saudi Arabia, “Hedjaz”.

Notes on type locality. Nothing is known about the exact places and circumstances of its collecting. The Hedjaz Range is a mountain range located in the Hejazi region, the western part of the country. It is very likely, as in the case of two Saudi Arabian species of *Acinopus*, *A. brittoni* Wrase & Kataev, 2016 and *A. arabicus* Wrase & Kataev, 2016 (Wrase and Kataev 2016), that *P. arabicus*

lives in higher altitudes where habitats with enough moisture are present.

Type material. **Holotype** ♀, ‘Hedjaz [w, h] // Ex-Musaeo / H.W. Bates / 1892 [w, p]’ (MNHN). Paratype: 1♀, ‘El Hahaz / Millinger [sic] [w, p] // El Hedjaz. / Millingen. / 1915–38.’ [w, p] // *Platyderus / languidus / Reiche / E.B. Britton det. / 1946 [w, h&p]’* (NHMUK).

Other material examined. Imprecise locality: 1♀, ‘Bagdad [w, h] // Ex-Musaeo / H.W. Bates / 1892’ [w, p] (MNHN).

TME: 3 specimens. TGE: 1♀.

Etymology. The specific epithet is a Latinized adjective, based on the name of the region in which this species can be found.

Diagnosis. Among members of “*languidus*” group, *P. arabicus* sp. nov. and *P. jordanensis* sp. nov. are taxa with pronotum most constricted toward apex (PW/PA: 1.44–1.48 and 1.39–1.52, respectively; Table 3). However, pronotal forms differ. Whereas the former has a subelliptic pronotum with sides to base straight or slightly convex and less constricted, the latter has a subquadrate pronotum with sides to base slightly concave and more constricted (PW/PB: 1.09–1.15 and 1.15–1.22, respectively). In addition, *P. arabicus* has a darker, brown or chestnut color of integument and 5–6 setiferous punctures of anterior side of mesofemur ventrally, whereas *P. jordanensis* sp. nov. has a lighter, reddish-brown to rufous color and 4 setiferous punctures of anterior side of mesofemur ventrally.

It is also closely related to *P. brunki* sp. nov. but two species differ by a set of morphometric ratios (see “Diagnosis”, under *P. brunki* sp. nov.).

Description. **Habitus.** Specimens of large size for *Platyderus* species (BL: 8.20–9.40 mm; BW: 2.85–3.25 mm), with elongate, moderately to rather convex body (Fig. 3B). **Measurements and ratios.** See Table 3. **Color and lustre.** Body and appendages uniformly dark reddish-brown, only terminal palpomeres slightly lighter. Integument slightly to moderately shiny, head and pronotum shinier than elytra. **Microsculpture and punctuation.** Pronotum with evident microreticulation throughout, sculpticells regular isodiametric to slightly stretched. Elytra (intervals, scutellum, basal margin and lateral gutter) with distinct isodiametric sculpticells. Ventral surface with well-impressed isodiametric or slight transverse sculpticells, only epipleura, mesosternum and middle coxa with sculpticells scarcely-visible. Head impunctate, smooth or nearly smooth, with a few, very shallow wrinkles on clypeus posterior half and frontal furrows laterally. Pronotum surface mostly smooth, only basal area between foveae longitudinally wrinkled and along lateral margin with few punctures that do not reach anterior half (paratype also with several wrinkles in front of anterior transverse impression). Elytral intervals impunctate or with scattered and very shallow punctures. Abdominal ventrite 1 wrinkled medially, 2–6 smooth, neither wrinkled nor punctate. **Head.** More than one-third narrower than pronotum wide (PW/HW= 1.41–1.43). Eyes

Table 3. Morphometric data for species of the ‘*languidus*’ group of *Platyderus*.

Species (number of samples)	BL/mm	BW/mm	PW/HW	PW/PL	PW/PA	PW/PB	PA/PB	EL/EW	EW/PW	EL/PL
<i>P. arabicus</i> sp. nov. (3♀♀)	8.20–9.40	2.85–3.25	1.41–1.43	1.07–1.11	1.44–1.48	1.09–1.15	0.76–0.79	1.54–1.62	1.44–1.49	2.47–2.56
<i>P. arabicus</i> sp. nov. (mean)	8.73	3.05	1.42	1.09	1.46	1.13	0.78	1.59	1.46	2.51
<i>P. brunki</i> sp. nov. (2 exx.)	–	3.30–3.45	–	1.02–1.05	1.38–1.42	1.14–1.22	0.80–0.88	1.58–1.59	1.48	2.40–2.44
<i>P. brunki</i> sp. nov. (mean)	–	3.38	–	1.04	1.40	1.18	0.84	1.59	1.48	2.42
<i>P. brunneus brunneus</i> Karsch (5♂♂, 4♀♀)	7.70–9.30	2.70–3.40	1.28–1.41	1.10–1.20	1.36–1.43	1.21–1.28	0.88–0.92	1.53–1.72	1.36–1.48	2.53–2.72
<i>P. brunneus brunneus</i> Karsch (mean)	8.60	2.99	1.35	1.16	1.39	1.25	0.90	1.61	1.41	2.63
<i>P. brunneus ferrantei</i> Reitter (1♂, 6♀♀)	7.60–9.00	2.70–3.20	1.29–1.39	1.14–1.21	1.34–1.42	1.12–1.23	0.82–0.89	1.52–1.60	1.35–1.46	2.46–2.58
<i>P. brunneus ferrantei</i> Reitter (mean)	8.53	3.01	1.32	1.16	1.38	1.17	0.85	1.56	1.41	2.53
<i>P. insignitus insignitus</i> Bedel (1♂, 4♀♀)	6.60–8.70	2.20–3.00	1.35–1.45	1.06–1.17	1.35–1.40	1.12–1.17	0.80–0.85	1.57–1.65	1.40–1.51	2.41–2.61
<i>P. insignitus insignitus</i> Bedel (mean)	7.72	2.67	1.38	1.10	1.39	1.15	0.83	1.61	1.45	2.55
<i>P. irakensis</i> sp. nov. (2♀♀)	8.30–9.00	2.90–3.20	1.30–1.32	1.13	1.34–1.38	1.09–1.11	0.79–0.83	1.62–1.63	1.45–1.47	2.65–2.72
<i>P. irakensis</i> sp. nov. (mean)	8.65	3.05	1.31	1.13	1.36	1.10	0.81	1.63	1.46	2.69
<i>P. languidus</i> (Reiche & Saulcy) (10♂♂, 10♀♀)	6.40–9.10	2.20–3.15	1.27–1.38	1.11–1.22	1.31–1.41	1.10–1.20	0.81–0.90	1.52–1.62	1.29–1.48	2.42–2.60
<i>P. languidus</i> (Reiche & Saulcy) (mean)	7.82	2.74	1.33	1.16	1.35	1.16	0.85	1.56	1.37	2.49
<i>P. jordanensis</i> sp. nov. (4♂♂, 1♀)	8.70–9.90	3.00–3.45	1.35–1.42	1.08–1.13	1.39–1.52	1.15–1.22	0.78–0.87	1.56–1.60	1.39–1.46	2.41–2.60
<i>P. jordanensis</i> sp. nov. (mean)	9.28	3.25	1.39	1.10	1.44	1.18	0.82	1.59	1.43	2.50

For abbreviations in line 1, see “Abbreviations to measurements and ratios” (section “Material and methods”).

moderately convex. Labrum subrectangular, slightly shorter than clypeus, with anterior margin concave. Frontoclypeal suture slightly distinct in middle, indistinct at sides. Frontal furrows very shallow, subfoveolate. Paraorbital sulci straight, backward barely reaching posterior margin of eye, not reaching level of posterior supraorbital pore. **Thorax.** Pronotum about one time and one tenth as wide as long (PW/PL = 1.07–1.11), with widest point at medial third. Anterior transverse impression indistinct to slightly distinct, posterior transverse impression barely distinct. Sides not sinuate, smoothly convex medially and anteriorly, nearly straight posteriorly; anterior bead present laterally, lack in medial 1/8–1/10; basal bead present laterally, reduced to varying degrees or non-existent in medial half. Metepisternum as long as wide, MA/MI = 1.00. **Elytra.** Elongate, about one and-a-half times as long as elytra wide (EL/EW = 1.54–1.62), two and a half times as long as pronotum (EL/PL = 2.47–2.56), and one and a half as wide as pronotum (EW/PW = 1.44–1.49), with widest point at beginning of third quarter. Parascutellar striole punctiform to sublinear, very shallow; striae 1–6 more impressed than striole and striae 7 and 8, moderately to indistinctly punctate; parascutellar striole short, not joining stria 1; base of stria 1 ending in parascutellar pore, striae 2–5 reaching basal bead, 6 and 7 ending little before. Interval 3 with three discal setiferous punctures on right elytron (medial one of left elytron lacking in two specimens). Umbilicate setiferous series with 15 punctures on left elytron and 16 on right elytron in holotype, with 16 punctures on each side in paratype. **Legs.** Posterior side of profemur with one seta in basal third and one in medial third. Mesofemur with 4 setiferous punctures on anterior side ventrally. Anterior side of metafemur ventrally with two to three long setae, one in basal third and one to two in apical half. **Male genitalia.** Unknown. **Female genitalia** (Fig. 14E). Apical gonocoxite with pointed apex and one dorsolateral ensiform seta. Spermathecal canal connected in basal third of receptaculum.

Comparisons. From *P. irakensis* sp. nov., that inhabits areas northeast of the Al-Hedjaz region, *P. arabicus* differs

in: (1) dark brown color of body (vs. orange-brown color of body); (2) head narrower, compared to pronotum (PW/HW: 1.41–1.43, vs. PW/HW: 1.30–1.32); (3) pronotum with anterior angles more pointed and sides to apex more constricted (PW/PA: 1.44–1.48), vs. pronotum with anterior angles less pointed and sides to apex less constricted (PW/PA: 1.34–1.38); (4) elytra less long, compared to pronotum (EL/PL: 2.47–2.56, vs. EL/PL: 2.65–2.72); (5) meso- and metatarsomeres dorsally neither flattened nor grooved (vs. meso- and metatarsomeres dorsally partly flattened and slightly grooved).

Habitat. Like other representatives of the “*languidus*” group with known habitat preferences (*P. languidus*, *P. brunneus*, *P. brunki* sp. nov.), *P. arabicus* sp. nov. could inhabit the wetter parts of desert and semi-desert habitats.

Distribution. The new species is known from the region of Hedjaz in Saudi Arabia, which includes the western part of the country (Fig. 19). Likely to be endemic to the Hedjaz Mountains. As far as the specimen with the locality “Bagdat” is concerned, we believe that this inscription is either due to a mislabeling or a genuine observation. If it is the latter case, then the species probably occurs in the Iraqi areas on the border with Saudi Arabia, southwest of the city of Baghdad.

Notes. The specimen from “Bagdat” differs from the two type specimens in the larger, more quadratic and slightly wider pronotum (vs. smaller and somewhat narrow pronotum) and having less prominent anterior angles (vs. somewhat more prominent anterior angles). That is why, we have some doubt if this specimen really belongs to *P. arabicus*.

14. *Platyderus (Eremoderus) brunki* sp. nov.

<http://zoobank.org/C5B5E518-02FF-4E24-A1C1-70F560699170>
Figs 3C, 14F, 19, Table 3

Type locality. Yemen, ‘Amran Governorate, Thula District, between Kaukaban and Shibam, approximate GPS coordinates: 15.503, 43.901.

Type material. *Holotype* ♀, ‘YEMEN, ~ 40 km NW Sanaa, / Kaukaban/Shibam, small waste- / waterstream, ruralic vegetation, / sand, 2700–2930 m Handaufsam. / 15°30'9.98"N, 43°54'2.66"E / 02. Dez. 2009, legit. Ingo Brunk [p, w] // Coll. / I. Brunk / Dresden/Germ [h, pn]' (cBRU).

Other material examined. Remains of a specimen of uncertain sex in bad condition (only pronotum and elytra preserved), ‘UNDER A STONE // YEMEN / El Errein, nr. Haz, / about 16 miles N.W. / of San'a, ca. 9,300ft. [= 2835 m] / 3.ii.1938.// B.M. Exp. to / S.W. Arabia. / H. Scott & / E.B. Britton. / B.M. 1938–246, // *Platyderus / languidus* / Reiche / E.B. Britton det. / 1946' (NHMUK). TME: 2 specimens. TGE: 1♀.

Etymology. Latinized patronym based on the surname of Ingo Brunk (Dresden, Germany), who collected the first well-preserved representative of the new species.

Diagnosis. *Platyderus brunki* sp. nov. readily differs from all other *Eremoderus*-taxa in its smallest value in ratio PW/PL (Table 3). It is most closely related to *P. arabicus*; both species are the only two within “*languidus*” group with darkest coloration of integument and sides of pronotum not sinuate from widest point to base (*P. irakensis* has also sides of pronotum not sinuate to base, but much lighter coloration of integument and higher value in ratio EL/PL). The new species is distinct from *P. arabicus* sp. nov., in: (1) pronotum with anterior angles more rounded at tips (vs. pronotum with anterior angles more pointed at tips, Fig. 3B, C); (2) pronotum nearly as long as wide, PW/PL: 1.02–1.05 (vs. pronotum appreciably wider than long, PW/PL: 1.07–1.11); (3) pronotum subcordate, less constricted anteriorly, PW/PA: 1.38–1.42, with greater value in ratio PA/PB: 0.80–0.88 (vs. pronotum subquadrate, more constricted anteriorly, PW/PA: 1.44–1.48, with smaller value in ratio PA/PB: 0.76–0.79); (4) elytra compared to pronotum slightly shorter, EL/PL: 2.40–2.44 (vs. elytra compared to pronotum slightly longer, EL/PL: 2.47–2.56). Females are different from all other representatives of the “*languidus*” group by the presence of two, instead of one, dorsolateral ensiform setae on the apical gonocoxite (Fig. 14F).

Description. *Habitus.* Specimens of large size for *Platyderus* species (BL of holotype: 9.50 mm; BW: 3.30 mm), with elongate, moderately convex body (Fig. 3C). **Measurements and ratios.** See Table 3. **Color and lustre.** Body and appendages uniformly reddish-brown, with palpi and antennae slightly lighter. Integument slightly to moderately shiny, head and pronotum shinier than elytra. **Microsculpture and punctuation.** Microreticulation of pronotum and elytra as in *P. arabicus* sp. nov. Ventral surface largely with well-impressed isodiametric or slight transverse sculpticells, epipleura, mesosternum and middle coxa with sculpticells less apparent. Head (holotype) nearly smooth, impunctate, wrinkles present only on clypeus and frons, including frontal foveae and area surrounding them. Pronotum surface largely smooth, only apical part medially in front of anterior transverse impression and basal area medially behind posterior transverse impression

longitudinally wrinkled, as well as each side along lateral margin with a few shallow punctures not reaching anterior half. Elytral intervals without apparent punctuation. Abdominal ventrites nearly smooth, impunctate, 3–5 with a few fine wrinkles at sides. **Head** (holotype). About two-thirds as wide as pronotum (PW/HW of holotype: 1.36). Eyes long, slightly convex. Labrum subrectangular, as long as clypeus, with anterior margin concave. Frontoclypeal suture distinct in middle, indistinct at sides. Frontal furrows shallow, subfoveolate. Paraorbital sulci straight, backward barely reaching posterior margin of eye, not reaching level of posterior supraorbital pore. **Thorax.** Pronotum almost as wide as long (PW/PL= 1.02–1.05), with widest point at second quarter (holotype) or medial fifth (specimen from “El Errein, nr. Haz”). Anterior and posterior transverse impressions slightly distinct medially, indistinct laterally. Sides not sinuate, smoothly convex anteriorly and medially, straight (specimen from “El Errein, nr. Haz”) or convex posteriorly (holotype); anterior bead present laterally, lacking in medial 1/8 to 1/10; basal bead present laterally, reduced to absent in medial half; posterior angles rounded (holotype) or obtuse (specimen from “El Errein, nr. Haz”). Metepisternum as long as wide, MA/MI= 1.00. **Elytra.** Elongate, about one and a half times as long as elytra (EL/EW= 1.58–1.59), two and a half times as long as pronotum (EL/PL= 2.40–2.44), and a one and half as wide as pronotum (EW/PW= 1.48), with widest point at medial third. Parascutellar striole scarcely distinct, very shallow; striae more impressed than striole, barely punctate; parascutellar striole not joining stria 1; striae 1–5 and sometimes 6 reaching basal bead, 7 ending little before. Interval 3 with three discal setiferous punctures, medial one larger than others, in midst of interval 3 (holotype) or near stria 2 (specimen from “El Errein, nr. Haz”), anterior and posterior punctures smaller, adjoining stria 3 (posterior puncture lacking on right elytron of holotype). Umbilicate setiferous series with 16 or 17 punctures of each elytron. **Legs.** Posterior side of profemur with one seta in basal third and one in medial third. Left mesofemur with 5, right one with 4 setiferous punctures on anterior side ventrally. Anterior side of metafemur ventrally with two long setae, one in basal third and one in medial third. **Male genitalia.** Unknown. **Female genitalia** (Fig. 14F). Apical gonocoxite with pointed apex and two dorsolateral ensiform setae. Spermathecal canal connected in medial third of receptaculum.

Habitat. The holotype was collected by sifting the waste-water vegetation and soil at a humid place where waste water falls down (Ingo Brunk, pers. comm.). The correct altitude of the type locality is ca. 2700 m a. s. l. The locality is situated approximately half-way on a very steep walking path starting from Kawkaban (town on the top of the Mount Kawkaban) downwards to Schibam Kawkaban (town on the bottom of the mountain). Together with the holotype, numerous specimens of *Trechus (Arabotrechus) rougemontiellus* Belousov, 2017 and few *Bembidion* spp. were collected.

Distribution. Yemen (Sana'a Governorate), see Fig. 19.

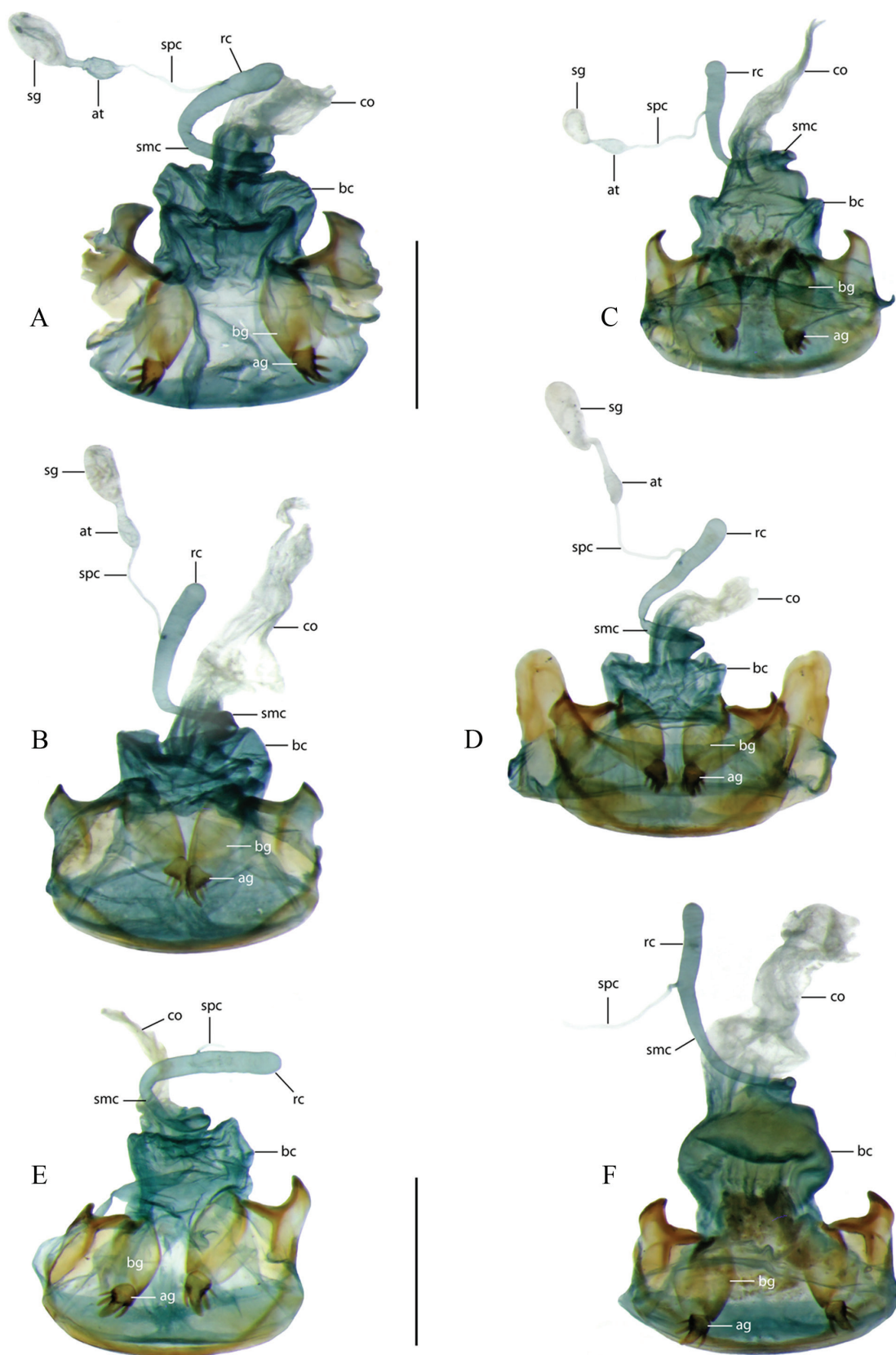


Figure 13. Spermathecal complex and gonocoxites, ventral view. **A.** *Platyderus (Eremoderus) weiratheri* Mařan, 1940, topotype female specimen; **B.** *P. (E.) felixi*, sp. nov., topotype female paratype; **C.** *P. (E.) iranicus*, sp. nov., topotype female paratype; **D.** *P. (E.) vanensis*, sp. nov., topotype female paratype; **E.** *P. (E.) vanensis*, sp. nov., female paratype, col de Buglan 1500 m, border area of Bingöl and Muş provinces, Turkey; **F.** *P. (E.) vrabeci*, sp. nov., topotype female paratype. Scale bars: 0.5 mm. Abbreviations: **ag** – apical gonocoxite; **at** – atrium; **bc** – bursa copulatrix; **bg** – basal gonocoxite; **co** – common oviduct; **rc** – receptaculum; **sg** – spermathecal gland; **smc** – seminal canal; **spc** – spermathecal canal.

15. *Platyderus (Eremoderus) brunneus* Karsch, 1881, stat. rev.

Figs 3D, F, 5H, 6A, B, 7I, J, 9C, D, 11B, C, 12J, K, 15A, B, 18, Table 3

Diagnosis. A species of *Platyderus (Eremoderus)*, with mesotarsomeres and metatarsomeres dorsally more or less flattened and grooved (Fig. 6A, B), cordate pronotum, with sides from widest point to base markedly (nominotypical subspecies) or barely concave (ssp. *ferrantei*) and posterior angles obtuse, with tips laterally more (nominotypical subspecies) or less protruding (ssp. *ferrantei*), and median lobe of aedeagus with basal bulb more slanting to shaft (Fig. 9C, D).

Redescription. Habitus. Moderately to large-sized species (BL: 7.60–9.30 mm; BW: 2.70–3.40 mm), with elongate and moderately convex body (Fig. 3D, F). **Measurements and ratios.** See Table 3. **Color and lustre.** Body, palpi, antennae and most of legs yellow-brown to reddish-brown, with head usually darker than pronotum and elytra and femora lighter than tibiae and tarsomeres. Integument slightly shiny (less shiny than in *P. languidus*). **Microsculpture and punctuation.** Pronotum with evident microreticulation, sculpticells regularly isodiametric. Elytral intervals, scutellum and lateral gutter with distinct isodiametric sculpticells; basal margin with reduced microreticulation. Ventral surface with impressed slight transverse sculpticells or with sculpticells scarcely-visible. Head impunctate, usually smooth, clypeus and areas laterad of frontal furrows sometimes with fine longitudinal wrinkles. Surface of pronotum impunctate, largely smooth, only basal area medially behind posterior transverse impression longitudinally wrinkled, rarely apical part medially in front of anterior transverse impression also wrinkled; basal foveae and adjacent lateral areas smooth, smoother than those in *P. languidus*. Elytral intervals without apparent punctuation. Abdominal ventrite 1 finely wrinkled in whole, 2–5 finely wrinkled at sides. **Head.** About one-third as wide as pronotum (PW/HW= 1.28–1.41). Eye long, moderately convex. Labrum subrectangular, as long as clypeus, with anterior margin concave medially. Frontoclypeal suture distinct in middle, reduced to disappeared at sides. Frontal furrows small, rather shallow, punctiform. Paraorbital sulci straight, fine, backward surpassing posterior margin of eye, nearly reaching level of posterior supraorbital pore. **Thorax.** Pronotum one-tenth to one-fifth wider than long (PW/PL= 1.10–1.21), with widest point at second quarter. Anterior transverse impression absent, posterior transverse impression short, barely distinct. Sides convex medially and anteriorly, slightly concave to straight in base; anterior bead present laterally, lacking or present in medial eighth to tenth; basal bead present laterally, reduced to absent in medial fifth to half. Metepisternum slightly longer than wide or nearly as long as wide, MA/MI= 0.87–1.00, with greater values occurring in specimens of ssp. *ferrantei*. **Elytra.** Oblong, about one-and-a-half times to one and two thirds as long as wide (EL/EW= 1.52–1.72), two-and-a-half times or little more as long as pronotum

(EL/PL= 2.46–2.72), and one and a third to a one-and-a-half times as wide as pronotum (EW/PW= 1.35–1.48), with widest point at medial third. Parascutellar striole and striae 1–7 very shallow to indistinct, stria 8 evident, clearly deeper than other striae (nominotypical form) or parascutellar striole and striae 1–7 distinct, slightly impressed, stria 8 somewhat deeper than other striae (ssp. *ferrantei*); parascutellar striole, if present, not joining stria 1; striae 1–8 superficially to moderately punctate; bases of striae 1–7 more or less reduced, not reaching basal bead (nominotypical form) or distinct, reaching basal bead (ssp. *ferrantei*). Interval 3 with three discal setiferous punctures. Umbilicate setiferous series with 16 or 17 punctures on each side. **Legs.** Posterior side of profemur with one or two setae in basal third and one or two in medial third. Mesofemur with 4–7 setiferous punctures on anterior side ventrally (Fig. 5H). Anterior side of metafemur ventrally with a few long setae, one in basal third and one to three in apical half. **Male genitalia.** Urite IX suboval, with proximal margin slightly asymmetrical, insignificantly turned to left (Fig. 7I, J). Median lobe of aedeagus in lateral view slender, with narrow basal bulb, long shaft and short, straight apex (Fig. 9C, D); median lobe in ventral view straight, 3.4–3.5 times longer than wide (Fig. 11B, C); apical lamella (dorsal view) short, scarcely asymmetrical, rounded at tip, with right side straight and left side slightly concave. Internal sac in lateral view (Fig. 9C, D) with ventral sclerite long, broadened and rounded distally; same in ventral view (Fig. 11B, C), with dorsal sclerite large, reticulate, with left-sided and right-sided protuberances distinct, and ventral sclerite narrow and distally very slightly curved to left. Right paramere as on Fig. 12J, K. **Female genitalia** (Fig. 15A, B). Apical gonocoxite with rounded apex and one dorsolateral ensiform seta. Spermathecal canal connected in basal third of receptaculum.

Notes. Due to minor morphological differences, the populations from the lower course of Nile River and Southwest Israel are treated as a distinct subspecies of *P. brunneus* (see Fig. 18). Moreover, no verifiable records of the species are so far known from the vast area between Misrata District (Libya) and Cairo Governorate (Egypt).

15.1. *Platyderus (Eremoderus) brunneus brunneus* Karsch, 1881

Figs 3D, E, 6A, 7I, 9C, 11B, 12J, 15A, 18, Table 3

Platyderus brunneus Karsch, 1881: 43 (type locality: “Bir Milrha”, Jabal Tarhūnah [Tarhuna plateau], Libya, based on lectotype designation), stat. rev.
= *Platyderus elegans* Bedel, 1900: 170 (type locality: “Sud de la Tunisie”), syn. n.

Notes on type locality. This taxon was described from “Bir Milrha” (Murqub District, Libya; locality cannot be localized) and “Uadi Mbellem” (Misrata District, Libya; locality with approximate GPS coordinates: 31.167,

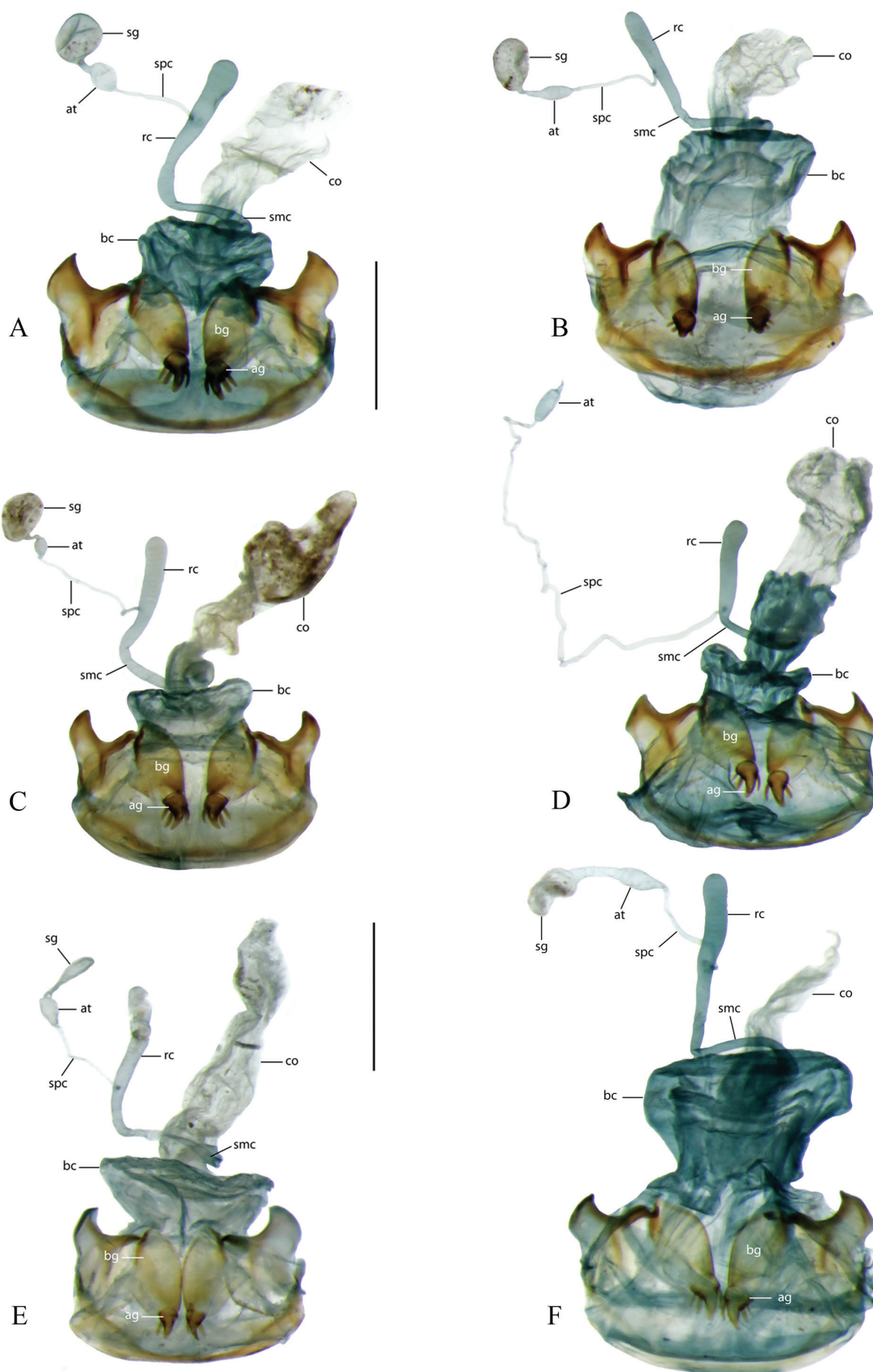


Figure 14. Spermathecal complex and gonocoxites, ventral view. **A.** *Platyderus (Eremoderus) lassallei*, sp. nov., female paratype, Iran, Mazandaran Province, E Qolqol; **B.** *P. (E.) ledouxi* Morvan, 1974, female specimen, 10 km SW Rudbarak, Mazandaran Province, Iran; **C.** *P. (E.) taghizadehi* Morvan, 1974, female specimen, Alburz Dizin, Tehran Province, Iran; **D.** *P. (Platyderus) umbratus* (Ménétriés), female specimen, Iran, Kohgiluyeh va Boyer-Ahmad Province, Sisakht; **E.** *P. (E.) arabicus*, sp. nov., holotype; **F.** *P. (E.) brunki*, sp. nov., holotype. Scale bars: 0.5 mm. For abbreviations see captions on Fig. 13.

15.050) both localities in the Gebèl Tarhúna Plateaux. As a result of current lectotype designation, the former place becomes the type locality of *P. brunneus brunneus*. *Platyderus elegans* was first discovered from “Sud de la Tunisie” (Bedel, 1900), and for the second time – from “Aïn Segoufta à l’O. du Dj. Bon-Hedma” (Bedel, 1902); the second location refers to present Jebel Bou-Hedma National Park, situated on Gafsa Governorate and Sidi Bouzid Governorate, Tunisia.

References. *Platyderus elegans*: Bedel 1902: 211, 214–215; Csiki 1931: 768; Lorenz 1998: 375; Hovorka and Sciaky 2003: 522; Lorenz 2005: 395; Hovorka 2017: 757. *Platyderus languidus* (data for *brunneus* Karsch): Bedel 1902: 211, 214–215; Csiki 1931: 769; Hovorka and Sciaky 2003: 521; Lorenz 2005: 396; Hovorka 2017: 756.

Type material. *Platyderus brunneus* Karsch, 1881. The original type series of Karsch consisted of six syntypes, 4♂♂, 2♀♀, all stored in MFNB. Their examination revealed the presence of two diagnosable taxa. One male and one female specimen were found to represent the subspecies *ferrantei* (see section “Type material” under *P. brunneus ferrantei*). The other four specimens belong to *P. brunneus brunneus*, the first of them designated lectotype and other three paralectotypes: ♂, ‘60906 [p, w] // Bir Milrha / Exp. Rohlf. [h, tq] // Hist.-Coll. (Coleoptera) / Nr. 60906 / *Platyderus brunneus* Klug, / Karsch* / Bir Milrha / Zool. Mus. Berlin [p, w] // SYNTYPE / *Platyderus / brunneus* Karsch, 1881 / labelled by MFNB 2017 [p, r]’; ♂, ‘Uadi M’bellem / Exp. Rohlf. [h, tq] // Hist.-Coll. (Coleoptera) / Nr. 60906 / *Platyderus brunneus* Klug, / Karsch* / Uadi M’bellem, Exped. / Rohlf. / Zool. Mus. Berlin [p, w] // SYNTYPE / *Platyderus / brunneus* Karsch, 1881 / labelled by MFNB 2017 [p, r]’; ♂, ‘gn 2469. [h, w] // Hist.-Coll. (Coleoptera) / Nr. 60906 / *Platyderus brunneus* Klug, / Karsch* / Bir Milrha & Uadi M’bellem, / Exped. Rohlf. / Zool. Mus. Berlin [p, w] // SYNTYPE / *Platyderus / brunneus* Karsch, 1881 / labelled by MFNB 2017 [p, r]’; ♀, ‘Hist.-Coll. (Coleoptera) / Nr. 60906 / *Platyderus brunneus* Klug, / Karsch* / Bir Milrha & Uadi M’bellem, / Exped. Rohlf. / Zool. Mus. Berlin [p, w] // SYNTYPE / *Platyderus / brunneus* Karsch, 1881 / labelled by MFNB 2017 [p, r]’.

The synonymy of *Platyderus brunneus* with *P. languidus* was proposed by Bedel (1902: 211). Revision of the type material and study of the original descriptions of the both aforementioned forms and that of *P. elegans*, as well the study of other *Eremoderus*-specimens from North Africa and the Levant, revealed that *P. brunneus* and *P. elegans* represent a single species in contrast with *P. languidus* which is a separate species not occurring in North Africa.

Other material examined. **Tunisia:** Medenine Governorate: 1♂, 1♀, ‘TUNISIA c. or. / 50 km W of Ben Gardane / 22.4.1998 / R. Borovec lgt. // *Platyderus / elegans* Bedel / JEANNE det. 2003 // COLL. WRASE / BERLIN’ (cWR).

Libya: Nuqat al Khams District: 1♀, ‘BUKAMASH [near Zuwarah City] / 04-II-2006 / LIBYA P.Weill’

(cWEI). Jafara District: 1♀, ‘AZIZIYAH P.Weill / 30-I-2010 LIBYE // *Platyderus / languidus*. R & S / Det. P. Weill 2010’ (cWEI). Tripoli District: 1♂, ‘02-III-2002 / JANZUR / LIBYA – TRIPOLITANIA // JC Ringenbach Leg. / *Platyderus languidus*’ (cWEI).

Three additional records from Libya that concern *P. brunneus brunneus* are pointed out for *P. languidus* in the webpage http://jcringenbach.free.fr/website/beetles/carabidae/Platyderus_languidus.htm, namely: ‘East of Tajura’, 04/01/2002, JCR Leg.’; ‘Road Yafran-Az Zintan, 25/12/2001, JCR Leg.’; ‘Sidi As Sa’ih 03/02/2006, PW Leg.’. The webpage is part of the database <http://jcringenbach.free.fr/website/beetles/carabidae/carablibya.htm> created by Jean-Claude Ringenbach (Pardies-Piétat, France) and Patrick Weill (Pau, France) and representing online checklist of Libyan ground-beetles.

TME: 9 specimens. TGE: 2♂♂, 1♀.

Diagnosis. Nominotypical subspecies differs from ssp. *ferrantei* in parascutellar striole and elytral striae 1–7 very shallow, almost indistinct, with bases not reaching basal bead (vs. parascutellar striole and elytral striae 1–7 distinct, slightly impressed, with bases reaching basal bead). In addition, the former has the pronotal anterior margin proportionally broader, compared to the posterior margin (vs. anterior margin of pronotum proportionally narrower, compared to posterior margin, see PA/PB, Table 3).

Habitat. Two of the three Libyan specimens were collected under stones or plant debris. Bukamash and Aziziyah are two biotopes of Tripolitania located in a semi-desert zone (Jaffarah Plain), with a few sparse trees and abundant ground vegetation, mainly in early spring (Patrick Weill, pers. comm.).

Distribution. Tunisia, Libya (Fig. 18).

Notes. Hovorka (2017: 757) placed *P. elegans* in *Platyderus* (s. str.). Present study proved however that the species currently validly known as *P. brunneus* is indeed a member of subgenus *Eremoderus*.

15.2. *Platyderus (Eremoderus) brunneus ferrantei* Reitter, 1909, stat. nov.

Figs 3F, 5H, 6B, 7J, 9D, 11C, 12K, 15B, 18, Table 3

Platyderus ferrantei Reitter, 1909: 29 (type locality: Egypt, “Cairo”).

Notes on type locality. Nothing is known about the exact locality and circumstances of collecting. At time of collecting, the city of Cairo was entirely situated on the east bank of the Nile River. Nevertheless, it is possible for the subspecies *ferrantei* to occur on both sides of the Nile River, as moisture should favor the species’ occurrence and distribution in certain less human-influenced habitats.

References. *Platyderus ferrantei*: Csiki 1931: 768; Lorenz 1998: 375; Hovorka and Sciaky 2003: 522; Lorenz 2005: 395; Abdel-Dayem 2012: 200–201; Hovorka 2017: 758.

Type material. *Platyderus ferrantei* Reitter, 1909. Holotype, female in HHNM, with the following labels: ‘Aegyptus / Cairo Ferrante’ [h, w] // *Ferrantei* / m. / Cairo. [h, w, written by Reitter himself] // coll. Reitter [p, w] // Holotypus 1909 / *Platyderus* / *Ferrantei* / Reitter [p, h, w/r, subsequently added]’.

The holotype designations in many type series, stored in HHNM, made by the late Zoltán Kaszab (or one of his co-workers) are invalid because in most cases these are syntypes. In this case, the labelling as holotype was correct, as it is only one specimen on which the description was based.

Type material. *Platyderus brunneus* Karsch, 1881. One female specimen and one male specimen from type series of *P. brunneus* are conspecific with the holotype of *P. ferrantei*. They are labelled as follows: 1♀, ‘2469 [p, w] // Hist.-Coll. (Coleoptera) / Nr. 2469 / Sphodrus brunneus / Aegypt., Ehrenberg / Zool. Mus. Berlin [p, w] // SYNTYPE / *Platyderus* / brunneus Karsch, 1881 / labelled by MFNB 2017 [p, r] // brunneus / m. Karsch* / Egypt Ehrbg. [h, tl]’ (MFNB); 1♂, ‘2470 [p, w] // Syria. Ehr: / lxxiii . 196. [h, y] // Hist.-Coll. (Coleoptera) / Nr. 2470 / Sphodrus brunneus / Syria, Ehrenberg / Zool. Mus. Berlin [p, w] // SYNTYPE / *Platyderus* / brunneus Karsch, 1881 / labelled by MFNB 2017 [p, r]’ (MFNB). The male specimen has non-chitinised genitalia and a paler coloration (see Karsch 1881: 44), indicating the immaturity of the specimen.

Other material examined. Israel: Southern District: 1♂, 1♀, ‘Israel / Holot Haluza / 1.iii.2008 / Ittai Renan’ (SMNH-TAU); 1♀, ‘Israel / Holot Haluza / 25.IV.2009 / I. Renan’ (SMNH-TAU); 2♀♀, ‘Israel / Holot Haluza / 2.iii.2010 / I. Renan’ (SMNH-TAU).

TME: 8 specimens. TGE: 1♂, 1♀.

Diagnosis. See “Diagnosis” under the nominotypical subspecies.

Comparisons. The subspecies considered here differs from easterly occurring representatives of the “*languidus*” group, i.e. *P. languidus*, *P. jordanensis* sp. nov. and *P. arabicus* sp. nov., by the meso- and metatarsomeres dorsally somewhat flattened and grooved. Its median lobe of aedeagus is more arcuate ventrally and with ventral margin of apex straight (this of *P. languidus* is appreciably less arcuate ventrally, whereas that of *P. jordanensis* has ventral margin of apex convex). Other differences between *P. brunneus ferrantei* and *P. jordanensis* sp. nov. are listed in section “Comparisons” under the latter taxon.

Supplementary distinctions between *P. brunneus ferrantei* and *P. arabicus* sp. nov., are: a/ head compared to pronotum wider, PW/HW: 1.29–1.39 (vs. head narrower, PW/HW: 1.41–1.43); b/ pronotum appreciably wider than long, PW/PL: 1.14–1.21, less constricted to apex, PW/PA: 1.34–1.42, with anterior margins compared to posterior margin long, PA/PB: 0.82–0.89 (vs. pronotum less wider, PW/PL: 1.07–1.11, more constricted to apex, PW/PA: 1.44–1.48, with anterior margin compared to posterior margin much narrower, PA/PB: 0.76–0.79).

P. irakensis and *P. brunneus ferrantei* share meso- and metatarsomeres dorsally flattened and slightly grooved. The two taxa can be reliably diagnosed by a combination of three ratios – PW/PB, EL/EW and EL/PL (Table 3).

Habitat. The Israeli site is located in the sand dunes of Western Negev. The species lives on the shifting dunes, together with *Atlantomasoreus groneri* Assmann, Renan & Wrase, 2015, *Discoptera arabica* Fairmaire, 1896, *Scarites striatulus* Dejean, 1825, *Thermophilum sexmaculatum* (Fabricius, 1787), *Graphipterus serrator* (Forsskål, 1775) (or *G. multiguttatus* (Olivier, 1790)), and a species of the *Cymindis setifeensis/suturalis* group(s). For a detailed description of the habitat see those of *Anthia sexmaculata*, *A. groneri* and *G. serrator* in Assmann et al. (2015a, 2015b) and Renan et al. (2018). Photographs of the habitat are given by Assmann et al. (2015a, fig. 7b, p. 62) and Renan et al. (2018, fig. 14, p. 59).

Distribution. Northeast part of Egypt (not yet found in Sinai Peninsula, but possibly occurring there), southwestern part of Israel (Southern District), see Fig. 18. The record from Holot Haluza is the first record for *P. brunneus* (s.l.) for Israel and for the Asian continent.

16. *Platyderus (Eremoderus) insignitus* Bedel, 1902

Figs 4A, 9E, 11D, 15C, Table 3

Diagnosis. This species differs from *P. brunneus brunneus* in pronotum less constricted to base (PW/PB: 1.12–1.17, vs. PW/PB: 1.21–1.28) and with apex appreciably narrower than base (PA/PB: 0.80–0.85, vs. PA/PB: 0.88–0.92). Median lobe of aedeagus somewhat longer than that in *P. brunneus* (s.l.), with ventral sclerite longer and not forming a distal kink (Figs 9E, 11D).

Redescription. Habitus. Moderately large species (BL: 6.60–8.70 mm; BW: 2.20–3.00 mm), with elongate, narrow and moderately convex body (Fig. 4A). **Measurements and ratios.** See Table 3. **Color and lustre.** Chestnut-colored as palpi, with antennae and legs usually lighter than rest of body, head somewhat darker than pronotum and elytra. Integument shiny. **Microsculpture and punctuation.** Pronotum and elytra with isodiametric sculpticells. Ventral surface with impressed slight stretched isodiametric sculpticells or with microsculpture less apparent or scarcely-visible. Head impunctate, usually smooth, but lateral areas adjacent to frontal furrows sometimes with fine wrinkles. Surface of pronotum impunctate, largely smooth, basal area medially behind posterior transverse impression longitudinally wrinkled, rarely apical part medially in front of anterior transverse impression also wrinkled; basal foveae and adjacent lateral areas smooth. Elytral intervals without apparent punctuation. Abdominal ventrite 1 finely wrinkled in whole, 2–5 finely wrinkled at sides. **Head.** About two thirds as wide as pronotum (PW/HW= 1.35–1.45). Eye long, convex. Labrum slightly shorter than clypeus, subrectangular, with anterior margin concave medially. Frontoclypeal suture more or less

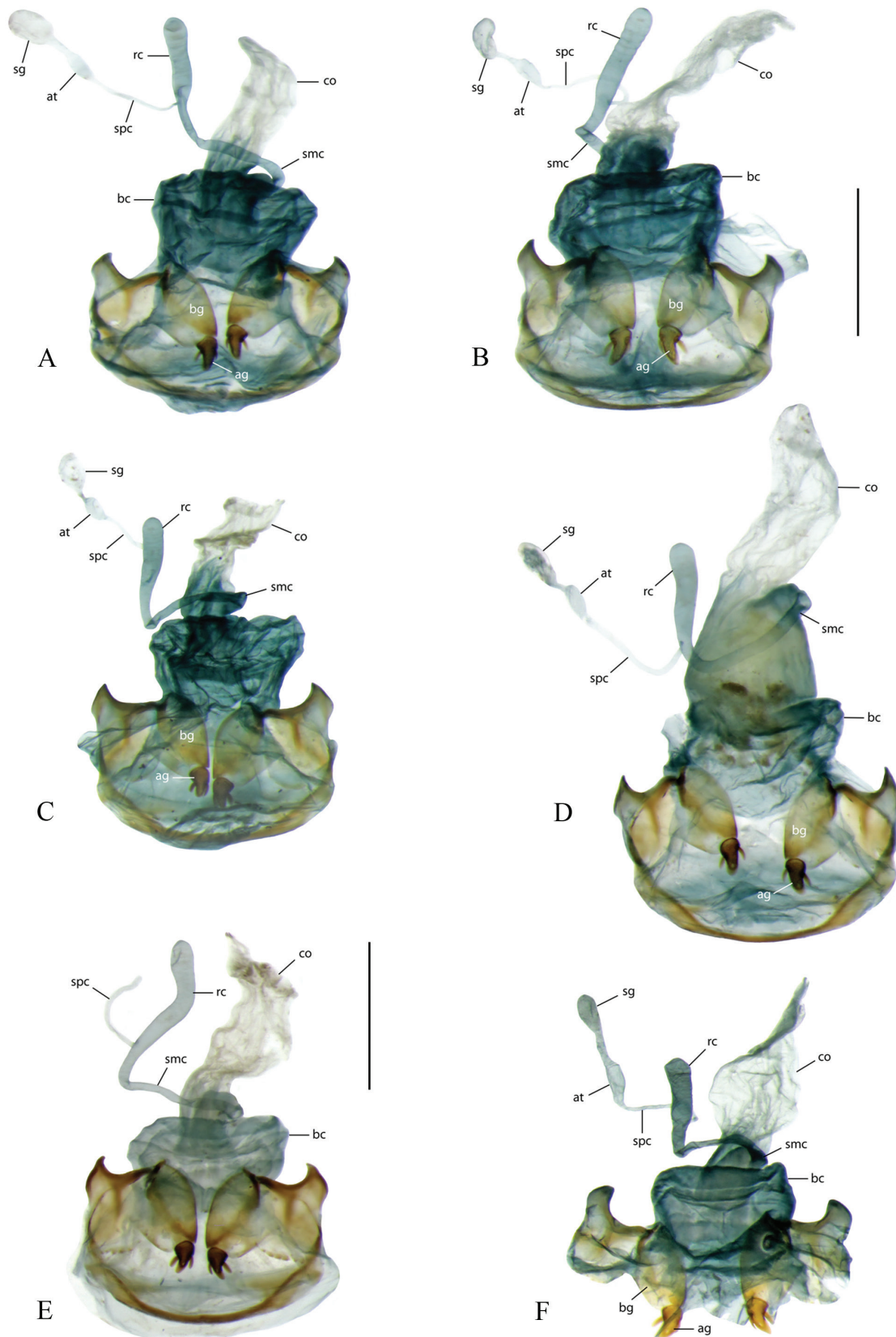


Figure 15. Spermathecal complex and gonocoxites, ventral view. **A.** *Platyderus (Eremoderus) brunneus brunneus* Karsch, 1881, female specimen, Bukamash, Nuqat al Khams District, Libya; **B.** *P. (E.) brunneus ferrantei* Reitter, 1909, female specimen, Holot Haluza, Southern District, Israel; **C.** *P. (E.) insignitus insignitus* Bedel, 1902, female specimen, Plage Aglou, Sous-Massa Region, Morocco; **D.** *P. (E.) irakensis*, sp. nov., holotype; **E.** *P. (E.) jordanensis*, sp. nov., female paratype, N Wadi Musa, Ma’an Governorate, Jordan; **F.** *P. (E.) languidus* (Reiche & Saulcy, 1855), female specimens, Israel, Netanya 22.xii.1996, Central District, Israel. Scale bars: 0.5 mm. For abbreviations see captions on Fig. 13.

distinct in middle, indistinct or disappeared at sides. Frontal furrows very small, shallow, punctiform. Paraorbital sulci fine, backward not reaching level of posterior supraorbital pore. **Thorax.** Pronotum about a tenth to a fifth wider than long (PW/PL= 1.06–1.17), widest point at second quarter. Anterior transverse impression absent, posterior transverse impression very shallow, barely distinct. Sides convex medially and anteriorly, slightly concave to base (somewhat more concave than in *P. brunneus*); anterior bead present laterally, reduced or lack in medial eighth to tenth; basal bead present laterally, reduced to absent in medial fifth to half. Metepisternum slightly longer than wide or nearly as long as wide, MA/MI= 0.79–0.86. **Elytra.** Oblong, about one-and-a-half times, or a little more, as long as elytra (EL/EW= 1.57–1.65), two-and-a-half times as long as pronotum (EL/PL= 2.41–2.61), and a half as wide as pronotum (EW/PW= 1.40–1.51), with widest point at medial third. Parascutellar striole and striae 1–7 rather shallow, impunctate or slightly punctate, stria 8 deeper than other striae; parascutellar striole not joining stria 1; bases of striae 1–7 mostly reduced, not reaching basal bead, rarely reaching it. Interval 3 with three discal setiferous punctures. Umbilicate setiferous series with 16 or 17 punctures on each side. **Legs.** Posterior side of profemur with one seta in basal third and one in medial third. Mesofemur mostly with 5–6 setiferous punctures on anterior side ventrally, rarely with 4 punctures. Anterior side of metafemur ventrally mostly with one seta in basal third and one in medial third or apical half (single specimen with two setae in basal half and two in apical half on one femur). **Male genitalia.** Median lobe of aedeagus in lateral view arcuate, with narrow basal bulb, long shaft and short, straight apex (Fig. 9E); same in ventral view straight, about 3.6–3.7 times longer than wide; apical lamella (dorsal view) short, almost symmetrical, rounded at tip and slightly concave at each side. Internal sac in lateral view (Fig. 9E) with ventral sclerite long, slightly broadened distally; same in ventral view (Fig. 11D), with dorsal sclerite large, forming two small left-sided protuberances and a broad right-sided protuberance, and with ventral sclerite narrow, straight and slightly broadened distally. **Female genitalia** (Fig. 15C). Apical gonocoxite with rounded apex and one dorsolateral ensiform seta. Spermathecal canal connected in medial third of receptaculum.

16.1. *Platyderus (Eremoderus) insignitus insignitus* Bedel, 1902

Figs 4A, 9E, 11D, 15C, 18, Table 3

Platyderus insignitus Bedel, 1902: 211 (type locality: “Mogador” [= Essaouira], Morocco).

References. *Platyderus insignitus*: Bedel 1902: 214; Csiki 1931: 769; Antoine 1957: 235–236; Jeanne 1996: 398; Lorenz 1998: 375; Hovorka and Sciaky 2003: 521; Lorenz 2005: 395; Machard 2017: 102; Machard 2019: 199. *Platyderus insignitus insignitus*: Hovorka 2017: 756.

Type material. Five syntypes should be present in MNHN, according to original description. Not examined.

Other material examined. **Morocco:** Casablanca-Settat Region: 1♀, ‘Marokko (region Doukkala-Abda) / Bir Jdid between El Jadida / and Casablanca / 4.2.2003, leg. M. Egger’ (cWR). Marrakesh-Safi Region: 1♀, ‘SW-Morocco, 31.28 N / 09.46W, DIABAT (4 km / S Essaouira), 60 m // J. Kaláb leg., 17.XI.2003 / bushes, sandy dunes, / steppe’ (cASL). Sous-Massa Region: 1♂, ‘MAROKKO, s. w. TIZNIT / umg. TIZNIT, 50 m / Strand-AGLOU / I. Puchner, 2.III.2000’ (cDOS); 1♀, ‘SW-Morocco, 29.48N/09.50W / AGLOU PLAGE, 30 m, / J. Kaláb leg., 26–28.xi.2004 / sandy/grassy places, / half-desert’ (cWR); 1♀, ‘MOROCCO, Plage Aglou / NW Tiznit / 29°45’N, 9°54’W / 6 m, 6.V.2011 / lgt. P. Kabátek’ (cWR).

TME: 5 specimens. TGE: 1♂, 1♀.

Diagnosis. See “Diagnosis” of *P. insignitus presaharensis*.

Habitat. Nothing is known about the bionomics of this species.

Distribution. According to the available data, *P. insignitus insignitus* is endemic to Morocco (Fig. 18). Antoine (1957: 236) stated that it is a sublittoral species living in the area between Oum er Rbia River to the north and the Anti-Atlas Mountain Range to the south. Machard (2017, 2019) noted that it inhabits the “Littoral atlantique de Casablanca à Agadir”. The new data from the environs of Tiznit show that the species occurs south of the city of Agadir as well.

16.2. *Platyderus (Eremoderus) insignitus presaharensis* Lagar Mascaró, 1978

Fig. 18

Platyderus insignitus presaharensis Lagar Mascaró, 1978: 31 (type locality: “cueva [cave] Kef Aziza, Tazzouguert”, Morocco).

References. *Platyderus insignitus presahariensis* [sic]: Hovorka 2017: 756.

Type material. Holotype probably in Museu de Ciències Naturals de Barcelona. Not examined.

Other material examined. None.

Diagnosis. Differs from nominotypical subspecies by pronotum sides more parallel to pronotum base and not sinuate before posterior angles, which are right and rounded, somewhat longer antennae, with antennomeres 9–11 exceeding pronotum base, and elytral striae well-impressed (Lagar Mascaró 1978: 31).

Habitat. The holotype was collected in the cave Kef Aziza, a 4.5 km long cave near river Oued Guir and village of Ksar Tazougart, one of the longest caves in Morocco. It seems to be a troglaxene or subtroglophile that tends to temporarily inhabit subterranean habitats, but also strongly associated with aboveground habitats.

Distribution. Errachidia Province, Drâa-Tafilalet Region, Eastern-Central Morocco (Fig. 18).

17. *Platyderus (Eremoderus) irakensis* sp. nov.

<http://zoobank.org/95E89306-626A-468D-BA68-F16489ABB9F3>

Figs 4B, 6C, 15D, 19, Table 3

Type locality. Iraq, Al Anbar Governorate, Ar Rutba District, ca. 115 km east of Ar-Rutbah Town.

Type material. *Holotype* ♀, 'IRAQ, Al-Anbar / Rutba, singled / 115 km. E of town / 8.I.1978 [w, h] // No. 350 / Topál & Zilahy [w, h]' (HNHM); *paratype* ♀, 'IRAQ, Al-Anbar / Rutba, singled / at 30 km W of / town, 9.I.1978 [w, h] // No. 351 / Topál & Zilahy [w, h]' (NMNHS).

TME: 2 specimens. TGE: 1 ♀.

Etymology. The specific epithet is a Latinized adjective, referring to the name of the country in which this new species was found.

Diagnosis. *Platyderus irakensis* is distinct from all other species of “*languidus*” group by the orange-brown color of integument (Fig. 4B), mesotarsomeres and metatarsomeres dorsally flattened and slightly grooved (Fig. 6C), pronotum with sides to base slightly convex and posterior angles laterally not prominent, and distal enlargement of bursa copulatrix (Fig. 15D); the last character may be an autapomorphy. Among Asian representatives of species group, it is the form with the highest mean values for EL/PL (= 2.69) and EL/EW (= 1.63), and, together with *P. arabicus* sp. nov., the one possessing lowest index for PW/PB (= 1.10).

Description. *Habitus.* Specimens of moderate size for *Platyderus* species (BL: 8.30–9.00 mm; BW: 2.90–3.20 mm), with elongate and fairly convex body (Fig. 4B). **Measurements and ratios.** See Table 3. **Color and lustre.** Body and appendages orange-brown, with head somewhat darker than the rest of the body and ventral surface lighter than dorsal surface. Integument slightly to moderately shiny, head and pronotum as shiny as elytra, ventral surface somewhat shinier than dorsal surface. **Microsculpture and punctation.** Pronotum with evident microreticulation, sculpticells regular isodiametric. Elytral intervals, scutellum and lateral gutter with distinct isodiametric sculpticells, sculpticells of basal margin more or less reduced. Ventral surface with isodiametric or slight transverse sculpticells, less apparent on epipleura and middle coxa. Head impunctate and smooth, only frontal furrows and lateral ends of clypeus, with very fine and short wrinkles. Pronotum surface mostly smooth, only apical part medially in front of anterior transverse impression and basal area medially behind posterior transverse impression longitudinally wrinkled; basal foveae and adjacent lateral areas shallowly punctate. Elytral intervals without evident punctures. Abdominal ventrites 1–3 finely wrinkled at sides, smooth medially. **Head.** About one time and a third as wide as pronotum (PW/HW= 1.30–1.32). Eyes long, moderately convex. Labrum subrectangular, barely shorter than clypeus, with anterior margin concave medially. Frontoclypeal suture distinct in middle, reduced at sides. Frontal furrows punctiform, shallow. Paraorbital sulci straight, fine, backward surpassing posterior margin of eye, not

reaching level of posterior supraorbital pore. **Thorax.** Pronotum about a tenth wider than long (PW/PL= 1.13), with widest point at medial third. Anterior transverse impression indistinct; posterior transverse impression indistinct to barely distinct. Sides not sinuate, shallowly convex anteriorly, barely convex posteriorly; anterior bead present laterally, lacking or present in medial ninth to tenth; basal bead present laterally, reduced to absent in medial third. Metepisternum slightly longer than wide, MA/MI= 0.91–0.95. **Elytra.** Elongate, about one and two thirds as long as wide (EL/EW= 1.62–1.63), two and two thirds as long as pronotum (EL/PL= 2.65–2.72), and almost one and a half times as wide as pronotum (EW/PW= 1.45–1.47), with widest point at first half of third quarter. Parascutellar striole and striae 1–8 shallowly impressed, superficially to indistinctly punctate; striole short, not joining stria 1; bases of striae not reaching basal bead (except for stria 2 in paratype). Interval 3 with three discal setiferous punctures (posterior puncture lacking on left elytron of holotype), all adjoining stria 2; one additional discal puncture adjoining stria 4 at anterior quarter of right elytron of paratype. Umbilicate setiferous series with 16 punctures on left elytron and 17 on right elytron in holotype, respectively, with 16 and 15 punctures in paratype. **Legs.** Posterior side of profemur with one or two setae in basal third and one in medial third. Mesofemur mostly with 4 or 5 setiferous punctures on anterior side ventrally. Anterior side of metafemur ventrally with a few long setae, one in basal third and one-two in apical half. **Male genitalia.** Unknown. **Female genitalia** (Fig. 15D). Apical gonocoxite with rounded apex and one dorsolateral ensiform seta. Bursa copulatrix two-chambered, with a shorter, but wider basal part and a longer, but narrower apical enlargement. Spermathecal canal connected in basal third of receptaculum.

Comparisons. In addition to characters mentioned in “Diagnosis”, the new species differs from *P. jordanensis* sp. nov., by: (1) head wider, compared to pronotum (PW/HW: 1.30–1.32, vs. PW/HW: 1.35–1.42); (2) pronotum with sides less constricted anteriorly and posteriorly (PW/PA: 1.34–1.38 and PW/PB: 1.09–1.11, vs. PW/PA: 1.39–1.52 and PW/PB: 1.15–1.22); (3) elytra longer compared to their width and the length of the pronotum (EL/EW: 1.62–1.63 and EL/PL: 2.65–2.72, vs. EL/EW: 1.56–1.60 and EL/PL: 2.41–2.60).

For differences between *P. irakensis* sp. nov. and *P. arabicus* sp. nov. and such between *P. irakensis* sp. nov. and *P. languidus*, see “Comparisons” under the latter species.

Habitat. Nothing is known about the bionomics of this species.

Distribution. It is currently known from two localities situated in the Ar Rutba District, which is the largest district of Al Anbar Governorate, Western Iraq (Fig. 19). The holotype was collected about 115 km east of Ar-Rutbah Town whilst the paratype was found about 30 km west of the same town. Most of the area of the Ar Rutba District is a high plateau.

18. *Platyderus (Eremoderus) jordanensis* sp. nov.

http://zoobank.org/A95FB1A6-43F7-4FFC-A202-05073CC72F90

Figs 4C, 6D, 7K, 9F, 11E, 12L, 15E, 19, Table 3

Type locality. Jordan, Ma'an Governorate, Al-Betrā' District, Little Petra, archaeological area, 30.3667, 35.4333.

Type material. *Holotype* ♂, 'JORDAN (Ma'an)/Little Petra, ca. 1000 m/archaeological area / 30°22'N/35°26'E / (narrow shaft beside / stony staircase) / 25.III.2016 Wrase & Laser [12B] [w, p]' (cWR). Paratypes: 1♀, 'Jordanien 1024 m / Prov Ma'an / W. Ziegler 9.3.2015 [w, p] // N Wadi Musa / 30°24'.15"N, 35°26'.53"E [w, p]' (cZIEG); 1♂, 'Jordania / Prov. Ma'an / n Wadi Musa 1023m / W.Ziegler 25.3.2016 [w, p] // Jabal al Bayda (Project / 30°24'29"N, 35°26'743"E [w, p]' (NMNHS); 1♂ 'S-Jordan: Wadi Rum / Qatar Spring / 29.51°N / 35.41°E / 1000–1100 m asl [w, p] // dry wadi with *Ficus* trees, 21.III.2017 / leg. Th. Assmann [w, p]' (cAL); 1♂, 'S-Jordan: Little Petra, ca. 1000m / wadis with Mediterranean trees in vicinity to the archaeological site / 30.34°N, 035.46°E / 25.III.2016 / leg. Th. Assmann [w, p]' (cAL).

TME: 5 specimens. TGE: 4♂♂, 1♀.

Etymology. The specific epithet is a Latinized adjective, based on the name of the country in which this species was found.

Diagnosis. Differs from all other species of the "languidus" group by the following set of characters: (1) meso- and metatarsomeres dorsally convex and smooth (Fig. 6D); (2) posterior angles of pronotum incompletely rounded, with tips protruding laterally (Fig. 4C); and (3) ventral margin of apex of median lobe (lateral view) evidently convex thus apex appears bent up (Fig. 9F).

Platyderus jordanensis sp. nov. and *P. languidus* share a trait that can be a mark for their close relationships, the apical gonocoxite without nematiform setae.

Description. *Habitus.* Specimens of large size for *Platyderus* species (BL: 8.70–9.90 mm; BW: 3.00–3.45 mm), with rather elongate and moderately convex body (Fig. 4C). *Measurements and ratios.* See Table 3. *Color and lustre.* Body and appendages uniformly light reddish-brown, palpomeres and legs somewhat lighter than rest of body. Integument slightly to moderately shiny, head and pronotum shinier than elytra. *Microsculpture and punctuation.* Surface of pronotum with evident microreticulation, sculpticells regular isodiametric. Elytra (intervals, scutellum, basal margin and lateral gutter) with distinct isodiametric sculpticells. Ventral surface largely with more or less impressed isodiametric or slight transverse sculpticells. Head impunctate, nearly smooth, with a few, fine and shallow wrinkles in and laterally of frontal furrows. Pronotum surface mostly smooth, only basal area between foveae longitudinally wrinkled and adjacent lateral areas with rare and superficial punctures that do not reach anterior half. Elytral intervals without apparent punctuation. Abdominal ventrite 1 finely wrinkled medially, smooth laterally, other ventrites neither wrinkled nor punctate. **Head.** One-third or more as wide as pronotum wide (PW/HW= 1.35–1.42). Eyes long, moderately convex. Labrum

subrectangular, shorter than clypeus, with anterior margin concave medially. Frontoclypeal suture distinct in middle, indistinct at sides. Frontal furrows small, punctiform. Paraorbital sulci straight, backward surpassing posterior margin of eye, hardly reaching level of posterior supraorbital pore. **Thorax.** Pronotum about a tenth wider than long (PW/PL= 1.08–1.13), with widest point at medial third. Anterior transverse impression absent; posterior transverse impression barely distinct. Sides sinuate, convex medially and anteriorly, slightly concave posteriorly; anterior bead present laterally, lacking or present in medial 1/10; basal bead present laterally, reduced to absent in medial third or medial half. Metepisternum somewhat longer than wide, MA/MI= 0.88–0.91. **Elytra.** Elongate, about one and a half times or little more as long as elytra width (EL/EW= 1.56–1.60), two-and-a-half-times as long as pronotum (EL/PL= 2.41–2.60), and a bit less than a half as wide as pronotum (EW/PW= 1.39–1.46), with widest point at medial third. Parascutellar striole linear, as impressed as other striae, not joining stria 1; striae 1–8 and striole slightly to indistinctly punctate; base of stria 1 ending in parascutellar pore, striae 2–5 reaching or barely not reaching basal bead, 6 and 7 ending little before basal bead. Interval 3 with three discal setiferous punctures. Umbilicate setiferous series with 16 punctures on each elytron in three specimens examined, including holotype. **Legs.** Posterior side of profemur with one or two setae in basal third and one in medial third. Mesofemora with 6 (holotype) or 5 (both paratypes) setiferous punctures on anterior side ventrally. Anterior side of metafemur ventrally with two long setae, one in basal third and one in medial third. **Male genitalia.** Urite IX subtriangular, with proximal margin symmetrical and pointed at apex (Fig. 7K). Median lobe of aedeagus in lateral view slender, with narrow basal bulb, shaft broad with proximal part slightly constricted, and short, straight apex (Fig. 9F); median lobe in ventral view straight, 3.7 times longer than wide; apical lamella (dorsal view) rather short, nearly symmetrical, rounded at tip, with sides straight to slightly concave. Internal sac in lateral view (Fig. 9F) with ventral sclerite slightly broadened and rounded distally; same in ventral view (Fig. 11E), with dorsal sclerite large, having small left-sided and large right-sided protuberance, and ventral sclerite straight and rather narrow. Right paramere as on Fig. 12L. **Female genitalia** (Fig. 15E). Apical gonocoxite with widely rounded apex and one dorsolateral ensiform seta. Spermathecal canal connected in basal third of receptaculum.

Comparisons. In additions to characters mentioned in "Diagnosis", *P. jordanensis* sp. nov. differs from geographically close *P. brunneus ferranei* by pronotum less wide (PW/PL: 1.08–1.13, vs. PW/PL: 1.14–1.21), with anterior margin narrower than posterior margin (PA/PB: 0.78–0.87, vs. PA/PB: 0.88–0.92).

For differences between *P. jordanensis*, from one side, and *P. languidus*, *P. irakensis* and *P. arabicus*, from other side, see sections "Comparisons" (under the first two species) and "Diagnosis" (under *P. arabicus*).

Habitat. In Little Petra *P. jordanensis* sp. nov. lives in wadis that have a canyon-like profile and some Mediterranean tree species. There it lives together with



Figure 16. Distribution of species from subgenus *Eremoderus* in the western Aegean Sea Region and Turkey: *Platyderus chatzakiae* sp. nov. (red circle), *P. weiratheri* (blue circles), *P. vanensis* sp. nov. (brown circles), and *P. vrabeci* sp. nov. (yellow circle).

Laemostenus quadricollisquadricollis L. Redtenbacher, 1843, *Trechus crucifer* Piochard de la Brûlerie, 1876, *Calathus cinctus* Motschulsky, 1850, *Cymindis andreae* Ménétris, 1832, and *Carabus impressus* Klug, 1832. In Wadi Rum the single specimen was found in a dry wadi with *Retama* shrubs and single *Ficus* trees in the shade of the walls of the head of the canyon-like valley. It occurs together with ground beetles that are mainly typical for desert habitats (*Laemostenus aegyptiacus* Schatzmayr, 1936, *Singilis flicornis* Peyerimhoff, 1907, *Cymindis hierichontica* Reiche & Saulcy, 1855, *Merizomena castanea* Klug, 1832, and *Amara maindroni* Bedel, 1907). A photograph of the habitat of the latter is given by Casale and Assmann (2017: 22, fig. 35).

Distribution. According to the data available, the species is the representative of the group “*languidus*” in the southern part of Jordan, stretching from the vicinity of Little Petra to areas close to the Saudi Arabian border (Fig. 19). As Wadi Rum is in the most southern part of Jordan, the species may also occur in Northwest Saudi Arabia.

19. *Platyderus (Eremoderus) languidus* (Reiche & Saulcy, 1855)

Figs 4D, E, 5I, 6E, 7L, M, 9G, H, 11F, G, 12M, N, 15F, 19, Table 3

Feronia (Argutor) languida Reiche & Saulcy, 1855: 610 (type locality: “Jordanis”, based on lectotype designation).
= *Sphodrus parumstriatus* Fairmaire, 1872: 47 (type locality: “inconnue... probably qu’il appartient à la faune méditerranéenne”).
Synonymy established by Bedel (1906: 91).

Note on type locality. The specimens were collected from: “Des bords du Jourdain et de la mer Morte” (Reiche and Saulcy 1855: 610).

References. *Platyderus languidus*: Chaudoir 1866: 108–109; Piochard de la Brûlerie 1876: 428, 430; Bedel 1902: 211; Sahlberg 1903: 3–4; Bedel 1906: 91; Csiki 1931: 769; Jedlička 1963: 20, 22; Israelso 1990: 165; Jeanne 1996: 398; Lorenz 1998: 375; Hovorka and Sciaky 2003: 521; Lorenz 2005: 396; Hovorka 2017: 756.

Type material. *Feronia languida* Reiche & Saulcy, 1855. Consists of four syntypes, 2♂♂, 2♀♀ in MHNG, all conspecific. All the specimens quite dirty and damaged. Three of them were preserved in pinned condition, whereas a male below designated as paralectotype, together with the extracted genitalia (without the urite preserved), was glued on a card; originally this specimen was pinned. The last specimen has been labelled as holotype by the late Claude Jeanne, but such a treatment was incorrect because at least four type specimens exist belonging to one species, all of them bearing the well-known yellow handwritten labels of Louis Jérôme Reiche (1799–1890); all specimens have the status of syntypes.

We chose for lectotype designation a male specimen with the label “Jordanis” in order to retain the type locality “Jordanis” that is in accordance with the locality that was given in the description (Reiche and Saulcy 1855). Although rather damaged, we took a picture of its habitus and examined its genitalia (Fig. 4D). Afterwards, the lectotype specimen was glued onto a white card, and its genitalia were embedded in Euparal on a second smaller white card pinned below the specimen.

The four specimens are labelled, as follows: lectotype ♂, ‘Jordanis [h, y] // Coll. Reiche [p, w] // PARATYPE *Feronia / languida* R. & S / C. JEANNE des. 1990 [p, h, r] // *Platyderus / languidus* R. & S. / JEANNE det. 1990 [p, w]’; paralectotype ♂, ‘*Platyderus / languidus*. Reiche / Soc. Ent. 1855. 610 / Syria [h, y] // Coll. Reiche [p, w] // HOLOTYPE *Feronia / languida* R. & S. / C. JEANNE des. 1990 [p, h, r] // *Platyderus / languidus*

R. & S. / JEANNE det. 1990 [p, w]'; paralectotype ♀, 'Nazareth [h, y] // Coll. Reiche [p, w] // PARATYPE Feronia / languida R. & S / C. JEANNE des. 1990 [p, h, r] // *Platyderus / languidus* R. & S. JEANNE det. 1990 [p, w]'; paralectotype ♀, 'Palæstina [h, y] // Coll. Reiche [p, w] // // PARATYPE Feronia / languida R. & S / C. JEANNE des. 1990 [p, h, r] // *Platyderus / languidus* R. & S. JEANNE det. 1990 [p, w]'

Besides, all the four specimens have two supplementary labels subsequently added (Fig. 4D), one printed in MHNG, '*Platyderus / languidus* [sic] Reiche / 'Syrie' [pencil crossed off] / Label MHNG 2010 [p, w]', and, one lectotype [or paralectotype] label added by the first revising authors in the context of this work.

A further fifth syntype exists in MNHN, but in view of its too damaged body and imprecise location, it was not subject of lectotype designation (see "Imprecise locality").

Other material examined. Imprecise locality: single specimen of uncertain sex, with missing left antennae, fore tarsi, middle and hind legs '*languida* Reiche [h, w] // cotype de Reiche cite par Chaudoir [h, w] // Ex Musæo Mniszech [p, w] // L. Bedel Vidit 1902. [p, w]', (MNHN; ex-collection Chaudoir, box N° 218 "*Platyderus Oxycrepis Stolonis Loxandrus*").

Israel: Northern District: 1♂, 'ISRAEL: Hammat / Gader / 8.v.1997 / V. CHIKATUNOV' (SMNH-TAU). Central District: 1♀, 'Beit-Berl / 13.2.68 // COLLECTED BY KUTY YEFENOF' (SMNH-TAU); 1♀, 'Israel Netanya / 30.11.96 / R. Hoffman' (SMNH-TAU); 1♂, 'Israel Netanya / 14.12.96 / R. Hoffman' (SMNH-TAU); 1♀, 'Israel Netanya / 21.12.96 / R. Hoffman' (SMNH-TAU); 1♂, 'ISRAEL: / Netanya 22.xii.1996 / V. Chikatunov' (SMNH-TAU); 1♀, 'Israel Netanya / 30.12.96 / R. Hoffman' (NMNHS); 2♀♀, 'Israel Netanya / 18.1.97 / R. Hoffman' (SMNH-TAU); 1♀, 'Israel Netanya / 1.3.97 / R.

Hoffman' (SMNH-TAU). Jerusalem District: 1♀, 'Jerusalem // *Tapinopterus insidiosus* Frm.' (MFNB); 1♂, 'Jerusalem / Syria // ex coll. A. Jedlička / National Museum / Prague, Czech Republic // languidus / Reiche / det. Ing. Jedlička' (NMPC); 1♀, 'Jerusalem 30.XII.25' (MIZ); 1♂, 'PALESTINE. / F.S. Bodenheimer. // Press by / Imp. Inst. Ent. / B.M. 1944-97. // Jerusalem / scopus / 26.XII.33' (NHMUK). Judea and Samaria Area: 1♀, 'PALESTINE / Jerusalem - / Jericho Road / Bytinski-Salz / km 18. / 14.ii.1940' (SMNH-TAU); 1♂, 'Jerusalem Jericho / Road km 18 / Palestine 17.ii.1940 / leg. Bytinski-Salz' (SMNH-TAU); 1♀, 'PALESTINE / Kv. Schiller / 25.ii. 19 / leg. Bytinski-Salz // *Platyderus / languidus* R. / det. Ing. Jedlička' (SMNH-TAU); 2♂♂, 1♀, 'ISRAEL: South-facing / slope of Nahal Perat [= Nahal Prat] / 28.ii.2007 / L. FRIEDMAN' (SMNH-TAU); 1♂, 'ISRAEL / Eshkolot / 18.iii.2007 / I. SCHKIRBERG' (SMNH-TAU). Southern District: 1♂, 1♀, 'W-Israel / Nizzanim / S of Ashdod // 5.XII.2008 / leg. Th. Assmann' (cASL); 1♀, 'Ashkelon / 7.4.2017 / I. Renan // FS' (cWR); 1♂, 'Ashdod / 11.4.2017 / I. Renan // GM' (SMNH-TAU).

TME: 30 specimens. TGE: 4♂♂, 2♀♀.

Diagnosis. A species of medium size for *Platyderus* (*Eremoderus*), with light reddish-brown integument, meso- and metatarsomeres dorsally convex and smooth (Fig. 6E), and pronotum from widest point to apex slightly to moderately constricted (PW/PA: 1.31–1.41), with sides to base straight (rarely slightly concave). Posterior angles of pronotum subrounded, with tips not protruding laterally (most cases) or very slightly protruding (few cases – as in *P. jordanensis* sp. nov.). Median lobe of aedeagus (lateral view) with proximal part, including basal bulb, rather long and slender, forming an angle with distal part of lobe smaller compared to other members of the "*languidus*" group (Fig. 9G, H).

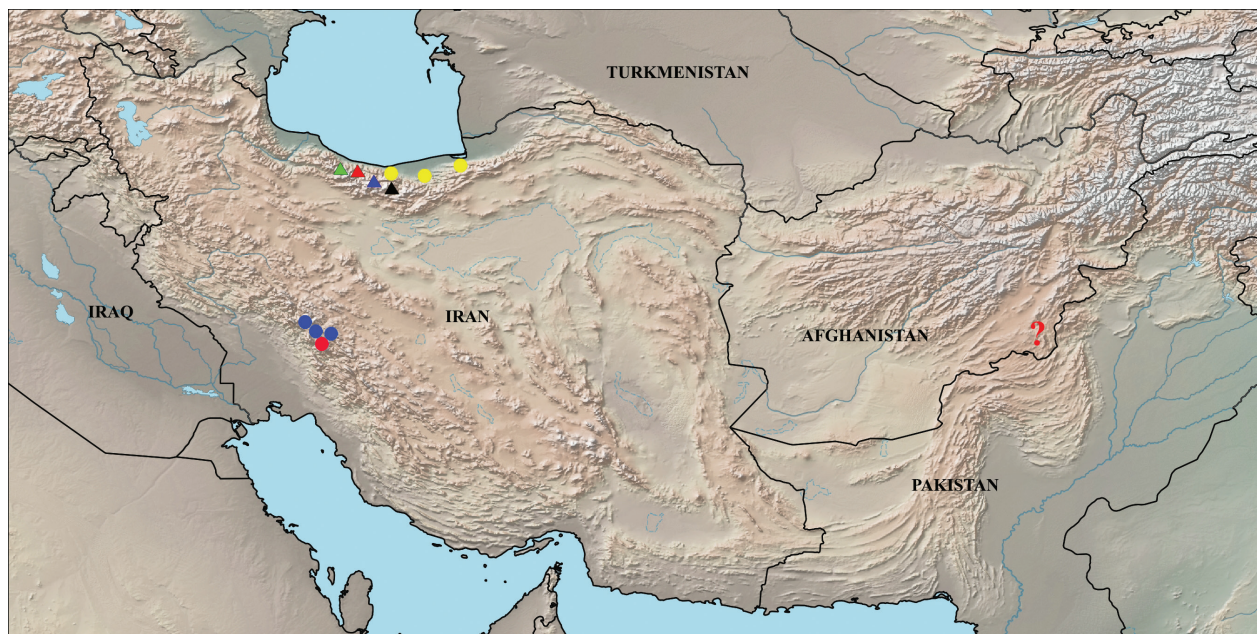


Figure 17. Distribution of species from subgenus *Eremoderus* in Iran and Afghanistan: *Platyderus felixi* sp. nov. (red circle), *P. iranicus* sp. nov. (blue circles), *P. lassallei* sp. nov. (yellow circles), *P. davatchii* (green triangle), *P. ledouxi* (red triangle), *P. taghizadehi* (blue triangle), *P. klapperichi* sp. nov. (black triangle), and *P. afghanisticus* sp. nov. (red question mark).

Redescription. Habitus. Specimens of moderate to large size for *Platyderus* species (BL: 6.40–9.10 mm; BW: 2.20–3.15 mm), with elongate and moderate convex body (Fig. 4D, E). **Measurements and ratios.** See Table 3. **Color and lustre.** Body and appendages uniformly yellow brown to reddish-brown, usually head darker than the rest of the body. Integument slightly to moderately shiny, head and pronotum as shiny as elytra. **Microsculpture and punctuation.** Pronotum with evident microreticulation, sculpticells regular isodiametric. Elytra (including intervals, basal margin and lateral gutter) with distinct isodiametric sculpticells. Ventral surface with more or less well-impressed isodiametric or slight transverse sculpticells or with sculpticells less apparent or scarcely-visible. Head smooth, including area of frontal furrows, sometimes clypeus with fine and shallow longitudinal wrinkles, disc micropunctate. Pronotum surface largely smooth, only apical part medially in front of anterior transverse impression and basal area medially behind posterior transverse impression longitudinally wrinkled; basal foveae and adjacent lateral areas mostly smooth, rarely shallowly punctate. Elytral intervals with very superficial and scattered punctures, or without such ones. Abdominal ventrites 1–3 finely wrinkled. **Head.** About one-third or more as wide as pronotum (PW/HW= 1.27–1.38). Eyes long, slightly to moderately convex. Labrum subrectangular, shorter than clypeus, with anterior margin concave medially. Frontoclypeal suture distinct in middle, reduced to disappeared at sides. Frontal furrows small, punctiform. Paraorbital sulci fine, backward surpassing posterior margin of eye, almost reaching level of posterior supraorbital pore. **Thorax.** Pronotum one tenth to one fifth wider than long (PW/

PL= 1.11–1.22), with widest point at second quarter. Anterior transverse impression absent, posterior transverse impression barely distinct. Sides sinuate, convex medially and anteriorly, straight to slightly concave posteriorly; anterior bead present laterally, lack or present in medial tenth; basal bead present laterally, reduced to absent in medial third to medial half. Metepisternum slightly longer than wide, MA/MI= 0.87–0.95. **Elytra.** Elongate, about one-and-a-half times or little more as long as elytra (EL/EW= 1.52–1.62), two-and-a-half-times as long as pronotum (EL/PL= 2.42–2.60), and a third to a half as wide as pronotum (EW/PW= 1.29–1.48), with widest point at medial third or third quarter. Parascutellar striae short, less impressed than other striae, not joining stria 1; striae 1–8 and striae superficially punctate; base of stria 1 ending in parascutellar pore, striae 2–6 reaching or not reaching basal bead, 7 ending before basal bead. Interval 3 with three discal setiferous punctures, as location of first varies (adjacent to stria 3, in midst of interval 3, or adjacent to stria 2). Umbilicate setiferous series mostly with 16 punctures on each elytron. **Legs.** Posterior side of profemur with one or two setae in basal third and one or two in medial third. Mesofemur mostly with 5 setiferous punctures on anterior side ventrally (Fig. 5I). Anterior side of metafemur ventrally with a few long setae, one in basal third and one to three in apical half. **Male genitalia.** Urite IX subovate to subtriangular, with proximal margin nearly symmetrical and subacuminate at apex (Fig. 7L, M). Median lobe of aedeagus in lateral view slender, with long and narrow basal bulb, long and broader shaft, and short, almost straight apex, as angle between front and rear halves relatively small (Fig. 9G, H); median lobe in ventral view straight, 3.5–

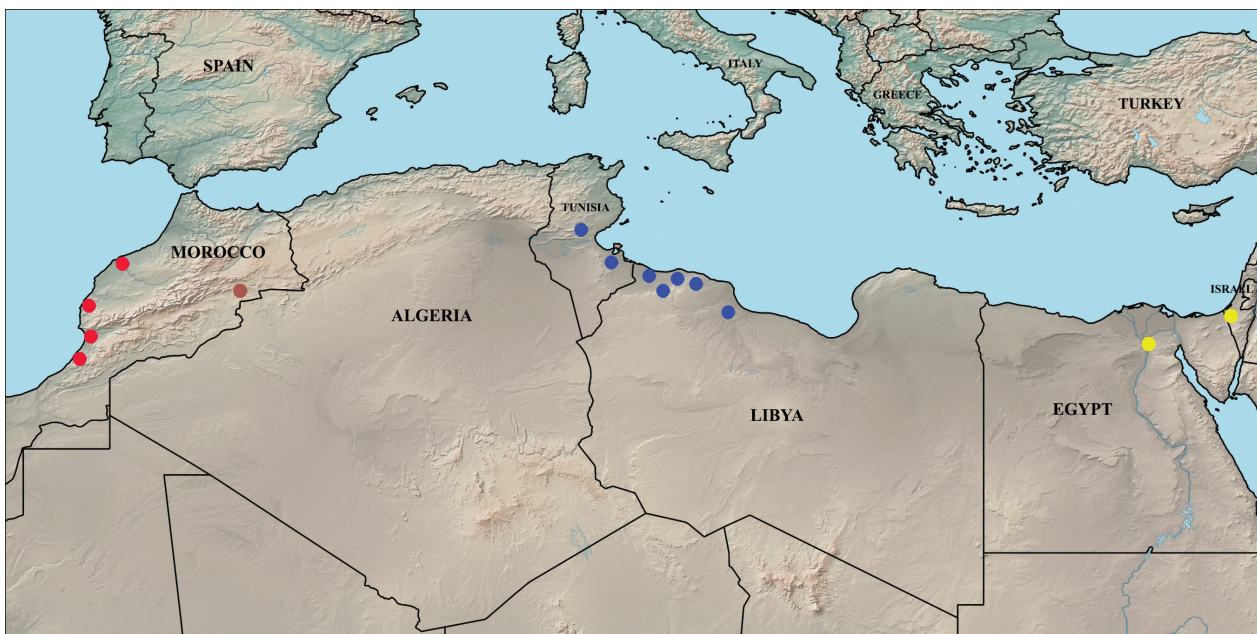


Figure 18. Distribution of species from subgenus *Eremoderus* in continental North Africa and the southern Levant: *Platyderus brunneus brunneus* (blue circles), *P. brunneus ferrantei* (yellow circles), *P. insignitus insignitus* (red circles), and *P. insignitus presaharensis* (brown circle).

3.7 times longer than wide; apical lamella (dorsal view) short, nearly symmetrical, rounded at tip, with right side straight to convex and left side barely concave. Internal sac in lateral view (Fig. 9G, H) with ventral sclerite broadened and rounded distally; same in ventral view (Fig. 11F, G), with dorsal sclerite large, reticulate, with lateral protuberances distinct, and ventral sclerite narrow and nearly straight. Right paramere as on Fig. 12M, N. **Female genitalia** (Fig. 15F). Apical gonocoxite semi-pointed apex and one dorsolateral ensiform seta. Spermathecal canal connected in basal third of receptaculum.

Comparisons. *P. languidus* and *P. jordanensis* sp. nov. differ in characters noted in “Diagnosis” under the latter species.

P. languidus distinguishes from both *P. brunneus* and *P. irakensis* sp. nov. by meso- and metatarsomeres dorsally neither flattened nor grooved (vs. meso- and metatarsomeres dorsally more or less flattened and grooved), see Fig. 6E. Additionally, it is distinct from *P. brunneus* in the pronotum less cordate, with sides less concave and less constricted toward base. The species differs from *P. irakensis* sp. nov. by the less long elytra compared to the length of the elytra and pronotum (EL/EW: 1.52–1.62 and EL/PL: 2.42–2.60, vs. EL/EW: 1.62–1.63 and EL/PL: 2.65–2.72).

Habitat. The records from the Coastal Lowlands of Israel refer to dune habitats close to the shores of the Mediterranean Sea. *Platyderus languidus* co-occurs there together with *Carabus impressus* Klug, 1832, *Masoreus aegyptiacus* Dejean, 1828, *Graphipterus sharonae* Renan & Assmann, 2018, and some eurytopic ground

beetle species (see habitat characterization in Assmann et al. 2008, 2015a; Renan et al. 2018). Photographs of this type of habitat are given in Assmann et al. (2008, fig. 17, p. 17, 2015a, fig. 8b, p. 63) and Renan et al. (2018, fig. 15, p. 63). The other habitats in Nahal Prat (= Wadi Kelt) must differ from these ones as there are no typical dune habitats.

Distribution. *Platyderus languidus* was cited for Morocco, Libya, Egypt (incl. Sinai), Syria and Israel (Jedlička 1963: 22; Hovorka 2017: 756). Machard (2017: 102, 2019: 199) included it in the list of the Moroccan Carabidae noting that its “Présence au Maroc non confirmée”. The review of published and new material showed that the species does not live in Africa. All examined material of *Platyderus* (*Eremoderus*) from Tunisia, Libya and Egypt should be referred to *P. brunneus* (see above). The species records of *P. languidus* for Morocco are also based on former misinterpretations and should concern *P. insignitus*. Certainly occurs only in Israel (Fig. 19). May live also in the southernmost area of Syria.

Notes. Léon Fairmaire described his *Sphodrus parumstriatus* without indication of an exact locality. This author mentioned only that it comes from “La localité qu’il habite est inconnue, mais il est plus que probable qu’il appartient à la faune méditerranéenne”. Later on, Bedel (1906: 91) established the synonymy of *S. parumstriatus* with *Feronia languida* and stated: “Le type, dont la provenance restait ignorée, provient manifestement des récoltes de F. de Saulcy en Palestine. J’ai pu l’examiner grâce à l’extrême amabilité de M. J. Magnin, son possesseur actuel”. In

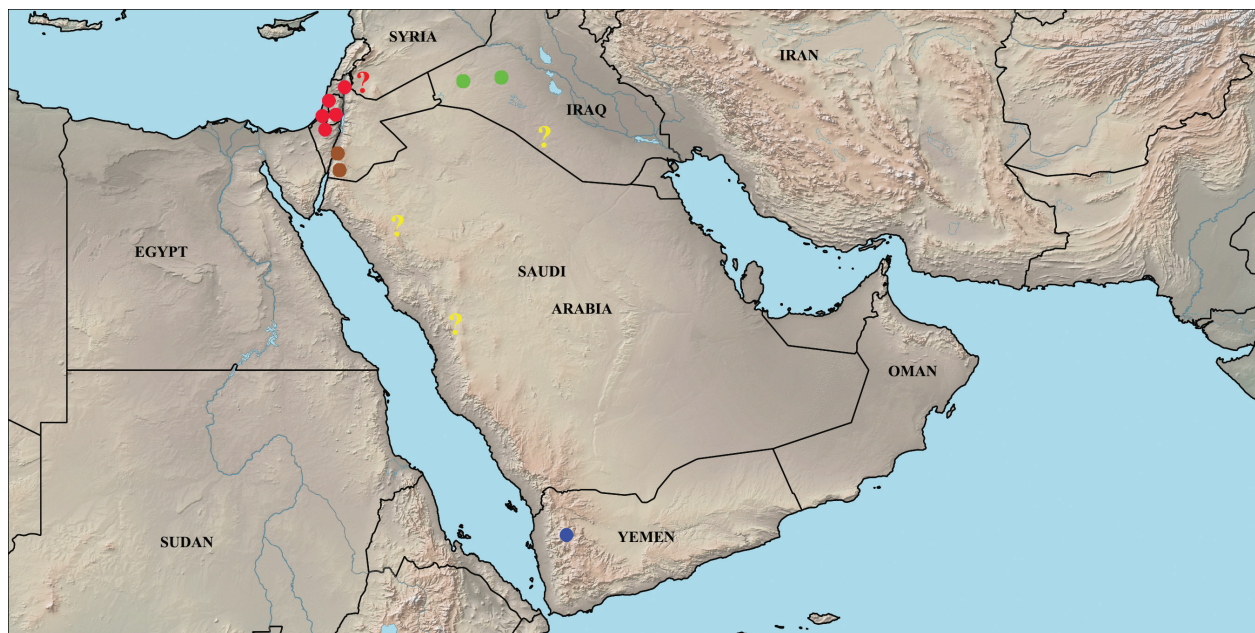


Figure 19. Distribution of species from subgenus *Eremoderus* in the Levant and the Arabian Peninsula: *Platyderus arabicus* sp. nov. (yellow question marks), *P. brunki* sp. nov. (blue circle), *P. irakensis* sp. nov. (green circles), *P. jordanensis* sp. nov. (brown circles), and *P. languidus* (red circles).

2016, one of us (BG) looked for the type material of *S. parumstriatus* in MNHN, a depository where the ex-collection of L. Fairmaire is housed now, but nothing has been found. Subsequently, in a correspondence with BG (pers. comm.), Dr. Th. Deuve said: “*Nous n’avons pas la collection Magnin et j’ignore où elle se trouve. Certains spécimens ont pu être dispersés et pourraient être dans la collection du Muséum, mais je ne connais pas le type de Sphodrus parumstriatus Fairmaire. De toute façon, les types de Fairmaire sont*

toujours très difficile à trouver. En général, nous n’en retrouvons que 50%”.

It is worth noting that the distance between the closest known localities of *P. brunneus ferrantei* and *P. languidus* in south Israel, respectively Holot Haluza (being the northeasternmost locality of the former species) and Ashkelon (being the southwesternmost one of the latter species), is about 65 km in a straight line. By supposition, the two species occur in different types of habitats.

Key to the male specimens of subgenus *Eremoderus* Jeanne from Africa and Southwest Asia

(key does not include *P. davatchii* Morvan, for which diagnostic characters remain unstudied)

- 1 Ventral sclerite of internal sac obliquely situated with respect to main axis of median lobe (ventral view) and distinctly bent in middle (lateral view) (Figs 8A, B, 10A, B) (“*weiratheri*” species group)..... 2
- Ventral sclerite of internal sac parallel to main axis of median lobe (ventral view) and straight (lateral view) (Figs 8C–I, 9B–H, 10C–I, 11A–G)..... 3
- 2 Width of body more than 2.7 mm. Elytra length / pronotum length small (EL/PL= 2.50 or less; Table 1). Anterior discal puncture in midst of elytral interval 3..... *Platyderus (Eremoderus) chatzakiae* sp. nov.
- Width of body less than 2.7 mm. Elytra length / pronotum length large (EL/PL= 2.55–2.83; Table 1). Anterior discal puncture adjoining elytral stria 3..... *Platyderus (Eremoderus) weiratheri* Mañan, 1940
- 3 Ventral sclerite of internal sac of median lobe (lateral view) significantly widened anteriorly, three and more times wider at distal 1/3 than at proximal 1/3 (Fig. 8C–F). Prosternum laterally and proepisternum coarsely and densely punctate (“*iranicus-vanensis*” species group) 4
- Ventral sclerite of internal sac of median lobe (lateral view) slightly widened anteriorly, a half to two times wider at distal 1/3 than at proximal 1/3 (Figs 8G–I, 9B–H). Prosternum laterally and proepisternum less coarsely and scarcely punctate 7
- 4 Size of body small (< 6.7 mm), except for *P. felixi* sp. nov. with EL/EW <1.6. Parascutellar striola and striae 1–8 finely punctate (Fig. 1C, D). Right paramere short, considerably crooked ventrally (Fig. 12C, D). Specimens from Iran..... 5
- Size of body large (> 6.7 mm), with EL/EW >1.6. Parascutellar striola and striae 1–8 moderately to coarsely punctate (Figs 1E, F, 2A). Right paramere long, less crooked ventrally (Fig. 12E). Specimens from Turkey 6
- 5 Pronotum narrow compared to head (PW/HW ≤1.45). Elytra more considerably wider than long (EL/EW ≥1.55). Small specimens (BL= 4.30–6.65 mm) *Platyderus (Eremoderus) iranicus* sp. nov.
- Pronotum wide compared to head (vs. PW/HW ≥ 1.45). Elytra less considerably wider than long (EL/EW ≤1.55, vs. EL/EW ≥1.55). Large specimens (BL= 6.00–7.00 mm) *Platyderus (Eremoderus) felixi* sp. nov.
- 6 Color light, rusty red. Elytral striae and striola less coarsely and deeply punctate (Fig. 1F); all intervals with distinct sculpticells. Apical lamella of median lobe (dorsal and ventral view) more symmetrical and somewhat shorter (Fig. 10F)..... *Platyderus (Eremoderus) vrabeci* sp. nov.
- Color dark reddish-brown (some specimens with elytra entirely black). Elytral striae and striola coarsely and deeply punctate (Fig. 1E); only intervals 6–9 with more or less distinct sculpticells. Apical lamella of median lobe (dorsal and ventral view) partly asymmetrical and somewhat more elongate (Fig. 10E)..... *Platyderus (Eremoderus) vanensis* sp. nov.
- 7 Basal foveae of pronotum and adjacent lateral areas as well as mesepisternum, metasternum laterally and metepisternum moderately punctate (Fig. 2B–E). Ventral sclerite of internal sac (ventral view) with distal end curved to left (Fig. 10G–I). Specimens from North Iran..... 8
- Basal foveae of pronotum and adjacent lateral areas as well as mesepisternum, metasternum laterally and metepisternum scarcely punctate to impunctate (Figs 3A–F, 4A–E). Ventral sclerite of internal sac (ventral view) with distal end straight throughout or curved to left (Fig. 11A–G). Specimens from other countries..... 11
- 8 Body (excl. appendages) black. Pronotum sides toward base nearly straight to slightly concave. Dorsal surface of head and base of pronotum with extensive and denser punctation. Median lobe of aedeagus less than those of the species of “*davatchii*” species group curved ventrally, with apex not turned upward (lateral view). Length of body: 8.00–8.50 mm *Platyderus (Eremoderus) lassallei* sp. nov.
- Body (excl. appendages) light to dark brown. Pronotum sides toward base significantly concave. Dorsal surface of head and base of pronotum with less extensive and sparser. Median lobe of aedeagus more curved ventrally, with apex somewhat turned upward (lateral view) (“*davatchii*” species group). Length of body less than 8.00 mm)..... 9

- 9 Pronotum in relation to head less wide (PW/HW= 1.27; Fig. 2C). Small specimens (BL less than 7 mm) *Platyderus (Eremoderus) klapperichi* sp. nov.
- Pronotum in relation to head wider (PW/HW >1.30; Fig. 2D, E). Large specimens (BL more than 7 mm) 10
- 10 Pronotum in relation to head wider (PW/HW >1.40), with apex compared with widest point more constricted (PW/PA >1.40). Elytra in relation to pronotum narrower (EW/PW <1.38). Anterior side of mesofemur ventrally with four setiferous punctures *Platyderus (Eremoderus) ledouxi* Morvan, 1974
- Pronotum in relation to head less wide (PW/HW= 1.31–1.33), with apex compared with widest point less constricted (PW/PA <1.40). Elytra in relation to pronotum wider (EW/PW >1.38). Anterior side of mesofemur ventrally with three setiferous punctures..... *Platyderus (Eremoderus) taghizadehi* Morvan, 1974
- 11 Disc of head and pronotum with reduced sculpticells. Pronotum wider (PW/PL >1.22, Table 2), with basal beads present throughout. Elytra in relation to pronotum longer (EL/PL =2.78). Specimens from Afghanistan *Platyderus (Eremoderus) afghanisticus* sp. nov.
- Disc of head and pronotum with complete microreticulation. Pronotum narrower (PW/PL ≤1.22), with basal bead reduced to absent in basal third to half. Elytra in relation to pronotum shorter (EL/PL <2.75). Specimens from other countries (“*languidus*” species group) 12
- 12 Meso- and metatarsomeres dorsally convex and smooth (Fig. 6D). Tips of posterior angles protruding laterally (Fig. 4C). Ventral margin of apex of median lobe evidently convex thus apex appears slightly bent up (Fig. 9F)..... *Platyderus (Eremoderus) jordanensis* sp. nov.
- Metatarsomeres dorsally convex or not (Fig. 6A, B, E). Ventral margin of apex of median lobe straight to apex (Fig. 9C–E, G, H)..... 13
- 13 Meso- and metatarsomeres dorsally somewhat flattened and slightly grooved (Fig. 6A, B) 14
- Meso- and metatarsomeres dorsally convex and not grooved (Fig. 6E)..... 15
- 14 Parascutellar striola and elytral striae 1–7 very shallow, nearly indistinct, with bases more or less reduced, not reaching basal bead. Width of pronotum posterior margin usually large compared to pronotum maximum width and width of anterior margin (PW/PB >1.1, PA/PB >0.88, Table 3) *Platyderus (Eremoderus) brunneus brunneus* Karsch, 1881
- Parascutellar striola and elytral striae 1–7 distinct, slightly impressed, with bases reaching basal bead. Width of pronotum posterior margin usually small compared to pronotum maximum width and width of anterior margin (PW/PB <1.23, PA/PB <0.89, Table 3) *Platyderus (Eremoderus) brunneus ferrantei* Reitter, 1909
- 15 Median lobe of aedeagus with basal bulb shorter and ventral sclerite of internal sac longer (Figs 9E, 11D). Disc of head impunctate. Specimens from Morocco..... *Platyderus (Eremoderus) insignitus* Bedel, 1902
- Median lobe of aedeagus with basal bulb longer and ventral sclerite of internal sac short (Figs 9G, H, 11F, G). Disc of head mostly micropunctate. Specimens from Syria and Israel..... *Platyderus (Eremoderus) languidus* (Reiche & Saulcy, 1855)

Key to the female specimens of subgenus *Eremoderus* Jeanne from Africa and Southwest Asia

(key does not include *P. davatchii* Morvan, for which diagnostic characters remain unstudied)

- 1 Pronotal disc with coarse and dense punctuation on basis that at sides reaches anterior half (Fig. 1C–F). Specimens from East Turkey or West- and Southwest Iran 2
- Pronotal disc with less coarse and dense punctuation on basis which usually does not reach anterior half (Fig. 1B, 2AC–E, 3A–F, 4A–E). Specimens from West Turkey (Western Toros Mts.), North Iran and other countries 5
- 2 Parascutellar striola and striae 1–8 less finely punctate impressed (Fig. 1C, D). Specimens from Iran 3
- Parascutellar striola and striae 1–8 moderately to coarsely punctate and impressed (Figs 1E, F, 2A). Specimens from Turkey 4
- 3 Pronotum narrower compared to head (PW/HW ≤1.45). Elytra more considerably wider than long (EL/EW ≥1.55). Small specimens, 4.30–6.65 mm *Platyderus (Eremoderus) iranicus* sp. nov.
- Pronotum wide compared to head (vs. PW/HW ≥ 1.45). Elytra less considerably wider than long (EL/EW ≤1.55, vs. EL/EW ≥1.55). Large specimens, 6.00–7.00 mm..... *Platyderus (Eremoderus) felixi* sp. nov.
- 4 Elytral striae and striola less coarsely and deeply punctate (Fig. 1F); all intervals with distinct sculpticells. Color light, rusty red *Platyderus (Eremoderus) vrabeci* sp. nov.
- Elytral striae and striola coarsely and deeply punctate (Fig. 1E); only intervals 6–9 with more or less distinct sculpticells. Color dark reddish-brown (some specimens with elytra entirely black)..... *Platyderus (Eremoderus) vanensis* sp. nov.
- 5 Specimens from Western Toros Mts., Southwest Turkey *Platyderus (Eremoderus) weiratheri* Mařan, 1940
- Specimens from other regions and countries 6
- 6 Base of pronotum and adjacent lateral areas (Fig. 2B–E), mesepisternum, metasternum laterally and metepisternum more coarsely and densely punctate. Specimens from North Iran 7
- Base of pronotum and adjacent lateral areas (Figs 3A–F, 4A–E), mesepisternum, metasternum laterally and metepisternum finely and scarcely punctate to impunctate. Specimens from other countries..... 10

- 7 Body (excl. appendages) black. Pronotum sides toward base nearly straight to slightly concave. Dorsal surface of head and base of pronotum with extensive and denser punctation. Length of body: 8.00–8.50 mm *Platyderus (Eremoderus) lassallei* sp. nov.
- Body (excl. appendages) light to dark brown. Pronotum sides toward base significantly concave. Dorsal surface of head and base of pronotum with less extensive and sparser punctation. Length of body less than 8.00 mm 8
- 8 Pronotum in relation to head less wide (PW/HW= 1.27; Fig. 2C). Small specimens, <7 mm *Platyderus (Eremoderus) klapperichi* sp. nov.
- Pronotum in relation to head wider (PW/HW >1.30; Fig. 2D, E). Large specimens, >7 mm 9
- 9 Pronotum in relation to head wider (PW/HW >1.40), with apex compared with widest point more constricted (PW/PA >1.40). Anterior side of mesofemur ventrally with four setiferous punctures *Platyderus (Eremoderus) ledouxi* Morvan, 1974
- Pronotum in relation to head less wide (PW/HW= 1.31–1.33), with apex compared with widest point less constricted (PW/PA <1.40). Anterior side of mesofemur ventrally with three setiferous punctures *Platyderus (Eremoderus) taghizadehi* Morvan, 1974
- 10 Color reddish brown. Pronotum with sides to base straight or slightly convex; posterior angles not projecting laterally (Fig. 3B, C). Specimens from the Arabian Peninsula 11
- Color orange brown. Pronotum either with sides to base slightly convex to base; posterior angles not projecting laterally (Fig. 4B) or with sides to base straight or slightly concave and posterior angles projecting laterally (Figs 3D, F, 4A–E). Species from North Africa, Israel, Jordan and Iraq 12
- 11 Pronotum nearly as long as wide (PW/PL= 1.02–1.05), less constricted anteriorly (PW/PA= 1.38–1.42), PA/PB large (Table 3). Apical gonocoxite with two dorsolateral ensiform setae (Fig. 14F) *Platyderus (Eremoderus) brunki* sp. nov.
- Pronotum slightly wider than long (PW/PL= 1.07–1.11), more constricted anteriorly (PW/PA= 1.44–1.48), PA/PB small (Table 3). Apical gonocoxite with one dorsolateral ensiform seta (Fig. 14D) *Platyderus (Eremoderus) arabicus* sp. nov.
- 12 Pronotum less constricted toward base (PW/PB ≤1.11), with sides weakly convex; posterior angles rounded, laterally not prominent (Fig. 4B). Bursa copulatrix long, with apical enlargement (Fig. 15D). Specimens from Iraq *Platyderus (Eremoderus) irakensis* sp. nov.
- Pronotum more constricted toward base (PW/PB >1.10), with sides straight or slightly concave; posterior angles rounded, laterally prominent or not. Bursa copulatrix short, without apical enlargement (Fig. 15A–C, E, F). Specimens from other countries 13
- 13 Meso- and metatarsomeres dorsally convex and smooth (Fig. 6D). Tips of pronotal posterior angles protruding laterally (Fig. 6D) *Platyderus (Eremoderus) jordanensis* sp. nov.
- Metatarsomeres dorsally convex or not (Fig. 6A, B, E) 14
- 14 Meso- and metatarsomeres dorsally somewhat flattened and slightly grooved (Fig. 6A, B) 15
- Meso- and metatarsomeres dorsally convex and not grooved (Fig. 6E) 16
- 15 Parascutellar striola and elytral striae 1–7 very shallow, nearly indistinct, with bases more or less reduced, not reaching basal bead. Width of pronotum posterior margin usually large compared to pronotum maximum width and width of anterior margin (PW/PB >1.1, PA/PB >0.88, Table 3) *Platyderus (Eremoderus) brunneus brunneus* Karsch, 1881
- Parascutellar striola and elytral striae 1–7 distinct, slightly impressed, with bases reaching basal bead. Width of pronotum posterior margin usually small compared to pronotum maximum width and width of anterior margin (PW/PB <1.23, PA/PB <0.89, Table 3) *Platyderus (Eremoderus) brunneus ferrantei* Reitter, 1909
- 16 Disc of head impunctate. Specimens from Morocco *Platyderus (Eremoderus) insignitus* Bedel, 1902
- Disc of head mostly micropunctate. Specimens from Israel and Syria *Platyderus (Eremoderus) languidus* (Reiche & Saulcy, 1855)

Discussion

While the taxonomic status of *Eremoderus* remained questionable, being insufficiently defined by a taxonomic point (see ‘Introduction’), new and interesting material from species supposedly belonging to it was collected and made available for study. The subsequent analysis shows that the group is considerably homogeneous and *Eremoderus* deserves to be treated as a separate subgenus.

At least four character states determine *Eremoderus* as a separate group distinct from *Platyderus* (s. str.): (1) ventral sclerite of median lobe of aedeagus in shape of an elongated drop at lateral view, straight, narrow and elongate at ventral view (Figs 8A–I, 9B–H, 10A–I, 11A–G), (2) seminal canal and receptaculum of comparable lengths

(Figs 13A–F, 14A–C, E, F, 15A–F), (3) ventral margin of anterior side of mesofemur with four or more, rarely three setiferous punctures ventrally (Fig. 5A–I), and (4) proximal margin appearing to be “apex” of urite IX symmetrical or nearly symmetrical (Fig. 7A–M). The corresponding states of the four characters in the nominotypical subgenus are, as follows: (1) ventral sclerite of median lobe S-shaped at lateral view, plate-like, wide in ventral view (Figs 8J, 9A, 10J, K), (2) spermathecal canal one-and-a-half to about three times longer than the spermatheca (Fig. 14D), (3) ventral margin of anterior side of mesofemur mostly with two, rarely three such punctures, and (4) proximal margin of urite IX clearly asymmetrical, turned to left (Fig. 7N, O). Forthcoming revisions of selected groups of *Platyderus* s. str. will confirm or reject

whether these traits are well-evaluated, and potentially reveal other important differences between both groups.

Schmidt (2009: 138) discussed the number of the setiferous punctures on the ventral margin of mesofemur from a phylogenetic perspective expressing two different, mutually exclusive one another probabilities. He has supposed that the mesofemoral polysetosy may have derived several times in the genus (i.e., to be a derived state); in the same paper, however, the author speculated that it could be a plesiomorphic state in *Platyderus*. Schmidt also stated (ibid.) that the Middle Asian taxa of the genus with four or more setae “am Innenrand der Mittelschenkel” are neither related to the Atlanto-Mediterranean species groups (i.e., the groups of “*languidus*” and “*insignitus*”, sensu Jeanne 1996) nor form a common monophylum with them. However, the present study based on a great number of specimens, has revealed that the higher number of setiferous punctures on the ventral margin of the mesofemur on its anterior side is always linked, in all the examined *Eremoderus* taxa, with the other three shared traits (see above).

As a rule, the species of *Eremoderus* share three or more setiferous punctures on the ventral margin of the mesofemur on the anterior side (cfr. Jeanne 1996; present study). It is the common morphological feature useful to differentiate them from species belonging to *Platyderus* (s. str.). In fact, most species of *Eremoderus* have four or more such punctures, only specimens of *P. taghizadehi* and some specimens of *P. weiratheri* have three such punctures; these last two taxa included in species groups supposed here to be more generalized. On the other hand, the members of the nominotypical subgenus have most frequently two, rarely three setiferous punctures on the ventral margin of the mesofemur on the anterior side.

Without any comments, Hovorka and Sciaky (2003) and Hovorka (2017) listed *P. alticola*, *P. lancerottensis*, and *P. haberhaueri* in *Eremoderus*, adding them to the two species already mentioned by Jeanne (1996) (see part ‘Introduction’). Actually, the former two species were long treated as subspecies of *P. languidus* (see Bedel 1902: 214; Israelson 1990: 165–166, figs 1–6). Inclusion of *P. haberhaueri* seems more interesting since no bibliographical data were found to substantiate such an inclusion. Nevertheless, a preliminary study of unpublished material from the Central Asian species *P. haberhaueri*, *P. tadjikistanus* Kryzhanovskij, 1968 and *P. foveipennis* (Casale, 1988) showed that these taxa also belong to *Eremoderus*. The systematic position of the Chinese *P. sinensis* Casale & Sciaky, 2003 remains questionable in view of the fact that the authors stated that it is “*evidently allied to P. haberhaueri*” (Casale and Sciaky 2003: 82).

Checklist of the species of *Platyderus* (subg. *Eremoderus*)

1. *afghanistanicus*, sp. nov. Afghanistan (“Habatah”)
- 2.1. *alticola alticola* Wollaston, 1864 Canary Islands (Tenerife)

- 2.2. *alticola descendens* Bedel, 1902 Canary Islands (Gran Canaria)
- 2.3. *alticola gomerensis* Machado, 1992 Canary Islands (La Gomera)
- 2.4. *alticola hierroensis* Machado, 1992 Canary Islands (El Hierro)
3. *arabicus*, sp. nov. Saudi Arabia, ? Iraq
4. *brunki*, sp. nov. Yemen
- 5.1. *brunneus brunneus* Karsch, 1881 Tunisia, Libya = *elegans* Bedel, 1900, syn. n.
- 5.2. *brunneus ferrantei* Reitter, 1909: 29, stat. n. Egypt, Israel
6. *chatzakiae*, sp. nov. Greece (Kalimnos)
7. *davatchii* Morvan, 1970 Iran
8. *felixi*, sp. nov. Iran
9. *foveipennis* Casale, 1988 (*Pseudotaphoxenus*) Kyrgyzstan
10. *haberhaueri* Heyden, 1889 Tajikistan, Uzbekistan
- 11.1. *insignitus insignitus* Bedel, 1902 Morocco
- 11.2. *insignitus presaharensis* Lagar, 1978 Morocco
12. *irakensis*, sp. nov. Iraq
13. *iranicus*, sp. nov. Iran
14. *jordanensis*, sp. nov. Jordan
15. *klapperichi*, sp. nov. Iran
16. *lancerottensis* Israelson, 1990 Canary Islands (Lanzarote)
17. *languidus* Reiche & Saulcy, 1855 (*Feronia*) Israel, ? Syria = *parumstriatus* Fairmaire, 1872 (*Sphodrus*)
Note: Except for old published data indicating Syria, no present reliable record is known from this country.
18. *lassallei*, sp. nov. Iran
19. *ledouxi* Morvan, 1974 Iran
20. *tadjikistanus* Kryzhanovskij, 1968 Tajikistan, ? Uzbekistan
Note: Kryzhanovskij (1968: 163) cited the locality “Джар-Курган” [Dzharkurgan] as situated in SE Uzbekistan. As a populated place with the same name occurs in south Tajikistan (Khatlon Region), the species presence in the adjacent country needs confirmation.
21. *taghizadehi* Morvan, 1974 Iran
22. *vanensis*, sp. nov. Turkey
Note: A separate form southward from the populations of *P. vanensis* may exist in the Karabet Pass, which taxonomic status needs further study.
23. *vrabeci*, sp. nov. Turkey (Nemrut Dağı)
24. *weiratheri* Mařan, 1940 Turkey

Acknowledgements

For the loan of specimens of which this study is based, we are grateful to the museum curators, collection managers and private collectors enumerated above.

Bernd Jaeger (MFNB), Boris Kataev (Zoological Institute, Russian Academy of Sciences, St. Petersburg, Russia), Jose Serrano (Universidad de Murcia, Murcia, Spain), Pier Mauro Giachino (Settore Fitosanitario Regionale, Torino, Italy), Thierry Deuve (MNHN)

and Ingo Brunk (Dresden, Germany) have been very helpful in finding bibliographic references not available to us. Thierry Deuve provided information about the type material of *Sphodrus parumstriatus* Fairmaire. Ingo Brunk, Maria Chatzaki (Democritus University of Thrace, Komotini, Greece), Bernard Lassalle (Boissy-les-Perche, France), Christoph Reuter (Hamburg, Germany) and Vladimir Vrabec (Czech University of Life Sciences Prague, Prague, Czech Republic) are highly appreciated for providing information about the type localities of some species. TA and DW thank the colleague Prof. Dr. Fares Khoury (American University of Ma'dabā, Ma'dabā, Jordan) for his collaboration and generous support of this work.

We extend our hearty thanks to James K. Liebherr (Cornell University, Ithaca, USA), Achille Casale (University of Sassari, Sassari, Italy), Joachim Schmidt (University of Rostock, Rostock, Germany), and Kipling W. Will (Essig Museum of Entomology, Berkeley, USA) for their very helpful comments and remarks on the penultimate draft of our work. We are grateful for their considerable efforts, which led to a substantially improved manuscript.

The European Union-funded Integrated Infrastructure Initiative “Synthesys” supported the work of BG in various EU national history institutions (applications AT-TAF–1470, DE-TAF–1568, FR-TAF–2938, GB-TAF–4263, NL-TAF–4177 and PL-TAF–4042).

References

- Abdel-Dayem MS (2012) An annotated checklist of the endemic Carabidae (Coleoptera) of Egypt. *Check List* 8(2): 197–203. <https://doi.org/10.15560/8.2.197>
- Anichtchenko A (2005) Nuevas especies de *Platyderus* Stephens, 1828 (Coleoptera, Carabidae) de España. *Boletín de SAE* 12: 31–45.
- Anichtchenko A (2011) Contribution to the knowledge [sic!] of *Platyderus* Stephens, 1827 (Coleoptera, Carabidae) from Spain. *Baltic Journal of Coleopterology* 11: 33–39.
- Anichtchenko A (2012) New species of *Platyderus* Stephens, 1827 (Coleoptera, Carabidae) from North Spain. *Baltic Journal of Coleopterology* 12: 99–104.
- Antoine M (1957) Coléoptères carabiques du Maroc (deuxième partie). *Mémoires de la Société des Sciences Naturelles et Physiques du Maroc* (N.S., Zoologie) 3: 179–314.
- Assmann T, Buse J, Drees C, Friedman ALL, Levanony T, Matern A, Timm A, Wrase DW (2008) The *Carabus* fauna of Israel – updated identification key, faunistics, and habitats (Coleoptera: Carabidae). *ZooKeys* 1: 9–22. <https://doi.org/10.3897/zookeys.1.23>
- Assmann T, Boutaud E, Buse J, Chikatunov V, Drees C, Friedman ALL, Härdtle W, Homburg K, Levanony T, Marcus T, Renan I, Wrase DW (2015a) The ground beetle tribe Cyclosomini (Coleoptera, Carabidae) in Israel. *Spixiana* 38(1): 49–69.
- Assmann T, Austin K, Boutaud E, Buse J, Chikatunov V, Drees C, Felix RFFL, Friedman ALL, Marcus T, Renan I, Schmidt C, Wrase DW (2015b) The ground beetle supertribe Zuphiitae in the southern Levant (Coleoptera: Carabidae). *Spixiana* 38(2): 237–262.
- Azadbakhsh S, Nozari J (2015) Checklist of the Iranian Ground Beetles (Coleoptera: Carabidae). *Zootaxa* 4024(1): 1–108. <https://doi.org/10.11646/zootaxa.4024.1.1>
- Bedel L (1900) Description d'un *Platyderus* nouveau (Col.) de la Tunisie méridionale. *Bulletin de la Société Entomologique de France* 1900: e170. <https://doi.org/10.3406/bsef.1900.22589>
- Bedel L 1902. *Catalogue raisonné des Coléoptères du nord de l'Afrique* (Maroc, Algérie, Tunisie et Tripolitaine) avec notes sur la faune des îles Canaries et de Madère, première partie. *Société Entomologique de France*, Paris, 209–220.
- Bedel L (1906) Communications. Synonymies de Coléoptères paléarctiques. *Bulletin de la Société Entomologique de France* 1906(8): 91–93. <https://doi.org/10.3406/bsef.1906.23895>
- Casale A (1988) Revisione degli *Sphodrina* (Coleoptera, Carabidae, Sphodrini). *Museo Regionale di Scienze Naturali, Monografie V*, Torino, 1024 pp.
- Casale A, Assmann T (2017) The *Sphodrina* of the southern Levant (Coleoptera: Carabidae, Sphodrini). *Fragmenta Entomologica* 49(1): 13–24. <https://doi.org/10.4081/fe.2017.226>
- Casale A, Sciaky R (2003) A second *Dimorphopatrobus* species from Tibet, and the first Eastern Himalayan *Platyderus* species from Sichuan (China) (Insecta: Coleoptera: Carabidae: Patrobini et Sphodrini). In: Hartmann M, Baumbach H (Eds) *Biodiversität und Naturausstattung im Himalaya*. Verein der Freunde & Förderer des Naturkundemuseums Erfurt e. V., Erfurt, 79–83.
- Csiki E (1931) Carabidae: Harpalinae V (Pars 115). In: Junk W, Schenkling S (Eds) *Coleopterorum catalogus*. Volumen II. Carabidae II. W. Junk, Berlin, 739–1022.
- de Chaudoir M (1866) Monographie du genre *Platyderus*. *Annales de la Société Entomologique de France* 6(4): 105–115.
- Fairmaire L (1872) Diagnoses et synonymies de divers coléoptères. *Annales de la Société Entomologique de France* 2(5): 47–48.
- Guéorguiev B (2009) Three new species of *Platyderus* from South Italy (Coleoptera: Carabidae: Sphodrini). *Zootaxa* 2268: 41–51. <https://doi.org/10.11646/zootaxa.2268.1.3>
- Hanley RS, Ashe JS (2003) Techniques for dissecting adult aleocharine beetles (Coleoptera: Staphylinidae). *Bulletin of Entomological Research* 93: 11–18. <https://doi.org/10.1079/BER2002210>
- Hovorka O (2017) *Atranopsina* Baehr, 1982. In: Löbl I, Löbl D (Eds) *Catalogue of Palaearctic Coleoptera*. Volume 1 Revised and Updated Edition. Archostemata – Myxophaga – Adepaga. Brill, Leiden – Boston, 755–760.
- Hovorka O, Sciaky R (2003) *Atranopsina* Baehr, 1982. In: Löbl L, Smetana A (Eds) *Catalogue of Palaearctic Coleoptera*. Volume 1. Archostemata – Myxophaga – Adepaga. Apollo Books, Stenstrup, 521–524.
- ICZN [International Commission on Zoological Nomenclature] (1999) *International Code on Zoological Nomenclature*. 4th Edn. Adopted by the International Union of Biological Sciences. International Trust for Zoological Nomenclature, London. <https://www.iczn.org/the-code/the-code-online/>
- Israelson G (1990) A *Platyderus* Stephens (Col., Carabidae) from Lanzarote, Canary Islands. *Vieraea* 19: 165–167.
- Jeanne C (1996) Le genre *Platyderus* Stephens: I. – Espèces nouvelles de la péninsule Ibérique (Coleoptera, Pterostichidae). *Bulletin de la Société Entomologique de France* 101(4): 397–412. <https://doi.org/10.3406/bsef.1996.17271>
- Jedlička A (1963) Neue Carabiden aus Anatolien und vom Balkan. *Koleopterologische Rundschau* 40–41(1962–1963): 16–22.

- JCR (2004) *Platyderus (Eremoderus) languidus* Reiche & Saulcy, 1855. http://jcringenbach.free.fr/website/beetles/carabidae/Platyderus_languidus.htm
- Karsch F (1881) Die Käfer der Rohlf'schen Afrikanischen Expedition 1878–79. Berliner Entomologische Zeitschrift 25: 41–50. [+ i pl] <https://doi.org/10.1002/mmnd.18810250108>
- Kryzhanovskij OL (1968) Novye i maloizvestnye zhuzhelitsy (Coleoptera, Carabidae) fauny SSSR i granichashchikh s nim stran. Entomologicheskoe Obozrenie 47: 160–175.
- Lagar Mascaró A (1978) Un nuevo *Platyderus* del Marroc. Coleoptera Pterostichidae. Excursionisme. Bulletin de la Unió Excursionista de Catalunya 41: 19–20.
- Lindroth CH (1956) A revision of the genus *Synuchus* Gyllenhal (Coleoptera: Carabidae) in the widest sense, with notes on *Pristosia* Motschulsky (Eucalathus Bates) and *Calathus* Bonelli. Transactions of the Royal Entomological Society of London 108: 485–576. <https://doi.org/10.1111/j.1365-2311.1956.tb01274.x>
- Lohaj R, Mlejnek R (2007) Two new species of *Laemostenus (Antisphodrus)* (Coleoptera: Carabidae) from Turkey and Syria. Acta Societatis Zoologicae Bohemicae 71: 7–14.
- Lorenz W (1998) Nomina Carabidarum – a directory of the scientific names of ground beetles (Insecta, Coleoptera “Geadephaga”: Trachypachidae and Carabidae incl. Paussinae, Cicindelinae, Rhysodidae). First edition. Wolfgang Lorenz, Tutzing, [ii +] 502 pp.
- Lorenz W (2005) Systematic list of extant ground beetles of the world (Insecta Coleoptera “Geadephaga”: Trachypachidae and Carabidae incl. Paussinae, Cicindelinae, Rhysodinae). Second Edition. Wolfgang Lorenz, Tutzing, [ii +] 530 pp.
- Machado A (1992) Monografía de los carábidos de las Islas Canarias (Insecta, Coleoptera). Instituto de Estudios Canarios, La Laguna, 734 pp.
- Machard P (2017) Un *Platyderus* nouveau du Maroc (Coleoptera, Carabidae). Coleopterist 20(2): 101–102.
- Machard P (2019) Catalogue des Coléoptères Carabiques du Maroc (Coleoptera, Carabidae). Coleopterist 21(3): 183–203.
- Machard P (2020) Dans le genre *Platyderus* Stephens, 1827: Description de deux espèces nouvelles (Coleoptera, Carabidae). Coleopterist 23(2): 107–112.
- Mařan J (1940) Nový druh rodu *Platyderus* Schaum z Malé Asie. Speciei novae generis *Platyderus* Schaum ex Asia minore descriptio (Coleopt. Carabidae). Časopis Československé Společnosti Entomologické 37: 25–26.
- Morvan P (1970) Contribution à la connaissance des coléoptères carabiques de l'Iran. Bulletin de la Société Entomologique de France 74 (1969): 192–198. <https://doi.org/10.3406/bsef.1969.21081>
- Morvan P (1974) Nouveaux coléoptères carabiques d'Iran (6eme note). Journal of Entomological Society of Iran 1: 143–156.
- Ortuño VM, Gilgado JD (2010) Update of the knowledge of the Ibero-Balearic hypogean Carabidae (Coleoptera): Faunistics, biology and distribution. Entomologische Blätter 106: 233–264.
- Piochard de la Brûlerie CJ (1876) Catalogue raisonné des coléoptères de la Syrie et de l'île de Chypre. 1^{re} partie (suite). Annales de la Société Entomologique de France [5] 5(1875): 395–448.
- Reiche L, Saulcy F (1855) Espèces nouvelles ou peu connues de coléoptères, recueillies par M. F. de Saulcy, membre de l'Institut, dans son voyage en Orient, et décrites par M.M. L. Reiche et Félix de Saulcy. Annales de la Société Entomologique de France 3: 561–645. [troisième série]
- Reitter E (1909) Espèces nouvelles de coléoptères égyptiens. Bulletin de la Société Entomologique d'Égypte 1: 29–32.
- Renan I, Assmann T, Friedberg A (2018) Taxonomic Revision of the *Graphipterus serrator* (Forskål) group (Coleoptera, Carabidae): An increase from five to 15 valid species. ZooKeys 753: 23–82. <https://doi.org/10.3897/zookeys.753.22366>
- Ruiz-Tapiador I, Anichtchenko A (2007) New species of *Platyderus* Stephens, 1827 (Coleoptera, Carabidae) from Iberian peninsula. Baltic Journal of Coleopterology 7: 185–190.
- Sahlberg JR (1903) Coleoptera Levantina mensibus Februario et Martio 1896 in Palaestina et Aegypto inferiore collecta. Öfversigt af Finska Vetenskaps-Societetens Förhandlingar 45[1902–1903](18): 1–36.
- Schmidt J (2009) *Platyderus anandi* n. sp., ein Tertiärrelikt im zentralen Nepal-Himalaya (Insecta: Coleoptera: Carabidae: Sphodrini). In: Hartmann M, Weipert J (Eds) Biodiversität und Naturlandschaft im Himalaya III. Verein der Freunde & Förderer des Naturkundemuseums Erfurt e. V., Erfurt, 137–140.
- Serrano J (2003) Catalogue of the Carabidae (Coleoptera) of the Iberian Peninsula. Monografias Sociedad Entomologica Aragonesa 9, Zaragoza, 130 pp.
- Serrano J (2013) New Catalogue of the Family Carabidae of the Iberian Peninsula (Coleoptera). Universidad de Murcia, Murcia, 192 pp.
- Shorthouse DP (2010) SimpleMapp, an online tool to produce publication-quality point maps. <http://www.simplermappr.net> [Accessed May 10, 2022]
- Wrase DW, Kataev BM (2016) Four new species of genus *Acinopus* Dejean, 1821, subgenus *Acinopus* from southern Iran, from Sinai, and from western Saudi Arabia, and faunistic and taxonomic notes on species previously described (Coleoptera, Carabidae, Harpalini, Harpalina). Linzer Biologische Beiträge 48(2): 1783–1806.